This item was submitted to Loughborough's Research Repository by the author.
Items in Figshare are protected by copyright, with all rights reserved, unless otherwise indicated.

The application of fluorescence spectroscopy to the study of drug–protein binding

PLEASE CITE THE PUBLISHED VERSION

PUBLISHER

© H.N. Sturley

PUBLISHER STATEMENT

This work is made available according to the conditions of the Creative Commons Attribution-NonCommercial-NoDerivatives 4.0 International (CC BY-NC-ND 4.0) licence. Full details of this licence are available at: https://creativecommons.org/licenses/by-nc-nd/4.0/

LICENCE

CC BY-NC-ND 4.0

REPOSITORY RECORD

Sturley, H.N.. 2019. “The Application of Fluorescence Spectroscopy to the Study of Drug–protein Binding”. figshare. https://hdl.handle.net/2134/34915.

LOUGHBOROUGH
UNIVERSITY OF TECHNOLOGY
LIBRARY

AUTHOR/FILING TITLE

STURLEY, H

ACCESSION/COPY NO.

005378/01

VOL. NO.

CLASS MARK

ARCHIVES
COPY

FOR REFERENCE ONLY

THE APPLICATION OF FLUORESCENCE SPECTROSCOPY TO THE STUDY OF DRUG-PROTEIN BINDING

by

H N Sturley

A Doctorial Thesis

Submitted in partial fulfilment of the requirement
for the award of
Ph.D. of the Loughborough University of Technology
December 1983

© by H N Sturley (1983)

Loughborough University
of Technology Library
Date July 84
Class
Acc. No. 005378/01

ABSTRACT

Many small molecules and drugs bind strongly to the plasma proteins and in particular to human serum albumin, or HSA. The degree of binding of a drug to HSA may limit its availability to the receptor sites and excretory systems and so have profound effects on its biological activity and half-life.

Various reports of harmful side-effects occurring in vivo and arising from competition between drugs for plasma binding sites have been published. In order to understand and possibly predict these sometimes lethal effects, it is important to develop rapid and reliable methods for studying drug-protein phenomena.

Fluorescence spectroscopy is an extremely sensitive technique and fluorescence titrations may be performed quickly and simply. The binding of the fluorescent probes warfarin and 8-anilino-1-naphthalene sulphonic acid has been studied in solutions of HSA and in human sera. An accurate procedure has been developed for the determination of binding constants for such interactions. The method requires no prior separation of protein-bound and unbound fractions. Computer programs have been written to process experimental data and generate binding curves and constants.

Displacement of the bound probes by competitors has yielded information on the number and nature of the binding sites of various drugs.

Results from the spectroscopic method were compared with those obtained from equilibrium dialysis experiments. Specially designed dialysis cells were tested, and the binding curves produced using these were similar to those yielded by the fluorescence titrations.

Flow-injection analysis has been used to automate procedures. Once optimized, the system could handle large numbers of samples rapidly with minimum reagent consumption. The binding and displacement of probes in both albumin and serum samples investigated with the flow-injection apparatus have given results in excellent agreement with those obtained from the 'static' fluorescence titrations.

The applicability of derivative and synchronous fluorescence spectroscopy to drug-protein binding work has been examined.

The clinical implications of certain results have been considered.

CONTENTS

ABSTRACT i

ACKNOWLEDGEMENTS ii

LIST OF FIGURES vi

LIST OF TABLES ix

CHAPTER 1 INTRODUCTION

1.1 An Overview of Drug-Protein Binding

1.1.1 The Effect of Protein Binding on Drug Distribution 1
1.1.2 The Effect of Protein Binding on Drug Metabolism 8
1.1.3 The Effect of Protein Binding on Drug Excretion 10
1.1.4 The Effect of Protein Binding on the Pharmacological Activity of Drugs 12

1.2 Factors Which Alter Drug-Protein Binding in Vivo

1.2.1 Drug Displacement Interactions 14
1.2.2 Disease States 22
1.2.3 Miscellaneous Factors 24

1.3 The Location of Drug Binding Sites in the Blood and Tissues

1.3.1 The Partitioning of Drugs Amongst Blood Components 25
1.3.2 Binding of Drugs to Tissue and Extravascular Proteins 31

1.4 Human Serum Albumin and the Nature of its Drug Binding Sites

1.4.1 The Molecular Structure and Pharmacological Properties of HSA 32
1.4.2 The Location of the Major Drug-Binding Sites of HSA 38
1.4.3 Binding Forces, Structural Requirements and Theoretical Aspects of the Binding of Drugs to HSA 46

1.5 A Review of Current Techniques Employed in the Study of Drug-Protein Binding 51

1.6 Molecular Fluorescence Spectroscopy

1.6.1 Introduction to Molecular Fluorescence 56
1.6.2 The Effect of Molecular Structure on Fluorescence 71
1.6.3 The Effect of Molecular Environment on Fluorescence 76
1.6.4 Practical Aspects of Fluorescence Spectroscopy 83

1.7 Mathematical Models and the Graphical Representation of Binding Data 90

CHAPTER 2 MATERIALS AND STANDARD EXPERIMENTAL METHODS

2.1 Chemicals

2.1.1 Source and Pretreatment 99
2.1.2 Preparation of Solutions 99
2.1.3 Determination of Concentrations 101
2.1.4 Storage of Chemicals 101

2.2 Instrumentation 101

2.3 Spectrophotometric Measurements 102

2.4 Fluorescence Measurements

2.4.1 Uncorrected Spectra 105
2.4.2 Corrected Spectra 107
2.4.3 Emission Intensities 108

2.5 Computational Methods 113

CHAPTER 3 DEVELOPMENT OF A HOMOGENEOUS FLUORESCENCE ASSAY FOR THE ACCURATE DETERMINATION OF PROTEIN BINDING CONSTANTS

3.1 Introduction 114

3.2 The Characterization of Probe Fluorescence

3.2.1 Production of a Calibration Curve for Unbound Probe 123
3.2.2 Production of a Calibration Curve for Bound Probe 128
3.2.3 A Detailed Examination of the Calibration Plots 133

3.3 The Production of Data for Binding Curves

3.3.1 Practical Aspects of Binding Titrations 149
3.3.2 The Analysis of the Results of Binding Titrations 150

3.4 The Presentation of Results 154

3.5 The Calculation of Binding Constants from Experimental Data 159

3.6 The Analysis of Errors 168

3.7 Derivative and Synchronous Fluorescence Spectroscopy in the Resolution of Spectral Contributions from Bound and Free Fluorescent Probes 178

APPENDIX A 190

CHAPTER 4 THE APPLICATION OF FLUORESCENT PROBES TO A STUDY OF DRUG BINDING SITES ON SERUM PROTEINS

4.1 Introduction 198

4.2 The Influence of Competitor Drugs on Probe Binding Curves

4.2.1 Practical Considerations 199
4.2.2 Results and Observations 203

4.3 A Rapid Method for the Characterization of Drug Binding Sites on Albumin and in Whole Serum 215

4.4 Discussion of Methods and Results 232

CHAPTER 5 EQUILIBRIUM DIALYSIS : A CLASSICAL TECHNIQUE FOR STUDYING DRUG-PROTEIN BINDING

5.1 Principle of the Method 242

5.2 Design of Dialysis Cells and Performance Tests 246

5.3 Application of Dialysing System to Drug-Protein Binding Studies

5.3.1 Control of Fluid Shifts and Other Factors 249
5.3.2 Experimental Procedures 258

5.4 Equilibrium Dialysis Results 261

5.5 Comparison of the Fluorimetric and Equilibrium Dialysis Methods for Studying Drug-Protein Binding 266

CHAPTER 6 THE AUTOMATION OF BINDING STUDIES BASED ON THE PRINCIPLE OF FLOW INJECTION ANALYSIS

6.1 Theoretical and Practical Aspects of Continuous Flow Analysis 273

6.2 The Application of FIA to a Study of Drug-Protein Binding using Fluorimetric Detection. 283

6.3 Results Obtained using the Flow System 292

6.4 Discussion of Methods and Findings 299

CHAPTER 7 DISCUSSION 301

REFERENCES 308

LIST OF FIGURES

1.1 Representation of the diffusion equilibria that occur to relate the concentration of drug in plasma to the drug concentration at the receptor site and subsequent intensity of drug effect. 3

1.2 The Problems of Multiple-Drug Administration. 15

1.3 Simultaneous Interactions Between Two Ligands and One Macromolecule. 15

1.4 Amino Acid Sequence and 9-Double-Loop Structure of Human Serum Albumin. 34

1.5 Generalized Molecular-Orbital Energy Diagram. 58

1.6 The Franck-Condon Principle and Vibronic Transitions. 62

1.7 Transitions Occurring in Electronically Excited Molecules. 64

1.8 Mean Decay Times for Transitions in Excited State Molecules. 67

1.9 A Transition State Diagram Showing Solvent Relaxation and Intersystem Crossing. 77

1.10 Major Components of an Instrument for Measuring Fluorescence. 85

1.11 Graphical Representation of Three Commonly Used Linear Transformations of the Binding Equation for a Single Site or a Single Class of Sites. 95

2.1 Chemical Structural Formulae of Drugs and Fluorescent Probes used in this Study. 100

3.1 Corrected emission spectra of bound and free warfarin illustrating fluorescence enhancement. 117

3.2 Corrected emission spectra of bound and free warfarin illustrating differences in peak maxima and spectral bandwidths. 119

3.3 Corrected emission spectra of bound and free ANS illustrating fluorescence enhancement. 120

3.4 Corrected emission spectra of bound and free ANS illustrating differences in peak maxima and spectral bandwidths. 120

3.5 Corrected excitation spectra of warfarin and ANS. Corrected emission spectrum of HSA. 121

3.6 Emission spectra of human serum albumin illustrating resonance energy transfer to acceptor molecule (warfarin). 121

3.7 Emission spectra of human serum albumin illustrating resonance energy transfer to acceptor molecule (ANS). 122

3.8 Corrected excitation spectrum of albumin-bound ANS. 122

3.9 Flow Diagram. 124

3.10 Calibration Curve for Unbound Fluorescent Probe (Warfarin). 126

3.11 Scheme Showing Methods of Sample Preparation. 127

3.12 Reverse Titration for ANS. 130

3.13 Calibration Curve for Bound Fluorescent Probe (Warfarin). 130

3.14 The Effect of Ethanol on the Fluorescence of Albumin-Bound Warfarin. 134

3.15 Diagram of a Fluorescent Molecule at Some Position (x_1, y_1) in a Fluorimeter Cell. 138

3.16 Diagram Showing a Central Symmetric, Irradiated Portion of a Fluorimeter Cell. 138

3.17 Illustration of Over- and Under-Estimations of k on Calibration Plots. 144

3.18 Calibration Plot for Unbound Fluorescent Probe (ANS). 147

3.19 Calibration Plot for Bound Fluorescent Probe (ANS). 147

3.20 Listing of a Segment of FLUORB. 152

3.21 Scatchard Plot Representing the Binding of Warfarin to HSA. 156

3.22 Double Reciprocal Plot Representing the Binding of Warfarin to HSA. 156

3.23 DF/R Versus R Plot Representing the Binding of Warfarin to HSA. 156

3.24 A Scatchard Plot Representing the Binding of ANS to HSA. 158

3.25 Segment of NKFIT. 162

3.26 A Scatchard Plot Representing the Binding of Warfarin to HSA. 165

3.27 Derivative Spectra of Bound and Free Warfarin. 182

3.28 Corrected Excitation and Emission Spectra of Bound and Free Warfarin. 186

3.29 Corrected Excitation and Emission Spectra of Bound and Free ANS. 186

3.30 Corrected Excitation and Emission Spectra of Human Serum Albumin. 186

3.31 Synchronously Excited Emission Spectrum of ANS in Free Solution. 187

3.32 Synchronously Excited Emission Spectrum of Bound ANS. 187

3.33 A Comparison of Conventional and Synchronous Fluorescence Spectra of Albumin-Bound ANS. 188

A.1 Position of Molecules in Fluorimeter Cell (One Coordinate). 192

A.2 Position of Molecules in Fluorimeter Cell (Two Coordinates). 196

4.1 Absorption Spectra for Several Drugs and their Relation to the Excitation Peak of Warfarin at 320nm. 200

4.2 The Effect of Phenylbutazone on the Binding of Warfarin to HSA. 204

4.3 The Effect of Sulphisoxazole on the Binding of Warfarin to HSA. 210

4.4 The Effect of Sulphisomidine and Sulphamerazine on the Binding of Warfarin to HSA. 211

4.5 The Effects of Sulphapyridine and Sulphadiazine on the Binding of Warfarin to HSA. 212

4.6 The Effect of a Number of Drugs on the Degree of Binding of Warfarin to HSA. 219

4.7 The Effect of a Number of Drugs on the Degree of Binding of Warfarin to HSA over an Extended Concentration Range. 220

4.8 The Decrease in the Fluorescence of Albumin-Bound Warfarin on addition of ANS. 222

4.9 The Increase in the Fluorescence of Albumin-Bound ANS on Addition of Warfarin. 223

4.10 The Effect of a Number of Drugs on the Degree of Binding of ANS to HSA. 225

5.1 An Illustration of a Dialysis Cell used in this Study. 247

5.2 The Pattern of Membrane Oxidation Following Dialysis of a Potassium Permanganate Solution. 247

5.3 Calibration Curve for Warfarin in Free Solution. 250

5.4 The Equilibration of Warfarin Across the Dialysis Membrane. 251

5.5 Escape Plot for Warfarin Using Data of Figure 5.4. 256

5.6 Scatchard Plot Describing the Binding of Warfarin to Human Serum Albumin. Equilibrium Dialysis and Fluorimetric Titration. 262

5.7 Calibration Plot for Sulphisomidine. 265

5.8 The Binding of Three Sulphonamide Drugs to HSA as Determined by Equilibrium Dialysis. 267

6.1 Configurations of Different Continuous Flow Systems. 274

6.2 Velocity Profiles and Shapes of Injected Sample Zones. 276

6.3 Diagrammatic Representation of Effects of Convection and Radial Diffusion on Concentration Profiles and Samples Monitored at a Suitable Distance Downstream from Injection. 276

6.4 Injection Valves. 285

6.5 The Displacement of ANS from Human Serum Albumin by Flufenamic Acid; Conventional FIA Technique. 287

6.6 The Displacement of ANS from Human Serum Albumin by a Number of Acidic Drugs : Merging Zone FIA Technique. 293

6.7 The Displacement of Warfarin from Human Serum Albumin by a Number of Acidic Drugs : Merging Zone FIA Technique. 297

6.8 The Binding of ANS to HSA as Measured by Fluorescence Titration and Merging Zone FIA. 298

LIST OF TABLES

1.1 A Scheme for Binding Regions Located on Serum Albumin. 40

3.1 The Effect of Temperature on the Fluorescence of Albumin-Bound Warfarin. 132

3.2 The Effect of Buffer Ionic Strength on the Sample Fluorescence. 132

3.3 The Optimization of k from Experimental Data. 145

3.4 The Data of One Binding Experiment as Represented by the Program FLUORB. 155

3.5 The Variation in the Gradient of the Linear, Corrected Calibration Plot at Each Point in a Titration When the Optimum Value of k is Used. 170

3.6 The Value of k Required to Transpose Each Data Point on to the Linear Calibration Plot. 172

3.7 A Summary of the Major Features of the Fluorescence Spectra of Human Serum Albumin, Warfarin and ANS. 183

4.1 Nine Determinations of the Inner-Filter Factor k for Sulphisomidine. 202

4.2 Mean Values of k for Some Sulphonamide Drugs. 202

4.3 The Data Used to Construct the Plots Shown in Figure 4.2. 205

4.4 Estimated Binding Constants for the Interaction Between Warfarin and HSA; the Effect of Phenylbutazone on These Values. 208

4.5 Estimated Binding Constants for the Interaction Between Warfarin and HSA; the Effect of Sulphisoxazole on These Values. 208

4.6 Estimated Binding Constants for the Interaction Between Warfarin and HSA; the Effect of Sulphisomidine and Sulphapyridine on These Values. 213

4.7 Results Illustrating the Competitive Displacement of Warfarin From HSA by Increasing Concentrations of a Number of Drugs. 216

4.8 The Displacement of ANS from HSA by Flufenamic Acid in the Presence of Sulphisoxazole. 226

4.9 The Displacement of ANS from HSA by Flufenamic Acid in the Presence of a Number of Ligands. 226

4.10 The Displacement of ANS from HSA by Ethacrynic Acid in the Presence of Sulphisomidine and Warfarin. 228

4.11 Displacement of ANS in Human Serum by a Number of Ligands. 230

4.12 Displacement of ANS from Albumin Binding Sites. 231

4.13 Displacement of Warfarin from HSA and Serum Binding Sites. 231

5.1 Results of an Experiment to Test Fluid Shifts Within the Dialysis Cells. 252

5.2 Approach to Equilibrium in Dialysis Cell with Warfarin as Ligand. 257

5.3 Influence of Initial Conditions and Fraction Unbound on the Time to Reach a Certain Fraction Away From the Equilibrium Concentration. 258

5.4 The Displacement of Warfarin from HSA as Determined by Equilibrium Dialysis. 264

5.5 Advantages and Disadvantages of Fluorimetric and Equilibrium Dialysis Methods for Studying Drug-Protein Binding. 268

6.1 The Displacement of ANS from its Albumin Binding Sites by Acidic Drugs. Comparison of FIA and Static Methods. 294

6.2 The Displacement of Warfarin from its Albumin Binding Sites by Acidic Drugs as Measured by FIA. 296

CHAPTER 1

Introduction

1.1 An Overview of Drug-Protein Binding

The biological activity of a drug is profoundly influenced by its interaction with protein molecules. Almost every drug exerts its pharmacological effect by binding to some kind of protein in the body. As well as being necessary for drug-receptor interactions and metabolism to take place, protein binding also governs the absorption, distribution and excretion characteristics of drugs. Consequently a thorough understanding of the nature and number of binding sites for specific ligands would lead to a better understanding of the therapeutic and toxic effects of drug administration.

Several comprehensive reviews of the literature on drug-protein binding have already been published. The first was Goldstein's classic report which surveyed and summarized the major contributions in the field up to 1949. Subsequently, Meyer and Guttman (1968) produced a review which contained comprehensive tabular data, similar in form to that employed by Goldstein (1949), but summarizing the findings of more recent studies. A sequel to this review has been compiled by Vallner (1977). An important series of papers from a conference covering all aspects of drug-protein binding was published in 1973 (Anton and Solomon, 1973); this has been extended by the general review of Bridges and Wilson (1976). Keen (1971) and Jusko and Gretch (1976) have compiled interesting works which focus mainly on the role of drug-protein binding in pharmacokinetics. The latest review (Wilkinson, 1983) covers some recent findings in the broad area of drug-protein binding but concentrates primarily on the effects of the phenomenon on pharmacokinetics in man.

The aim of this, the first section of the introduction, is to examine the biological significance of drug-protein binding; the importance of the more specific areas covered in later sections may then be appreciated.

1.1.1 The Effect of Protein Binding on Drug Distribution

Most drugs are carried from their sites of absorption to their sites of action and elimination by the circulating blood. Drugs, other xenobiotics and endogenous compounds may be transported in the blood stream in simple solution, as a suspension or associated with blood constituents such as albumin, globulins, lipoproteins and erythrocytes. The binding of drugs to plasma proteins is probably completely reversible but it is only unbound or free drug which diffuses through the capillary walls, reaches the site of action, and is subject to elimination from the body. The relationship of plasma protein binding to the processes that establish the concentration of drug at the receptor site are shown in Figure 1.1.

Whatever the route of administration, almost all therapeutic agents reach their sites of action via the systemic circulation. The capillary wall, through which the blood is in contact with the tissue fluids, is the initial barrier to drug distribution. Indeed, the exchange of water and solutes between the blood and the tissue fluids takes place almost entirely through the walls of the capillaries.

Blood capillaries are lined with endothelial cells. These cells are about 0.2 micron in diameter and contain most of the organelles present in other cell types, including pinocytotic vescicles that probably serve specific transport functions for macromolecules. The capillary endothelial cells are surrounded by a basement membrane of about 20 to 30nm thickness which resembles the ground substance.

Most capillaries in muscle and skin are of the continuous type with no discontinuities between cells. The exchange of material across their walls is largely by the diffusion of very small molecules in accordance with concentration gradients. The bulk movement of water and permeable substances is therefore determined by osmotic and hydrostatic pressures.

More permeable capillaries termed fenestrated capillaries have pores between the cells of the endothelial wall. Many vascular channels consist of fenestrated capillaries but they are particularly abundant in the renal glomeruli and the intestinal mucosa. Their pores allow low molecular weight compounds to pass directly from the circulation to the extravascular space while restricting the passage of plasma proteins and other high molecular weight constituents of the blood. As a result only that fraction of a drug which is not bound to serum proteins or red blood cells can cross these capillaries by passive diffusion.

Even more permeable endothelial walls are present in the sinusoids of organs such as the liver, spleen and bone marrow. Sinusoids are capillary-like structures with large diameters. They are termed discontinuous capillaries because there are large gaps in the abutments between the endothelial cells. There is no impairment to the passage of even the largest macromolcules and blood cells can enter or leave the circulation through the gaps.

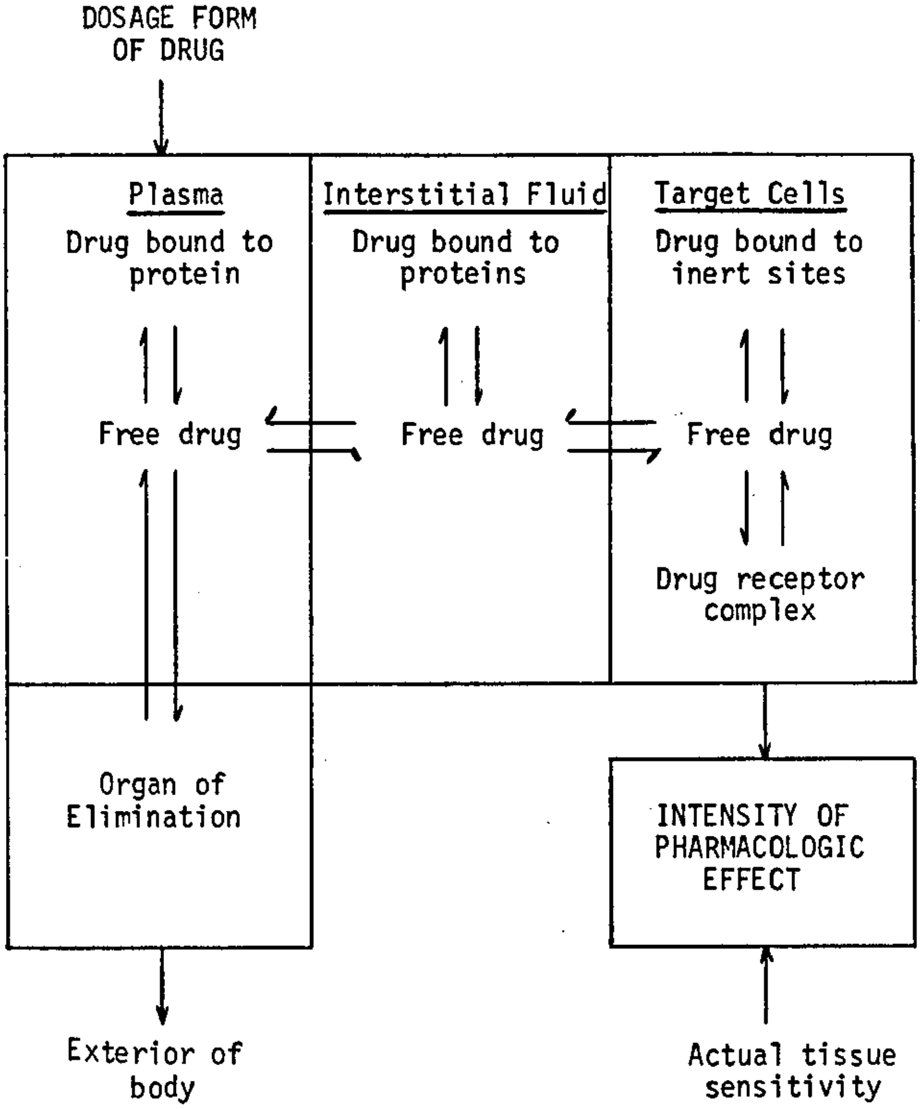
DOSAGE FORM OF DRUG
Plasma
Drug bound to protein
Free drug
Interstitial Fluid
Drug bound to proteins
Free drug
Target Cells
Drug bound to inert sites
Free drug
Drug receptor complex
Organ of Elimination
Exterior of body
INTENSITY OF PHARMACOLOGIC EFFECT
Actual tissue sensitivity

FIGURE 1.1 Representation of the diffusion equilibria that occur to relate the concentration of drug in plasma to the drug concentration at the receptor site and subsequent intensity of drug effect (From Reidenberg, 1981).

A number of body compartments, including the eye, mammary gland, the foetus and the greater part of the brain, are effectively separated from the circulation by membranes lacking the pores which render the capillary walls permeable to drugs. Free drug tends to come into equilibrium across these membranes but the rate of attainment of equilibrium is determined by the degree of ionization of the drug and its lipid solubility. Lien (1981) has examined the relationship between the structural and physiochemical properties of drugs and their passage across various body membranes.

Evidence that only the unbound fraction of a drug is available for transport to extravascular sites has been provided by studies of the antibacterial action of sulphonamide drugs. In 1943 Davis postulated that the bound fraction of a sulphonamide was probably devoid of bacteriostatic action. Anton (1960) was able to demonstrate experimentally that albumin-bound sulphonamide is not available for antibacterial action and that the potency of these agents is due to the free drug.

Providing they do not bind preferentially or irreversibly to tissue sites, it is clear that highly protein-bound drugs are likely to be localized initially in the plasma compartment, particularly at doses where the high affinity sites are not saturated. Under these circumstances plasma protein-bound drugs can serve as a reservoir replenishing by dissociation some of the free drug that diffuses out of the bloodstream through the capillary membranes and is lost by metabolism and excretion. This equilibration process depends on the readily reversible binding of drugs to plasma proteins and tends to maintain the concentration of unbound drug at a therapeutically useful concentration over a considerable range of total plasma concentrations. Thus plasma proteins have an important buffering role for many drugs enabling them to be given only a few times a day rather than by continuous infusion. Plasma protein binding could also reduce the free concentration of some drugs below that required to elicit a toxic response, thus rendering the drug safe for therapeutic use.

Once drug distribution is complete, the concentration of unbound drug in the tissues and the tissue compartments of the extracellular fluid can equal that in the plasma. This has been shown experimentally by Howell et al (1972) who measured unbound levels of penicillin in synovial fluid and serum samples. As shown in Figure 1.1, it is not the total but rather the free drug concentration in the serum that correlates with the concentration at the sites of action.

The rate of reaching an equilibrium distribution between the drug in the blood and in a tissue depends largely on the tissue's rate of perfusion. Equilibrium between drug in plasma and tissue is rapidly achieved in the lung, brain, liver and kidney which are richly perfused. Muscle (at least, when in a resting state) is less rapidly perfused and equilibrium distributions are reached more slowly. Adipose tissue does not have an extensive blood supply and equilibration of drugs into it from the blood is even slower than with muscle.

In the steady state, the concentration of bound drug in the plasma will depend on the quantities of binding material present in both plasma and tissues, and on the affinity of the drug for the binding sites of these materials. For drugs which are highly bound in both plasma and tissues, the tissue binding will tend to draw free drug from the plasma leading to a lowered plasma drug concentration. With tricyclic antidepressants and phenothiazines, for example, almost all of the drug in the serum is bound to albumin, however, because of extensive tissue binding, the circulating drug in the plasma represents only a small fraction of the total drug in the body (Koch-Weser and Sellers, 1976).

The extent to which a drug is distributed through the body is usually measured in terms of its 'apparent volume of distribution'. At distribution equilibrium the volume of distribution of total drug is:

$$\text{Vd} = \frac{\text{amount of drug in body}}{\text{plasma concentration of drug}}$$

It is the apparent volume of fluid a drug would occupy if the total amount administered were in solution at the same concentration as in plasma.

Depending on its physical and chemical properties, a drug exhibits different apparent volumes of distribution. For some drugs Vd may correspond to an anatomical or physical compartment such as plasma volume, extracellular fluid, or total body water. Thus a drug that is tightly bound to plasma proteins has a volume of distribution of about 3l which corresponds to the plasma volume. Warfarin is extensively bound to plasma proteins and has a small apparent volume of distribution - indeed, its Vd is identical to that of injected albumin (Tillement, 1978).

Drugs that pass through the capillary endothelium but not through cell membranes, and which are not protein-bound or lipid soluble, have a volume of distribution of about 9l equal to that of the extracellular fluid volume. If the drug passes through cell membranes but is not bound to any tissue constituents or selectively taken up into any particular cells, it will be evenly distributed through the body water when equilibrium is reached and will have a volume of distribution of about 42l: such a drug is ethanol. However, if a drug is selectively bound to constituents of tissues or is taken up by tissue cells, the apparent volume of distribution is a purely mathematical concept: some drugs may have volumes of distribution several hundred times the body volume. The volumes of distribution of many of the most commonly administered drugs have been tabulated by Bowman and Rand (1980).

The apparent volume of distribution is a function of the relative binding of a drug in blood and tissue. Clearly a decrease in blood binding will lead to an increase in the volume of distribution, whereas a decrease in tissue binding will lead to a decrease in the volume of distribution. A simple theoretical model to explain quantitatively the effects of plasma protein binding on the steady-state drug distribution in the body has been described by Martin (1965). Using this model it has been calculated that the binding of drugs to plasma proteins will have an effect on distribution only if associations constants are greater than 10^4 M^{-1}. At low plasma levels a drug with a high association constant, say 10^5 M^{-1}, will be almost completely bound to plasma proteins. When the concentration of the drug increases, however, available plasma protein binding sites become fewer as saturation approaches, more of the drug diffuses into the tissues and the fraction remaining within the vasculature is reduced. For such drugs there will be a concentration range over which small changes in the plasma level may exert a profound influence on the distribution of the drug within the body. The simple model suggests that the controllable therapeutic dose range may be narrow for highly bound drugs. Levy (1973) has demonstrated that the distribution and elimination of the highly bound drug dicoumarol is affected by its plasma protein binding but emphasized that such effects are likely to be less pronounced for drugs not so extensively bound.

The simplified model of Martin (1965) made early contributions to an understanding of the effects of drug-protein binding and drug dosage on pharmacokinetics. However, the analysis assumed that drug binding to the plasma proteins was only important in the intravascular compartment. As outlined below, there is now evidence to suggest that plasma proteins are widely distributed throughout the extravascular fluids.

Despite its high molecular weight, albumin is not exclusively retained in the plasma. The extravascular space consists of many different anatomical compartments of varying pool size, each of which has its own characteristic exchange rate with the vascular compartment. Most plasma disappearance curves of albumin can be resolved into three components. The component with the longest half-life of about 17 to 18 days reflects the catabolism of albumin. The other two components with half-lives of 6 hours and about 28 hours indicate that there are at least two distinct groups of extravascular compartments which contain albumin and are in equilibrium with the vascular compartment. The model most often used to depict albumin distribution is therefore a three-compartment model with an intravascular (plasma) compartment and two extravascular compartments. In those tissues with discontinuous capillaries such as the liver, spleen and intestine, and high plasma perfusion rates, distribution occurs rapidly as is represented by the extravascular compartment with the smaller volume of distribution. Those tissues with continuous capillaries, such as muscle and skin, and with smaller plasma perfusion rates are represented by the larger and more slowly exchanging extravascular compartment (Courtice, 1971).

The total amount of extravascular albumin in the body has been computed by several kinetic methods: it appears that about 55 to 65% of the total exchangeable albumin is located outside the plasma (Jusko and Gretch, 1976). Once it is realized that an appreciable quantity of albumin is distributed both extravascularly and intravascularly, it is logical to extend the analysis of Martin (1965) to account for the binding of drugs in an extravascular compartment, namely in the interstitial fluid. This yields a three-compartment model which illustrates some further theoretical and practical aspects of the effect of the drug-protein interaction on drug distribution. Nevertheless, this model is still a simplified representation of what actually occurs in the body under steady-dosing conditions. Other factors such as binding to tissue proteins and partitioning into fatty deposits could serve to further complicate drug distribution. More sophisticated models are required to describe adequately the distribution of most drugs.

Physiological pharmacokinetic models have been used successfully to describe the distribution and elimination of certain drugs: this work has been reviewed by Jusko and Gretch (1976). All the parameters used in such models have a specific physiologic or physiochemical basis. The major regions of the body known to be of importance in drug distribution are considered and each tissue region is separated into three compartments, the capillary plasma volume, the internal water and the extracellular water. The different tissue regions receive a designated plasma flow and realistic plasma and tissue albumin concentrations are employed.

Øie and Tozer (1979) have produced equations which should be helpful in analysing and predicting alterations in the volume of distribution of any drug not only when there is a change in the unbound fraction in the plasma, but when there is a change in the unbound fraction in the extracellular fluids outside the plasma, in the volumes of the extracellular fluids, or in the extravascular to intravascular plasma protein ratios as occurs in many diseases and other abnormal physiological states. Faed (1981) has also stressed the importance of considering drug binding in the interstitial fluid as well as in the plasma when examining the pharmacokinetics of drugs which are highly bound to plasma proteins and have a small apparent volume of distribution.

1.1.2 The Effect of Protein Binding on Drug Metabolism

The main organ concerned with drug metabolism is the liver, and many drugs are substrates for the microsomal enzyme systems of hepatocytes. Hepatocytes constitute about 60% of the mass of the liver: Bowman and Rand (1980) have discussed the structures and metabolic functions of these cells in some detail.

Although hepatocytes are the major sites of drug metabolism, the kidney, lung, intestinal mucosa, plasma and nervous tissue also contain important drug-metabolizing enzymes. The reactions in tissues other than the liver may have important local consequences due to the formation of end-products with altered pharmacological activity or toxicity which exert their effects in the vicinity of the sites of production. While the same may be true of the liver, reactions taking place in this organ can have far-reaching consequences arising from the inactivation of endogenous hormones, drugs and toxic substances - that is, detoxifications, and the formation of pharmacologically active metabolites from inert precursors or prodrugs. In general, the metabolism of a drug renders it more soluble.

A number of qualitative and semiquantitative observations have indicated that the binding of drugs to plasma proteins can influence their rates of metabolism. Newbould and Kilpatrick (1960) showed that the rate of acetylation of two long-acting sulphonamides in a perfused liver preparation decreased when plasma was added to the perfusion fluid and the rate of metabolism was dependent on the concentration of unbound drug. Anton and Boyle (1964) showed that albumin interfered with the acetylation of sulphamethoxypyridazine in an in vitro enzyme system. Wiseman and Nelson (1964) reported a rank-order correlation between the rates of in vivo metabolism of a number of sulphonamides and the degree of protein binding. These and other results suggest that only free sulphonamide is accesible to the drug-metabolizing enzymes. For most drugs, however, it is not known whether only free or total drug is available for metabolism in the liver (Jusko and Gretch, 1976).

Theoretical considerations of the effect of protein binding on drug-metabolism have been published by Gillette (1971). These suggest that if the activity of drug-metabolizing enzymes in the liver are so high that virtually all the drug is cleared from the blood as it passes through the liver, then an elevation in the binding of the drug to plasma proteins will accelerate its metabolism by increasing the rate at which it is carried to the liver. So for drugs with high extraction ratios, plasma protein binding may have a transport function, bringing the drugs to the metabolizing organ. Alternatively, if very little of a drug is metabolized as it passes through the liver, that is, if the drug has a low extraction ratio, an increase in plasma protein binding may either decrease its metabolism or have little effect; in these circumstances, protein binding may have a storage function.

In considering the possible mechanisms that restrict the metabolism of highly bound drugs, one might conclude that the plasma could be completely cleared of unbound drug as it passes through the liver and that the rate of dissociation of the drug-protein complex limits the elimination of the bound form. For this mechanism to be limiting, however, the half time for dissociation of the complex would have to be about equal to or greater than the mean transfer time of the blood through the sinusoids of the liver. Gillette (1973) has provided evidence to suggest that the rate of dissociation of the drug-protein complex is seldom rate limiting in the metabolism of drugs. Lassman (1981), on the other hand, concludes that the dissociation of some albumin-bound drugs could be the rate limiting step in their clearance from the liver.

In a recent development, Weisiger et al (1981) have considered the uptake of long-chained fatty acids in the liver. Although tightly bound to albumin, these compounds are effectively removed from the plasma during its passage through the liver. Uptake of fatty acids has been attributed to their spontaneous dissociation from albumin in the bulk aqueous phase and the subsequent diffusion of free ligand to the surface of the liver cells. Weisiger et al (1981) present evidence that the uptake of long-chain fatty acids takes place by a saturable binding of the fatty acid-albumin complex with a receptor for albumin on the liver cell surface: their data suggest that the concentrations of albumin and albumin-bound fatty acid are the principal determinants of uptake. The existence of a hepatocyte receptor for albumin may also be supported on theoretical grounds. Under physiological conditions only about 0.1% of long-chain fatty acids are not bound to albumin. If this small fraction alone were to account for uptake, its regeneration from the fatty acid-albumin complex would need to be extremely rapid to account for the overall extraction observed during a single pass through the liver. However, the half-life for the dissociation of long-chain fatty acids from high-affinity sites on albumin is significantly longer than the time required for blood to pass through the liver (Svenson et al, 1974). Thus the putative albumin receptor may provide a mechanism by which the probability of uptake of fatty acids can be increased. Participation of the hepatic albumin receptor in the uptake of other endogenous and exogenous ligands has yet to be demonstrated.

According to Bridges and Wilson (1976), newly synthesized serum albumin may be involved in the removal of metabolites from the liver. Large quantities of serum albumin are synthesized on the hepatic endoplasmic recticulum and secreted out of the cell. It is possible that this newly synthesized albumin might bind drug metabolites which are being formed on the endoplasmic recticulum and facititate their clearance from liver cells. This mechanism would explain the lack of hepatic damage caused by some active metabolites formed in the liver cells.

1.1.3 The Effect of Protein Binding on Drug Excretion

Three processes contribute to renal excretion: glomerular filtration, tubular secretion and tubular reabsorption. The first two processes remove drugs and their metabolites from the blood, whereas the latter diminishes renal clearance. The effect of plasma protein binding on the renal excretion of a drug depends on the relative importance of these processes.

Glomerular filtration relies upon the passive diffusion of unbound ligand across the glomerular membrane. There is no appreciable movement of plasma proteins through the glomerular membrane but the free fraction of almost all drugs is readily filtered. Hence the concentration of drugs in the glomerular filtrate generally equals the free drug concentration in the serum. For this reason, Keen (1971) has described the glomerular filtrate as a true ultrafiltrate of plasma. Since only free drug is filtered by the glomeruli, plasma protein binding of a drug will tend to have a retaining effect. The glomerular elimination of highly albumin-bound drugs can be extremely slow. Kakemi et al (1962) found an approximate inverse relationship between the binding of a series of salicylates and their rates of excretion. However, such a correlation is likely to hold only when elimination is predominantly determined by the rate of glomerular filtration.

Tubular secretion is primarily an active process and has a certain selectivity towards acids, bases and various endogenous compounds. Consequently, it can be inhibited by compounds that compete for the same transport system. Unlike glomerular filtration, the tubular secretion of drugs is not generally limited by protein binding. Only free drug can be secreted by the tubules, and in contrast to glomerular filtration, active tubular secretion decreases the concentration of free drug in the blood. However, the dissociation of the drug-protein complex is usually so rapid that any free drug withdrawn from the serum by active transport mechanisms can be replaced virtually instantaneously. Consequently, even drugs which are more than 90% bound to serum albumin at therapeutic concentrations, can be removed almost completely from the blood by tubular secretory mechanisms during a single pass through the kidney (Koch-Weser and Sellers, 1976a). Nevertheless, it is probable that protein-binding accelerates the rate of elimination of a drug which is actively secreted by the tubules because it increases the plasma drug concentration and so delivers more drug to the sites of secretion.

As with hepatic clearance, it is possible to distinguish between drugs with high and low renal extraction ratios. As the rate of glomerular filtration is about 120ml/min, a drug which has a high renal clearance approaching renal blood flow (1500ml/min) must be predominantly secreted and not reabsorbed. Clearly, the elimination of such a drug is affected by change in renal blood flow rather than by changes in protein binding or the capacity of active transport systems; for a lowly cleared drug the opposite is true.

The importance of plasma protein binding in hepatic biotransformation is generally analogous to that in the renal excretion of drugs. Thus drugs that enter the hepatocyte by simple diffusion are protected from biotransormation to the extent of their binding to plasma proteins, while on the other hand, the biotransformation of drugs that are concentrated in the hepatic cell by active transport mechanisms is unlikely to be limited by their protein binding.

Lipophilic nonionized drugs are passively reabsorbed from tubular urine across an intact tubule membrane. In general, ionized drugs are not reabsorbed but if the degree of ionization of a drug can be altered by changing urine pH, then its reabsorption and hence renal clearance will be affected. According to Koch-Weser and Sellers (1976a) binding to serum albumin can limit the rate of elimination of drugs that are lipid soluble at the pH of tubular fluid by increasing their back-diffusion from the glomerular filtrate into the blood.

Drugs may be actively secreted into bile. Consequently protein binding is unlikely to limit biliary secretion. Indeed, it has been suggested that protein binding may assist biliary excretion. However, the effect of plasma protein binding on biliary excretion is still a matter of conjecture (Keen, 1971).

Salivary excretion of drugs appears to involve a process of passive diffusion which excludes the protein bound fraction. Nevertheless, it should be noted that when the pH of the saliva differs from that in the plasma, free drug may be unequally distributed between the two fluids.

1.1.4 The Effect of Protein Binding on the Pharmacological Activity of Drugs

Since protein binding inhibits the activity of a number of drugs, it is generally considered that only free drug can reach the sites of action and exert a pharmacological effect (Anton, 1960; Keen, 1971; Kunin et al, 1973; Koch-Weser and Sellers, 1976a). The finding that the biological effect of drugs and endogenous ligands increases when they are displaced from plasma protein binding sites (Aggeler et al, 1967; Anton, 1973) also suggests that it is the unbound fraction which is active.

Binding to serum albumin decreases the maximum intensity of action of a single dose of most drugs because it lowers the peak concentration of unbound drug at the receptor sites. The magnitude of this effect is directly proportional to the fraction of the administered dose which binds to serum albumin.

Binding to plasma proteins slows the elimination of drugs that are removed from the serum by glomerular filtration or by passive diffusion to the sites of hepatic biotransformation. It therefore increases the duration of action of a single dose of such drugs. Indeed, the duration of action of many drugs correlates with the degree of their albumin binding. However, drugs that are highly bound to plasma proteins may have a high degree of binding at inactive tissue sites which would also lead to a long half-life and duration of action. On the other hand, by increasing the rate of delivery to the sites of elimination, binding to plasma proteins may shorten the duration of action of drugs that are actively transported into renal tubules or hepatic cells. Clearly, the effects of protein binding on the pharmacological activity of a drug are not simple but depend on the particular pharmacokinetic characteristics of the compound.

The rate of intravenous injection of highly albumin-bound drugs can be important for the intensity of their pharmacological action. During rapid intravenous injection of such drugs the binding capacity of the plasma proteins in the limited blood volume with which the drug mixes may be exceeded. If this occurs, the rapid introduction of strongly bound drugs into the circulation produces a much higher concentration of free drug than when administration is slow enough to allow mixing with the entire blood volume during the injection. The increased level of free drug in the serum can be reflected in a higher drug concentration at the sites of action in rapidly perfused tissues. A more intense pharmacologic action after rapid rather than slow intravenous injection has been demonstrated for highly bound drugs that act on tissues with a high perfusion rate.

It is apparent that it is usually only the free drug and drug metabolite concentration in the plasma which could be expected to correlate directly with the therapeutic and toxicological effects of the drug. Most often, however, it is the total drug blood level which is measured in clinical pharmacology studies (Greenblat et al, 1982; Marks, 1979a). Interpretation of data based on total blood levels rests on the assumption that there is a simple correlation between free drug levels and total drug blood levels. For moderately or poorly bound drugs this may be valid, but it is frequently not justified for highly bound drugs. When the protein binding sites of a highly bound drug are nearly saturated, small changes in the total blood level may mask very significant increases in free drug levels. It is hardly surprising that for many strongly bound drugs poor correlations have been reported between biological effects and total drug blood levels. The use of total drug measurements to guide therapy may sometimes lead to errors in dosing (Koch-Weser, 1972). This point is further emphasized in the book by Wartak (1983) which provides a general account of the application of pharmacokinetic principles to drug therapy. There is considerable interest in the possibility that saliva might prove more useful than blood as the fluid in which drug assays should be performed. One advantage is that for many drugs their concentration in saliva reflects, more or less accurately, the concentration of unbound drug in the plasma; unfortunately this is not true for all drugs (Marks, 1979b).

It is by no means certain, however, that a protein-bound drug is invariably therapeutically and toxicologically inactive. The fact that drugs which are deliberately covalently bound to serum albumin often cause specific antibodies to be produced when the drug-protein complex is injected into experimental animals implies that drugs bound to proteins may still be able to interact with some receptor sites. It is possible that large polar drug molecules which are not normally able to pass across cell membranes may be taken up into cells by pinocytosis when bound to protein. For cells active in protein uptake the possibility of drug absorption in the albumin-bound form should not be discounted (Weisiger et al, 1981).

The effect of tissue binding on the pharmacological activity of drugs is obviously very important. If an alteration of plasma protein binding is to be pharmacologically significant, it must be associated with a simultaneous and corresponding change in tissue binding (Kurz and Ficktl, 1983). Should tissue binding remain constant or change in the opposite direction, the displacement of a drug from plasma binding sites is of little significance or has no pharmacological effect at all. The consequences of altered drug-protein binding in vivo are considered in the next section.

1.2 Factors Which Alter Drug-Protein Binding in Vivo

1.2.1 Drug Displacement Interactions

The plasma proteins have only a limited capacity for binding drugs, and competition for binding sites between concomittantly administered drugs is a common cause of drugs interactions in man. However, while the problems associated with multiple-drug therapy are very widely appreciated (Figure 1.2), it is important not to overestimate or overstate the importance of plasma protein binding displacement as a mechanism of drug interaction.

There are a number of proteins in the blood which bind drugs, and each protein may have several binding sites. The sites that avidly bind one drug may be different from those that avidly bind another. For this reason not all highly bound drugs displace one another from plasma proteins. Nevertheless, when two or more drugs bind to the same sites on a macromolecule, there will be a simple competition between the drugs for these sites (Figure 1.3) the mutual displacement of the interacting drugs is a function of their concentrations and their relative affinities for the common binding sites. Compounds with a high affinity will tend to displace drugs with a lower affinity and so the mutual displacement of interacting drugs tends to take place to differing extents. When two drugs compete for binding sites, the displacement of only one drug is likely to be clinically important. The latter is referred to as the displaced drug (Koch-Weser and Sellers, 1976b), while the other component of the interaction is called the displacing agent.

Drug displacement interactions can also occur between compounds which bind to different sites on a protein molecule. When a drug binds to

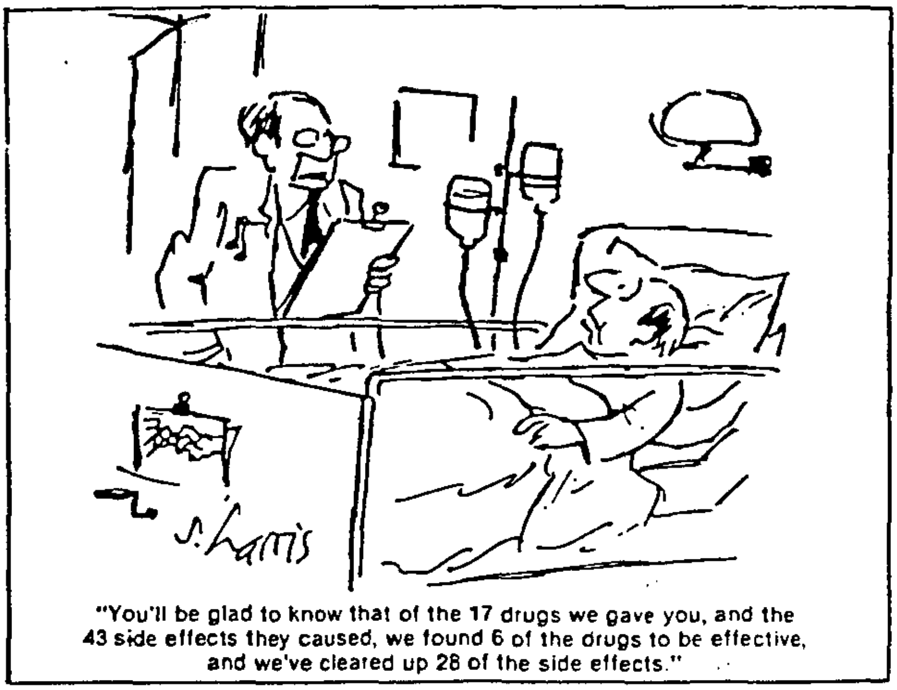
S. Harris
"You'll be glad to know that of the 17 drugs we gave you, and the 43 side effects they caused, we found 6 of the drugs to be effective, and we've cleared up 28 of the side effects."

FIGURE 1.2 The Problems of Multiple-Drug Administration (From Current Contents, Life Sciences 26 (23), June 7, 1982).

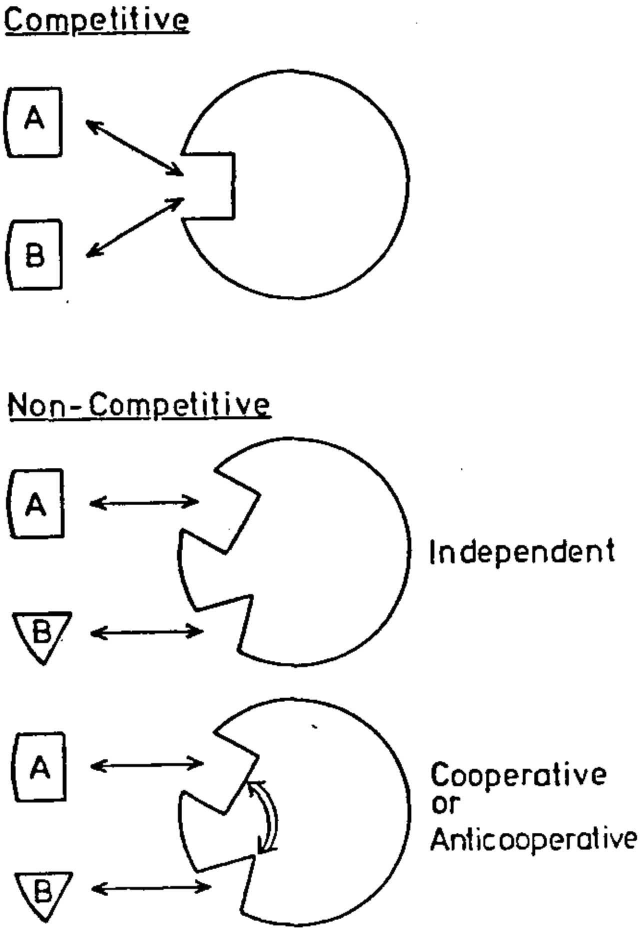
Competitive
A
B
Non-Competitive
A
B
Independent
A
B
Cooperative
or
Anticooperative

FIGURE 1.3 Simultaneous Interactions Between Two Ligands and One Macromolecule.

a serum protein, it may induce structural changes in the tertiary conformation of the macromolecule which modify the shape of specific binding sites for other groups of drugs. This modification may lead to a non-competitive displacement interaction (Figure 1.3).

A wide range of drugs are bound to plasma proteins and may thus enter into interactions involving binding displacement. Many potential drug-drug interactions have been identified, but the majority of drug displacement interactions are probably of insufficient magnitude to have a clinical effect or may be obscured by other factors in vivo.

Sometimes the metabolite of a drug rather than the drug itself may be involved in a displacement interaction. For example, trichloroacetic acid, a metabolite of chloral hydrate displaces warfarin from its albumin binding sites (Sellers and Koch-Weser, 1970). Some drugs may be converted in the body to metabolites that compete with the parent compound for binding to serum and tissue proteins (Gillette, 1973).

An unusual mechanism is responsible for a number of displacement interactions involving aspirin. The acetyl group of aspirin can become covalently attached to lysine residues on albumin molecules. The albumin binding of flufenamic acid, phenylbutazone and possibly other anionic drugs is modified in the presence of aspirin (Pinkard et al, 1973).

Rondanelli et al (1983) have considered some general aspects of the clinical pharmacology of drug interactions. The clinical significance of interactions which involve the displacement of drugs from plasma protein and tissue binding sites has been discussed by D'Arcy and McElnay (1982) and McElnay and D'Arcy (1983). The pharmacokinetics of drug displacement interactions and the factors which determine their severity have also been reviewed by McElnay and D'Arcy (1980). Koch-Weser and Sellers (1976b) have considered the clinical consequences of the competition between drugs for serum albumin binding sites, and pharmacokinetic models of drug-drug interactions have been reviewed by Aarons (1981). Some of the more important aspects of drug displacement interactions will be examined below.

If a bolus injection of a displacing drug is given to a patient, displacement of the primary agent will be almost immediate while distribution and therefore re-equilibration will take a short time. This means that the free drug plasma concentration will rise and total drug concentration will remain the same immediately after injection. During this initial period, the displacement of even a small amount of highly bound drug can cause a large increase in the free fraction of the drug in serum.

Thus displacement from albumin of 1% of a 99% bound drug will double the free fraction. It is important to stress that this does not mean that the free drug concentration in the plasma will be doubled: the displaced drug does not remain confined to the circulation but quickly distributes throughout the body and may localize in tissues. Hence displacement interactions are often of a transient nature.

After redistribution, any remaining increases in the free drug concentration in the serum and extracellular fluid depend on the new volume of distribution of the drug. If this volume is large, changes in the plasma free drug pool caused by displacement from plasma proteins are too small to affect the total body free drug pool and therefore too small to have a significant effect on free drug concentration in the plasma or tissues after re-equilibration. Since the apparent volume of distribution of most drugs far exceeds the plasma volume (an exception is warfarin), D'Arcy and McElnay (1982) have suggested that the ultimate consequence of the majority of plasma protein binding displacement interactions is a decrease in the total drug concentration in the plasma while the free drug concentration remains essentially unchanged. Since pharmacological actions, including toxicities, correspond to free drug in the plasma, such drug displacement interactions would have no adverse side-effects. On the other hand, if much of the displaced drug is normally present in the circulation, that is, the apparent volume of distribution is small, the concentration of free drug in the serum and at its receptor site may rise sufficiently after redistribution to increase the intensity of drug action in a clinically important fashion. Gillette (1973) has calculated that the displacement of drugs from plasma proteins will be important when more than 90% of the drug in the blood is bound; only then will the plasma bound fraction represent a significant proportion of the total drug in the body.

The major consequence of a drug displacement interaction is an increase in the free drug concentration leading to an augmentation of the therapeutic response and a possible increase in toxic side-effects. Potentiation of a drug's pharmacologic action is not the only consequence of its partial displacement from plasma proteins; both drug elimination and metabolism may be affected by displacement interactions.

After displaced drug has diffused out of the plasma into the tissue compartment and a new equilibrium distribution established, the total drug concentration in the plasma will be at a new, reduced level. Thus for drugs that are removed from the circulation by active transport mechanisms in the kidney or liver, displacement from plasma proteins decreases the rate at which drug is delivered to the sites of elimination. This can temporarily increase the half-life of a drug.

An elevated free drug level, if it occurs, will also tend to increase the free drug concentration at the sites of metabolism and elimination. For drugs which are removed primarily by glomerular filtration or passive diffusion into hepatic cells, this action results in a higher rate of elimination which is reflected in a shortened half-life. This compensatory mechanism will minimize the expected increase in the therapeutic effect of the displaced drug.

The pharmacokinetic time course of the displacement interaction between two drugs is quite complex. It is determined by the rate and extent to which the interacting drugs accumulate in the body - which is a function of their half-life and dosing schedules - and by the sequence of their administration. If metabolites of one or both drugs also compete for plasma protein binding sites, the interaction becomes even more complicated.

The clinical significance of a drug-drug interaction depends on the magnitude of the change in the concentration of the active species at their sites of pharmacological action and the degree of change that can be tolerated. The latter is determined by the therapeutic index of the drug. The smaller the difference between toxicity and efficacy, the greater the likelihood that a drug interaction will have serious therapeutic consequences.

There are a number of instances when the displacement of one drug by another is likely to be dangerous. When the displacing agent is administered by rapid intravenous injection the concentration of unbound drug could be increased almost instantaneously and thus the richly perfused organs such as the endocrine glands, liver, heart and brain, could be exposed to very high and possibly toxic concentrations of unbound drug during the period of redistribution. Aarons and Rowland (1981) have discussed methods of moderating drug displacement by adjusting the rate and timing of administration of the displacing agent.

If a patient's plasma protein binding is decreased due to drug-drug competition for binding sites, then the monitored total drug level will be lowered. However the corresponding plasma free drug level, and hence the therapeutic effect, are virtually unaltered by the majority of drug displacement interactions. Nonetheless, because drug monitoring is usually concerned with total drug in the plasma, the patient's dosage may be increased in response to the low total concentration; the total body pool of drug will increase and with it both total and free concentrations in the plasma. As most drugs being monitored in patients have a narrow therapeutic range (this is the reason for monitoring), the increase in free concentration after dosage adjustment is likely to give rise to toxicity (D'Arcy and McElnay, 1982).

Another important facet of drug displacement interactions at plasma protein binding sites is the displacing agent may resemble the displaced drug so closely that it also blocks active transport systems in the kidney or drug-metabolizing enzymes in the liver and other organs. Thus, after repeated administration of the drug and the displacing agent, the steady-state level of unbound drug could increase, not because of drug displacement, but because the compensatory elimination mechanism is inhibited (Gillette, 1973).

From the foregoing discussions it is clearly possible to predict which drugs are likely to be involved in clinically important displacement interactions. Such drugs are highly bound to plasma proteins at normal doses, have a small apparent volume of distribution, and display a relatively narrow range of therapeutic concentrations at their sites of action. As few highly bound drugs satisfy the second and third criteria, the proportion which are subject to clinically significant displacement-induced potentiation of their actions is very much smaller than suggested by the many albumin binding interactions that have been demonstrated in vitro.

The coumarin anticoagulants are involved in the most hazardous interactions (Koch-Weser and Sellers, 1976b; Stratton et al, 1982). The most frequently cited cases involve the displacement of warfarin by highly acidic drugs such as phenylbutazone, indomethacin, mefenamic acid, oxyphenylbutazone, trichloroacetic acid and various sulphonamides, leading to an increased anticoagulant effect which may give rise to spontaneous haemorrhage. Further details concerning the pharmacology and pharmacokinetics of warfarin are included in the review by Sawyer (1983). The displacement of the oral hypoglycaemic drug tolbutamide by phenylbutazone and other drugs also has clinical significance since it can result in a sudden hypoglycaemic crisis (Christensen, 1963). Anton (1960) showed that phenylbutazone displaces certain long-acting sulphonamides from serum albumin and thereby enhances their antibacterial action, but the clinical significance of these and other interactions remains in doubt (Koch-Weser and Sellers, 1976b).

Some clinically important drug interactions that are usually attributed simply to changed albumin binding of one or both drugs actually involve other mechanisms as well. D'Arcy and McElnay (1982) suggest that there are probably no major drug interactions in which plasma protein binding displacement alone is the evoking mechanism. Certainly, the interaction between warfarin and phenylbutazone in man is multifactorial (O'Reilly, and Goulart, 1981).

Endogenous, as well as exogenous compounds, can compete with drugs for serum protein binding sites. The displacement of highly bound drugs by fatty acids and other naturally occurring substances may have important implications for the effectiveness or safety of drug therapy. Furthermore, when attention is focused on drugs as displacing agents, competition with endogenous compounds is known to have serious toxicological consequences.

Despite reports in the literature, the involvement of endogenous material in the displacement of drugs from plasma proteins is sometimes overlooked. Tsutsumi et al (1975) have shown that at therapeutic concentrations of diazepam, binding to HSA is inhibited by laurate. Wosilait and Ryan (1979) have demonstrated that the binding of warfarin to HSA is affected in a complex fashion depending on the concentration of free fatty acid. Spector et al (1973) also produced evidence to suggest that changes in free fatty acid concentration within the physiological range alter the binding of certain drugs to serum albumin. The presence of one or more lipid-soluble endogenous binding inhibitors in human plasma can alter the binding characteristics of salicylate (Cham et al 1982).

An example of an extensively studied and important competitive binding effect is the displacement of bilirubin by a number of strongly bound drugs. At a time when premature babies were routinely treated with sulphisoxazole to protect them against infection, it was noted that toxic jaundice and lethal kernicterus were significantly more frequent than in children receiving penicillin (Silverman et al, 1956). Sulphisoxazole can displace bilirubin from serum albumin (Odell, 1959) and following redistribution free bilirubin may enter the brain to give rise to the toxic symptoms. Many studies have since been conducted to examine the effects of other drugs on the displacement of bilirubin from albumin and Lamola and co-workers (1979) have shown that albumin is the major binding protein for bilirubin in whole blood. Salicylate displaces bilirubin from human serum albumin (Brodersen, 1974) and so could also potentiate the risk of bilirubin encephalopathy in jaundiced human neonates. Ahlfors et al (1982) have recently studied this interaction in vivo and make a detailed assessment of its clinical significance.

The hypothesis that free unconjugated bilirubin enters the central nervous system causing subsequent cellular damage has recently been questioned (Ritter et al, 1982; Levine et al, 1982). Levine et al support the alternative hypothesis that kernicterus results from the uptake of albumin bound bilirubin following breakdown of the blood brain barrier. However, this view has been seriously challenged by Wennberg and Ahlfons (1982) and by Odell (1982).

There are other instances when the ability of drugs to displace endogenous ligands has important clinical consequences. It has been suggested that the activity of nonsteroidal anti-inflammatory agents such as phenylbutazone, salicylate and indomethacin may be related to their ability to displace corticosteroids from plasma proteins (Brodie, 1965). McArthur et al (1971) have proposed the view that the antirheumatic activity of certain drugs may be mediated through their ability to displace endogenously plasma protein-bound tryptophan and other small peptides.

So far only plasma protein binding displacement interactions have been discussed; for many compounds, competition for tissue binding sites may be of greater significance. Indeed the ratio of tissue mass to albumin mass is of the order of 100:1. It is also important to recall that displacement can occur from both intravascular and extravascular albumin.

Since the apparent volume of distribution of most drugs far exceeds the plasma volume, the bulk of the total drug pool of the body is in the tissues. Tissue binding displacement will give rise to an increase of free drug in the tissues. The diffusion of free drug into the plasma compartment will produce equilibration of this displaced drug and there will be an increase of both free and bound concentrations in the plasma. As the plasma volume is relatively small for most drugs, the distribution of displaced drug into the plasma will be unable to buffer the impact of the increased pool of free drug in the body. For the majority of drugs, then, tissue binding displacement approximates to a reverse of the effects seen with plasma protein binding displacement.

It is quite possible that a displacing agent may displace a primary drug from both plasma and tissue sites simultaneously. Such an interaction would certainly lead to an increased free drug concentration in the plasma. However, until methods are developed for quantifying tissue binding and displacement, measurements of free and bound levels in plasma must serve as the sole tool for the examination of drug displacement interactions whether they take place in the plasma or in the tissues.

1.2.2 Disease States

The plasma protein binding of drugs has been seen to be an important determinant that can affect the distribution, elimination and pharmacological activity of drugs. The extent of drug plasma protein binding may be altered by changes in protein concentration and distribution, pH, ionic strength and temperature, and by endogenous ligands and metabolic products. In a number of pathological conditions, drug levels may be affected by changes in one or more of these factors. As pointed out by Wandell and Wilcox-Thole (1983), the most life-threatening and clinically complex disease states are frequently those that exhibit the largest variation in protein binding.

An assessment of the effect of diseases on plasma drug levels was compiled by Jusko and Gretch (1976). In a recent review Tillement et al (1978) have examined the pathophysiological mechanisms which modify drug binding to plasma proteins and discussed the pharmacological consequences of a number of disease states. Some further developments will be considered in this section. Piafsky (1980) has summarized the effects of disease-induced changes in the plasma binding of basic drugs. The course of action of a drug is dependent upon the normal functioning of a number of organs which combine to absorb, distribute, metabolise and excrete the drug at a characteristic rate; Wilson and Bromberg (1981) have reviewed the effects of a number of pathological conditions on drug pharmacokinetics.

Hypoalbuminemia is characterized by a decrease in the plasma concentration of albumin. The extent of drug binding depends on the quantity of binding protein available and when this decreases so does the amount of bound drug. The phenomenon is important only for highly bound drugs with a low volume of distribution; these are usually weakly acidic drugs. Hypoalbuminemia is associated with severe stress or altered nutrition as well as with nephrosis, hepatitis, cirrhosis, cancers, gastrointestinal diseases, heart disease and hypothyroidism. Hyperalbuminemia is so rare to be regarded as a result of dehydration (Peters, 1975). Thus, variations in plasma albumin levels are relatively narrow and if significant, almost always in the direction of decreasing concentration.

Basic drugs bind to lipoproteins and α_1-acid glycoprotein as well as to albumin. The former show large fluctuations due to both physiological and pathological conditions α_1-acid glycoprotein, the acute phase protein, is raised above normal in a large number of conditions characterized by physiological stress, in response to inflammation such as seen in rheumatoid arthritis and other diseases, and in malignancy. Associated with these changes in binding protein both increases and decreases in the plasma protein of basic drugs have been recorded.

The distribution of free and protein-bound drug in the body is illustrated in Figure 1.1. Distribution of bound drug clearly follows that of its carrier protein. In the case of albumin, plasma and interstitial fluid contain about 40% and 60% respectively of the total quantity in the body. The succession of equilibria between free and bound drug may be upset in a number of disease states in which there is known to be an increase in the concentration of albumin in the interstitial fluid at the expense of the plasma compartment.

A change of pH is known to alter the protein binding of drugs (Newbould and Kilpatrick, 1960). The organ and tissue selectively of certain drugs may be partly due to pH-dependent differences in unbound concentration. Henry and co-workers (1981) have developed a model for the pH-dependence of drug-protein binding which suggests that acidosis and alkalosis could produce alterations in the duration and intensity of action of a wide variety of drugs.

In some pathalogical conditions the reduced protein binding of drugs may be due to a structural modification of the carrier molecule. The role of physiological inhibitors of drug-protein binding, such as fatty acids and bilirubin, has already been considered: reduced protein binding in disease states may also be due to the existence of pathological binding inhibitors. The identification of the latter in uraemia is the focus of much current research.

Uraemia is associated with a decreased protein binding of weakly acid drugs such as salicylate, warfarin and sulphonamides. The defect is related somewhat to a decrease in serum albumin levels but can not be accounted for by hypoalbuminemia alone (Reidenberg, 1976). Two major hypotheses have been offered to explain the reduced binding in uraemia. The first hypothesis that there may be alterations in the structure of serum proteins in uraemic patients is supported by the differences in amino acid compositions of purified normal and uraemic albumin (Boobis, 1977). The second hypothesis is that certain toxic metabolic products which are normally excreted by the kidneys in healthy individuals, accumulate in renal failure. These compounds would bind to albumin and interfere with the binding of weakly acidic drugs either by direct competition for binding sites or by modifying the protein conformation (Sjoholm et al, 1976; Kober et al, 1979; Bowmer and Lindup, 1982). This theory is supported by the fact that the binding defect is rapidly arrested by renal transplant and by active charcoal treatment of uraemic sera (Grafnetterová et al, 1979). The endogenous metabolites responsible for these binding defects have yet to be recovered. Very recently, however, Lichtenwalner et al (1981) have partially purified and characterized drug binding inhibitors extracted from uraemic sera. When added to normal human serum these compounds were capable of inducing binding defects similar to those seen in uraemia. In addition, Schwertner and Hawthorne (1980) observed a fluorescent material in the serum of patients with chronic renal disease and established that the fluorescence is not attributable to albumin itself but to the binding of certain unidentified species. The chemical characterization of these agents is awaited. Calvo et al (1982) have investigated the binding of sulphisoxazole and diazepam in plasma samples from healthy and uraemic patients in an attempt to establish the effect of the disease on the binding of drugs to two distinct sites on albumin.

While considerable attention has focused on the biochemical characterization of albumin from sufferers of chronic renal failure or uraemia, Itoh et al (1981) have used the fluorescent probe, ANS, to examine the ligand-binding properties of nephrotic albumin.

The binding of acidic drugs is reduced in patients with chronic liver disease (Urien et al, 1981). This finding may be explained only partially by hypoalbuminemia (Jahnchen et al, 1981). Thus endogenous binding inhibitors may also be a factor in the decreased protein binding of drugs in liver disease (Kober et al, 1978).

Although abnormal binding of L-tryptophan has been reported in patients with rheumatoid arthritis (McArthur et al, 1971), Wanwimolruk et al (1982) found that the protein binding of several drugs is unaltered in patients with this disease.

Feely et al (1981) examined the plasma protein binding of propranolol (basic drug) and warfarin (acidic drug) in patients with thyroid disorders. Their results suggest that the binding of both acidic and basic drugs is altered by thyroid disease.

1.2.3 Miscellaneous Factors

There are a number of miscellaneous conditions which can alter the protein binding of drugs. They are included here for completeness and help to put into perspective the significance of plasma protein binding displacement interactions in determining free drug levels.

The plasma protein binding of drugs may be altered in pregnancy (Perucca and Crema, 1982; Perucca et al, 1981). This is hardly surprising because the normal human pregnancy is associated with considerable changes in the concentrations of plasma proteins, free fatty acids and possibly other endogenous substances which interfere with drug binding.

McNamara et al (1980) have reported an apparent effect of tobacco smoking on drug binding to human serum proteins. Adir et al (1982) found that the plasma protein binding of an acidic drug decreased with age but the results could be explained partly by the lower albumin concentrations in elderly subjects. Wood and Wood (1981) have investigated age-related changes in α_1-acid glycoprotein and related these to plasma drug binding in the newborn infant. There may be sex-related differences in the plasma protein binding of certain drugs (Routledge et al, 1981).

As stated previously, the bound drug concentration depends on the quantity of binding protein available. The latter may be dependent on nutritional status (Varma, 1981). Stress, injury, alcohol and the accilimalization to heat are known to decrease albumin production (Rothschild, 1973) and so could lead to a significant increase in free drug blood levels for highly bound drugs. Morrison et al (1979) have shown that the concentrations of a number of serum constituents, including albumin, vary in characteristic patterns during the course of the day. Levels of α_1-acid glycoprotein have been reported to be raised after surgery, resulting in a reduction of the free fraction of basic drugs (Fremstad et al, 1976).

1.3 The Location of Drug Binding Sites in the Blood and Tissues

1.3.1 The Partitioning of Drugs Amongst Blood Components

Before considering molecular aspects of the binding of drugs to plasma proteins, it is worth examining the physiological role of the proteins involved and the relative contributions they make to the binding of drugs in plasma.

Many detailed reviews of the composition, structure and function of the plasma proteins have appeared (Neurath, 1965; Jonas, 1972; Putnam, 1975) consequently only limited aspects will be covered in this section.

Of the hundreds of proteins present in the plasma of healthy individuals only a few are known to be important in the binding of drugs. The best known example is human serum albumin (HSA).

Serum albumin is the most abundant and the most extensively studied protein in the blood. Approximately 60% of the total serum protein is albumin. While other plasma proteins tend to have single, fairly specific functions, albumin appears to have several important physiological roles. It is the principal agent responsible for the osmotic pressure of the blood and hence contributes to the maintenance of the circulating fluid within the vascular system. Albumin has a major role in the binding and transport of long chain fatty acids, and in the binding and detoxification of unconjugated bilirubin. Although albumin binds thyroxine and numerous steroid hormones less tightly than do specific binding proteins, it is present in larger quantities and so acts as a buffer when the primary binding proteins become saturated. Albumin can therefore stabilize the plasma concentrations of hormones and other endogenous ligands. The latter include tryptophan which is the only amino acid bound reversibly to albumin (cysteine is able to bind covalently to the thiol group of the protein), and calcium. The binding of the calcium ion constitutes a weak association but is important physiologically due to the abundance of albumin in the plasma. The minor nutritive role of albumin arises from its availability to cells through pinocytosis: it contributes about 5% of the amino acids used by peripheral tissues. Recent findings suggest that the biological function of albumin may also be associated with the regulation of prostaglandin synthesis in vivo (Saeed et al, 1981).

The physiological importance of serum albumin is reflected in the fact that the concentration of albumin in blood has been used as a major index in health and disease over the years. The normal level of HSA in the serum of healthy adults is 42g/l with a range of 35-50g/l (Peters, 1977). However, a stable serum albumin level depends upon an equilibrium between three processes: distribution, degradation and synthesis.

As mentioned earlier, the albumin of the blood is involved in active exchange with that of the other body fluids. While equilibrium within the vascular pool is rapid, a slow but constant extravascular exchange occurs such that distribution equilibrium between intravascular and extravascular pools is usually achieved in man within 7-10 days. At any one time, however, only about 40% of the exchangeable albumin pool is located in the plasma.

The normal half-life of circulating albumin is approximately 19 days. This corresponds to a daily degradation of 14g. The breakdown of albumin follows first-order kinetics and is probably the result of continual uptake of droplets of circulating plasma into cells by pinocytosis. The free amino acids produced by complete digestion of the protein mix with the amino acid pool of the tissues concerned before entering the circulating pool. However, the factors that regulate the degredation of serum proteins are unknown and no specific organ has been identified which is predominantly responsible for albumin breakdown.

Albumin is synthesized almost exclusively by the liver. Of the many factors influencing albumin synthesis, the most important appears to be adequate nutrition, or more specifically, the supply of amino acids at the sites of synthesis. Albumin production increases very rapidly after each protein-containing meal. Nonetheless, negative feedback processes tend to regulate albumin synthesis. Thus, the circulating albumin level and the colloid osmotic pressure contribute to homeostasis. Albumin synthesis is also affected by the total hormonal balance (Kernoff, 1971). It appears that albumin is synthesized as a precursor form called proalbumin which contains a small additional peptide segment (Quinn et al 1975). Further information on the biosynthesis of albumin is contained in the review by Peters (1977).

Aside from its physiological interactions with numerous endogenous ligands, human serum albumin makes the predominant contribution to the plasma protein binding of drugs and other exogenous ligands including metals (Pedersen, 1981; Perrin, 1982; Lau et al, 1979), surfactants (Sukow et al 1980), dyes (Meyer and Guttman, 1968), insecticides (Fang, 1980) and pesticides (Maliwal and Guthrie, 1983). On the other hand, in cases of severe albumin deficiency such as analbuminemia, other plasma proteins appear to compensate partly for the deficiency by serving a significant transport role for endogenous and exogenous ligands (Frohlich et al, 1981). Nevertheless, Bridges and Wilson (1973) have suggested that with the exception of cytochrome P-450, albumin is probably unique in its capacity for binding ligands of diverse chemical and physical properties. The physiochemical and structural properties of albumin which allow it to bind such a wide range of compounds are reviewed in the next section.

Human serum albumin is clearly not the only circulating plasma protein involved in drug binding. For a certain class of drugs, α_1-acid glycoprotein and not albumin is the major binding protein in plasma. It is also well-known that some drugs can bind to lipoproteins.

α_1-acid glycoprotein (orosomucoid) is a globulin present in normal human plasma. The structure and properties of this protein have been reviewed in detail by Schmid (1975). From this report it is clear that α_1-acid glycoprotein has several features which allow it to be distinguished from the other plasma proteins. For example, it has a very high carbohydrate content amounting to about 55% of its weight. In fact the carbohydrate moiety of α_1-acid glycoprotein accounts for about 10% of the protein bound carbohydrate of normal plasma. α_1-acid glycoprotein exhibits a significant degree of homology with the immunoglobulins. Furthermore, Schmid et al (1973) have shown that there are multiple amino acid substitutions of α_1-acid glycoprotein, a property shared as far as is known only by the immunoglobulins.

α_1-acid glycoprotein is synthesized in the liver and the half-life of this γ-globulin is about 5 days. Plasma levels of α_1-acid glycoprotein are rather low showing a normal mean level of 90mg/100ml with a normal range of 55-140mg/100ml (Putnam, 1975). However, as discussed in Section 1.2.2, α_1-acid glycoprotein is an acute phase reactant and increased blood levels are associated with induced inflammation, pregnancy and various unrelated disease states including cancer, pneumonia and rheumatoid arthritis. In addition, normal individuals who undergo a major operation will also produce an increased plasma concentration of α_1-acid glycoprotein. The physiological role of α_1-acid glycoprotein remains to be elucidated, but the parameter common to the above states, namely cell proliferation, is known to effect an increasing synthesis of α_1-acid glycoprotein in the liver. As this protein has been found to be homologous to the immunoglobulins, it is conceivable that higher concentrations are required to protect the increased cell population. Other observations pertaining to the possible biological function of α_1-acid glycoprotein suggest that it may influence blood clotting, have a minor role in binding some steroids and be involved in the formation of striated collagen.

The plasma lipoproteins constitute an extremely heterogeneous group of compounds and contain variable proportions of lipid, protein and carbohydrate. The protein content varies from as low as 2% in the chylomicrons to a high of only about 50% in the high density lipoprotein (HDL) class.

The lipoproteins are normally separated into classes that are characterized by their flotation rates: chylomicrons, very low density lipoproteins (VLDL), low density lipoproteins (LDL), high density lipoproteins (HDL), and very high density lipoproteins (VHDL). Since the interactions of the lipid and protein components are noncovalent and the classes are heterogeneous, the term molecular weight does not have true meaning. However, the majority of lipoproteins present in serum are in the range 200,000 to 10,000,000 daltons.

The major biological function of circulating lipoproteins is the transport of lipids. The complex lipoprotein system ensures the transport of a remarkably heterogeneous group of lipids which include unesterified fatty acids, mono-, di- and triglycerides, various phospholipids, cholesterol, and other minor components such as hydrocarbons and glycolipids (Scanu et al, 1975). The solubilization of otherwise water unsoluble substances by lipoproteins is the basis of many fundamental metabolic mechanisms occurring in vivo.

Both the liver and intestinal mucosa are capable of serum lipoprotein synthesis. Normal serum lipoprotein concentrations range from about 200 to 700mg/100ml and are influenced by age, sex and diet (Romach et al, 1981).

The α, β and γ globulins are an important group of binding proteins in serum. Several α and β globulin have a high affinity, but relatively low capacity, for a number of endogenous substances and chemically related synthetic compounds. For most drugs though, binding to these proteins is negligible. The metal containing globulins, transferrin and ceruloplasmin interact strongly with iron and copper respectively and have an essential biological function in the transport of these ions. Binding globulins have also been identified for other endogenous compounds including corticosteroids, testosterone, oestradiol, progesterone, thyroxine and several vitamins. The plasma γ globulins probably do not interact significantly with drugs except where they occur as specific antibodies to them.

α -fetoprotein (AFP) is a serum protein made and secreted by the fetal liver and yolk sac of all mammals so far studied. The serum concentration of AFP decreases rapidly during fetal development to a residual level in adulthood but rises again in individuals with hepatomas or germ-cell tumours. Elevation of AFP levels is also observed in a variety of pathological conditions and in certain human fetal malformations such as neural tube defects. The exact function of AFP is unclear, although similar biological and physicochemical properties suggest that it may be the fetal counterpart of adult serum albumin. Recently, Law et al (1981) have shown that the amino acid sequence and primary structure of AFP reveals extensive homology to serum albumin. AFP is known to bind estradiol (Grigorova et al, 1980), but the drug-binding capability of this protein remains to be established; it is a prime candidate for future study.

Having considered the major binding proteins in serum and examined their biological functions it is pertinent to discuss the manner in which bound drugs are distributed between the various serum components.

An appreciation of the ability of albumin to bind a large number of acidic and non-acidic drugs may be obtained from the comprehensive tabular summaries of Meyer and Guttman (1968) and Jusko and Gretch (1976). Numerous studies have demonstrated the high affinity binding of anionic drugs to HSA, and it is generally believed that at therapeutic levels of these drugs, albumin represents the major binding protein in plasma (Tillement et al, 1982). For the majority of drugs therefore, it appears that the binding to serum albumin is quantitatively by far the most important and often accounts for almost the entire drug binding in plasma.

Recently, however, sufficient evidence has accumulated to suggest that the blood binding of basic (cationic) drugs differs from that of acidic compounds; while albumin is the major binding protein for the latter, many basic drugs exhibit only a moderate affinity for albumin and bind more avidly to other blood components such as α_1-acid glycoprotein and lipoproteins (Glasson et al, 1979 Brinkschulte et al, 1981 Romach et al 1981). Meuldermans et al (1982) have considered the possible contribution of red blood cells as well as α_1-acid glycoprotein and lipoproteins to the binding of basic drugs in blood. For cationic drugs the protein bound fraction in plasma is clearly a heterogeneous one.

The widely held belief that albumin can account for almost all the anionic drug binding in plasma has, nonetheless, been challenged somewhat by the recent findings of Urien et al (1982). These authors present evidence for the binding of certain acidic drugs to α_1-acid glycoprotein. Although α_1-acid glycoprotein is present in plasma in far lower concentrations than is human serum albumin, the association constants of some acidic drugs with α_1-acid glycoprotein are high enough to suggest that binding to α_1-acid glycoprotein will contribute significantly to the plasma bound fraction of these drugs (Urien et al, 1982).

Up to now, the binding of drugs to erythrocytes and other cell components appears to have received little attention. The ability of organic bases to penetrate and associate with red blood cells has been known for many years ; more recently it has been shown that a number of basic drugs bind to red blood cell membranes and their contents (Piafsky, 1980). Although the amount of bound drug is usually small, it should not be ignored and on occasion the binding to blood cells can even exceed that to plasma proteins (Ehrnebo et al, 1974).

1.3.2 Binding of Drugs to Tissues and Extravascular Proteins

The binding of drugs to blood components has been extensively studied primarily because the blood is readily accesible to sampling, can be easily separated into its constituent macromolecules, and is amenable to quantitative analysis. Tissue binding studies have none of these advantages and so despite its clinical significance, the binding of drugs to tissue components has received only limited attention. Kurz and Fichtl (1983) have summarized the methodological problems associated with tissue binding studies; this review also covers the current evidence for the binding of drugs to constituents of muscle, kidney, liver and lung tissue.

60 to 65% of the exchangeable albumin pool is located in extraplasma sites, notably in the skin and muscle. Consequently, not only does albumin have a major role in the binding of drugs in the blood, but it is the principle drug binding protein in tissues. However, a number of other substances have been found to be involved with the uptake of drugs by tissues. For example, it appears that drug binding proteins in the cytoplasm of hepatocytes may hasten metabolism by increasing the amount of drug available to the enzymes located towards the centre of the cells. Two hepatic cytoplasmic proteins called Y and Z proteins have been isolated and are known to bind a number of endogenous and exogenous substances. Y protein or ligandin has been shown to be a major determinant of the selective hepatic uptake of a number of small anions and may influence the flux of metabolites from the liver to the plasma or bile. Z protein appears to bind the fluorescent dye ANS (Sugiyama et al, 1980). It is likely that a number of specific and nonspecific cellular binding proteins will be isolated and characterized in the future and this should lead to a better understanding of tissue-binding phenomena.

Many drugs bind to microsomal components, particularly to cytochrome P450 (Bridges and Wilson, 1976). A number of drugs whose structures are planar combine with DNA by intercalation between the base pairs. Dabrowiak (1983) has recently outlined methods which can be used to examine the specificity of drug-DNA interactions and includes a survey of the sequence specifications of several small ligands which interact with DNA. Some planar aromatic drugs are concentrated in the pigmented structures of the eye; melanin is probably responsible for the binding of these drugs. The binding of drugs to lysozyme, one of the major proteins in human tears has been demonstrated by El Nimr et al (1981). Other tissue components which can bind drugs include calcified materials such as bone and teeth.

Kurz and Fichtl (1983) suggest that in general the binding of drugs to tissues is governed by similar mechanisms in all tissue and exhibits a lower degree of specificity than does plasma protein binding.

1.4 Human Serum Albumin and the Nature of its Drug Binding Sites

1.4.1 The Molecular Structure and Physiochemical Properties of HSA

As the simplest plasma protein to prepare in a relatively pure form, albumin has been known for over a century. The term albumin was originally used to designate a group of plasma proteins with certain solubility characteristics. Serum proteins were separated into two fractions, albumin and globulin, according to solubility. With the advent of electrophoresis in the 1940s, it was found that one electrophoretic fraction produced the most conspicuous peak and accounted for at least 95% of the protein in the albumin fraction, whereas globulin turned out to be a highly complex mixture of proteins. The protein of this peak was called serum albumin (or plasma albumin). A detailed historical perspective of the development of methods for isolating and purifying serum albumin is included in the review by Peters (1975).

Although purified preparations of albumin are now widely available, a microheterogeneity is present even in the albumin of a single donor. Polymorphism of a donor population is clearly not the cause. Removal of tightly bound fatty acids decreases but does not eliminate this microheterogeneity. Intramolecular disulphide bond interchange (Sogami et al, 1969) or the modification of circulating molecules such as acetylation of ε-amino groups by aspirin are more likely explanations for the observed heterogeneity. The drug or metabolite induced heterogeneity of albumin produces variants which have been called bisalbumins (Scheurlen, 1955). There is no reason to suspect that the plasma of a normal individual contains albumin species differing in amino acid sequence, although very occasionally inherited albumin variants or alloalbumins have been detected in the serum of clinically healthy subjects (Giuliani et al, 1981). The inherent heterogeneity of albumin preparations and the variation between commercially available samples helps to explain why many aspects of albumin structure remained obscure for so long.

It is now firmly established that albumin is an example of a simple protein, that is, one consisting only of amino acid residues. Albumin alone among the major plasma proteins contains no carbohydrate. Fatty acids that are present are bound tightly but not covalently. The amino acid compositions in terms of residues per molecule of albumin have been determined for several mammalian albumins and show characteristic features. The high levels of glutamic and aspartic acids and lysine are consistent with the polarity of albumins. In comparison to most other proteins the cystine contents are high, whereas tryptophan, methionine, isoleucine and glycine levels are low.

The major impetus for much recent work on albumin stems from the elucidation of the complete amino acid sequences of bovine and human serum albumins. These are the considerable achievements of Brown and co-workers (Brown, 1975; Behrens et al 1975), Meloun and co-workers (Meloun et al, 1975), and others. Minor divergences have existed, but it now seems probable that the final sequence of the human protein is as shown in Figure 1.4. The primary structure deduced from the disulphide bridging pattern was proposed by Brown (1974). The model produces a unique pattern of nine double loops held together by disulphide bridges (Figure 1.4). The existence of the independent double loops was confirmed by the isolation of various peptide fragments without rupturing disulphide bridges.

It has been estimated that the secondary structure of human serum albumin contains 45 to 50% α helix (Sogami and Forster, 1968), about 15% β-pleated sheet (Reed et al, 1975), and the remainder random coil. McLachlan and Walker (1978) on the other hand have calculated probabilities of helix structure throughout the amino acid sequence of albumin and estimate that there is probably 75% or more of helix, and little, if any, β sheet.

The tertiary structure of albumin is also a matter of some conjecture. According to hydrodynamic studies, bovine albumin at pH 5 to 8 is a prolate ellipsoid with major and minor axes of 140 and 40Å. Within this shell the tertiary structure is discernible only by inference, since X-ray crystallographic studies of the configuration of albumin are in their infancy. One can assume that strong associative forces between some of the loops of the peptide chain are responsible for the compact molecule observed at neutral pH. It is also likely that association of the loops forms globular regions or domains. A model showing a linear arrangement of such domains with transverse clefts has been proposed by Anderson and Weber (1969) in order to satisfy their observations on the polarity of the fluorescence of complexes with ANS.

Peters (1975) has discussed the grouping of the double loops of the albumin peptide chain into domains. Arrangements are of necessity based on the rapid cleavage of the connecting link, 3-4, by trypsin and

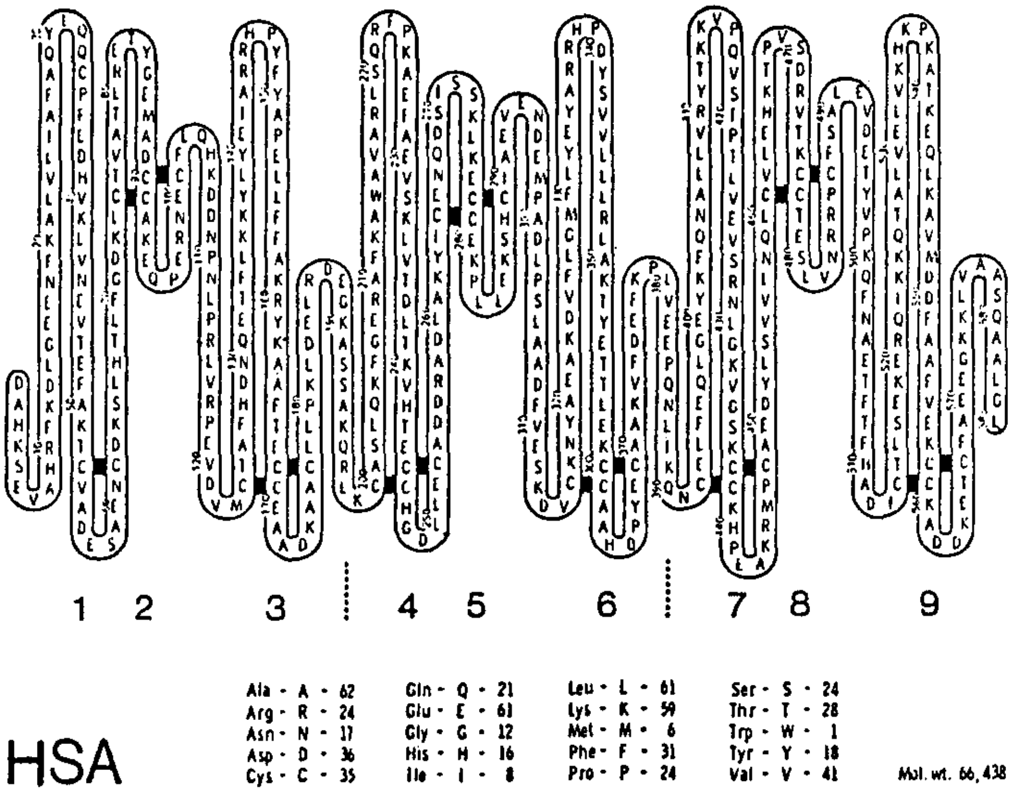
1
2
3
4
5
6
7
8
9
HSA
Ala - A - 62
Arg - R - 24
Asn - N - 17
Asp - D - 36
Cys - C - 35
Gln - Q - 21
Glu - E - 61
Gly - G - 12
His - H - 16
Ile - I - 8
Leu - L - 61
Lys - K - 59
Met - M - 6
Phe - F - 31
Pro - P - 24
Ser - S - 24
Thr - T - 28
Trp - W - 1
Tyr - Y - 18
Val - V - 41
Mol. wt. 66,438

FIGURE 1.4 Amino Acid Sequence and 9-Double-loop Structure of Human Serum Albumin

Dotted lines signify a possible arrangement of the double loops of the peptide chain into domains.

by pepsin, and on the fact that loops 3 and 4 each have a net positive charge which would tend to repel one from the other. Loops 7-8-9 are suggested as a second domain; the long connecting link 6-7 is particularly susceptible to attack by both trysin and pepsin, and loop 7-8-9 can be isolated as an intact fragment which retains a fatty acid-binding site. The split between loop 6 and loop 5 rests on more tentative evidence - the high net negative charges of loops 5 and 6 and the cleavage of link 5-6 by pepsin at pH 3.7 and subtilisin at pH 9 in the presence of a denaturant. Under these conditions changes in charge distribution may have altered the protein structure. The final, tentative subdivision of the molecule is into domains of loops 1-2-3, 4-5, 6 and 7-8-9; the division between 4-5 and 6 is the least clearly defined of the three.

Brown (1978) has put forward a slightly different model for the tertiary structure of albumin. In this case the albumin molecule is seen as consisting of three linearly arranged globular elements, or domains, of loops 1-2-3, 4-5-6, and 7-8-9. The strong homologies in the amino acid sequences of these domains has led Brown to propose that they form similar three-dimensional folding-patterns. It is suggested that each domain consists of six α-helices (three double loops) forming a cylindrical structure; the albumin molecule is then visualized as an association of the three cylindrical domains. The suggestion that albumin is composed of three domains is supported by low angle X-ray scattering studies (Bloomfield, 1966).

Other mammalian species and lower animals have proteins with similar structures and properties to those of HSA. The amino acid compositions of mammalian albumins exhibit many common features and these proteins tend to cross react serologically. Immunochemical relationships have helped to define evolutionary differences; work on the phylogenetic origins of albumin has been reviewed by Peters (1975). The repeating double loop structure of albumin and the presence of recurrent amino acid sequences in the different loops has led to proposed evolutionary pathways for albumins. (McLachlan and Walker, 1977). It appears that the modern protein probably descended from a primative albumin consisting of a single double-loop structure by a train of gene duplication and depletion.

Despite their probable common ancestry, albumins from different species have been found to exhibit marked variations in their capacities for binding drugs (Genazzani and Pagnini, 1963; Seller et al, 1977).

Albumin has been a model protein for physical chemists. A selection of the most important physiochemical data has been tabulated by Peters (1975). Steinhardt et al (1971) have reviewed the major differences between the physical, chemical and spectroscopic properties of bovine and human serum albumins. It is possible to reconcile many of the properties of albumin with its amino acid sequence and structure.

Albumin is characterized by its high solubility, total charge, net negative charge, stability and flexibility, and by its ability to bind a diverse range of endogenous and exogenous ligands. The flexibility or 'conformational adaptability' of the albumin molecule can be explained by the proposed loop-link pattern of Figure 1.4.

The more than 200 positive and negative charges distributed over the molecule give albumin a hydrophilic character and contribute to its high solubility in aqueous media. The titration curve in the pH range 2-12 can be closely reconstructed as a composite of the ionizable groups of the constituent amino acid residues. Albumin is a strong buffer at pH 4 and pH 10 but a weak buffer at pH 7. The isoionic point of HSA is near pH 5.2 and is close to the pH at which all basic groups are protonated and carboxyl groups are still negatively charged. Hence the isoionic point of albumin is also the pH of maximum total charge with about 100 positive and 100 negative charges. At plasma pH 7.4 albumin has a net negative charge of 18 but, as discussed in the next section, it can nevertheless interact strongly at this pH with anions as well as cations.

In the pH range from 2 to 4, ultracentrifugation, viscosity and diffusion measurements indicate that the albumin molecule expands, becoming larger and more asymmetric. The helical structure decreases (Wallevik, 1973) and the molecule unfolds so that interior regions become accessible; about 150 additional hydrogen atoms exchange D_2O and more tyrosine residues become exposed to the solvent. With exposure of hydrophobic regions, the molecule becomes less soluble in aqueous solutions.

The hydrogen-ion dependent transitions in the acid pH range can be divided into two regions, the exact limits being contingent upon temperature (Wallevik, 1973). The major reversible change in the conformation of the albumin molecule which occurs between pH 3.8 and 5.0 has been attributed by Foster (1960) to a transition from a normal or N form to a species with faster electrophoretic mobility called the F-form. The normal-fast, or N-F, transition represents an unfolding of the albumin molecule as the pH is reduced. The second stage of the transition is the acid expansion which occurs between pH 2.6 and 3.8. From about pH 2.0 to 2.6 the albumin conformation is independent of pH and corresponds to the acid-expanded form of the molecule. The expansion of albumin in acid probably begins as a separation of domains such as those described above.

The full expansion of the molecule in highly acidic media can be pictured as a dissociation of individual loops of the peptide chain into a long viscous molecule.

In the region of pH from 5 to 7 the albumin molecule does not seem to undergo major changes of conformation. A limited change, the neutral-base, or N-B, transformation takes place about pH 7 to 8 and is characterized by a small net loss of α helical structure (Wallevik, 1973). Kremer et al (1982) have described the effect of the N-B transition on the kinetics of the binding of warfarin to human serum albumin.

On the alkaline side of neutrality, beginning about pH 9, a less well-characterized isomerization has been detected by electrophoresis. A slow process of aging takes place when albumin is stored in mildly alkaline solutions resulting in the A form (Nickel and Foster, 1971). The process is probably a rearrangement of intramolecular disulphide bonds, catalysed by the single, free sulphydryl group of the protein (Stroupe and Foster, 1973). A more extensive unfolding of the albumin molecule takes place in a narrow interval of pH between 11.2 and 12.0.

In contrast to the pH-dependent transitions of HSA, the thermal unfolding of albumin appears to involve broad, continuous transitions with no detectable intermediate stages. Thermal transitions may represent the sum of simultaneous but more or less independent unfoldings of different regions of the molecule (Wallevik, 1973).

The spectroscopic properties of albumin have been examined in detail by a number of authors (Steinhardt et al, 1971; Longworth, 1981; Waldmeyer et al, 1982) and Dale (1975) has reviewed the more general aspects of protein luminescence. Ultraviolet absorption spectra of albumins are quantitatively similar to those of other simple proteins, but the absorption near 280nm is lower due to the low tryptophan content of albumins. Human albumin with one tryptophan has an absorptivity about 20% less than that of bovine albumin which has two. If albumin is excited at about 280nm, the fluorescence contains contributions from both tyrosine and tryptophan residues. The tryptophan fluorescence originates not only from direct excitation by the incident radiation but also from tryptophan residues which have been excited by radiationless energy transfer from tyrosine side chains. However, if the exciting wavelength is increased to between 295nm and 305nm, all of the tryptophan emission is the result of direct excitation by the incident radiation; under these conditions tyrosine does not absorb radiation and so neither emits nor transfers energy.

The structural and physiochemical properties of HSA underline its unique ability to bind and transport a diverse range of small molecules. Changes induced in the physical and chemical properties of albumin by the binding of small molecules provide a means for studying ligand-albumin interactions. Current theories concerning the major drug-binding sites on HSA are considered in the next section and experimental methods are reviewed in Section 1.5.

1.4.2 The Location of the Major Drug-Binding Sites of HSA

Literally hundreds of in vitro studies have supplied information on the binding of drugs to human serum albumin. The purpose of this review is to examine the methodolgies employed, and to highlight some of the more recent attempts to rationalize the accumulated data in terms of the binding process at the molecular level.

It is now generally accepted that there are only a small number of high affinity drug-binding sites on HSA (Meyer and Guttman, 1968). Many drugs appear to compete for common sites on the albumin molecule and much recent work has been concerned with the identification and classification of the specific drug binding sites.

Two specific sites for acidic drugs have been characterized using fluorescent probe techniques by Sudlow et al (1975) and were designated sites I and II. Site I is the warfarin binding site, and warfarin and 5-dimethylaminonaphthalene 1 sulphonamide (DNSA) were used as selective fluorescent probes for this binding site. Site II was labelled with the fluorescent probe dansylsarcosine. By observing the competitive displacement of these fluorescent probes, Sudlow et al (1975) were able to associate a number of drugs with either one or both of the specific binding sites on HSA.

In a similar manner Müller and Wollert (1975) used tritiated L-tryptophan as a marker for a single binding site on human serum albumin.

Sudlow et al (1975) gave some evidence for a third drug-binding site on HSA but could not find a specific ligand for it. Sjöholm et al (1979) used warfarin and diazepam as markers for two specific drug-binding sites and proposed that digitoxin binds to a third high affinity site on albumin.

Goya et al (1982) have synthesized a fluorescent probe which is displaced from its primary binding site on HSA by digitoxin. Furthermore, site I and site II drugs on the basis of Sudlow's classification do not significantly displace the fluorescent probe. The results of Goya et al

(1982) clearly support the suggestion of Sjöholm et al (1979) that the digitoxin binding site is independent of the drug binding sites I and II.

Wanwimolruk and Birkett (1982) have demonstrated that the N-B transition of albumin provides a further distinction between site I and site II binding characteristics. The N-B transition of HSA involves a change in conformation at site I which results in the increased binding of drugs and fluorescent probes at this site, whereas there is no corresponding effect on acidic drug binding at site II.

On the other hand, Bruderlein and Bernstein (1979) suggest that the distinctions between sites I and II are not clear-cut. They used the fluorescent probes DNSA and dansylsarcosine to investigate the location of the L-tryptophan receptor site on HSA in relation to the established drug binding sites I and II. Their observation that L-tryptophan has a single binding site on albumin but displaced both probes in an apparently competitive fashion led them to conclude that sites I and II may be overlapping.

Based on a comprehensive survey of competitive binding results in the literature, Kragh-Hansen (1981) has proposed that there are at least six binding regions on the albumin molecule. A summary of the proposal is given in Table 1.1. It is suggested that binding region numbers 1, 4 and probably 5 are very specific, whereas binding regions numbers 2, 3 and 6 seem to be less specific and capable of high-affinity interactions with several different ligands. Although only one of these binding regions has been allocated to drugs, the author concedes that there are probably other important drug binding sites on the albumin molecule. However, in this review (Kragh-Hansen, 1981) and in a subsequent paper (Kragh-Hansen, 1983), caution is stressed in the interpretation of competitive binding results. For example, before assignment of the high-affinity binding sites of two different ligands to the same binding region of the protein, it is essential to determine whether an apparent decrease in the binding of one of the ligands,caused by the simultaneous addition of the other ligand, is the result of direct competition or of some other effect: the latter may arise when conformational changes of the drug-albumin complex are induced by the binding of the second ligand to another region of the protein, or when, in a fluorimetric study, the fluorescence of a probe molecule is reduced through energy transfer to a second bound ligand. (Some further modulatory effects are considered later). Another complicating factor is that ligands are usually bound not only to one or two high affinity sites but to a greater number of low affinity binding sites.

Binding Region or Site	Ligand Bound With High Affinity
1	Long chain fatty acids
2	L-thyroxine L- and D-tryptophan Octanoate Chlorazepate p-iodobenzoate Chloride ion
3	Bilirubin Certain dyes (eg. phenolsulphonphthalein dyes) Iopanoate
4	Cu^{2+} and Ni^{2+} ions
5	Haemin
6	Salicylate Sulphaethidole Sulphathiazole Chlorpropamide Tolbutamide Indomethacin

TABLE 1.1 A Scheme for Binding Regions Located on Serum Albumin (From Kragh - Hansen, 1981;1983).

An important aspect of the characterization of specific binding sites on HSA is the identification of the amino acid residues which line the binding regions. This information is useful in testing the validity of the common site models derived from competitive binding studies, and leads to a better understanding of the structural requirements for the binding of ligands to specific regions of the albumin molecule.

A recognized approach is to modify certain amino acid residues of the protein by reactive compounds and to compare the ligand binding properties of the modified and native albumin. Such studies can be supplemented by a sequence analysis to determine the position of the covalently attached modifier. Unfortunately, there are a number of inherent difficulties in the chemical modification technique. The reagent is seldom specific and so more than one kind of amino acid residue may be modified. Conformational changes are often induced in the protein molecule during the labelling procedure, although these can be minimized by a careful control of the experimental conditions. A specific labelling of the hydrophobic amino acids of albumin (except for tryptophanyl and cysteinyl) has not been achieved but a knowledge of the amino acid sequence of the molecule may permit an assignment of the identity and positions of the hydrophobic residues in the vicinity of the binding regions. Since the finding that acetylsalicylic acid specifically acetylates only one lysine of HSA (Hawkins et al, 1968), many other amino acids of HSA have been more or less specifically modified, for example, the lone tryptophan residue (Fehske et al, 1978), the lone cysteine residue (Walker, 1976), the highly reactive tyrosine residue (Fehske et al, 1979) and lysine, histidine and arginine residues sensitive to different reagents. The binding of site specific ligands to the modified albumin derivatives clearly indicates whether or not the modified amino acid residues participate in the binding sites.

Another approach is to cleave the albumin molecule into definite fragments using reagents such as cyanogen bromide, trypsin and pepsin. The binding of drugs to isolated fragments has been used to localize specific binding sites. Again, however, the secondary and tertiary structure of the fragments may differ from that of the same sequence in the native protein. Thus, it can be difficult to decide whether the failure to find binding to a particular fragment depends on the location of the binding site in another part of the molecule or on the destruction of the binding site due to conformational changes in the fragment under investigation.

Perhaps the most advanced approach to localize a binding site might be to synthesize peptide analogues. Lakusta and Sarkar (1979) and Sankaranarayana Iyer et al (1978) have achieved this for the divalent metal ion binding site which is located at the amino terminus of HSA. As yet, no drug-binding sites have been constructed in this way.

Despite the difficulties, biochemical techniques such as those outlined above, have supplied useful information on the structure and amino acid composition of drug-binding sites on HSA, and on the location of these sites within the secondary and tertiary structure of the protein. Much of the recent work has been summarized by Fehske et al (1981).

Probably the best characterized binding site of HSA is the indole and benzodiazepine binding site (Müller and Wollert, 1979) called site II by Sudlow et al (1975). This site binds several indole derivatives and benzodiazepines with a high degree of structural specificity. The interaction of tryptophan with HSA is an outstanding example of stereospecific binding. Specific markers for this site are L-tryptophan (Müller and Wollert, 1975), diazepam (Sjöholm et al, 1979), dansylsarcosine (Sudlow et al, 1975) and iopanoic acid (Mudge et al, 1978). Many other drugs of very different chemical structures also bind to the indole and benzodiazepine binding site with high affinity (Sjöholm et al, 1979).

Contradictory evidence exists for the localization of this specific binding site within the HSA molecule and for the amino acids involved. Since hydrophobic forces seem to be important for the binding of indoles and benzodiazepines, participation of lipophilic amino acid residues is very likely. Among the three lipophilic aromatic amino acid residues tryptophan, tyrosine and phenylalanine, the lone tryptophan residue was, until relatively recently, the most likely candidate as an important part of the indole binding site of HSA (Gambhir and McMenamy, 1973 Swaney and Klotz, 1970). However, using a specific modification by 2-hydroxy-5 nitrobenzlbromide, Fehske et al (1978) have demonstrated that the lone tryptophan of HSA is not directly involved in the indole and benzodiazepine binding site.

Fragments of HSA have been investigated with respect to the position of the indole binding site. The major locus for the indole binding site in HSA occurs in cyanogen bromide fragment C (residues 124-298) as concluded from the binding of L-tryptophan and diazepam (Gambhir and McMenamy, 1973 Sjöholm and Ljungstedt, 1973). Part of the binding site may also be located in fragment A (residues 299-585) which binds both marker ligands, although to a much smaller extent than fragment C. The third major cyanogen bromide fragment, called fragment B (residues 1-123) does not bind L-tryptophan and diazepam.

Within fragment C, His 146 and Lys 194 have been shown to be involved in the specific indole and benzodiazepine binding to HSA (Roosdorp et al, 1977) the most important is probably Arg 145 (Fehske, 1981). It is interesting to note that the amino acid sequence in the vicinity of His 146 and Arg 145 contains lipophilic residues (Tyr 138, 140, 148, 150) and cationic charged residues, which provides a favourable environment for the binding of small organic anions.

Employing a selective chemical modification procedure, Fehske et al (1979) tested the hypothesis that tyrosine residues participate in the specific indole binding site. A single highly reactive tyrosine residue of HSA was shown to be part of the indole and benzodiazepine binding site. Although the authors suggested that the highly reactive residue could be one of the four tyrosines in the vicinity of Arg 145, it is now established that this tyrosine is Tyr 411 (Means and Wu, 1979 Fehske et al, 1980) and so located within fragment A not fragment C. Sjödin et al (1977) isolated a trypsin-resistant fragment of HSA (residues 182-585) which retained diazepam binding properties. The highly reactive tyrosine (Tyr 411) and Lys 194 are located within this fragment, but His 141 and Arg 145 are not.

The data are definitely not consistent with previous assumptions that the indole and benzodiazepine binding sites can be located on a single amino acid sequence of the HSA primary structure. Rather it seems that sequences and amino acid residues of very different parts of the albumin primary structure are involved in this site. This is an agreement with the original hypothesis of Gambhir and McMenamy, 1973 that the indole binding site is located between fragments A and C as they exist in native albumin. Accordingly, the indole and benzodiazepine site must be finally formed by the HSA tertiary structure.

The location of the warfarin binding site,or site I of HSA is, probably less well-defined than that of the indole and benzodiazepine binding site. From the work of Sjohölm and Ljungstedt (1973), at least one part of the warfarin binding site seems to be located in fragment C (residues 124-298). The only amino acid residue clearly involved in the warfarin binding site is the lone tryptophan residue of HSA, trp 213 (Swaney and Klotz, 1970). The amino acid sequence in the neighbourhood of the lone tryptophan is striking in having a cluster of apolar residues. Ala-Trp-Ala-Val-Ala, bracketed by two cationic residues, Lys and Arg. Swaney and Klotz (1970) suggest that this is a particularly appropriate environment for interactions with a small organic anion.

Modification of the lone tryptophan residue by two different reagents has been shown to reduce the binding of warfarin to its specific high-affinity binding site on HSA (Fehske et al, 1979), while the modification of tyrosine residues has very little effect. The location of the tryptophan residue within the warfarin binding site has also been demonstrated by spectroscopic measurements (Chignell, 1970).

In large contrast to the above findings are recent observations that the tryptophan modification does not affect the binding of phenylbutazone and azopropazone even though both of these drugs readily displace warfarin from its albumin binding sites. These observations have led Fehske et al (1982) to propose that the warfarin binding site is actually a larger binding area consisting of the overlapping subsites of warfarin and azopropazone. The lone tryptophan residue of HSA, previously established as part of the warfarin binding site, could be located in the non-overlapping part of the warfarin subsite so that its modification affects only the binding of drugs to the warfarin and not to the azopropazone subsite of this large binding area. In general, it appears that drugs interacting with one of the two subsites will displace drugs bound to the other subsite, although the degree of displacement for both subsites may vary considerably.

Unfortunately the role of the tryptophan residue of human serum albumin is still not resolved. The latest work in this field (Sakamoto et al, 1983) suggests that the tryptophan residue of HSA lies in or near the indole and benzodiazepine binding site and not in the primary binding site of warfarin and phenylbutazone. These findings are clearly at odds with those of Fehske and colleagues (1978 and 1982).

The third specific drug binding site of HSA is the digitoxin binding site which is clearly independent of both sites I and II and binds only very few drugs (Sjöholm et al, 1979). Little information is available about the location of this site. Neither the lone tryptophan nor the highly reactive tyrosine seem to be involved, although the modification of 9 out of 18 tyrosine residues strongly reduces the binding of digitoxin to this site (Fehske et al, 1981).

Although fatty acids are not drugs, a discussion of the fatty acid binding site will be included in this section; there is evidence to suggest that their binding is associated with a reduced or enhanced binding of drugs to HSA through both competitive displacement and allosteric mechanisms. However, the relationship of the fatty acid binding site to other specific binding sites on HSA is still not clear.

Many observations have contributed to the assertion that serum albumin binds long and medium chain fatty acids at different sites (Kragh-Hansen, 1981). Demarkations seem to exist between unbranched fatty acids of 10 carbon atoms or less and those of 12 carbon atoms or more. Soltys and Hsia (1978) used a spin label probe for the bilirubin site and showed that fatty acids of chain length less than 10 carbon atoms competively displace the spin label from albumin while fatty acids of longer chain length enhance the binding of the label allosterically. These results support the hypothesis that serum albumin has two distinct sets of endogenous binding sites for fatty acids of different chain lengths. This phenomenon is of additional interest because fatty acids of different chain length appear to have different effects on the binding of drugs to HSA.

Experimental evidence suggests that the high affinity binding site of long chain fatty acids is not identical with the binding sites of other organic ligands, but that long chain fatty acids can profoundly influence other ligand binding sites on the albumin molecule via allosteric mechanisms. Chakrabarti (1978) chose oleic acid as a representative long chain fatty acid and demonstrated a cooperative interaction between warfarin and the oleate ion for albumin binding. Similarly for site II, the other major drug binding site of albumin, Sjödin (1977) concludes that the displacement of bound diazepam by oleic acid occurs primarily through an allosteric mechanism. In contrast, Tstutsumi et al (1975) studied the binding of a benzodiazepine derivative to HSA in the presence of rather high molar concentrations of laurate over HSA and found a significant inhibitory effect on the binding which they suggested was competitive.

Clearly different from the high affinity binding site of long chain fatty acids is the high affinity binding site for medium chain fatty acids. The primary binding site of fatty acids with 10 or fewer carbon atoms seems to be identical with the indole and benzodiazepine binding site of HSA (Koh and Means, 1979 Sollene and Means, 1979). 5-(dimethyl-amino)naphthalene-1-sulphonic acid may be a useful fluorescent probe of the medium chain fatty acid binding site of serum albumins (Doody et al, 1982).

Brown et al (1982) have recently presented evidence for the existence of distinct albumin binding sites for short chain fatty acids (7 or less carbon atoms) and medium chain fatty acids (8 or more carbon atoms). Moreover, from these preliminary results it appears that the short chain fatty acid site may lie in the same region as the warfarin/

azopropazone binding area of HSA.

Bilirubin is not a drug but it binds strongly to HSA and merits discussion because of its clinical importance (Brodersen, 1979). Although bilirubin has been shown to bind to a number of different fragments of HSA the evidence for the location of the high affinity binding site is contradictory. While the bilirubin binding site is clearly independent of the diazepam binding site of HSA, that is, site II (Roosdorp et al, 1977 ; Brodersen et al, 1977), its relation to the warfarin binding site is not fully understood. Bilirubin reduces the binding of many drugs typical of the warfarin binding site (Sjöholm et al, 1979) but modification of the lone tryptophan of HSA does not affect the binding of bilirubin (Jacobsen, 1972).

While important progress has been made recently concerning the possible location of the major ligand binding sites of the albumin molecule, the only site which is fully characterized is the metal ion binding site at the N-terminal end of the protein. For all other ligand binding sites the complete structure and location are not yet known. One reason why this is so may be related to the increasing evidence which suggests that quite different parts of the albumin primary structure are involved in the binding of organic ligands. Thus, it is questionable whether binding sites can be located only within one fragment of the HSA amino acid sequence. A more complete characterization of binding sites may well depend upon a better knowledge of the albumin tertiary structure. A second reason for the lack of knowledge about the location of albumin drug binding sites may be that some of the binding sites consist of several subsites. The expression 'binding area' (Fehske et al, 1981) might be a better term for this type of binding site. The structure and location of the drug binding sites of HSA may therefore be more complicated than previously believed.

1.4.3 Binding Forces, Structural Requirements and Theoretical Aspects of the Binding of Drugs to HSA

A fundamental question concerning drug-albumin interactions is the nature of the binding forces involved. The fact that anionic drugs are preferentially bound to HSA suggests some form of electrostatic interaction, and at one time the binding of drugs to albumin was attributed to a simple electrostatic interaction between the ionic form of the drug and a charged group on the protein. More recent work suggests that while the initial attraction and specificity of orientation of a drug molecule towards its binding site on albumin may be an electrostatic interaction, it is probably reinforced by hydrophobic, van der Waals and hydrogen-bonding.

Hansch et al (1965) examined the binding of a large number of compounds to bovine serum albumin and analysed the data in terms of the partition coefficients of the compounds between octanol and water. The authors of this much-cited study concluded that the binding was rather nonspecific and was best described as being due to hydrophobic bonding.

Several attempts have been made to correlate the binding strengths of structurally related sulphonamides with their physiochemical properties. These and similar studies have aimed to uncover the nature and relative contributions of the binding forces involved in drug-albumin interactions and to illustrate the relationship between structural features and binding affinities. In an early study of the binding of sulphonamide drugs to bovine serum albumin, Moriguichi et al (1968) concluded that electrostatic forces dominate in the binding of acidic compounds to albumin. Ågren et al (1971), on the other hand, demonstrated a direct correlation between the lipophilicity and albumin binding of 13 sulphonamides to HSA. Hsu et al (1974) investigated the binding of 11 sulphonamide and 7 penicillin derivatives and showed that the binding affinities of these drugs were greatly affected by their side-chain substituents: the binding was enhanced by hydrophobic substituents and decreased by hydrophilic substituents on the parent molecule.

Studies have been performed with other classes of drug and many are discussed in the papers by Bridges and Wilson (1976) and Jusko and Gretch (1976). Since these reviews, Wojcikowski and Szlabowicz (1977) and Goto et al (1978) have shown that hydrophobic and, to a somewhat lesser degree, electrostatic forces are involved in the binding of sulphonylurea derivatives to HSA; Judis (1982) has demonstrated that the binding of phenol compounds to albumin primarily involves hydrophobic bonds, while Otagiri et al (1978) suggest that the binding of four anionic drugs to HSA includes considerable contributions from van der Waals forces and hydrogen-bonds. Whereas the view that most of the energy of drug-albumin interactions is due to hydrophobic forces may be receiving increasing support, the above studies illustrate the problem of data interpretation when more than one potential binding force is involved. A recognised complication is that estimations of the thermodynamic contributions of hydrophobic groups to form a drug-protein complex may sometimes be obscured by the simultaneous contribution of the protein molecule due to 'conformational adaptivity' (see later). Thus, the relative contributions of electrostatic, hydrophobic and other forces to the binding process is still not fully established.

Similarly, it is not possible to make accurate predictions about the albumin properties of a drug simply from a knowledge of its structure. However, based on a diverse range of drugs some rough guidelines for the effects of substituents on drug-protein binding constants may be discerned. These have been summarized by Bridges and Wilson (1976) and include the rule that substituents which cause an enhancement of hydrophobicity tend to increase binding. Since many drugs are small, aliphatic anions, the carboxylic fatty acids have been frequently used in albumin binding studies as they provide a convenient homologous series of ligands with similar charge but varying chain length and lipophilicity. Indeed chain length and hydrophobicity have been suggested as important determinants of ligand-albumin binding (Bird and Marshall, 1967). Structure-activity studies have shown linear relationships between lipophilicity (octanol/water partition) and albumin binding affinity for various ligands including the fatty acids (Hansch, 1968). However, the chain length of unbranched fatty acids appears to affect the location of binding to the albumin molecule (Brown et al, 1982) and so binding affinity is not simply related to lipophilicity.

The particular structural parameters which determine the selectivity of drugs for the major drug binding sites on HSA are not yet known. Some drugs (dicoumarol, indomethacin, tolbutamide, ethacrynic acid) can bind to both sites I and II, and in certain cases apparently very small changes in the chemical structure of drugs can dramatically alter the site selectivity (Mudge et al, 1978). Nonetheless, Bruderlein and Bernstein (1979) have designated structural requirements for binding at each site. Drugs which bind to site II are all aromatic carboxylic acids which are largely ionized at physiological pH. The net negative charge is located on the COO^- group, away from the nonpolar region. Drugs which bind to site I are also all aromatic acids with a delocalized negative charge generally at the centre of a large nonpolar molecule.

Large numbers of different ligands can bind to albumin, but the binding is clearly not nonspecific. As already mentioned, the substitution of ligands with relatively simple groups can cause profound changes in their binding properties. For example, iopanoate and iophenoxate, which differ only by the former having an amino group and the latter a hydroxyl group, are bound to different high affinity binding sites of HSA (Mudge et al, 1978). In some cases ligand binding to albumin is stereospecific. D-tryptophan binds to HSA with a binding constant about 100-fold lower than that of L-tryptophan (McMenamy and Oncley, 1958). On the other hand, the affinities of d- and l- warfarin are very much alike (Brown et al, 1977). Finally, isomeric compounds may not only have different affinities for binding albumin but may even bind to separate sites (Kragh-Hansen, 1981).

The evidence presented in the previous section shows categorically that the actual number of high affinity binding sites of the HSA molecule is rather small. In fact only three major drug binding sites have been identified and one of these binds only a very limited number of compounds. Site I and site II, on the other hand, are able to bind many drugs of very different chemical and parmacological properties. The capacity to accommodate a wide range of structural forms must be reconciled with the almost receptor-like specificity and even sterospecificity exhibited by these binding sites. The explanation for this apparent discrepancy may be the conformational adaptivity of the albumin binding sites.

There is now increasing evidence that the binding of ligands to HSA may induce small conformational changes in the environment of the binding sites (Müller and Wollert, 1979). The N-B transition is a well known pH-dependent conformational change in bovine and human serum albumins and may be affected by the binding of ions such as Cl^-, Ca^{2+} and Mg^{2+} as well as H^+ (Van der Geisen and Wilting, 1983). Warfarin which has a much higher affinity for the B than for the N form can shift the conformational equilibrium of albumin to the B state (Janssen et al, 1981). Ligands may therefore induce conformational changes in the albumin tertiary and quaternary structures. Lassman and Reitbrock (1982) suggest that the observed conformational changes in the HSA molecule after the binding of warfarin may be a necessary process in achieving the high affinity of albumin towards anionic drugs. In a study of the binding of a series of long chain fatty acids to HSA, Ashbrook et al (1975) concluded that the selectivity that albumin contributes to the binding process may be due to varying degrees of conformational adaptivity of its binding site as the fatty acid increases in length. The reasons why the binding sites of HSA can adapt in some cases but not in others (for example, the enantiomers of tryptophan) ~~is~~ are not known. The increased stability of the albumin molecule when ligands are reversibly bound to it may be due to some conformational change of the protein (Gumpen et al, 1979).

Cooperative and antagonistic binding of ligands to albumin are other manifestations of ligand-induced conformational changes. Weber (1975) has speculated that non-competitive mechanisms may more often be the rule than the exception in ligand-protein interactions. Madsen and Ellis (1981) have recently proposed a cooperative mechanism for the displacement interaction between warfarin and phenylbutazone and suggest that a cooperative viewpoint of displacement phenomena will provide a more stable framework for further understanding than continuing amendments to the common-site model.

The concept of conformational adaptivity of the albumin sites may parallel the allosteric transition theories of enzyme-activity modification (Koshland, 1958; Monod et al, 1963) and the mode of antigen-antibody interactions (Roitt, 1979). In order to account for its binding to a wide range of compounds though, a high, if not unique, conformational adaptivity must be attributed to HSA.

Isotope exchange experiments reveal that proteins in solution are not static structures but molecules changing between different conformational states. The rates at which hydrogen atoms in the protein exchange with those in aqueous solution depend upon their location in the molecule. Hydrogens on the protein surface readily exchange with deuterium in the solvent whereas hydrogens buried in the protein cannot exchange unless contact with the solvent is established. Such contact can only be brought about by relatively large-amplitude fluctuations, or 'breathing', of parts of the protein. There is evidence to show that albumin is able to change conformation by both large and small amplitude motions (Kragh-Hansen, 1981). Moreover, hydrogen exchange measurements support the view that serum albumin is able to change conformation more readily than other proteins which do not share its ability to bind ligands with a high affinity.

The existence of various conformational fluctuations of albumin with time constants differing by several orders of magnitude has been demonstrated (Kragh-Hansen, 1981). The large-amplitude motions probably occur at or close to the protein surface and may play an important role in ligand binding. However, many details of the conformational changes are unknown.

Two theories have been proposed to explain the influence of ligand binding on the conformation of albumin. Firstly, albumin in solution may be envisaged not as a system of identical molecules but as a collection of isomeric proteins of approximately equal energy in thermal equilibrium with each other (Karush, 1950). Addition of a ligand to the protein solution produces a preferential interaction between the ligand and the isomeric form of albumin which results in the most stable complex. This may be understood in terms of the symmetry or two-site model of Monod et al (1965) which was used to explain the activation of enzymes by small molecules and required the existence of protein tautomeric forms in equilibrium but with different affinities for the ligand.

Secondly, it is proposed that the albumin molecule has a high degree of flexibility or adaptability and during the binding process a ligand molecule is able to modify the conformation of a binding region so that a greater congruence occurs between the ligand and the binding site. This is the theory of conformational adaptivity and is similar to the sequential or induced-fit model of Koshland et al (1966). A number of kinetic studies are in accordance with this idea. For example, Scheider (1979) has shown that the binding of oleate to HSA occurs in two steps. The first step is diffusion controlled and involves a nonspecific attachment of the ligand. The second step is rate limited by a negative entropy of activation and involves a rearrangement of the protein fatty-acid conformation.

Daniel and Weber (1966) studied the cooperative nature of the binding of ANS to bovine serum albumin. The authors concluded that the observed cooperative binding phenomenon could not result from equilibria of the simple type invoked by Monod et al (1965). Moreover, the results appeared to indicate the existence in the protein molecule of relaxation effects upon binding and dissociation of the ligand. Gibson and Levin (1977) have made important distinctions between the two-state (Monod et al, 1965) and induced-fit model (Karush et al, 1966) for cooperative ligand binding.

Suzukida et al (1983) have recently developed a method for measuring distances between several amino acid residues in HSA. It will be interesting to see how these distances are affected by the binding of various ligands to the albumin molecule and to discover whether these changes are consistent with the induced-fit model.

To conclude, there are clearly regions of the albumin molecule which can be regarded as drug binding sites and certain steric and structural requirements have to be satisfied by the ligand before high affinity binding can occur. Nevertheless, these binding regions exhibit a degree of adaptability which allows them to bind a wide range of chemical compounds. The degree of adaptability is not unlimited, however, as demonstrated by the specificity of albumin binding.

1.5 A Review of Current Techniques Employed in the Study of Drug-Protein Binding

The methods which can be used to investigate drug-protein binding cover a diverse range of chemical and physical techniques. Most of the available methods have been applied to the study of the binding of drugs to human serum albumin. It is beyond the scope of this introduction to assess each approach in turn, although some of the more general aspects will be considered.

Bridges and Wilson (1976) have identified twelve principal techniques and approximately twenty less commonly used methods for studying drug-protein interactions. Bush and Alvin (1973) reviewed the 'classical' methods for estimating the levels of free and bound drug, namely dialysis, ultrafiltration and gel filtration. Physical methods for studying drug-protein binding, both spectroscopic and nonspectroscopic, have been examined in some detail by Chignell (1971). The same author has considered the ways in which fluorescence spectroscopy can be used to study the interactions of drugs with biological systems in general (Chignell, 1972). The review by Meyer and Guttman (1968) includes a discussion of the methods in use at that time. Enzymatic digestion and biochemical labelling techniques for investigating molecular aspects of the drug binding sites of HSA were considered in Section 1.4.2.

Classical methods for estimating the degree of protein binding of a drug are based on the physical separation of the unbound drug from the drug-protein complex. The most widely used techniques are those of equilibrium dialysis, ultrafiltration and gel filtration. The main value of these methods lies in their direct quantitative application to the measurement of drug-protein binding since their use in deriving structural information regarding the nature of the interaction is extremely limited. In practice it is important to ensure that the equilibrium between free and bound drug is not disturbed during the experimental runs and to determine the degree of non-specific absorption to the dialysis membrane, gel, or walls of the apparatus. An assessment of the strengths and weaknesses of the equilibrium dialysis approach is given in Chapter 5.

A number of techniques have been developed from the classified methods and include micro- and non-equilibrium dialysis which require much shorter experimental times (Eisen, 1971; Colowick and Womack, 1969; Hiji et al 1978). Nonetheless equilibrium dialysis remains the most commonly used method for determining drug-protein binding in clinical pharmacokinetic studies.

Several chromatographic techniques have been adapted to the study of drug protein binding. Keresztes-Nagy et al (1972) compared the use of equilibrium dialysis and frontal analysis chromatography in the examination of salicylate binding to HSA. The immobilization of albumin by covalent coupling to agarose gel matrices has allowed Lagercrantz and co-workers (1979) and Nakano et al (1982) to employ continuous frontal affinity chromatography to investigate the binding of drugs to bovine and human serum albumins, respectively. Sebille et al (1978) have determined drug-protein binding parameters using high-performance liquid chromatography.

The above techniques simply involve the physical separation of the bound and free drug. Subsequent to this separation there must be some measurement of the free or bound drug. It is normal practice to assay the former and the most widely used methods involve the use of radiolabelled drugs. In equilibrium dialysis experiments tracer amounts of radiolabelled drugs are added on either side of the dialysis membrane, but more usually on the buffer side. After dialysis has reached equilibrium the free fraction of the drug can be assessed from liquid scintillation measurements. Although this is a very sensitive and conceptually simple technique, Bjornssen et al (1981) have shown that radiochemical impurities can introduce large errors into the assay and suggest an extensive purification of radiolabels prior to dialysis. Hertl and Odstrchel (1982) recently patented a method for separating free ligand (including radiolabelled ligand) from radioactive breakdown products in the dialysate. The technique involves the use of an immobilized antibody specific for a given ligand. While this approach means that the extensive purification of radiolabels can be avoided, it still constitutes a rather complicated and costly adaptation of the basic concept of equilibrium dialysis.

A somewhat different method for the classification and identification of drug-binding sites on HSA has recently been described by Kurono et al (1981) and Kurono and Ikeda (1982). It makes use of the observation that the binding of drugs to human serum albumin can inhibit the esterase-like activity of the protein for the substrates p-nitrophenyl acetate and 5-nitroaspirin.

Spectroscopic techniques such as ultraviolet and visible absorption spectroscopy, fluorescence spectroscopy, optical rotatory dispersion and circular dichroism, nuclear magnetic resonance and electron spin resonance are playing an increasingly important role in protein binding studies. Compared to the more classical methods of assessing drug-protein binding, spectroscopic techniques have several advantages. Since membranes and gels are not involved and measurements can be made rapidly, absorption problems and concerns over the disturbance of equilibrium conditions are often minimized. Moreover, spectroscopic measurements can not only be used to measure the amounts of free and bound drug in a given system but can yield additional information on the nature of drug-protein interactions.

The interpretation of nuclear magnetic resonance and electron spin resonance spectra tends to be rather difficult but they may reveal which group or part of a drug molecule is involved in the binding process (Jardetsky and Wade-Jardetsky, 1965). By recording electron spin resonance spectra from enantiomeric labels, Hsia et al (1982) have examined the stereospecificity of the bilirubin binding sites of HSA.

Optical rotatory dispersion and circular dichroism may yield information on the three-dimensional nature of the drug binding site. These techniques can also provide quantitative data, although the interpretation of spectra may not be straightforward. Ekman et al (1980) have recently used circular dichroism as an aid in the characterization of the indomethacin binding sites of HSA.

When drugs bind to proteins their visible absorption spectra and those of the proteins often show marked changes. Since the degree of spectral change is usually proportional to the concentration of the drug-protein complex, this change may be used to measure the degree of drug binding to albumin. Spectral changes below 300nm are often small and are best observed by means of ultraviolet difference spectroscopy.

Fluorescence spectroscopy is a particularly powerful and sensitive technique with which to examine the binding of drugs to HSA. The wavelengths of maximum excitation and emission, the quantum yield of fluorescence, the degree of polarisation and the fluorescence lifetime of a drug may be markedly affected when it binds to albumin. Changes in the fluorescence characteristics of the protein molecule may also be affected by the binding of a drug. Fluorescence measurements can provide quantitative information on the degree of binding and qualitative information concerning the environment of the drug binding site. Fluorescence energy transfer measurements may be used to determine the distances between the lone tryptophan residue of HSA and specific drug binding sites.

A particularly important development which has extended the use of fluorescence spectroscopy in albumin binding studies is the identification of site-specific 'probe' molecules. These include ANS (Dodd + Radda, 1969), L-kynurenine (Churchich, 1972), warfarin (Chignell, 1970), dansyl amino acids (Sudlow et al, 1975), 7 anilinocoumarin-4 acetic acid (Goya et al 1982), and bilirubin. Fluorescent probes may be used to investigate the protein binding characteristics of a drug by measuring its ability to displace the probe molecule from albumin. Fluorescent probes can frequently be used over a wide concentration range and the displacement method has the particular virtue that it allows the assessment of the protein-binding properties of even those drugs which are intrinsically difficult to assay. A major part of this thesis is concerned with attempts to exploit this approach to the full. The possibility that a drug could alter the spectroscopic characteristics of a fluorescent probe via a modification of the protein conformation rather than by its direct displacement from a specific binding site is examined by comparing results with those of a more conventional method.

The measurement of the thermodynamic parameters governing the binding of a drug to a protein can provide important information on the nature of the interaction at the molecular level. Most of the various separation and spectroscopic techniques mentioned above can be performed at different temperatures and so, with the aid of the van't Hoff equation, permit the calculation of entropy and enthalpy changes for a given interaction. This is only rarely attempted in practice, an example being the study of Whitlam et al (1979). On the other hand, calorimetric techniques allow these parameters to be measured directly. Otagiri et al (1978) have used microcalorimetry to estimate thermodynamic parameters for the binding of four anionic drugs to HSA. They interpreted the results in terms of the relative contributions of hydrophobic, electrostatic, van der Waals and hydrogen-bonding to the binding process. A microcalorimetric method for the study of the competitive binding of ligands to HSA has been described by Coassolo et al (1978).

When spectroscopic methods are used in conjunction with stopped-flow or relaxation techniques, it is possible to study the kinetic parameters of drug-protein interactions. Lassman (1981) has used this approach to investigate the kinetics of the binding of warfarin to HSA. The binding process was followed by observing the enhancement in warfarin fluorescence which occurs on binding of the drug to albumin. Lassman and Reitbrock (1982) have used this new technique to investigate the pH-dependent binding kinetics of warfarin. These studies should lead to a better understanding of the binding process at the molecular level ; the kinetic parameters may also have important pharmacokinetic consequences.

The classical separation techniques used in the study of drug-protein binding tend to be rather tedious and time-consuming. Spectroscopic methods which do not involve any physical separation of the bound and free drug are more convenient to perform and are particularly suited to automation. A further aim of this study is to investigate the possibility of automating drug-protein binding studies.

1.6 Molecular Fluorescence Spectroscopy

The aim of this section is to cover some important theoretical and practical aspects of molecular fluorescence spectroscopy. Particular emphasis is placed on the effect of the molecular environment on fluorescence spectra: it is the extreme sensitivity of fluorescent probes to changes in their environment which makes a study of the spectroscopic properties of these molecules so useful in drug-protein binding studies.

There are a number of textbooks and reviews concerned with both the principles and the applications of fluorescence spectroscopy. Probably the best and most comprehensive of these are the works by Parker (1968), Ewing (1970), Winefordner et al (1972) and Guilbault (1973). Bowen and Wokes (1953), Becker (1969) and Simons (1971) have written important books on the theoretical aspects of luminescence, while Udenfriend (1962 and 1969), White and Argauer (1970), and Gifford (1981) have discussed the use of fluorimetric analysis in biochemistry and medicine. These publications contain further references to the extensive literature on fluorescence spectroscopy.

1.6.1 Introduction to Molecular Fluorescence

Descriptions of the transitions which give rise to molecular fluorescence invariably include a simplified representation of the available molecular energy levels. Various excited state processes are described with reference to this simple diagram. It is convenient to do so, and since only limited information exists concerning the available energy states of individual molecules, it is usually necessary. Nevertheless an appreciation of the radiative and non-radiative transitions in excited molecules requires some further understanding of molecular structure. Without this, simplified diagrams can obscure important aspects of fluorescence.

Those characteristics of molecular structure which are relevant to a discussion of fluorescence will be covered in this section. More detailed descriptions are given in standard textbooks such as that on molecular quantum mechanics by Atkins (1970).

The molecular orbitals within a molecule are foremost in determining its chemical and spectroscopic properties. The electronic charge in a σ bond is strongly localized between the nuclei it binds. Electronic repulsion, as well as the limitation of the Pauli exclusion principle, prevents the formation of more than one σ bond between any two atoms. Since the electrons involved in σ bonding are concentrated between the bonded atoms, they are held very tightly and a great deal of energy is required to promote these electrons to vacant molecular orbitals (see Figure 1.5). Π bonds are generally weaker than σ bonds as the overlap charge does not occur immediately between the nuclei. This means that Π electrons are freer to move within the molecule than are σ electrons.

So if several atoms are σ bonded in series and each has a p or d orbital with the correct spatial orientation to form a π bond with the others, a set of π bonds is formed whose electrons are spread over the entire series of atoms. The π bonds are therefore delocalized and in some cyclic organic molecules this delocalization extends over the whole molecule. Such aromatic compounds are of primary interest in molecular luminescence spectroscopy.

The symmetrical nature of the σ bond about its axis means that rotation is possible around such bonds. The π bond is symmetrical by reflection in its molecular plane but not with respect to rotation about the intramolecular axis. Hence rotation about a π bond destroys the parallelism needed for the overlap of its constituent p orbitals. Thus the double bond is in effect rigid and cannot rotate. Indeed π-systems are often to be found in extensive planar molecules.

In systems containing π and n electrons the spectral features and chemical reactivity are sometimes assigned exclusively to these electrons. The localized σ electrons are regarded as providing a σ-bond framework relative to which the distribution of π electrons is discussed. This approach is called the π-approximation. It is not completely valid because the π charge on a certain atom can repel the σ cloud and vice versa. Moreover, in excited states there is usually an alteration in one or other of the charge density distributions which then affects other distributions. However, while it is wrong to treat the σ electrons and the nuclei as together establishing a rigid core, it is almost inevitable to do so and theories concerned with π electrons alone have been very successful. This is due to two factors : the fundamental difference in symmetry between σ and π electrons and the greater polarizability of the π electrons which allows them to respond more readily than do σ electrons to any disturbance or perturbation. For spectroscopic purposes, then, and within the limits of the π-approximation, the entirety of the molecular electronic structure can be seen as consisting of occupied π orbitals at lowest energy, the occupied n orbitals at slightly higher energy than the π electrons, and the unoccupied π* orbitals to which n or π electrons are promoted for the electronically excited states. This is shown in Figure 1.5.

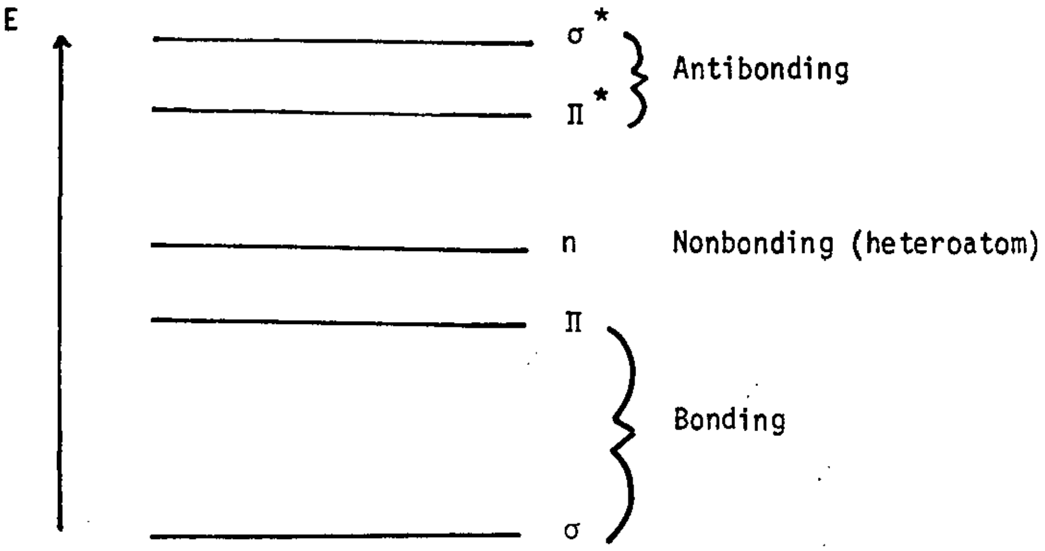

FIGURE 1.5 Generalized molecular-orbital energy diagram.

The electronic spectra of molecules are complex and their interpretation merits a description of more than just the electronic energy levels. The energy associated with rotational transitions is usually less than that associated with vibrational transitions which in turn is less than associated with electronic transitions. Consequently, although it is possible to observe pure rotational spectra, when a vibration is excited in a molecule then so are rotational transitions. Similarly, electronic spectra do not involve purely electronic transitions, both vibrational and rotational transitions are excited. While the gross structure of electronic spectra can be described in terms of the available electronic energy levels, the widths of absorption bands and the position of maximum absorption depend strongly on the molecular vibrational and rotational energy levels. Vibrational transitions have a particularly strong influence on the spectral properties of fluorescent molecules.

The energy of a bond between two atoms changes if the nuclei are disturbed from their equilibrium positions. A number of functions have been put forward to describe the potential energy curves of vibrating molecules. These functions may be used in the Schrödinger equation to compute the quantised vibrational energy levels. The allowed energy levels may be represented as a series of horizontal lines on the potential energy curve. For molecules undergoing anharmonic oscillations, the quantised energy levels are less well spread at high energies than at low, and vibrational transitions are governed by the selection rule $\Delta v = \pm 1, \pm 2, \pm 3, \ldots$ The vibrations of polyatomic molecules are complex and cannot be considered to be a property of individual bonds but must involve the entire molecule. While a detailed discussion of the possible vibrational modes is not merited, the role of molecular vibrations in governing the electronic spectra of various compounds will be considered.

The vibrational wavefunctions and probability density functions for an oscillating molecule can be used to calculate the probability of finding the vibrating nuclei at any distance from their equilibrium positions. For the lowest vibrational states the probability distribution function has a maximum at the centre of the vibration; higher vibrational states have a maximum probability near the turning points. A knowledge of the most likely location of the vibrating nuclei in a particular energy state can be used to determine the probability of transitions from one state to another.

Of course these transition probabilities also depend upon the population of the available energy states. The intensity resulting from the transition of a molecule from some initial state of energy to a final state depends on the number of molecules that have the initial energy. If there are two energy levels from which transitions to a third are equally possible then the most intense spectral line will come from the level which initially had the greater population. The Boltzman distribution may be used to calculate the population of available levels. This asserts that at equilibrium the ratio of the numbers of molecules in the states with energies E_i and E_j is

$$\frac{n_i}{n_j} = \exp \frac{-\Delta E}{kT}$$

where n_i and n_j are the numbers of molecules with energy E_i and E_j respectively, k is Boltzman's constant, T is the absolute temperature, and $\Delta E = \Delta E_i - E_j$. When ΔE is much less than kT, n_i is negligible with respect to n_j. At room temperature the energy difference between the first excited molecular electronic state and the ground state is much greater than kT. Consequently, an absorption spectrum normally shows transitions originating exclusively from molecules in their electronic ground states. Vibrational spectra of samples at room temperature can also usually be accounted for entirely in terms of transitions from the lowest vibrational states because the first vibrational excited state lies well above the ground state and is only slightly populated. In constrast, for molecular rotational levels the spacing is much smaller and even at room temperature many levels are populated. A rotational absorption spectrum contains lines due to transitions of molecules from a range of populated rotational levels.

Like all molecular electronic spectra, fluorescence originates in the absorption of visible or ultraviolet radiation by molecules in their ground states. The conventional system for representing electronic transitions is one in which the upper state is written first and the lower second (Atkins, 1970). The direction of the arrow then indicates emission $(A \longrightarrow X)$ or absorption $(A \longleftarrow X)$.

A transition between two stationary electronic states can be induced by radiation provided its frequency is $(E_j - E_i)/h$ where E_i and E_j are the energies of the states and h is Plank's constant. The frequencies at which electronic bands occur are determined by the energy separations between the ground state and the various excited levels. The electronic spectrum is normally divided into three regions: the visible between 400 and 750nm, the near ultraviolet between 200 and 400nm and the far or vacuum ultraviolet below 200nm.

Since a large input of energy is required to promote electrons involved in σ bonding to vacant molecular orbitals (see Figure 1.5), molecular electronic spectra concerning σ electron transitions occur well into the vacuum ultraviolet and are not available to, or of interest in, conventional luminescence spectroscopy. Π electrons are not as tightly bound as σ electrons and so their electronic spectra occur at lower frequencies. For molecules with isolated multiple bonds, transitions involving Π electrons are on the borderline of the near ultraviolet and the vacuum ultraviolet. When two or more multiple bonds are conjugated, however, molecules contain delocalized Π electrons and have Π electron spectra in the near ultraviolet. Highly delocalized Π systems such as aromatic molecules have intense $\Pi^* \leftarrow \Pi$ transitions ranging from the near ultraviolet for small molecules to the near infra red for large molecules. While the $\Pi^* \leftarrow \Pi$ transition is often intense, it tends to reduce the strength of the bond because a binding electron is transferred to an antiboding orbital. Electron pairs in n orbitals, on the other hand, are unavailable for conventional covalent bonding but are potential contributors to the spectral features of molecules that possess them.

In contrast to the narrow spectral lines of atoms, molecular electronic spectra usually appear as broad bands. This is because each molecular electronic state is accompanied by a manifold of vibrational and rotational states. As mentioned earlier, to explain the shapes of molecular spectra, transitions that involve both the electronic and vibrational levels must be considered. These are often referred to as vibronic transitions.

Electronic transitions in molecules occur very quickly. The time required for a molecule to pass from the ground state to an electronically excited state upon absorption of a quantum of radiation is of the order of 10^{-15}s. In contrast, vibrational transitions that require rearrangement of the position of nuclei take about 10^{-12}s. It is therefore reasonable to assume that electronic transitions occur so rapidly that the nuclear framework of a vibrating molecule remains unchanged. This is the basis of the Franck-Condon principle.

The Franck-Condon principle is extremely helpful in predicting which vibrational transitions accompany the transitions between molecular electronic levels and in explaining the intensity with which each vibronic transition occurs. The qualitative application of this principle may be understood by reference to Figure 1.6 which shows hypothetical potential energy curves for the ground and first excited electronic states of a diatomic molecule. The horizontal lines indicate the vibrational levels associated with each electronic state and approximate probability density functions are included.

The variations of potential energy with respect to nuclear configuration may be similar in the ground and excited states (Figure 1.6(a)). When an electronic transition occurs the molecule is excited to the state represented by the upper curve in Figure 1.6(a). Since the lowest vibrational level of the ground state is the most densely populated at room temperature, most transitions occur from this level. However, although there are no restrictions on the change in the vibrational quantum number during an electronic transition, the vibrational lines in a progression are not of the same intensity. According to the Franck-Condon principle, the nuclear coordinates remain constant during an electronic transition and so a vertical line has been drawn on the diagram to represent such a transition. In the vibrational ground state the most probable conformation of the nuclei when the transition occurs is that in which they are at their equilibrium positions. The lowest vibrational wavefunction has a maximum at this position. The vibrational transition may cut through several vibrational levels of the excited electronic level. When the nuclear configuration is similar in the ground and excited electronic states, there is strong overlap between the v=0 vibrational wavefunctions of the

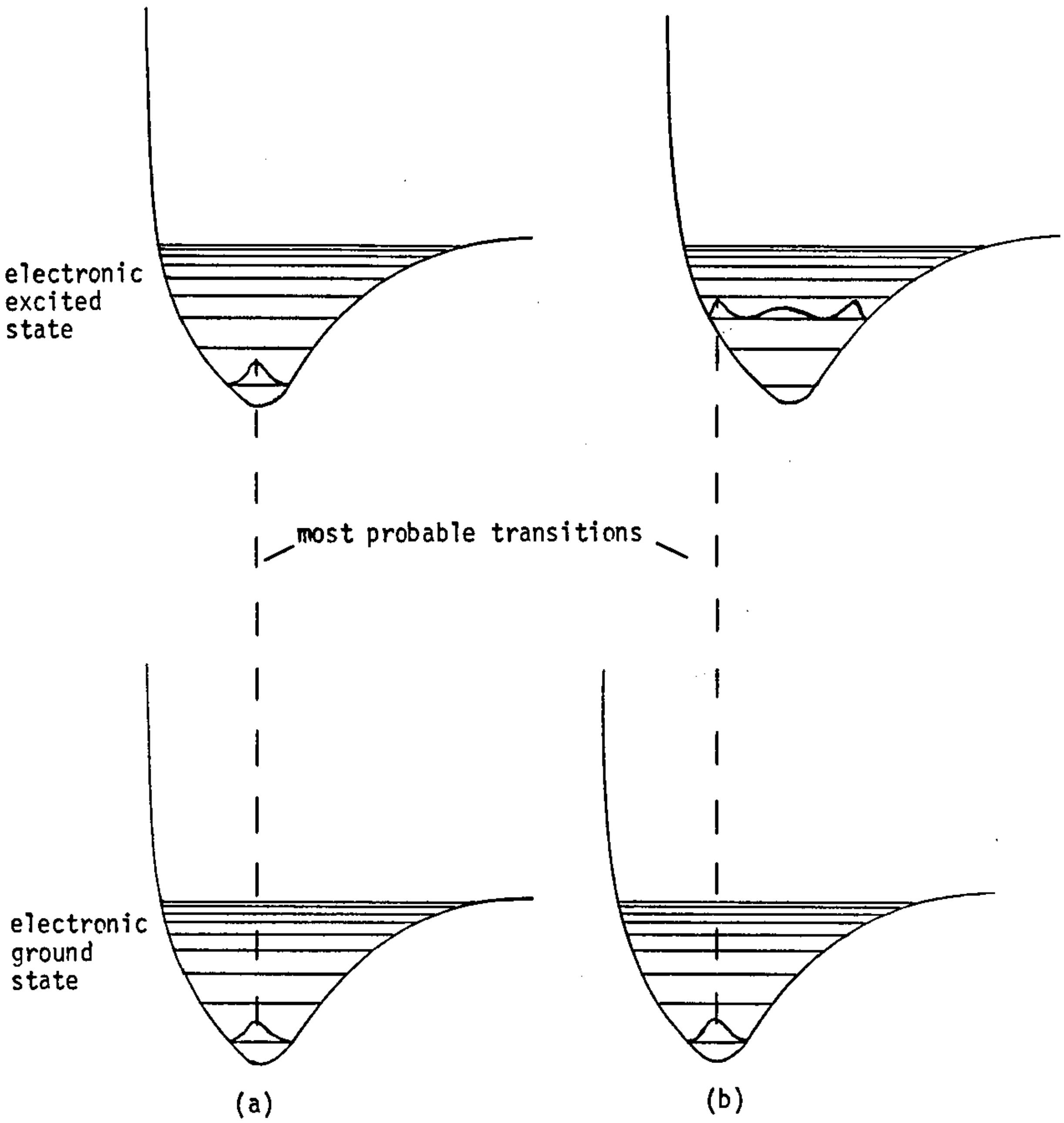
electronic
excited
state
most probable transitions
electronic
ground
state
(a)
(b)

FIGURE 1.6 The Franck-Condon Principle and Vibronic Transitions

Potential energy curves are shown for two electronic states of diatomic molecules with probable spectroscopic transitions.

electronic states and so the (0←0) transition is the most intense. Nevertheless transitions to other vibrational levels retain some probability since although the nuclei are most likely to be located at or near their equilibrium displacement in the v=0 state, a finite probability exists for them to be at the extremities of their vibration. Because the v=0 wavefunction is finite even for these nuclear configurations, overlap is quite possible with wavefunctions for other vibrational states. Of course, the (1←0), (2←0) and other transitions are of lower intensity than the (0←0) line. The (0←0) transition normally defines the low frequency (high wavelength) limit of the absorption band. At high temperatures, though, other vibrational levels may be appreciably populated and radiation of longer wavelength than the (0←0) line may be absorbed.

Quite often the equilibrium nuclear configuration of the ground electronic state is considerably different from that of the electronically excited state. Indeed, the upper potential energy curve is usually displaced to the right of the lower curve, that is, to longer bond lengths. This is so because an electronic transition often involves an increase in the antibonding character of a bond. In these circumstances the intensity of the vibronic transitions will differ from those in Figure 1.6(a). Vertical transitions may reveal that the most probable transition is now from the lower v=0 level to the upper v=3 state (Figure 1.6(b)). The upper state most probably reached depends on the displacement of the upper and lower potential energy curves. A lot of vibrational structure is indicative of considerable displacement of the two states.

In a molecule, electronic transitions are accompanied by changes in the rotational as well as the vibrational states. Thus the precise width of absorption bands and the position of maximum absorption depend on the structure caused by rotational as well as vibrational transitions. However, molecules are most often studied in solutions at room temperature and as a result of intermolecular collisions the rotational structure is invariably blurred. In fact vibrational as well as rotational structure is lost from most molecular electronic spectra and the result is a broad band spectrum.

Upon absorption of radiation of the correct frequency, a molecule can be excited to one of the vibrational levels of the electronically excited singlet states. There are several mechanisms by which the molecule can return to the ground state only one of which is fluorescence. The various mechanisms are illustrated in Figure 1.7.

The radiationless relaxation processes - those that involve direct

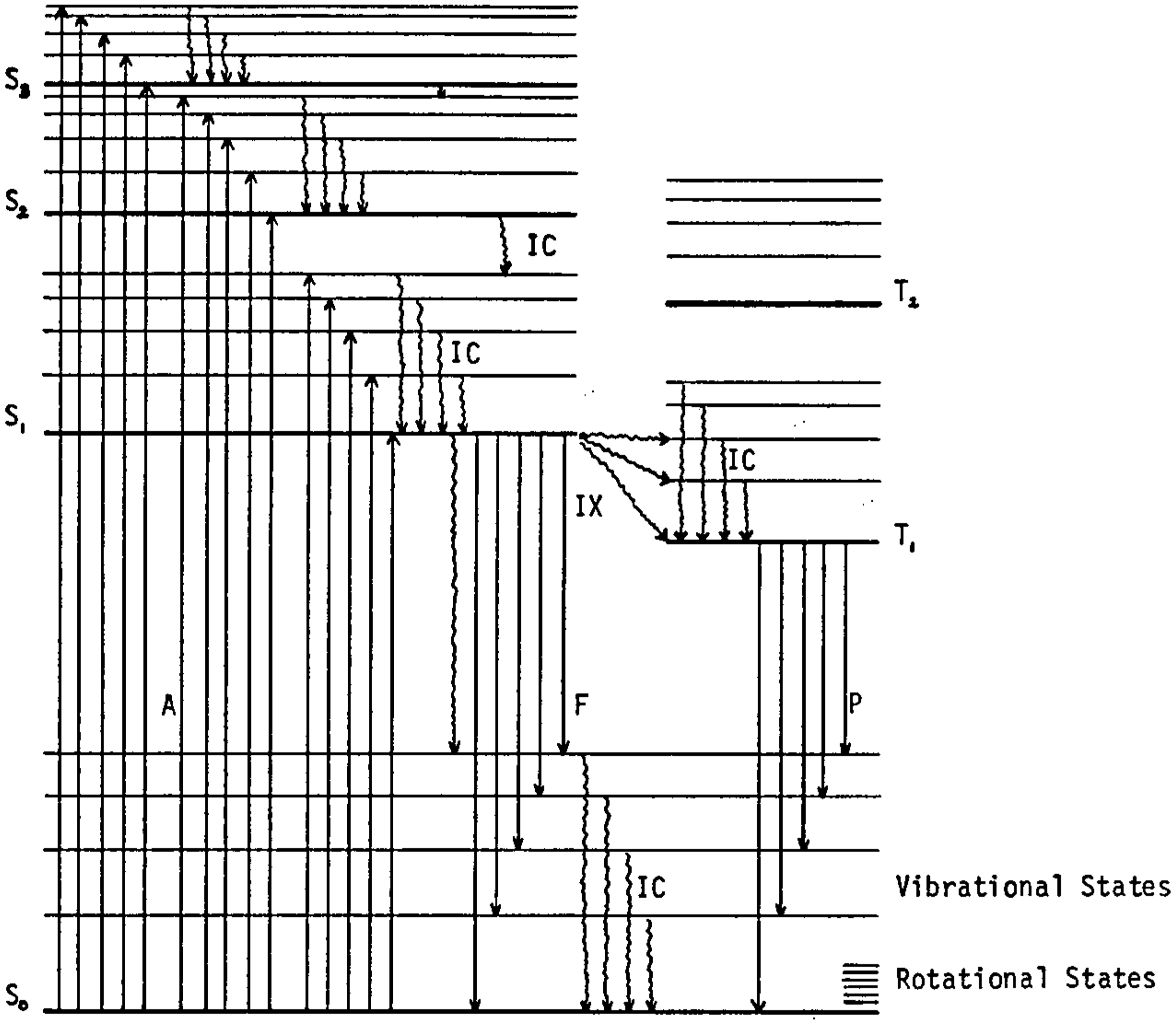
S₃
S₂
IC
T₂
IC
S₁
IC
IX
T₁
A
F
P
IC
Vibrational States
Rotational States
S₀

FIGURE 1.7 Transitions Occurring in Electronically Excited Molecules

S_0 - Electronic ground singlet state

S_1, S_2, S_3, - Electronically excited singlet states

T_1, T_2, - Electronically excited triplet states

A - absorption

F - fluorescence

P - phosphorescence

IC - internal conversion

IX - intersystem crossing

vibrational coupling or quantum mechanical tunneling between electronic states, and those due to thermal degredation of the vibrational and electronic levels through molecular collisions - are known as internal conversion. The probability of such processes occuring is extremely high; indeed radiative emissions other than those from the first excited electronic state are extremely rare. The various mechanisms which constitute internal conversion are discussed below.

The most common means by which excited molecules return to the ground state is via thermal decay. If an excited molecule is subjected to frequent collisions with molecules in its environment - with the solvent molcules if it is in solution - then the colliding species may act as an acceptor for the excess energy. In this manner excess vibrational energy may be dissipated with each collision removing a quantum of vibrational energy. Collisions may also transfer the electronic energy of excited molecules into the vibrational modes of acceptor molecules in the environment. Water, for example, has widely spaced vibrational energy levels which coincide with a range of typical electronic excitation energies. The energy may be distributed even more widely as the vibrational energy of the acceptor molecules is transferred by further collisions into the rotational and translational modes of the system. Through this relaxation process the excitation energy is degraded into heat as the absorbing molecule returns to the ground state. The lifetime of the excited electronic state depends on the efficiency of the transfer of energy into the vibrational modes of the neighbouring molecules.

The proportion of the excitation energy lost by this collisional process is difficult to determine. For some large molecules interactions of any kind with the solvent may be unnecessary for the decay from high to low excited electronic states. The transition occurs not only in solution but in rigid media and in the gas phase where the number of collisions may be severely diminished or even zero. Indeed it has been shown that upon excitation into their second excited singlet states, naphthalene, anthracene and naphthacene exhibit radiationless conversion into the first excited singlet state under conditions where no collisions occur during the lifetime of the second excited singlet state (Watts and Strichler, 1966). These observations suggest there must be other, intramolecular radiationless transitions in excited state molecules.

The potential energy surfaces of two electronic states may cross and the higher vibrational levels of the lower electronic state overlap the lower vibrational levels of the higher electronic state. This means the nuclear configuration and energies of the two electronic states are identical or very similar during a low level vibration of the upper and a high level vibration of the lower electronic state. Following a vibration in the upper electronic level, a high probability exists that in the next and succeeding vibrations, the molecule will be vibrating in a manner appropriate to the lower level. The transient thermal equilibrium between the electronic states permits population of the lower state. This coupling of the neighbouring electronic states by a vibronic perturbation represents a breakdown of the Born-Oppenheimer approximation: the electronic states are not independent of the nuclear vibrations.

If the vibrational levels of one electronic state do not overlap those of another but are separated only by a few vibrational quanta, a molecule in the upper electronic state may still convert to the lower by a tunneling mechanism. Tunneling is permitted quantum mechanically because the wave function characterizing a particle does not vanish at distances away from the most probable distribution but decreases asymptotically. So there is always some overlap of vibrational levels in different electronic states. The possibility of tunneling, and hence internal conversion, decreases as the difference in energy between the lower vibrational levels of the upper and the upper vibrational levels of the lower electronic state increases.

If there is a considerable separation between an upper and a lower electronic energy level, direct vibrational coupling of the electronic states will be impossible and tunneling highly improbable. Nonetheless, the probability of radiationless transitions between the closely-spaced higher electronic states is extremely great. Internal conversion is at least a thousand times more likely than is radiative emission from any excited singlet above the first excited singlet (Becker, 1969). However, as may be appreciated from the lifetimes of the excited states shown in Figure 1.8, internal conversion from the lowest excited state to the ground state is often much slower than it is between the higher states. This is because the energy separation between the ground state and the first excited state is larger than between the higher electronic levels. Hence other processes, including fluorescence, can sometimes compete successfully with internal conversion for depopulation of the lowest vibrational level of the first electronically excited state. Of course, in a molecule where there is significant overlap between the lower vibrational levels in the first excited state and the upper vibrational levels in the ground state, the fluorescence will be weak or absent.

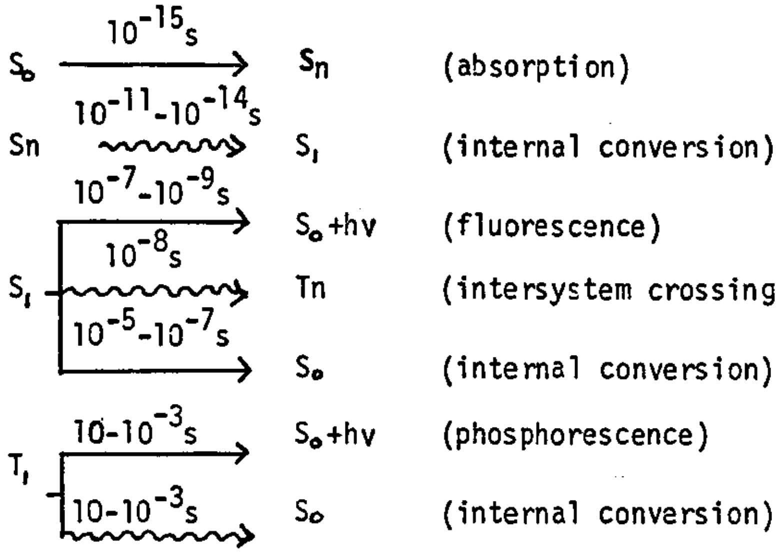
$S_0 \xrightarrow{10^{-15}s} S_n$ (absorption)
$S_n \xrightarrow{10^{-11}-10^{-14}s} S_1$ (internal conversion)
$S_1 \xrightarrow{10^{-7}-10^{-9}s} S_0+hv$ (fluorescence)
$S_1 \xrightarrow{10^{-8}s} T_n$ (intersystem crossing
$S_1 \xrightarrow{10^{-5}-10^{-7}s} S_0$ (internal conversion)
$T_1 \xrightarrow{10-10^{-3}s} S_0+hv$ (phosphorescence)
$T_1 \xrightarrow{10-10^{-3}s} S_0$ (internal conversion)

FIGURE 1.8 Mean decay times for non-radiative and radiative transitions in excited state molecules.

In general a radiative transition between electronic states is called luminescence. The term fluorescence is used when the upper and lower electronic states are of the same multiplicity. Fluorescence involves the spontaneous emission of a photon of visible or ultraviolet radiation. The emission of the radiation is spontaneous in the sense that it is not stimulated by incident photons of the same frequency. The mechanism of spontaneous emission is such that it becomes very important only at high frequencies ; the time required for a nucleus to reverse its magnetic moment in a magnetic field is astronomical. For molecular fluorescence the mean lifetime of the excited state is about 10^{-8}s. This is still quite long on a molecular scale since the excitation process takes only about 10^{-15}s.

The frequency at which fluorescence bands appear is proportional to the difference in energy between the ground state and the lowest, or very exceptionally the second, excited singlet state. The shapes and intensities of the fluorescence spectra are governed by the Franck-Condon principle which was discussed in connection with absorption spectra. Vertical transitions from the lowest vibrational level of the first electronically excited state terminate in any one of a number of vibrational (and rotational) levels in the ground electronic state (Figure 1.7). The result is a band spectrum. For molecules having identical nuclear configurations in the ground and first excited state, of the many possible vibronic transitions, the one between the v=0 levels of the two states will be the most probable. If, as is usual, the equilibrium nuclear configurations of the ground and excited states are slightly different, the emission band maximum will correspond to the frequency of some other transition. Which one will depend on the amount of displacement between the configurations.

Since at room temperature virtually all the radiative transitions in fluorescence originate from the same (v=0) vibrational level of the lowest excited singlet state, the vibrational structure of the emission spectrum is characteristic of the ground state. Indeed, this provides a method for studying the vibrational structure of the ground state. On the other hand, the corresponding absorption spectrum originates from the lowest vibrational level of the ground state and its vibrational structure is characteristic of the excited electronic states. It is not surprising, therefore, that there are many accounts in the literature of an approximate mirror-image relationship between the absorption and emission bands. This is to be expected if the spacings between the vibrational levels, and if the equilibrium nuclear configurations are similar in the ground and excited states. The mirror-image relationship should not be considered as general, however, since quite often considerable differences in the vibrational frequency and geometry of the two states can modify this relationship. In addition, while a molecule may show a number of bands in its absorption spectrum, it will never have more than one fluorescence band. Absorption may occur from the ground state to a number of electronically excited levels: fluorescence normally only originates from the first excited singlet state and terminates in the ground state. Thus quinine sulphate has two absorption bands corresponding to ($S_2 \leftarrow S_0$) and ($S_1 \leftarrow S_0$) but one emission band ($S_1 \rightarrow S_0$).

In returning the excited molecule to the lowest vibrational level of the first electronically excited state, the dissipation of absorbed energy by internal conversion means that fluorescence occurs at a longer wavelength, that is at lower energy, than does absorption. The ($0 \rightarrow 0$) transition of fluorescence is the high frequency limit of fluorescence and the low frequency limit of absorption for the same electronic states (Figure 1.7). This implies that the fluorescence maximum always occurs at a lower frequency, that is higher wavelength, than the corresponding absorption maximum. In fact this is nearly always so except, of course, when the 0—0 band is both the fluorescence and the absorption maximum. Even then the bulk of the fluorescence band is at lower frequency than the absorption band. As discussed previously, the absorption and emission band maxima are usually centred around some other than the 0—0 transition.

The absorption and fluorescence may then be well separated. The displacement to longer wavelength of the emission band maximum with respect to the excitation band maximum is constant for a given molecule. It is called the Stokes shift.

Anti-Stokes fluorescence, the emission of radiation at a shorter wavelength than that of the existing radiation can only occur if thermal energy is added to the excited state or if the molecule has many highly populated vibrational levels. This type of fluorescence is only observed in dilute gases at high temperature. Almost all fluorescence in solutions at ordinary temperatures is of the Stokes type.

Inspection of Figure 1.7 shows that fluorescence must not only compete with internal conversion for depopulation of the various excited states, but with intersystem crossing to the triplet manifold. So far, the role of the triplet state in electronic transitions has not been considered.

Molecules with an even number of spin-paired electrons have singlet electronic levels. The pairing means that the molecule as a whole has no set electronic magnetic moment. If the spin of a single electron in such a molecule is reversed, there will be two unpaired electrons. The multiplicity is three and the electronic state is triplet.

According to Hund's rule for atoms, electrons with parallel spins are lower in energy than the corresponding pair with opposed spins. By analogy, a triplet state in a molecule will always have lower energy than the corresponding singlet electronic state. This drop in energy to the triplet suggests another pathway by which the energy of an excited singlet state may be dissipated. However, electronic transitions between states of different multiplicity are forbidden. In practice the selection rule may break down to varying degrees under the influence of certain perturbations. These perturbations increase the extent of spin-orbital coupling in molecules and may bring about the electron spin reversal necessary for triplet formation.

Even in the absence of perturbing species, some spin-orbital coupling occurs in almost all atoms. An electron has spin and so possesses a magnetic moment. An electron with orbital angular momentum is effectively a circulating current and so gives to a magnetic field with a strength proportional to its angular momentum. Spin-orbital coupling occurs when the magnetic moment due to the spin of the electron interacts with the magnetic field of its orbital motion. This interaction means that some degree of intersystem crossing should occur in the excited states of practically all molecules.

For intersystem crossing to be effective, though, strong perturbations, such as those produced by heavy atoms, paramagnetic ions and heteroatoms, need to be present in the molecule or its immediate environment. These are discussed later.

The possibility of intersystem crossing also depends on the overlap of the vibrational wavefunctions of the singlet and the corresponding, but slightly lower, triplet electronic state. In fact, intersystem crossing may be considered to be a spin-forbidden internal conversion mechanism. Intersystem crossing is normally only important between the first excited singlet and triplet levels. Intersystem crossing involving higher singlet and triplet electronic states is severely limited by the great rate of internal conversion between the more energetic singlets (see Figure 1.8). Even if some intersystem crossing results in the population of higher triplet levels, internal conversion amongst the triplet states is so rapid that only the lowest excited triplet is of interest in conventional spectroscopy. Internal conversion in the lowest excited triplet level continues until the ground vibrational level is reached (Figure 1.7).

A radiative transition from the lowest vibrational level of the first excited triplet state to the electronic ground state is forbidden since it involves a change in multiplicity. The molecule may return to the ground state via the first excited singlet state if enough energy can be acquired from the environment to raise it back to the region where the first excited singlet and triplet levels cross. Under these conditions, the spectral distribution of the subsequently emitted radiation is the same as that produced by normal fluorescence but has a considerably longer lifetime. Such a transition is unlikely to occur, especially at low temperatures but when it does it is called delayed fluorescence.

Although a forbidden transition, radiative emission may still occur from the lowest vibrational level of the first excited triplet to the ground singlet state. Since intersystem crossing has already arisen between the first excited singlet and triplet levels, a perturbation must be present that can mix the multiplicities and break the selection rule. In addition return to the first excited singlet from the lower triplet is improbable. The emission of energy via a radiative transition from the triplet state must therefore retain some probability. This transition is known as phosphorescence.

Phosphorescence appears at a longer wavelength than the exciting radiation, and since the triplet is lower in energy than the corresponding singlet state, it is also at a longer wavelength than the fluorescence band of the molecule. The vibrational structure of the phosphorescence band is characteristic of the ground singlet state. The relative intensities of the individual vibronic transitions and so the shape of the band are again determined by Franck-Condon transitions.

Since phosphorescence involves a change in multiplicity, the lifetime of the process is very much longer than that of fluorescence (Figure 1.8). Phosphorescence often continues to be emitted long after the excitation is withdrawn. Due to the long lifetime of the triplet state, phosphorescence must compete with physical and chemical processes for deactivation of the lowest triplet state. Thus the triplet state may participate in photochemical reactions rather than return to the ground state. This is the basis of photochemistry and explains why the triplet state is more important than the singlet state in most photochemical reactions. In solution at room temperature the long-lived triplet state is very susceptible to non-radiative deactivation through collisional processes. For this reason, phosphorescence is normally observed in rigid or non-viscous media at very low temperatures.

The excitation of phosphorescence by the direct absorption of radiation from the ground state singlet to the excited triplet is extremely rare. Spin-orbital coupling and so intersystem crossing can only occur to any reasonable degree if there is a small energy difference between the singlet and triplet states concerned. This is so for the excited singlet states and the corresponding excited triplet states. The probability of intersystem crossing between these levels is therefore very much greater than is the direct transition from the ground state singlet to the well-removed first or higher excited triplet states.

Figure 1.8 shows that intersystem crossing is still fast enough to compete with fluorescence and give triplet state occupation. In many circumstances the relative rates of the two processes may be altered to favour intersystem crossing with a consequent high or even total occupation of the triplet state and a resulting complete absence of fluorescence. Molecular fluorescence is therefore very sensitive to structural and environmental factors.

1.6.2 The Effect of Molecular Structure on Fluorescence

The first requirement for fluorescence is an absorbing structure. The greater the ability of a molecule to absorb radiation, the more intense is likely to be its fluorescence. The $\Pi^* \leftarrow \Pi$ transitions in aromatic compounds are usually strongly allowed and many of these compounds are highly fluorescent.

$\Pi^* \leftarrow \Pi$ transitions in isolated carbon to carbon double bonds occur at about 180nm. When the double bonds are part of a conjugated system the absorption band is shifted to longer wavelengths; highly conjugated systems are often coloured. Aromatic compounds being cyclic conjugated systems show a similar effect; the larger the aromatic molecule the lower the frequency of any given absorption band.

As in the case of absorption spectra, luminescence bands tend towards higher wavelengths as the size of the Π system is increased. In addition, the intensity of the fluorescence often increases as the degree of conjugation increases. For a given number of aromatic rings, linear ring systems fluoresce at longer wavelengths than nonlinear systems.

For aromatic molecule containing carbonyl groups, and in heterocyclic compounds, n electrons are available for excitation into Π^* orbitals. $\Pi^* \leftarrow n$ transitions, however, are much less intense than $\Pi^* \leftarrow \Pi$ transitions. This is so because an important feature governing the intensities of electronic transitions is the spatial orientation of the orbitals between which transitions occur. In heterocyclic molecules such as pyridine, the ground state n orbitals are directed into the molecular plane whereas the Π^* orbitals are directed perpendicular to it. Consequently, there is poor overlap between the n and Π^* orbitals and $\Pi \leftarrow n$ transitions appear weakly with respect to $\Pi^* \leftarrow n$ transitions. On this basis alone, aromatic carbonyl compounds and heteroatoms would be expected to be less strongly fluorescent than aromatic hydrocarbons.

As noted in Figure 1.5, the energy of $\Pi^* \leftarrow n$ absorption will usually be lower than the lowest $\Pi^* \leftarrow \Pi$ transition. Such transitional characteristics are due to the n orbitals in the ground state of the molecule being higher in energy than the occupied Π orbitals. $\Pi^* \rightarrow n$ fluorescence should therefore occur at longer wavelength than $\Pi^* \rightarrow \Pi$ fluorescence. This is not always the case because, as discussed later, solvent-n electron interactions can alter the position of the fluorescence bands.

In saturated hydrocarbons there are no Π -binding or nonbonding electrons and all electronic transitions must involve σ electrons. All transitions involving σ electrons require a large input of energy and bond dissociation may accompany absorption. The probability of fluorescence is low. Some saturated hydrocarbons do fluoresce, though emission is very weak. In aliphatic carbonyl compounds $\Pi^* \leftarrow n$ transitions can occur, but fluorescence intensities are again very low.

Some non-aromatic, but highly conjugated compounds are quite fluorescent due to the occurrence of $\Pi^* \leftarrow \Pi$ transitions. In general, however, the vast majority of intensely fluorescent compounds are aromatic.

To explain the relation of molecular structure to fluorescence, it is insufficient simply to consider those aspects of structure which make for strongly absorbing species. Following excitation, fluorescence must compete with a variety of other excited state processes. Structural features and functional groups that enhance internal conversion and intersystem crossing may substantially reduce, or perhaps totally prevent, the emission of fluorescence from evenly strongly absorbing molecules.

Whether a molecule employs internal conversion or fluorescence to pass from a higher to a lower electronic state depends on the energy separation between the two states and the number of vibrational levels associated with each electronic state. The latter property is important because it determines the probability of vibrational overlap of the electronic states. If a molecule has a large number of modes of vibration then the vibrational levels of different electronic states are likely to overlap and internal conversion will be favoured. This method of dissipating the excitation energy explains why fluorescence is only rarely exhibited by aliphatic molecules and others that do not have rigid molecular skeletons. Such molecules posses many vibrational degrees of freedom. Aromatic molecules with their rigid ring structures are the class of compounds that most frequently show fluorescence.

Since internal conversion between the first excited singlet and the ground electronic state is generally unimportant in aromatic hydrocarbons, the principle process competing with fluorescence in these compounds is intersystem crossing. The presence of a heteroatom in an aromatic molecule usually means that the lowest excited singlet state is an (n,Π^*) singlet. Fluorescence rarely occurs from this state and if it does, it is extremely weak; indeed it is a hundred to a thousand times lower in intensity than $\Pi^* \rightarrow \Pi$ fluorescence. As mentioned before, it is a consequence of the symmetry forbiddeness between the excited state and the ground state and means that the radiative lifetime of (n,Π^*) singlets tends to be considerably longer than those of (Π,Π^*) singlets. Consequently, intersystem crossing can compete effectively with fluorescence for molecules whose lowest singlets are (n,Π^*). Moreover, energy differences between the first excited singlet and triplet states are frequently much larger for (Π,Π^*) than for (n,Π^*) excited states (Winefordner et al, 1972; Guilbault, 1973). Since the probability of intersystem crossing decreases as the energy separation of the states to be mixed increases, the process is more likely to occur for heteroatomic molecules than it is for their hydrocarbon analogoues. Thus, greatly enhanced phosphorescence to fluorescence ratios are observed as a result of heteroatom substitutions.

Certain simple generalizations may be made concerning the effects of meta- and of ortho-, para-directing substituents on the fluorescence of aromatic hydrocarbons. Ortho-, para-directing substituents often enhance fluorescence, whereas meta-directing substituents tend to increase the extent of intersystem crossing and repress fluorescence (Guilbault, 1973).

By providing strong perturbations, heavy atoms, paramagnetic ions and heteroatoms enhance intersystem crossing through spin-orbit coupling. Since the orbital angular momentum of an electron is located at the nucleus, whereas the spin angular momentum is located roughly on the electronic orbital, the spin-orbital coupling is weak unless the electron has a high probability density near the nucleus. Generally, then, only atoms with high nuclear charge (heavy atoms) exhibit appreciable spin-orbital coupling. Spin changes and hence intersystem crossing are readily brought about by the intense fields near to the nuclei of such atoms. Heavy atoms substituents can increase the rate of singlet to triplet intersystem crossing and triplet to ground state phosphorescence. Thus, when the substituent series F, Cl, Br, I is traversed for the halonaphthalenes, the ratio of the quantum yields of phosphorescence to fluorescence increases.

Paramagentic ions may quench fluorescence by forming charge-transfer complexes with potential fluorescers. The charge-transfer state may mix the multiplicities of the singlet fluorescer and the high spin paramagnetic species in the same way as spin-orbital coupling mixes the singlet and triplet states of the same molecule. Certain metallo-organic complexes contain paramagnetic ions. The strong inhomogenous magnetic field due to the paramagnetic ion is similar to that produced by a heavy atom and may likewise increase the chance of intersystem crossing.

Another process which may have a profound effect on the fluorescent properties of a compound is intramolecular energy transfer. Molecules containing more than one separate aromatic ring system may exhibit this effect and it is particularly important in proteins.

The commonest type of energy transfer is singlet-singlet transfer which involves a normally fluorescent donor whose excitation energy passes to an acceptor that may or may not be fluorescent. For energy to be transferred between different parts of the same molecule, certain spatial and steric requirements must be met and the emission spectrum of the donor must overlap the absorption spectrum of the acceptor moiety (Förster, 1951). The interaction is due to dipole-dipole coupling and does not involve the overlap of electronic orbitals. Energy transfer may therefore occur over relatively long distances up to about 100 Å.

The proximity of absorbing residues in proteins means the conditions are highly favourable for resonance energy transfer. This process, often referred to as the Förster mechanism is seen to have a considerable effect on protein fluorescence. The intrinsic fluorescence of proteins is due to the presence of aromatic amino acids. The aromatic residues phenylalanine, tyrosine and tryptophan fluoresce in water with emission band maxima at 282nm, 303nm and 348nm, respectively. However, the characteristics of protein fluorescence are extremely dependent on the structure of the protein and so cannot be fully described by simply specifying the fluophors themselves.

The fluorescence of phenylalanine is of very little importance in proteins due to its low quantum yield and efficient quenching by energy transfer to other chromophores. Class A proteins contain phenylalanine and tyrosine but no tryptophan. In these, phenylalinine fluorescence cannot normally be detected and the emission spectra are characteristic of tyrosine. Class B proteins contain tryptophan as well as phenylalanine and tyrosine. Usually the only fluorescence observed from class B proteins is that due to tryptophan. The absent or diminished tyrosine fluorescence in these proteins is probably due to energy transfer from tyrosine to tryptophan is feasible over the distances encountered in proteins.

There are, nonetheless, several other mechanisms by which tyrosine fluorescence may be quenched in proteins. These mechanisms may explain why the quantum yield of tyrosine is frequently so low in native proteins, even those containing no tryptophan. Due to the overlap of the absorption and emission spectra of tyrosine, whose maxima are centred at 280nm and 303nm, respectively, energy transfer between tyrosine residues may occur. This process is known to happen and its existence makes it possible for a nonfluorescent tyrosine to dissipate the energy of other residues. Thus it is believed that an ionized tyrosine residue can act as an effective quencher of the fluorescence of unionized tyrosines via energy transfer (Winefordner et al, 1972). An iodinated, and hence non-fluorescent, tyrosine may perform the same function. Tyrosine fluorescence quenching in proteins may also occur via peptide bonds and by hydrogen-bonded groups.

Unlike tyrosine, however, tryptophan fluorescence in proteins may have fluorescence quantum yields lower, about the same, or even higher than that of the free amino acid. This illustrates clearly how the fluorescence of aromatic amino acid residues is very dependent on the structure of the protein in which they reside. Indeed, if a single protein contains more than one tryptophan residue, the fluorescence from each may not be identical.

Much work has been performed over the last ten years in an attempt to understand the luminescence of proteins in relation to structure and conformation. The reviews of Chen (1973), Dale and Brand (1975) and Galley (1979) cover this field.

1.6.3 The Effect of Molecular Environment on Fluorescence

During electronic transitions, whether absorption or emission, the nuclei remain essentially stationary. This was the conclusion of the Franck-Condon principle. When a molecule in the ground state absorbs a photon it is promoted to a metastable excited state. This is the Franck-Condon excited state in which the molecular geometry and solvent configuration are those characteristic of the ground state. In solution at room temperature solvent reorientation follows within 10^{-12} to 10^{-11}s of excitation and produces an equilibrium state in which the solvent configuration is optimal for the geometry and electronic distribution of the excited molecule. Relaxation of the solvent molecules will tend to lower the energy of the excited state: this is shown in Figure 1.9. Thus if emission of radiation occurs, it will be from the equilibrium excited state to a Franck-Condon ground state. Relaxation of the solvent cage will take place again and return the molecule to the equilibrium ground state.

The energy differences between the Franck-Condon states and the equilibrium states depend on the nature of the interaction between the solute molecule and the solvent. If the solvent and solute are such that one is polar and one is nonpolar, or both are nonpolar, there may be only a small energy difference between the Franck-Condon and the equilibrium states. Under these circumstances the 0-0 bond in absorption and emission may be expected to be coincident, or nearly so, since the energy change is similar. Often, however, especially when both solvent and solute are polar, the energy separating the Franck-Condon and equilibrium states is relatively large. The ground and excited states involved in absorption and fluorescence are then quite different. As a

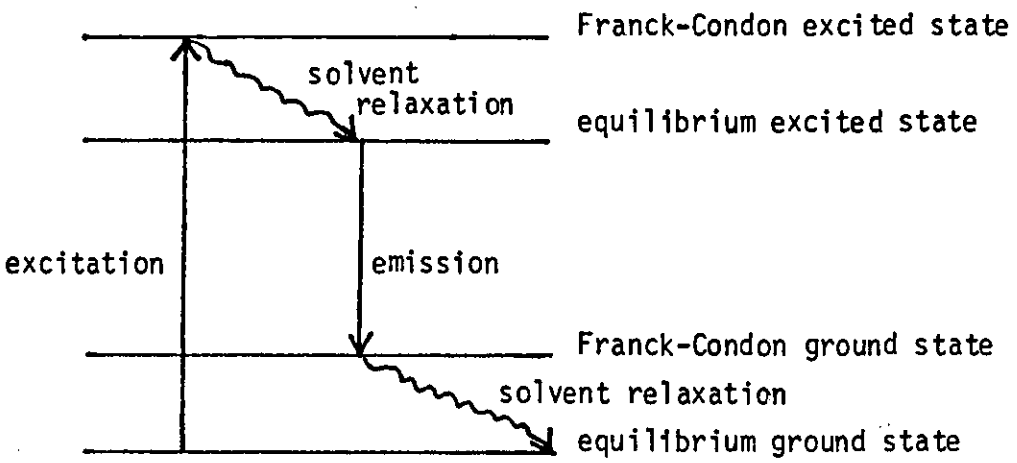
Franck-Condon excited state
solvent relaxation
equilibrium excited state
excitation
emission
Franck-Condon ground state
solvent relaxation
equilibrium ground state

FIGURE 1.9 The effect of solvent relaxation on the separation between excitation and emission frequencies.

result, the 0-0 bands in absorption and emission may be well separated.

For transitions involving (Π, Π *) states a change in solvent polarity has a characteristic effect. The ground state Π orbital is largely unaffected by the solvent polarity. On the other hand, the excited singlet state is more polar than the ground state and may drop substantially in energy. through electrostatic interaction with polar solvents. The greater the polarity of the solvent, the smaller is the energy difference between the highest occupied Π orbital of the ground state and the excited states of the molecule. Hence, (Π , Π*) transitions are shifted to lower frequencies as the dielectric constant of the solvent increases. Generally, then, the transfer of a fluorescent dye from a nonpolar to a polar solvent results in a red shift in the fluorescence emission maximum. Since the excited state interacts more strongly with the solvent than does the ground state, the spectral shift is larger in fluorescence than it is in absorption.

Direct evidence for solvent reorientation during the excited state lifetime of 2-p-toluidinonaphthalene-6-sulphonate (TNS) and 1-anilino-8-naphthalene sulphonate (ANS), both in viscous solvents and when absorbed to proteins has been obtained using the technique of nanosecond time-resolved emission spectroscopy (Brand and Gohlke, 1971). McClure and Edelman (1966) have suggested that the increased interaction between the chromophore and the solvent which accompanies solvent relaxation produces a greater number of vibrational levels in the state resulting from emission. This would account for the increase in spectral bandwidth observed in polar solvents.

For transitions involving (n, Π *) states, the effect of a polar solvent is generally more pronounced on the energy of the ground state n orbital than it is upon the excited state. The positive end of a solvent dipole exerts an attractive force on the n electrons in a solute molecule thereby lowering their potential energy. This has the effect of lowering the energy of the n orbitals relative to that of the Π orbitals. The Π orbitals being more symmetrically bound by the molecule as a whole do not experience the electrostatic interaction to a considerable extent. Although the energy of the excited (n, Π *) singlet is lowered by solvent relaxation, the decrease in energy of the ground state nonbonded orbitals accompanying electrostatic interaction with the solvent is greater. Hence the more polar the solvent, the greater is the difference between the highest occupied n orbitals in the ground state and the excited states of the molecule (n, Π *) transitions are shifted to higher frequency with increasing solvent polarity. In the limit, when the nonbonded pair enters into coordinate covalent bonding with the solvent, the energy of the n orbitals, which is transferred into a σ orbital, drops well below the energy of the occupied Π orbitals and (n, Π *) transitions are eliminated from the visible and near ultraviolet.

The generalizations than n orbitals are higher in energy than the occupied Π orbitals, and that (n, Π *) transitions always occur at lower frequencies than (Π , Π *) transitions in the same molecule therefore needs some qualification. In polar solvents (n, Π *) transitions are shifted to higher frequencies (shorter wavelengths), whereas (Π , Π *) transitions move to lower frequencies (longer wavelengths). If a solvent becomes polar enough, the (Π , Π *) transitions may actually overtake the (n, Π *) transitions and become the lowest energy band in the spectrum.

The effect of solvent polarity on the quantum yield of fluorescence is even more dramatic than the effect on the emission maxima. In molecules where the (n, Π *) state is the lowest excited singlet, fluorescence is rare and extremely weak when it does occur. As discussed in Section 1.6.2 this is a consequence of the symmetry forbideness of the transition between the excited state and the ground state. Phosphorescence is usually the most important emission in such molecules. However, because (n, Π *) and (Π , Π *) singlet states are often close together, they may be reversed in energy relative to one another by a change of solvent. An example is quinidine where the lowest excited singlet is (n, Π *) in nonpolar solvents and (Π , Π *) in polar solvents. The interchange effects the probability of intersystem crossing to the triplet and may have dramatic consequences on the relative intensities of fluorescence and phosphorescence. Thus the fluorescence of quinidine is 30 times greater in ethanol than in benzene, and 30 times greater in water than in ethanol.

Very often, however, the fluorescence of a molecule may be quenched as the solvent polarity increases. Since in polar solvents the separation between the ground state and the (Π, Π*) state is decreased, internal conversion to the ground state may be enhanced from both the lowest excited singlet and triplet states. Luminescence is quenched, and both the fluorescence and phosphorescence lifetimes are decreased, although the effect on the fluorescence lifetime is usually greater.

A further explanation for quenching in polar solvents involves the enhancement of intersystem crossing. It is to be expected that the dipole moment of the triplet state is less than that of the first excited singlet state (Jackson and Porter, 1961). In polar solvents, then, solvent reorientation may considerably decrease the separation of the first excited singlet and triplet states facilitating intersystem crossing and thereby quenching fluorescence. Seliskar and Brand (1971a) have used this mechanism to explain the low quantum yield of the N-arylaminonaphthalenesulphonates in liquid polar solvents. Additional evidence for solvent relaxation during the first excited singlet lifetime of N-(p-tolyl)-2-aminonaphthalene-6-sulphonate has been obtained by Brand and Gohlke (1971).

The arguments developed above may suggest plausible mechanisms to explain the spectroscopic properties of fluorescent probes of protein structure. These molecules fluoresce intensely when bound to proteins or when dissolved in nonpolar solvents, but have low quantum yields of fluorescence in aqueous solutions. Studies of ANS in a variety of solvents (Stryer, 1965) have supported the concept that observed changes in the fluorescence quantum yield, emission maximum and emission band width are related to the polarity of the environment around the fluorescent species and that these molecules can serve as probes for hydrophobic sites on proteins. Turner and Brand (1968) have also studied the fluorescence of N-arylaminonaphthalenesulphonates in different solvents in an attempt to quantify the relationship between polarity and fluorescence characteristics. The effect of solvent environment on the fluorescence of these compounds is discussed further in the review of Brand and Gohlke (1972).

Environmentally sensitive fluorescent probes usually contain two groups, an electron donor and an electron acceptor, attached to an aromatic ring system. A red shift of the emission maximum with increasing polarity of the solvent environment is dependent upon a large increase in dipole moment in the fluorescent state over that of the ground state. So, other things being equal, the greatest effects may be expected when the electron donor and acceptor groups are as far apart as possible in the parent molecule. With this in mind, Weber and Farris (1979) have described the synthesis, characterization and interesting spectroscopic properties of 6-propionyl-2-(dimethylamino) naphthalene (PRODAN), a compound that fulfills the above conditions. Following the same principles, Prendergast and co-workers (1983) have recently synthesized a polarity-sensitive fluorescent probe which selectively labels thiol groups in proteins.

Other factors may influence the spectroscopic properties of fluorescent molecules. For example, the fluorescence spectra of most aromatic compounds containing acidic or basic functional groups are very sensitive to alterations in the pH of the solvent. The ionizable groups can exist in solution at various stages of dissociation depending on the hydrogen ion concentration. Moreover, because ionization of the acidic or basic groups produces a considerable change in the electronic structure of the molecules which contain them, pH changes may affect both absorption and fluorescence. The ionized and unionized forms may be regarded as separate species each with their own spectral characteristics.

Hydrogen-bonding with the solvent can have profound effects on the spectra of luminescent solutes. Hydrogen-bonding may involve the ground or excited states of a molecule. In the former case both the absorption and fluorescence spectra may be affected. When hydrogen-bonding occurs after excitation, only the emission will be perturbed by the interaction. It has been seen how the luminescence of a molecule is highly dependent on whether the lowest excited singlet or triplet states are (n, Π^*) or (Π, Π^*) states. In hydroxylic solvents the (Π, Π^*) states are shifted to lower energies, while the (n, Π^*) singlets increase in energy. It is possible for a molecule whose lowest singlet is (n, Π^*) in nonpolar media to be (Π, Π^*) in hydrogen-bonding solvents. This is the case with some aromatic carbonyl compounds which are very weakly fluorescent in aprotic solvents and highly fluorescent in hydrogen-bonding solutions.

Many compounds exhibit a blue shift in their fluorescence spectra when the temperature is lowered and the solvent becomes more viscous. The increase in the energy of low temperature fluorescence compared to that at room temperature is due to the fact that the low temperature emission arises from a Franck-Condon state. At room temperature the solvent molecules reorientate themselves around the electronically excited solute molecules in about 10^{-11}s. Since the lifetime of fluorescent states is about 10^{-8}s, room temperature fluorescence is never observed from the Franck-Condon state. Nevertheless, if the temperature is lowered sufficiently, the time required for reorientation of the solvent may be greater than the lifetime of the excited state and emission from the Franck-Condon state may be observed.

The low temperature blue shift in fluorescence is, in fact, an effect of viscosity rather than temperature. A similar blue shift in room temperature fluorescence can be obtained for compounds embedded in rigid matrices. Thus the importance of solvent relaxation is supported by the finding that the fluorescence of TNS in ice resembles that in organic solvents (Seliskar and Brand, 1971a). Although the dye is surrounded by polar molecules in ice, they are not free to relax during the lifetime of the excited state. Similarly, the emission maximum of TNS in glycerol is temperature dependent (Seliskar and Brand, 1971b), shifting to the red (lower energy) with increasing temperature. Not surprisingly, at about 300°K where the relaxation time of glycerol is similar to the fluorescence lifetimes of N-arylaminonaphthalenesulphonates, the emission spectrum of TNS is particularly temperature-sensitive.

The rates of radiationless decay of electronically excited molecules in solution are also temperature dependent. The probability of deactivation of the excitation energy through collisions of the excited species with the solvent, or with other solute molecules, rises as the temperature of the medium increases. In fact the long lifetime of phosphorescence makes it so susceptible to competition from radiationless processes that this type of emission is not normally obtained in solution at room temperature. It is usually necessary to employ rigid media at very low temperatures in order to detect phosphorescence. Similarly fluorescence intensities increase at low temperatures. Moreover, luminescence spectra in rigid media at low temperatures often show well-resolved vibrational structure. In solution at room temperature such structure is lost due to collisional processes.

The effect of temperature is clearly complex due to the separate temperature dependent factors of diffusion, intramolecular energy conversion, excited state processes such as hydrogen-bonding with the solvent, and the effect of temperature on equilibria in solution.

Important spectroscopic characteristics including the quantum yield of fluorescence, may show a concentration-dependence. At low concentrations, the fluorescence intensity of a given solute may increase linearly with concentration. At high concentrations the fluorescence may reach a maximum and even decrease with further increases in concentration. Several processes may be responsible for this 'concentration quenching.'

The low frequency tail of the absorption spectrum of a solute may overlap the high frequency end of its fluorescence spectrum. The fluorescence emitted by an excited state molecule may therefore be reabsorbed by a ground state molecule of the same solute. The magnitude of the effect increases with rising solute concentration. The self-absorptive process can appreciably distort the shape of the emission band.

Many ground state aromatic molecules may form dimers or aggregates in particular solvents. The tendency to form dimers increases at high concentrations, and if the dimer is less fluorescent than the monomer, the overall fluorescence will be quenched. It is also possible for an electronically excited molecule to form an excited dimer, or excimer, with a ground state molecule of the same solute. So, in some cases, as the solute concentration is increases a gradual dissapearance of the initial fluorescence and the appearance of a new spectrum is observed.

Dimer and excimer formation can also occur between different solute molecules. When a complex forms between a luminescent species and a quencher, an excimer of mixed character is produced and the process is called collisional quenching. It occurs at, or near the diffusion controlled rate and is strongly dependent upon the viscosity of the medium. Collisional quenching is normally rendered negligible by adjusting the solution so that no solute is present at a concentration greater than about 10^{-3}M. Many quenching reactions involve specific interactions between the fluophor and a quenching agent. For example, heavy atoms in a solvent may quench the fluorescence of a solute molecule by increasing singlet to triplet intersystem crossing and phosphorescence when the solute interacts with the solvent sheath.

Intermolecular energy transfer provides another pathway by which the emission of a fluophor may be quenched in solution. Intermolecular energy transfer may be significant for high concentrations of donor and acceptor molecules but diminishes with dilution of the solution. This is so because with dilution the average intermolecular distance may increase beyond the range of dipole-dipole coupling. When two absorbing species are combined into a single molecule, the probability of energy transfer, which is then an intramolecular process, increases enormously. If the combination is such that the two parts of the molecule are within the range of dipole-dipole coupling, then the phenomenon of energy transfer will always be observed even in very dilute solutions.

It has been seen how simple self-absorption can effect the emission spectrum of a fluorescent compound. When other compounds are present in solution which absorb a significant proportion of the excitation or fluorescence radiation, the observed fluorescence may be diminished by what is known as an inner-filter effect. The non-specific trivial attenuation of the exciting or emitted beam is usually significant only if the concentration of an interfering species is sufficiently large for its absorbance to be greater than about 0.005.

1.6.4 Practical Aspects of Fluorescence Spectroscopy

For dilute solutions the intensity of the fluorescence emission is directly proportional to the concentration of the fluorescent species. In concentrated solutions the linear relationship between fluophor concentration and fluorescence intensity may break down because of inner-filter effects or concentration-dependent self-quenching mechanisms.

The quantity of fluorescence which is emitted by a sample is dependent on the intensity of the absorbed radiation multiplied by the quantum efficiency of fluorescence. So for any given concentration of analyte, the strength of the measured fluorescence signal may be increased simply by raising the level of the exciting radiation. Powerful light sources are therefore used in fluorimetry to ensure good sensitivity. Very intense sources, however, may produce photodecomposition of the sample. In absorptiometry the signals which are measured are often larger than those detected in fluorimetry; the intensity of the radiation emitted by a molecule is less than that which is absorbed. Nevertheless, for many organic compounds, luminescence methods are considerably more sensitive than absorptiometric procedures. This may be explained in terms of the manner in which the signals are measured.

In absorptiometry the detector must distinguish a small difference between two large signals, each of which may contain an appreciable noise level. On the other hand, in fluorimetry the detector need only measure a small signal against a zero, or perhaps, very small background noise. This is feasible because fluorescence is emitted in all directions and the detector may be positioned at an angle to the incident beam. Thus the sensitivity of fluorimetry is often 10 to 1000 times greater than that of absorptiometric methods.

In contrast, curvature of the analytical curves at high concentrations is a more severe problem in fluorimetry than it is in absorption spectroscopy. Consequently, absorptiometry is generally the preferred technique for high and intermediate concentrations of absorbers.

Apart from their greater sensitivity, luminescence methods have another useful quality. This is their high selectivity. Many molecules that absorb radiation have no emission spectra. Thus there are inherently fewer interferences when a luminescence rather than an absorptiometric method is employed. In addition another parameter may be used to enhance selectivity. In luminescence measurements both excitation and emission wavelengths can be selected to minimize interferences whereas in absorptiometry only the wavelength of absorption is variable.

Phosphorescence may be even more selective than fluorescence since phosphorescence decay times offer an additional parameter for differentiating between two phosphorescent species. This forms the basis of time-resolved phosphorimetry. Recently, however, techniques have become available for performing analysis using time-resolved fluorimetry.

Larger bandwidths are possible in phosphorimetry than in fluorimetry because scattering problems are essentially nonexistent in the former but relatively severe in the latter. Consequently the sensitivity of phosphorescence methods is often greater than for fluorescence methods. The disadvantage of phosphorimetry is that it is far more complicated experimentally than either fluorimetry or absorptiometry.

As a result of Franck-Condon considerations, absorption spectroscopy can yield information on only the average ground state of molecules which absorb light. Only solvent molecules which are immediately adjacent to the absorbing species can affect its absorption spectrum. Thus absorption spectroscopy is not sensitive to molecular dynamics. In contrast, fluorescence spectroscopic parameters are sensitive functions of dynamic processes which occur during the lifetime of the excited state and these processes can involve other molecules which are over 10nm away from the fluorphor at the moment of excitation. The lifetime of fluorescence emissions (10^{-7} to 10^{-9}s) is a long time relative to the motions of small molecules in fluid solution, and it is a time span which is comparable to the rotational diffusion of proteins and membrane-bound fluorescent probes. Thus fluorescence spectroscopy can reveal the dynamic properties of proteins, membranes and nucleic acids on the nanosecond timescale (Lakowicz, 1980; Horie et al, 1982).

A block diagram showing the essential components of a typical fluorimeter or spectrofluorimeter is given in Figure 1.10. The source of the exciting radiation is usually provided by an arc lamp. A shutter is included in the incident light path so that irradiation of the sample can be restricted to the period of measurement. The desired wavelength region of excitation may be selected by means of the excitation monochromator.

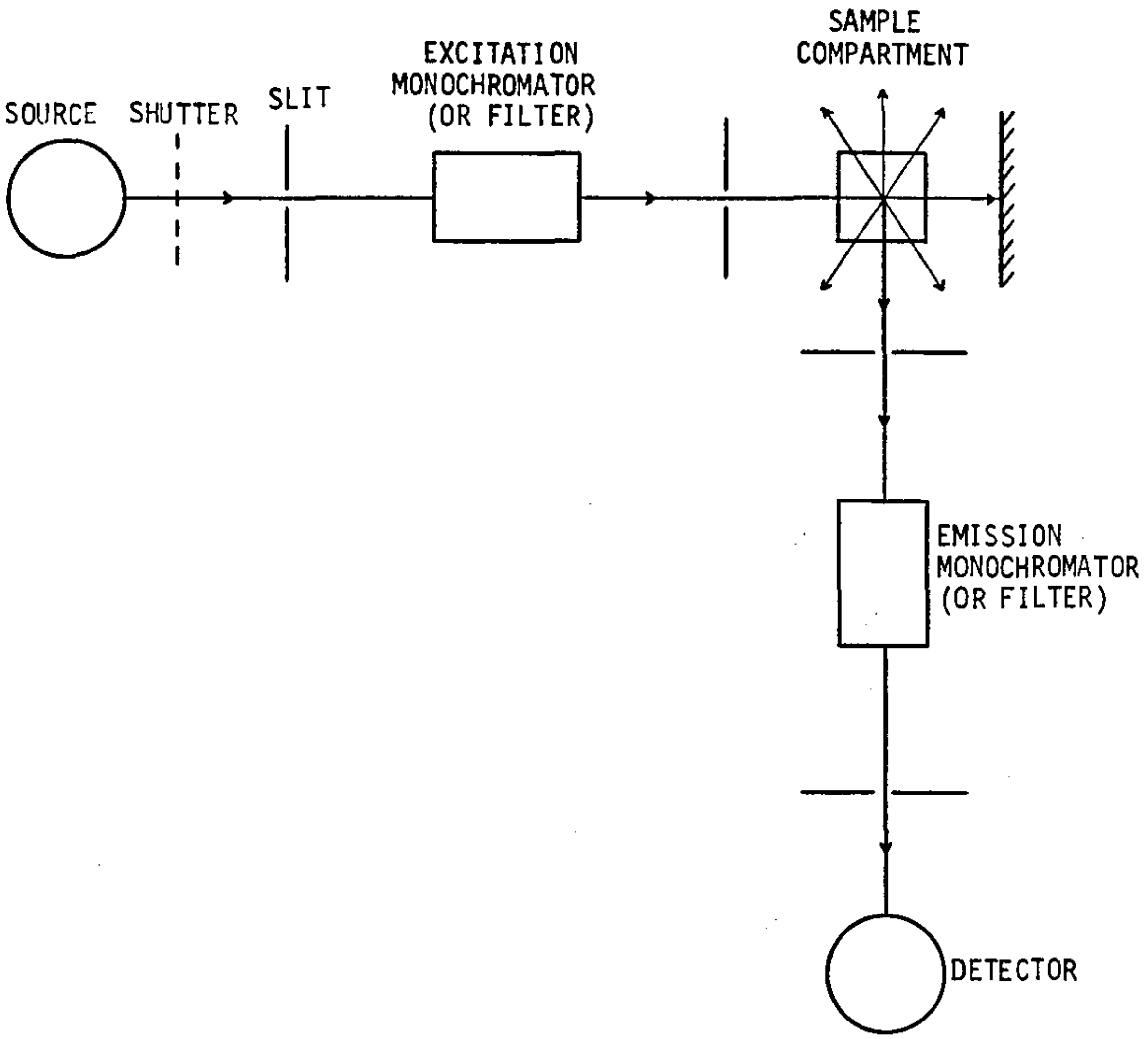
SAMPLE
COMPARTMENT
EXCITATION
MONOCHROMATOR
(OR FILTER)
SOURCE
SHUTTER
SLIT
EMISSION
MONOCHROMATOR
(OR FILTER)
DETECTOR

FIGURE 1.10 Major Components of an Instrument for Measuring Fluorescence.

Fluorescence is emitted by the sample in all directions but only a portion of the emission is sampled by the detection system at some angle, usually 90°, from the axis of the exciting beam. The detection system consists of an emission monochromator which selects the wavelength region of the fluorescence emission to be measured; a photomultiplier which converts the fluorescence radiation into an electrical signal; and the amplifier-readout system. The latter amplifies and processes the electrical signal as required and displays it in a convenient form. Often one or more choppers are placed in the light paths in an attempt to decrease the effect of signal noise. The simpler instruments use optical filters in place of monochromators and are called filter fluorimeters. The more versatile spectrofluorimeters employ grating or prism monochromators. The term 'photo' sometimes appears in the naming of luminescence instrumentation and implies photoelectric detection of the emitted radiation.

Equipment should provide reasonably high spectral resolution, sensitivity and signal-to-noise ratio over the desired wavelengths of excitation and emission. Spectral resolution is a function of the design and adjustment of the monochromator system, or, in filter instruments, the choice of filters. Most noise arises from the radiation source, the detector and to a lesser degree, the amplifier-readout system.

A spectrofluorimeter is capable of scanning the wavelength spectrum continuously and usually automatically. A fluorimeter is always a manual instrument best suited for measurements at fixed wavelengths, a change in filter being required each time the wavelength is altered. The spectrofluorimeter, having two monochromators, can therefore measure both excitation spectra in which the intensity of the fluorescence band is recorded as a function of the wavelength of the exciting light, and emission spectra in which the fluorescence intensity is measured as a function of the emission wavelength for a fixed wavelength of excitation. For analytical purposes the emission spectrum is normally used, although it is standard practice to run an excitation spectrum to select the optimum excitation wavelength.

The intensity of the radiation source and the response of the detector are both wavelength dependent. Hence, the exact shapes of the recorded excitation and emission spectra will rely upon the precise characteristics of the instrument used to make the measurements. The spectra, termed apparent or uncorrected spectra, may be grossly distorted versions of the true spectra. It is possible, however, to make allowances for the source and detector characteristics and to generate true, that is, corrected spectra (Parker and Rees, 1960).

There are also a number of problems associated with the application of fluorimetry to quantitative analysis. Light scattering in particular may seriously limit the sensitivity and reproducibility of a fluorescence assay. Rayleigh scattering is commonly encountered in fluorimetry and occurs at the same wavelength as the incident radiation. This type of elastic scattering takes place in all directions with respect to the incident radiation and has a relatively symmetrical intensity distribution. The intensity of the Rayleigh scattering, however, varies as the inverse fourth power of the wavelength of the incident radiation and so becomes increasingly significant at short wavelengths.

For Rayleigh scattering to occur the scattering centres must have dimensions much smaller than the wavelength of the incident radiation and be distributed in a medium of refractive index different from their own. Thus, in measuring the fluorescence of solutions, Rayleigh scattering is often observed from both solvent and solute molecules.

Light scattering may also arise from particles in the colloidal range of sizes, where the particulate matter has dimensions greater than a tenth but less than about one and a half times the wavelength of the incident radiation. This is Tyndall scattering. In contrast to Rayleigh scattering, the characteristic intensity pattern for large particle scattering is predominantly in the forward direction. Indeed, for very large particles only well-defined refracted and reflected beams remain.

In general, then, light scattering is relatively non-specific and may be exhibited by sample containers, optical surfaces and dust particles, as well as by the solvent and solute molecules of the sample. So while electronic excitation is a selective process and produces relatively few excited molecules, light scattering may occur from a large proportion of the molecules in solution.

Rayleigh-Tyndall scattering may be a problem in fluorimetry especially when absorption and fluorescence peaks are close together and when the intensity of fluorescence is low compared to the intensity of the exciting radiation. The effects of scattered radiation may be diminished by narrowing monochromator slit widths on both the excitation and emission side or by introducing a secondary cut-off filter. With spectrofluorimeters it is sometimes worthwhile to reduce the overlap of scattered and fluorescence peaks by lowering the wavelength of excitation and/or increasing the wavelength at which the fluorescence is measured. The geometry of the cell and cell holder may greatly influence the amount of scattered radiation incident on the detector; thus, it is common practice to measure the emitted radiation at right angles to the exciting beam.

An effect related to Rayleigh scattering may also give rise to spectral interferences in the measurement of fluorescence. Raman scatter is observed from many pure solvents. Raman bands are displaced by a fixed frequency from the incident radiation irrespective of the wavelength of excitation. This displacement arises because during the Rayleigh scattering process some of the incident energy may be abstracted and converted into vibrational or rotational energy. As a result of the inelastic process, the radiation that is scattered has a correspondingly lower energy than the incident radiation and is called the Stokes Raman band. On the other hand, a small proportion of the molecules encountered by the incident radiation will already be in higher vibrational and rotational energy states and may contribute this extra energy to the scattered photons. This leads to scattered radiation of higher energy than the incident beam and it is termed anti-Stokes Raman scatter. The difference in frequency between the Raman bands and the exciting radiation is characteristic of the irradiated molecule and corresponds with certain vibrational and rotational frequencies of that molecule. The Raman bands are usually much fainter than the corresponding Rayleigh scatter peak. Of the the two types of Raman band, the longer wavelength satelite is by far the more intense.

Raman scatter is of primary concern in fluorimetry when it occurs in the same region of the spectrum as a fluorescence peak. Although usually sharper than fluorescent bands, when monochromator slits are narrower Raman peaks can be mistaken for part of the analyte spectrum. When it occurs at a slightly shorter wavelength than fluorescence, troublesome Raman scatter may be minimized by the use of a suitable emission cut-off filter which removes all wavelengths below and including the Raman band. A better separation of the Raman and fluorescence peaks is achieved in a spectrofluorimeter when the excitation wavelength is lowered. This produces a corresponding shift in the Raman peak to a shorter wavelength, but since the wavelength of fluorescence is independent of the wavelength of excitation, the fluorescence becomes separated from the Raman scatter.

Both Rayleigh-Tyndall and Raman scatter differ from fluorescence in their degree of polarization and can be removed from fluorescence spectra by the proper use of polarizers. Thus, although they may diminish the measured signal somewhat, polarized filters may increase the sensitivity of fluorimetry for certain quantitative analyses (Lim et al, 1978).

Another practical problem encountered in analytical fluorimetry is the well-known inner-filter effect. Although it has no influence on the primary process of emission from excited state molecules, it may lead to a serious reduction in the intensity of the observed fluorescence through absorption of the excitation or emission radiation within the sample itself. The phenomenon is responsible for the distortion of otherwise linear calibration plots of observed fluorescence intensity versus concentration. Since inner-filter effects operate through the absorption of radiation within the sample, the distortion of analytical curves becomes more marked at high concentrations of fluophor where the absorption is high. As a self-absorption process, the effect is clearly dependent on the light paths through the sample and can be controlled experimentally by a suitable adjustment of the sample cell geometry. Absorption may be reduced by minimising the path-length through the sample for both the excitation and emission beams. This is commonly achieved by placing the cell excentrically within the sample compartment and allowing the incident or emitted radiation to pass through only a portion of the sample cell. For highly concentrated solutions it is possible to increase the linear concentration range by the use of microcuvettes.

Front-surface illumination of samples in fluorimetry has been employed in attempts to minimise the problems of inner-filter effects. Unfortunately the application of this technique is often limited by difficulties associated with light scattering and background fluorescence. Methods for the correction of fluorescence measurements for inner-filter effects have been described by Mertens and Kägi (1979) and Christmann et al (1980). Due to the temperature sensitivity of fluorescence, it may be necessary to ensure that the sample is maintained at a constant temperature prior to measurement. For accurate work thermostated cell holders may be required.

A final practical consideration concerns the stabilization of the recorded fluorescence intensities. Even with fixed instrumental settings the recorded signal may vary with time. This variation is normally due to instrumental drift and necessitates the use of stable fluorescent standards in quantitative analysis. The standards are used to detect and monitor changes in the instrumental response.

1.7 Mathematical Models and the Graphical Representation of Binding Data

As discussed in Section 1.5, many studies are concerned with drug-protein systems at equilibrium and with the determination of the degree of binding as a function of the composition of the sample. This is so because in principle it is possible to determine the number of classes of binding sites, the number of sites in each class, and the affinity constant of each class from estimations of the free and bound fraction of the ligand. In practice, however, the analysis of binding data is a fundamental problem and the focus of much current research.

Clearly, the model which best describes the collected data must be sought. It is preferable if the model is an accurate reflection of a real biochemical or biophysical process, but it may simply be a mathematical tool for interpolating data. There should be sufficient experimental data to generate precise estimates of the parameters of the model. Within the constraints of the model, efforts should be made to interpret these parameters in physiochemical terms such as those described above. The aim of this section is to discuss the theory and application of some mathematical models of drug-protein binding.

Consider the general case of the completely reversible association of a ligand A with n unoccupied, prexisting sites of a macromolecule P, each site being capable of interacting with the ligand. Assume initially that activities are equal to concentrations and all sites interact independently with the ligand A. The kinetic reaction for an individual binding site is described by

$$P + A \underset{k'}{\overset{k}{\rightleftharpoons}} PA$$

and can be characterized by the differential equation

$$\frac{d\,[PA]}{dt} = k\,[P]\,[A] - k'[PA]$$

where [ ] denotes molar concentration; and k and k' are the rate constants of the forward and reverse reactions. At equilibrium $\frac{d[PA]}{dt} = 0$ and the intrinsic microscopic association constant is

$$K_1 = \frac{k}{k'} = \frac{[PA]}{[P][A]}$$

K_1 in this case is also called the apparent association constant or the Scatchard association constant. The fraction of occupied sites is

$$r_1 = \frac{[PA]}{[P] + [PA]} = \frac{K_1 [A]}{1 + K_1 [A]}$$

where r_1 and $[A]$ are the variables that are usually measured. This equation also defines the probability that a ligand binds to a given site.

Since it is assumed that all the binding sites are independent and equivalent, the probabilities may be summed over the n sites to obtain the average number of molecules bound,

$$r = \sum_{i=1}^{n} r_i \quad \frac{n \ k_1 [A]}{1+k_1 [A]} \qquad (1.1)$$

If there are m classes of sites, all of which are independent but not equivalent then for each class i having n_i sites with an apparent association constant k_i, equation 1.1 can be generalized so that

$$r = \sum_{i=1}^{m} \frac{n_i \ k_i [A]}{1+k_i [A]} \qquad \text{or}$$

$$r = \frac{n_1 k_1 [A]}{1+k_1 [A]} + \frac{n_2 k_2 [A]}{1+k_2 [A]} + \cdots\cdots + \frac{n_m k_m [A]}{1+k_m [A]} \qquad (1.2)$$

This is called the generalized Scatchard model (Scatchard, 1949) and assumes that the binding of a drug molecule at one site does not influence the binding at another site. This model has been applied very widely to calculate the classical binding parameter n_i, k_i and m_i.

The difficulty with the Scatchard model is that a number of the fundamental assumptions used in its formulation are open to question. For example, the Scatchard analysis assumes that all of the binding sites exist initially and compete independently for available ligands. This is inconsistent with observations that the binding of certain organic ligands to albumin produces conformational changes in which binding sites are altered or formed (see Section 1.4.3). In the case of ionized drugs, a modification of binding may arise when there is a resultant overall change in the electrostatic environment of the protein which affects the binding of further drug molecules.

From a theoretical viewpoint, the stepwise multiple equilibria model is the most satisfactory theory on which to base the analysis of drug-protein binding data. The binding of a ligand to a macromolecule that contains no subunits can be described as a sequence of n stepwise equilibrium reactions (Klotz, 1953) where

$$\begin{array}{lcllcl}
P + A & \underset{k_1'}{\overset{k_1}{\rightleftharpoons}} & PA_1 & K_1 & = & \dfrac{[PA_1]}{[P]\,[A]} \\[2ex]
PA_1 + A & \underset{k_2'}{\overset{k_2}{\rightleftharpoons}} & PA_2 & K_2 & = & \dfrac{[PA_2]}{[PA_1]\,[A]} \\
\vdots \quad \vdots & & \vdots & \vdots & & \\
PA_{n-1} + A & \underset{k_n'}{\overset{k_n}{\rightleftharpoons}} & PA_n & K_n & = & \dfrac{[PA_n]}{[PA_{n-1}]\,[A]}
\end{array} \qquad (1.3)$$

This model does not presuppose the existence of n fixed sites, but only that n associations of a ligand to a macromolecule can occur sequentially. Clearly such a model is not based upon the assumption that the 'sites' bind independently. In fact, additional sites can be created or eliminated by the process of binding to an existing site. Thus the model can incorporate cooperative binding effects.

Since the number of moles of bound ligand equals the number of moles of PA, plus twice the number of moles of PA , and so on, the weighted average of the number of ligands bound per mole of macromolecule can be written as

$$r = \frac{[PA_1] + 2\,[PA_2] + \cdots\cdots + [PA_n]}{[P] + [PA_1] + [PA_2] + \cdots\cdots + [PA_n]}$$

Thus in view of equation (1.3)

$$r = \frac{K_1[P][A] + 2K_1K_2\,[P][A]^2 + \ldots\ldots + n(K_1K_2\ldots K_n)\,[P][A]^n}{[P] + K_1[P][A] + K_1K_2[P][A]^2 + \ldots\ldots + (K_1K_2\ldots K_n)\,[P][A]^n}$$

or

$$r = \frac{K_1[A] + 2K_1K_2[A]^2 + \cdots\cdots + n(K_1K_2\cdots K_n)\,[A]^n}{1 + K_1[A] + K_1K_2[A]^2 + \cdots\cdots + (K_1K_2\cdots K_n)\,[A]^n} \qquad (1.4)$$

This is the generalized equation for the extent of binding according to the theory of multiple equilibria (Klotz, 1953).

The Scatchard model and the sequential equilibria model appear to be quite different. The classical thermodynamic analysis of binding (Klotz, 1946; Klotz, 1953), which forms the basis of the stepwise multiple equilibria model, does not depend on any recognition of specific sites. The stepwise binding constants so obtained express the equilibria in purely stoichiometric terms and may have no meaning as actual site-binding constants (Klotz, 1983). It has long been acknowledged, nonetheless, that the stoichiometric (also known as macroscopic or classical) binding constants must be related to the site (or microscopic) binding constants for certain systems. General relationships between stoichiometric and site binding constants have been described for a multisite system by Fletcher et al (1970). Using these relationships, and supposing that n sites prexist and that all of these n sites have the same intrinsic microscopic association constants, it can be shown that the general stepwise equilibria model, equation 1.4, contains the Scatchard model, that is equation 1.2, as a special case (Fletcher et al, 1970; 1973; Klotz, 1953).

Despite the fact that most laboratories have easy access to computing facilities, the graphical representation of binding data has lost none of its appeal. The earliest approach to the plotting of protein binding data was the adsorption method by Freudlich (1907) and Langmuir (1917) where r is plotted against [A]. This approach is unsatisfactory since curved plots result and large changes in binding at high drug:protein ratios result in only a small alteration in curvature. The most commonly used representations employ various linear transformations of equation 1.1: three examples are shown below.

$\frac{1}{r} = \frac{1}{nk_1}\,\frac{1}{[A]} + \frac{1}{n}$ (1.5), the double-reciprocal plot (Klotz,1946);

$\frac{[A]}{r} = -\frac{1}{n}\,[A] + \frac{1}{nk_1}$ (1.6), (Klotz, 1953);

$\frac{r}{[A]} = -k_1 r + k_1 n$ (1.7), the Scatchard plot (Scatchard, 1953).

The graphical equivalents of equations (1.5), (1.6) and (1.7) are shown in Figure 1.11 (a), (b), and (c) respectively, and are particularly useful when fitting equation 1.1 to experimental data. Some less frequently used graphical representations are discussed by Bridges and Wilson (1976).

Equation (1.1) applies only to a single class of independent binding sites with the same intrinsic binding constant. When there are two or more independent classes of sites, or interacting sites, the functions represented by the coordinates in Figure 1.11 will no longer give linear graphs. It may still be possible to determine the limiting slopes and intercepts on the coordinate axes for the curves but the relation of these graphical parameters to the site binding constants is not what seems to be commonly assumed on intuitive grounds. The general expressions for the graphical parameters have been derived by Klotz and Hunston (1971), nevertheless the widespread misinterpretation of curved binding plots still pervades the literature on drug-protein binding. Norby et al (1980) reviewed 50 publications which contained various errors of graphical construction: many authors continue to use incorrect methods to estimate binding constants. Some of the more common mistakes are discussed below.

In a large number of studies authors have based their conclusions on insufficient and sometimes rather imprecise data. Straight line graphs have been fitted by eye or by least-squares methods to a few scattered points covering only a small fraction of the binding isotherm. The number of binding sites and the apparent association constants have been derived from the intercepts on the axes. Unfortunately, to obtain proper estimates of the binding constants, reliable measurements must be available over an extensive range of ligand concentrations. Klotz (1982) has recently pointed out the problems of calculating the total number of binding sites from Scatchard plots and suggested that it is better to estimate this parameter from a semilogarithmic plot of bound ligand concentration versus the logarithm of free ligand concentration; the advantage of the semilogarithmic plot is that interpretation of the characteristic sigmoidal curve matches it imperative to take measurements over a wide range of ligand concentration. A particular problem encountered with the interpretation of curved Scatchard plots was highlighted by the survey of Norby et al (1980): many authors appeared to have preconceived ideas urging them to obtain limiting intercepts corresponding to whole numbers on the abscissa. Since the intercept on the abscissa represents an n-value only in extreme cases (Klotz and Hunston, 1971), the dangers of subjective influencies on

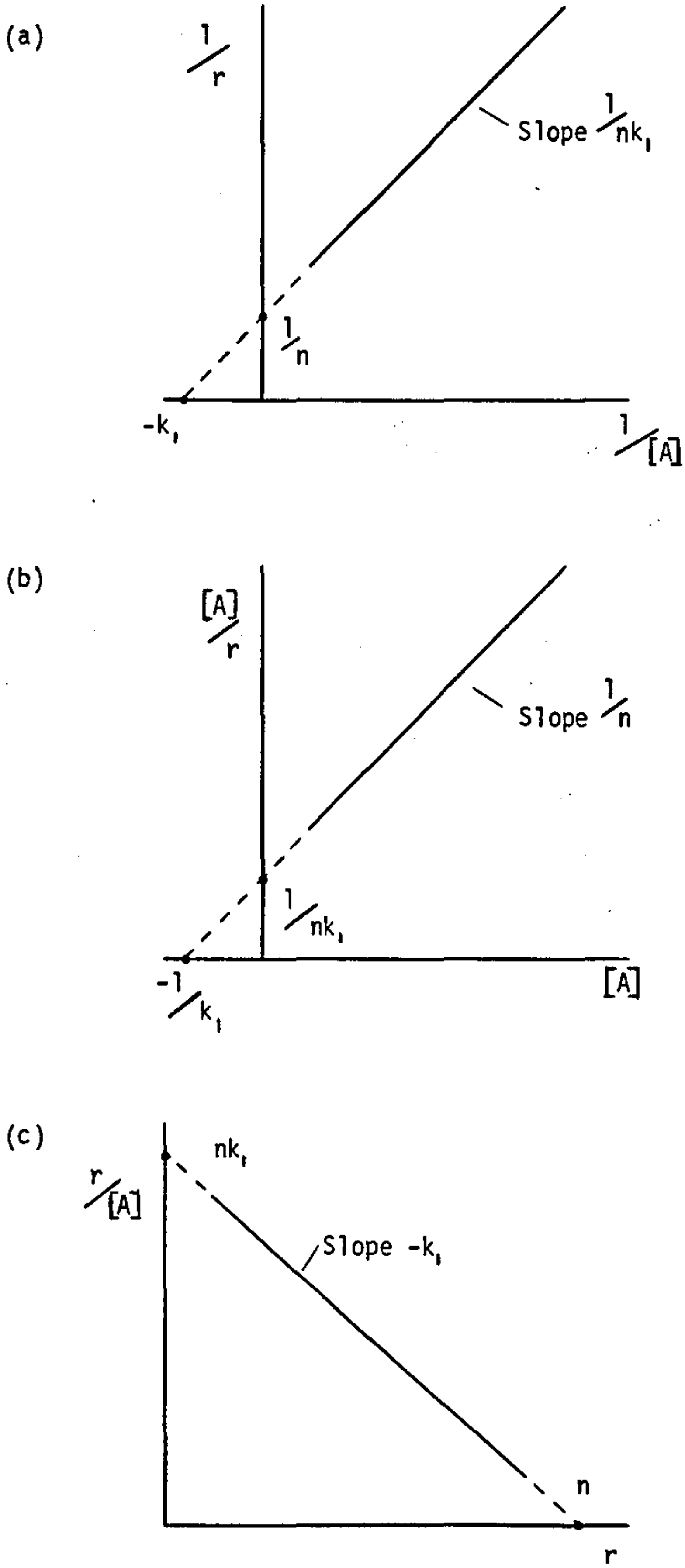

FIGURE 1.11 Graphical Representation of Three Commonly Used Linear Transformations of the Binding Equation for a Single Site or a Single Class of Sites.

The slopes and intercepts of the straight lines are indicated.

the decomposition of the plot are clear.

Manual procedures have been developed for fitting the parameters of the Scatchard model to sets of experimental data when more than one class of binding sites exist (Rosenthal, 1967; Pennock, 1973). Although theoretically sound, the manual graphical methods for determining binding parameters in complex systems are tedious and rather subjective. Fletcher et al (1973) have used a computerized method for accomplishing a least squares fit of the generalized Scatchard model to experimental data. A flexible curve-fitting program which uses a nonlinear least squares procedure has been developed by Munson and Robard (1980) to analyse the results of ligand binding studies; the analysis is based, in part, on the theoretical considerations of Feldman (1972). The report of Feldman (1972) includes graphical methods for the estimation of binding parameters from the Scatchard curve in those cases where the curve reduces to a hyperbolic form, and computational methods for fitting parameters to experimental data from more complex ligand-binding systems.

Although it is possible to resolve non-linear Scatchard plots into two or more independent components by fitting the generalized Scatchard model (equation 1.2) to the data, the curvature of the binding plots may be due to cooperative interactions rather than to the presence of several classes of independent binding sites. In these circumstances, the assumptions inherent in the Scatchard model have been violated and the Scatchard constants derived from the curve-fitting procedure are not meaningful as binding constants. Thus, the mechanism of the binding process need not necessarily satisfy the Scatchard assumptions even though the data are adequately fitted by the Scatchard model.

The slope of a Scatchard plot of the data may, however, reveal useful information about the form of the binding model that should be chosen for fitting the data. It can be shown that the slope of the Scatchard plot is always negative (Fletcher et al, 1973), that is, the data on the Scatchard plot must have an everywhere negative slope if this model is to be fitted. Therefore, if the Scatchard plot of the data has a slope that is non-negative over any range of its values, only the stepwise form of the model can be applied. On a plot of $\frac{r}{A}$ versus r, a positive slope signifies that as ligand binds to the macromolecule the probability of more ligand binding increases: this is the phenomenon of positive cooperativity, an allosteric effect on the binding process. José and Larralde (1982) have presented a qualitative graphical analysis of the sensitivity of the Scatchard plot to site-site interactions based on a computerized simulation of the stepwise binding model of Klotz (1953). They have shown that Scatchard plots may aquire very unusual shapes with several inflection points when there is a mixture of positive and negative intramolecular interactions.

Since the stepwise model is completely general and applies to all multiple equilibrium reactions, even when a variety of cooperative effects are present, it is an extremely powerful theory on which to base the analysis of drug-protein binding data. However, when n is greater than 2 in equation 1.4, fitting this equation by means of a non-linear curve-fitting procedure requires reliable starting estimates for the stoichiometric binding constants. Fletcher and co-workers (1970 ; 1973) have proposed a practical means for fitting binding data to the stepwise equilbria model. An initial indication of the nature of the binding can be obtained from the Scatchard plot of the data. If the data indicate an everywhere negative slope, the results can be fitted to the generalized Scatchard model. This does not imply that the assumptions in the generalized Scatchard model are satisfied but only that it can not be distinguished from the stepwise model at this point. The mathematical equivalence of the stepwise and Scatchard models means that approximate values of the stoichiometric binding constants can be derived from the parameters of the Scatchard model. These estimates are then refined by a least-squares fitting procedure which analyses the data in terms of the stepwise equilibria constants. Whenever the Scatchard model is not applicable, for example when the Scatchard plot has a positive slope in some region, the starting estimates of the stiochiometric binding constants must be obtained by trial and error or from other independent information.

Although the stepwise multiple equilibria model is more general than the independent-site model (the basis of the Scatchard plot), in that no a priori assumptions are made about the existence or nature of the binding sites, the amount of physical insight that can be obtained from the stepwise equilibrium constants is limited. Furthermore, whenever the assumptions of the Scatchard model are not violated, the microscopic (or site) binding constants represent the true association constants.

Monot et al (1983) have considered difficulties in applying the Scatchard model of ligand binding to proteins. The problems encountered in applying the stepwise equilibria model are as formidable. A practical limitation associated with the use of these models stems from the large numbers of parameters they contain. A great deal of highly accurated experimental data is required to estimate the values of even a small number of the binding parameters. It is often meaningless to fit anything more complicated than a two-site Scatchard model to a set of data; this model contains four unknowns n_1, n_2, k_1 and k_2. Monot et al (1983) propose other models with only two parameters, but despite the simplification they bring to curve-fitting, these models are primarily mathematical tools and offer no insight into the binding process.

It can be argued that the Scatchard plot, the double-reciprocal plot and the like are of limited value in representing drug displacement interactions since they display only one drug and can be potentially misleading. When both drugs are present at approximately the same concentration and both occupy a substantial fraction of the available binding sites, then the mutual displacement of each drug should be considered. Aarons et al (1979) have proposed that a superior method of analysing drug displacement interactions is in terms of the stepwise equilibria model and discusses the considerable numerical problems associated with the fitting of this kind of model to experimental results. Interpretation of the significance of the stepwise equilibrium constants may also be difficult. The same authors have experimented with a different kind of representation of drug displacement interactions. This involves a three dimensional plot in which the abscissa are the total concentrations of the two drugs and the ordinate is the unbound concentration of either drug (Aarons et al, 1979). As pointed out by Rowland (1980), when there are more than two species interacting at a common binding site, a quantitative interpretation of the underlying events is virtually impossible.

There clearly remain several theoretical and practical difficulties associated with the analysis of drug-protein binding data. The limitations of the different models of analysis must be appreciated if binding experiments are not to be misinterpreted.

CHAPTER 2

Materials and Standard Experimental Methods

This chapter describes the basic procedures which were followed repeatedly during the practical work. More specific and non-routine methods are discussed fully in later chapters.

2.1 Chemicals

2.1.1 Source and Pretreatment

Human serum albumin, or HSA, of 100% electrophoretic purity was purchased from Hoechst. No attempt was made to remove fatty acids from the commercial preparation.

Warfarin, phenylbutazone, ethacrynic acid, 2-p-(chlorophenoxy)-2-methyl propionic acid (CPMP), and the sulphonamide drugs sulphisoxazole, sulphamerazine, sulphadiazine, sulphapyridine and sulphisomidine were produced by the Sigma Chemical Company and flufenamic acid by Parke, Davis and Co. They were used without further purification.

The ammonium salt of 8-anilino-1-naphthalene sulphonic acid (ANS) was obtained from Sigma Chemical Co. It was purified by several recrystallizations from saturated magnesium chloride solutions following the procedure used by Dodd and Radda (1969). The green crystals of the magnesium salt, $(C_{16}H_{12}NSO_3)_2Mg \cdot 2H_2O$, were dried in an oven at 110°C for 24 hours to yield the stock reagent (see Figure 2.1 for chemical structural formulae).

Quinine sulphate and Tris, that is, Tris-(hydroxymethyl)-methylamine, were manufactured by B.D.H. Chemicals Ltd. Aristar grade Tris was used in fluorimetry. Other laboratory reagents were of analytical grade.

2.1.2 Preparation of Solutions

Unless otherwise stated, solutions were made up in 0.1M Tris-HCl buffer at pH 7.40. The buffer was prepared using good quality double-distilled water that had been collected in glass. The pH was adjusted with a small quantity of concentrated hydrochloric acid. Those drugs having low water-solubilities were first dissolved in small volumes of ethanol or 0.1M sodium hydroxide before making up to the required concentrations in the aqueous buffer. To avoid frothing of the solution and a possible denaturation of the protein, albumin was carefully dissolved in the buffer with little or no stirring.

Quinine sulphate solutions were produced in 0.05M sulphuric acid.

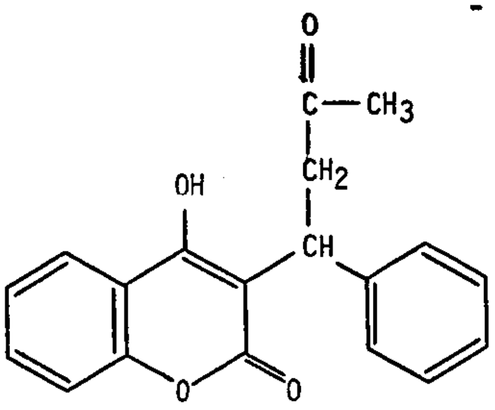

Warfarin

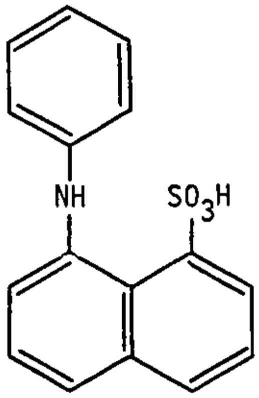

ANS

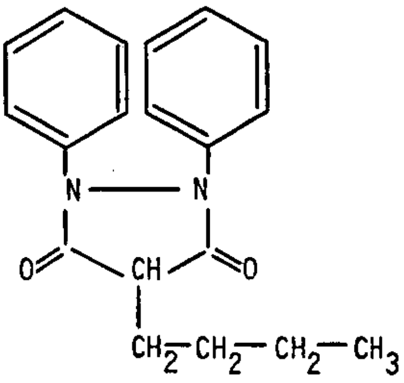

Phenylbutazone

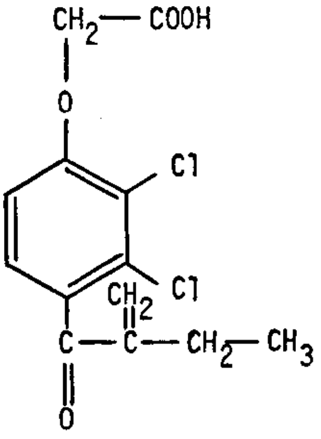

Ethacrynic Acid

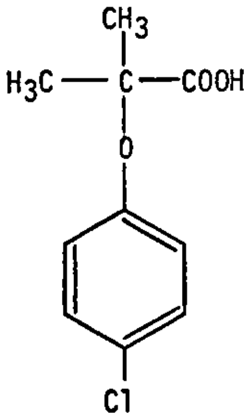

CPMP

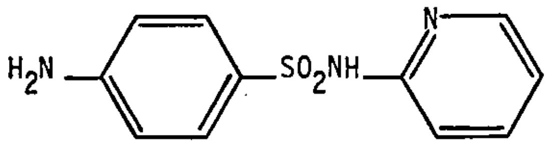

Sulphapyridine

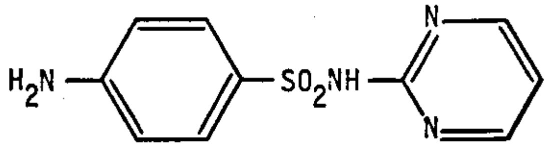

Sulphadiazine

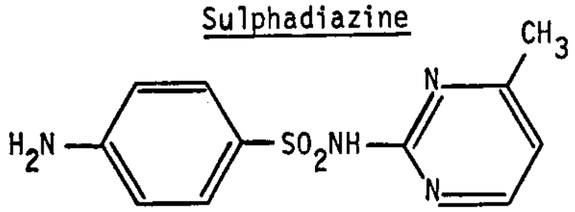

Sulphamerazine

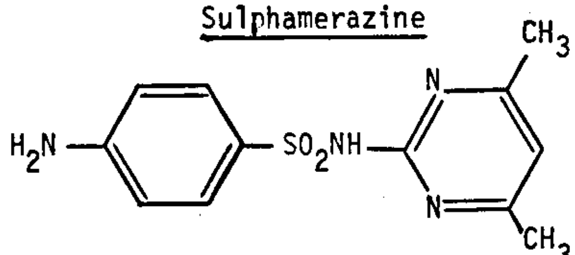

Sulphisomidine

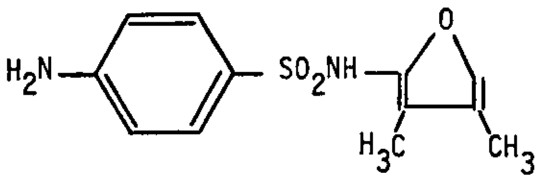

Sulphisoxazole

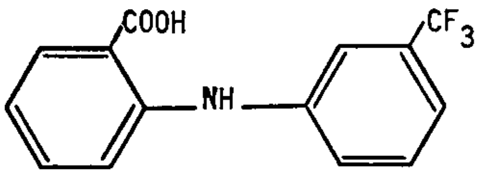

Flufenamic Acid

FIGURE 2.1 Chemical Structural Formulae of Drugs and Fluorescent Probes used in this Study.

2.1.3 Determination of Concentrations

For quantitative work it was necessary to control the concentrations of reagents in the standard solutions as accurately as possible.

After heating in a vacuum oven and reweighing at hourly intervals, all the commercial drug samples were found to contain less than 1% water by weight. Accordingly, solution concentrations could be deduced from accurate measurements of dry-weights. As a safeguard the water-content of powdered stock samples was checked periodically.

Routine determination of HSA was achieved by measuring the absorbance of solutions at 280nm and using an extinction coefficient, $E_{1cm}^{1\%} = 5.30$ (Chignell 1969a);a molecular weight of 66,500 (Meloun et al 1975) was used to calculate the corresponding molar concentrations.

2.1.4 Storage of Chemicals

All chemicals were stored as recommended by the manufactures. Thus for sulphisoxazole the instruction "store dark and desiccated at 0.5°C" was adhered to.

Whenever possible solutions were stored in the dark. To minimize bacterial contaminations all solutions containing Tris-HCl buffer were kept at 4°C and used as soon after preparation as possible. If, despite the precautions, solutions became cloudy through bacterial growth they were immediately discarded. This avoided the necessity of adding preservatives such as sodium azide or thiomercal.

Serum samples were separated into convenient volumes and stored neat at -4°C. Dilutions were made up as required.

2.2 Instrumentation

Absorbance spectra were run on a Pye Unicam SP8000 Ultraviolet Recording Spectrophotometer. This instrument was used for qualitative purposes only.

Quantitative absorbance readings at fixed wavelengths were produced with a Pye Unicam SP600 UV Spectrophotometer. Unless otherwise stated, matched 1cm x 1cm silica cells were used to contain sample and reference solutions.

Fluorescence intensity measurements were obtained at preselected settings of the excitation and emission monochromators on a Baird-Atomic Fluoripoint Spectrofluorimeter fitted with manual wavelength controls. Fluorescence excitation and emission spectra were generated using a Baird-

Atomic Fluoricord instrument. This machine has an automatic wavelength drive.

A Perkin Elmer MPF44B Fluorescence Spectrophotometer with a differential corrected spectra unit attachment, the DCSU-2, was employed to measure fluorescence intensities at fixed wavelengths and to produce corrected and uncorrected excitation and emission spectra. This versatile instrument was also used for the recording of synchronous and derivative spectra.

For certain fluorescence titrations it was desirable to minimize temperature fluctuations within the sample solutions. This necessitated the acquisition of a thermostatically controlled water-bath, a combined temperature-block and cell holder capable of installation into the fluorimeter cell compartment, and a reliable water pump. Water from the bath was pumped through the temperature-block and cell holder, and efficient heat-exchange between the circulating water and the fluorimeter cell walls meant that the sample solution could be easily maintained at a constant temperature.

The fluorimeter cells were a matched pair of 1cm x 1cm silica cells (Spectrosil Code Q Type 3, Chemlab Instruments Ltd) with a low absorbance in the ultra-violet region.

Buffer pH was adjusted with the aid of the EIL 7050 (Electronic Instruments Ltd) or the PHM 64 Research pH Meter (Radiometer Ltd).

Other equipment, notably that designed or modified to perform specific tasks, is described in the appropriate sections of the thesis.

2.3 Spectrophotometric Measurements

Absorption spectra and absorbance valves at fixed wavelengths were produced by standard procedures. As is common practice in spectrophotometry, reference solutions contained everything in the sample except the analyte. In most cases this simply meant using a diluent buffer as the reference. Sample and reference solutions were always equilibrated at room temperature prior to insertion in the spectrophotometer. They were inspected before and after measurement to ensure bubbles were not adhering to the cell surfaces.

For any substance the wavelength of maximum absorption could be determined by running a spectrum. Whenever possible this peak wavelength was chosen for quantitative measurements of absorbance. Basic theoretical considerations reveal why this is the most suitable choice.

Close to the absorption peak, the absorbance of the sample varies little with the wavelength. This is in contrast to other regions of the spectrum where the absorption curve is steep. Using the absorption maximum as the analytical wavelength minimizes the effect any irreproducibility or error in the wavelength setting may have on the precision or accuracy of the absorbance measurement.

Another obvious justification for taking readings at the maximum in the absorption spectrum is that the highest available sensitivity can normally be achieved at this wavelength. Furthermore, this procedure minimizes apparent deviations from Beer's law when the incident radiation is of a wide bandwidth (Olsen, 1975).

Having decided on a suitable wavelength for quantitative work, it became necessary to define a sensible range over which absorbance values could be accurately determined. In this context it is worthwhile to consider the Beer-Lambert law.

The Beer-Lambert law may be expressed as:

$$\log_{10} (Io/I) = A = \varepsilon cl \qquad (2.1)$$

Io and I are the intensities of the incident and transmitted light respectively, and $\log_{10}$ (Io/I) is defined as the absorbance A. C is the concentration of the absorbing species and ε is the molar absorptivity (the absorbance of a 1M solution in a 1cm cell). If Equation (2.1) is used to find the concentration of the absorbing species, and assuming the Beer-Lambert flow is applicable, then the maximum precision in the determination of c must correspond to the maximum precision in A.

Random errors associated with the measurement of absorption impose a limit on the degree of precision attainable. At low absorbances the instrument must discern a small difference between two large signals both of which includes an appreciable noise level. At high absorbances, where only a small amount of radiation is incident on the detector, a high amplification gain is required and an accurate measurement of the transmitted intensity is unlikely. So the range over which accurate absorbance values may be generated has well-defined upper and lower limits.

If the error in measuring the intensity of the transmitted radiation is constant over the operating range, differentiation of Equation (2.1) allows the relative error in the absorbance reading to be calculated. As expected, the error function, which is sometimes called the Twyman-Lothian curve, passes through a minimum. The absorbance corresponding to the minimum error is found by differentiating the Beer-Lambert equation again and setting the second derivative equal to zero. As it transpires, the minimum relative error occurs at an absorbance of 0.434. More significantly, the error function helps to define the useful range for taking absorbance measurements; outside the interval 0.2 to 0.7 absorbance units, readings are subject to rapidly increasing errors. A further discussion of the precision of spectrophotometric measurements is presented by Gridgeman (1952).

The Beer-Lambert law was used in the determination of unknown sample concentrations. Steps were taken to ensure absorbance measurements were made under conditions conducive to attaining maximum or near maximum precision. Two approaches were used. In the first, linear calibration plots were produced from measurements taken on solutions of known concentration. Unknown solutions were subsequently determined by recording sample absorbances and reading the corresponding concentrations off the calibration plots. The second approach made use of published absorptivity values. In the routine determination of HSA, for example, absorbance measurements were taken at 280nm and transformed into albumin concentrations by means of the accepted $E_{1\%}^{1cm}$ value.

In all quantitative work sample absorbances were adjusted to lie within the optimum range as defined in the preceeding theory. To determine solutions of high concentrations it was necessary to take accurate dilutions of the sample until the absorbance reading fell within the required limits. For very dilute samples, on the other hand, the absorbance of a suitably concentrated stock solution was first determined. This solution could then be diluted to the required strength.

An allowance was made for slight differences in the transmission properties of the absorption cells. With one cell containing the reference solution and the other acting as the sample cell, the absorbance of the sample solution was measured several times. The mean $\bar{A}$, and the standard deviation σ, were calculated for these results. The roles of the cells were then reversed. That is, the cell that had contained the sample solution was thoroughly rinsed and used to hold the reference solution, while the former reference cell was washed and filled with sample solution. Values for the sample absorbance were obtained again, and the mean $\bar{A}_2$ and standard deviation σ of several measurements recorded. Writing $\bar{A} = (\bar{A}_1 + \bar{A}_2)/2$ and $\sigma = \surd(\sigma_2^1 + \sigma_2^1)$ allowed the calculation of $\bar{A}$, the absorbance corrected for cell-mismatching, and if required, enabled the corresponding standard deviation σ to be reported.

Large differences between $\bar{A}_1$ and $\bar{A}_2$ were viewed with suspicion as they suggested at least one of the cells was dirty. In such circumstances cells were cleaned and measurements retaken. When coefficients of variation were calculated from σ they were typically 1.5% or less.

2.4 Fluorescence Measurements

2.4.1 Uncorrected Spectra

Excitation and emission spectra were produced by scanning excitation monochromators at fixed wavelengths of emission, and by scanning emission monochromators at fixed wavelengths of excitation, respectively. Both types of spectra were run on Baird-Atomic Fluoricord and Perkin-Elmer MPF44B spectrofluorimeters. In all cases the fluorescence was detected at right angles to the incident radiation.

The following paragraphs outline the main steps taken in the production of fluorescence spectra.

All solutions were allowed to equilibrate at room temperature before transferring to the fluorimeter cells. If air bubbles formed on the cell surfaces, they were removed. Strict temperature control of sample solutions was unnecessary except when quantitative measurements of spectral intensities were required.

Since the presence in solution of materials which absorb a significant proportion of the exciting or fluorescent radiation will diminish the observed fluorescence by an inner-filter effect, the concentrations of such substances and of the fluorescent species itself were maintained at levels corresponding to a low absorbance at the wavelengths of interest. Consequently, prior to recording a fluorescence spectrum, it often proved worthwhile to examine the absorption characteristics of a sample.

After allowing a suitable warm-up time to elapse, the correct focusing and alignment of the lamp was assured. This was essential if a reasonable level of irradiation of the sample were to be achieved. Notwithstanding this, significant adjustments to the Perkin-Elmer lamp settings were seldom called for.

To obtain reasonable spectra a suitable selection of the instrumental parameters was required. The most important parameters were those governed by the slit-width, time constant, scan speed and gain controls.

General guidelines exist which are helpful in deciding the settings to use. A choice of monochromator slit widths may be partially determined by the type of spectrum being recorded, that is, whether it be an excitation or an emission spectrum. To obtain the desired resolution, excitation spectra should be recorded with a sufficiently narrow excitation monochromator slit width; the emission monochromator slit may be wider, though, in order to give the intensity required for a good signal-to-noise ratio. Conversely, emission spectra may be recorded with a narrow emission monochromator slit width and a wider excitation monochromator slit width. On the other hand, if high resolution is not required, wide slit widths may be used for both monochromators. In general though, the minimum slit widths consistent with acceptable signal-to-noise ratios were sought.

A poor choice of response times and scan speeds may result in gross distortions of recorded spectra. Fluorescence excitation and emission spectra are usually obtained by scanning the appropriate monochromator wavelength drive at a constant rate and recording the emission signal versus time.

The response time is an indication of how quickly the output, pen position, needle recording, etc., follows changes in the input signal, be it current or voltage. A system with a short response time faithfully displays rapid changes in the input signal, whereas a system with a long response time smooths out and perhaps attenuates input signal changes. As a rule, random noise in the output of an analytical system may be reduced by increasing the response time. However, there is a limit to which the response time may be profitably increased. Excessively long response times may distort fluorescence spectral peaks and blur out details of fine structure. A similar effect arises with fast scan speeds, or a combination of fast scan speeds and long response times. The optimum scan speed obviously depends on the choice of response time and on the structure of the spectrum.

The time constant is a measure of the response time of an instrument. It is the time taken for a signal to decay to $^1/e$ of its initial value. For faithful spectral reproduction the time allowed for a signal to change full-scale should be at least five time constants. So, with a 0.1s time constant the signal should change in 0.5s or longer. For a scan speed of 4nm s^{-1} this amounts to a 2nm change.

A time constant of 0.3s and a scan speed of 2nm s^{-1} were found suitable for most purposes. In fact, only in the derivative mode was spectral distortion a problem.

Having selected appropriate slit widths, time constant, and scan speed, the photomultiplier gain was adjusted so that the peak signal in the spectrum was of a convenient magnitude, say 80% of full scale. If at the maximum gain only a small fluorescence signal could be obtained with the chosen slit widths, or if the signal-to-noise ratio was unacceptably low, the slits were widened. Should this cause an appreciable loss in resolution or, indeed, fail to generate a large enough signal, the concentration or composition of the sample was adjusted.

For each sample, the instrumental settings involved in the production of fluorescence spectra were invariably reported alongside the chart record.

Sample solutions were only irradiated during the relatively short periods required to measure the spectra. At all other times the shutter was kept closed. This was an attempt to minimize photodecomposition of samples.

Immediately after use, cells were cleaned by washing thoroughly in tap water and then rinsing in distilled water. Synthetic detergents were avoided whenever possible as many of these agents are known to be intrinsically fluorescent (Udenfriend, 1962). Occasionally deposits of protein or other substances formed on the walls of the cuvettes and had to be removed with nitric acid. After such treatment, the cells were carefully washed in the usual manner. Rather than leaving to soak in distilled water, the clean cells were dried in air. The disadvantage of the former procedure was that after a few days microorganisms became apparent in the soaking solution.

2.4.2 Corrected Spectra

Similar considerations applied to the production of both corrected and uncorrected spectra. However, to generate corrected, or true spectra, it was necessary to make allowances for the source and detector characteristics of the fluorimeter.

Interfaced with the MPF44B fluorimeter, the DCSU-2 microprocessor unit permitted corrected spectra to be produced automatically. Before running a corrected spectrum, the DSCU-2 unit had to be programmed as outlined in the manufacturers handbook. This involved the use of a Rhodamine B standard which enabled correction factors to be calculated and stored in the microprocessor unit every 0.2nm over the specified range. Corrected excitation or emission spectra could be generated simply by selecting the appropriate mode on the DCSU-2 unit and running the spectrum in the usual manner.

2.4.3 Emission Intensities

Quantitative measurements of fluorescence intensity were made at fixed wavelengths of excitation and emission on standard solutions of known concentrations. These standards were dilutions of an accurately produced stock solution. The results were expressed as calibration plots of fluorescence intensity versus concentration for various fluorescent species. They were used to determine the unknown analyte concentrations in different sample solutions. In so doing, the sample and standard fluorescences were measured under identical conditions.

The choice of instrumental settings in the recording of fluorescence intensities was largely guided by an inspection of the relevant excitation and emission spectra. For a given sample, the highest sensitivity, and hence the lowest limit of detection, are normally achieved when the observed signal is a maximum. So, for analytical work the peak wavelengths in the fluorescence excitation and emission spectra are the obvious ones to employ. Moreover, as in absorption spectroscopy, using the maximum in the excitation and emission spectra tends to minimize the effects of any errors in the wavelength settings.

Unfortunately, however, complications may arise in fluorimetry; the sensitivity and reproducibility of a fluorescence assay may be diminished by interferences due to scattered radiation. Not surprisingly therefore, further considerations are often necessary if optimal wavelength settings are to be achieved.

Most scattered radiation has the same wavelength as that of the exciting beam. If there is only a small Stoke's shift between the fluorescence excitation and emission maxima, Rayleigh-Tyndall scattering from the sample may interfere with the measurement of fluorescence. Under these conditions, of course, scattering from cell surfaces, optics and slits will tend to aggravate the problem.

To avoid collecting scattered radiation together with the sample fluorescence, it may be necessary to select narrow monochromator slit widths or to employ a suitable cut-off filter. Both techniques were used in the practical work.

As suggested previously, however, it is often feasible to reduce the overlap of scattered and fluorescence radiation by an adjustment of the wavelength settings. Lowering the wavelength of excitation produces a corresponding shift in the location of the Rayleigh-Tyndall scatter. At the same time, though, such an operation has no effect on the position of the fluorescence band. Consequently, selecting a shorter wavelength for excitation tends to improve the resolution of scatter and fluorescence peaks. Measuring the fluorescence at a longer wavelength than that of maximum emission may similarly reduce the effects of scatter. So although the recorded signal is greatest when the monochromators are set at the wavelengths of maximum excitation and emission, lowering the wavelength of excitation, or increasing the wavelength of emission, or doing both these operations, may actually increase the sensitivity of an assay. Hence, the monochromator settings used in the measurement of fluorescence intensities did not necessarily correspond exactly to the peak wavelengths in the excitation and emission spectra.

Raman scattering, which is a physical property of the pure solvent, could be readily distinguished from fluorescence because Raman peaks are always at a fixed frequency difference from the incident radiation irrespective of the wavelength of excitation. Although usually of very low intensity, Raman scattering can nonetheless be a problem when small fluorescence signals are to be measured. Fortunately, should the Raman band of the solvent coincide with the fluorescence emission from the sample, separation can again be achieved by changing the exciting wavelength to a lower value, when the Raman band will be similarly displaced. Since the wavelength of fluorescence is independent of the exciting wavelength, this method allows the fluorescence to be separated from the Raman scatter.

In practice it was often helpful if the position of Raman peaks could be predicted, or at least identified, for any wavelength of excitation. The problem demanded that a shift in frequency be related to a shift in wavelength, and so required differentiation of the relationship,

$= \lambda\ c/\nu$ where and ν are the wavelength and frequency of the radiation, respectively, and c is the speed of light. This gave:

$$d\lambda = -c/\lambda^2 \; d\nu$$

$$\text{that is,} \quad d\lambda = -\lambda^2/c \; d\nu \qquad (2.2)$$

The negative sign in Equation (2.2) signifies that a decrease in frequency (negative $d\nu$) corresponds to an increase in wavelength (positive $d\lambda$).

Since c is a constant, knowing the fixed frequency shift $d\nu$ between the Raman band and the exciting radiation allows the equivalent wavelength displacement $d\lambda$ to be determined for any excitation wavelength λ. The Raman peak will be located at $(\lambda + d\lambda)$. A corresponding anti-Stoke's Raman band will be centred at the wavelength $(\lambda - d\lambda)$ but is normally of low intensity and anyway does not interfere with the measurement of fluorescence.

Aqueous buffers were invariably used as solvents in fluorimetry. The three modes of vibration in the water molecule are all Raman-active but only the symmetrical stretch gives a strong Raman band. The value of $d\nu$ corresponding to this band was used in Equation (2.1) along with the proposed wavelength of excitation to predict the location of the Raman peak. Such simple calculations proved useful in the interpretation of spectra; moreover, for quantitative work, they indicated how suitable instrumental parameters could be chosen to separate fluorescence emissions and Raman scatter peaks.

In the absence of interfering species, resolution of the fluorescence and scattered radiation resulted in low blank signals. The minimization of blank signals is always desirable since the subtraction of a large blank signal from an only slightly larger blank plus sample signal is extremely prone to error.

Theoretically, the blank solution should contain everything in the sample except the analyte. In most cases true blank solutions were available. For example, if the emission intensity of a fluorescent probe was to be measured when protein-bound, a blank solution could be prepared in which the protein concentration, buffer ionic strength and pH were identical to those in the sample solution.

The blank and sample fluorescences were measured with the same instrumental settings and under the same experimental conditions. The blank value was subtracted from the sample fluorescence. Although the blank fluorescence, sometimes called the background fluorescence, was usually extremely small, suitable blanks were invariably prepared and sample readings blank-corrected at all times.

As well as minimizing the effects of Raman and Rayleigh-Tyndall scatter, it is important to check the purity of solvents if low fluorescence blanks are to be maintained. Thus, "Aristar" grade Tris and good quality double-distilled water were used in the preparation of buffer solutions. A less expensive batch of Tris was found to give an unacceptably high background emission. The water was always collected and stored in glass rather than in plastic vessels; organic additives and plasticizers have been known to leach out of plastic containers and into solution where they may interfere with spectroscopic measurements. Even if non-fluorescent, these contaminants can act as quenchers.

Similarly, all glassware used in fluorimetry was thoroughly washed in water to remove traces of impurities such as chromic acid and detergents which may have an intrinsic fluorescence.

The growth of microorganisms in buffer or sample solutions was seen to result in higher blank values, presumably through an increase in the amount of light scattered. To overcome this, solutions made up in buffer were always stored at $4^{o}C$ and discarded at the first signs of contamination.

For accurate fluorescence work control over certain environmental factors was of great importance. In all quantitative experiments the temperature of sample solutions was maintained at $23^{o}C \pm 0.2^{o}C$ using the apparatus described in Section 2.2. Strict temperature regulation was necessary for two reasons. Firstly, the fluorescence of a sample of constant composition could be varied simply by altering the temperature. This was not unexpected, since as discussed in Section 1.6.3 the quantum yields of many substances are temperature-sensitive. However, the second need for temperature control lay in the nature of the specific system under investigation. When a drug interacts with a protein, the equlibrium between the bound and unbound fractions is dependent on the temperature. So even if the total amounts of protein and drug are fixed, temperature changes can alter the composition of a sample as measured by the ratio of bound to unbound drug. Consequently, shifts in the solution temperature could not be tolerated if further complications in the interpretation of fluorescence data were to be avoided.

Another factor carefully monitored was the sample pH. This was necessary since relatively small changes in pH can sometimes have pronounced effects on the intensity and spectral characteristics exhibited by a sample. Of equal relevance to this work is the fact that interactions between small molecules and proteins are sensitive to changes in pH. Presumably, this sensitivity is a result of structural perturbations. At all times, therefore, buffers were made up accurately and the pH carefully adjusted to 7.40.

Subsequent to sample preparation, and having chosen the instrumental conditions, the actual reporting of measured fluorescence intensities needed some attention. Due to fluctuations in instrumental variables such as lamp intensity and photomultiplier sensitivity, it is normally impossible to obtain the same readings on a fluorimeter from one day to the next. In fact measurements may differ from hour to hour. This means that if precise quantitative fluorescence readings are to be recorded, some standardization of the equipment is required. A solution of a stable fluophor of known concentration may be used to maintain the instrument at a given sensitivity. Adjustments are best accomplished by varying the amplifier gain or photomultiplier voltage rather than the monochromator band widths. On the other hand , gradual changes in the instrumental sensitivity may be tolerated if the sample fluorescence is always measured with respect to the emission of the stable reference solution.

One of the most widely accepted fluorescence standards is quinine sulphate. Solutions of quinine sulphate in 0.05M sulphuric acid were always used when quantitative fluorescence measurements were required. Nevertheless, as with all other standards, there are certain limitations on the application of this substance in fluorimetry which are worthy of consideration.

Quinine sulphate undergoes decomposition at very low concentrations. Bowen and Wokes (1953) reported that whereas quinine sulphate solutions containing 10^{-6}g/ml or more are unaffected by prolonged irradiation, solutions of 2 x 10^{-8}g/ml or less deteriorate under continued exposure to ultra-violet light. It is apparent that decomposition of reference standards can lead to serious errors in the measurement of fluorescence. To minimize such errors, the concentrations of quinine sulphate reference solutions were normally 10^{-6}g/ml or above, and stock solutions were always stored in the dark.

Aside from the problem of photodecomposition, there is another good reason for avoiding very low concentrations of quinine sulphate. If adsorption of the solute on to glass surfaces is appreciable, then the effect will become more pronounced as solutions are diluted. Gradual removal of the fluorescent species from solution would produce an unacceptable decrease in the reference signal.

Whenever the sample fluorescence was measured with respect to the emission of a reference solution, it was preferable if the two signals to be compared were of a similar magnitude. This could be achieved by adjusting the strength of the reference solution but bearing in mind, of course, the above constraints on the concentration to use. If the sample and reference measurements differed by a factor of ten or more, then unduly small pen or needle deflections corresponding to either the sample or reference fluorescence would have to be monitored and large errors of measurement introduced. So for calibration plots extending over a wide range of fluorescence intensities, several reference solutions of differing concentrations were required.

Reference solutions are normally only useful for substances which fluoresce in the same region of the spectrum. Fortunately, quinine sulphate, with its wavelengths of maximum excitation and emission at 350nm and 450nm respectively, was particularly suitable for our purposes and no other fluorescent standards were needed.

Once instrumental drift had been allowed for, the values of the observed fluorescence intensities could be used to generate the calibration plots of fluorescence versus analyte concentration, mentioned at the beginning of this section. When these plots were extended over a wide concentration range, they showed a non-linear response. This was a result of inner-filter effects, the origins of which have been discussed in Section 1.6.4. Attempts were made to correct for these and in so doing to construct the more useful linear transformations.

2.5 Computational Methods

Routine calculations and the statistical analysis of certain results were performed with a Casio Fx-80 hand-held calculator. When more complicated processing of data was necessary, computer programs were devised. These were written in FORTRAN IV and all routines were run on an IBM 1900 computer using the card input and lineprinter output facilities.

CHAPTER 3

Development of a Homogeneous Fluorescence Assay for the Accurate Determination of Protein Binding Constants

3.1 Introduction

The clinical importance of the interactions between drugs and plasma proteins is well established. In particular, the degree binding of a drug to HSA may limit its availability to the receptor sites and excretory systems. Consequently, the affinity of a drug for binding albumin can have a profound influence on its biological activity and half-life. It is not surprising, then, that the strength of such an interaction, which is usually expressed as an apparent association constant, is an important parameter to determine.

An argument which was developed further in Chapter 1 concerned the displacement of drugs from plasma binding sites. It was seen how harmful side-effects may arise when several active drugs compete for a similar class of binding sites on albumin. Experimental evidence suggests that there are only a small number of high affinity drug binding sites on HSA. It would be useful if individual sites could be characterized more completely as this might help to identify potential drug interactions based on displacement and redistribution.

A major aim of this study was to develop simple and reliable methods for investigating drug-protein binding in vitro. At first, particular attention was paid to the application of fluorescence techniques to the determination of binding constants. The work with fluorescent probes formed a basis from which to examine the properties of separate sites on albumin.

Prior to 1977 fluorescence spectroscopy had already been widely used to study the binding of drugs and other small molecules to the plasma proteins. Much of this work has been reviewed by Chignell (1974) and Wilson and Bridges (1976). An early objective of this project was to search the literature and find out whether accurate procedures were available for quantifying the interactions between fluorescent probes and albumin. It soon became clear, however, that it would be extremely difficult to repeat and assess a standard protocol from the literature. There were two main reasons for this.

Firstly, the reporting of experimental procedures often gave too little detail for the work to be reproduced faithfully. Approximations were frequently introduced to simplify calculations of the concentrations of protein-bound and unbound fluorescent probe. These were sometimes difficult to justify especially when the full experimental conditions went unreported.

Secondly, and perhaps more importantly, the results of binding experiments were commonly misinterpreted. Even though binding data were generally expressed in a similar form - usually as a Scatchard plot, the methods of extracting binding constants from the results took many courses. The literature contains numerous examples in which linear binding plots have been constructed on the basis of insufficient data covering only a fraction of the binding isotherm. Even more frequently, however, curved Scatchard plots have been produced but the authors have simply extrapolated apparently linear portions of the curves and translated the intercepts on the axes directly into binding constants. The use of these constructions is unfounded, and the complex relationship between the intercepts and the site binding constants is rarely acknowledged. A further discussion of the problems encountered with the decomposition of binding curves is presented in Section 1.7.

Due to the lack of a suitable procedure in the literature, a new method was devised for measuring binding constants for the interactions between fluorescent probes and proteins.

In general, if a fixed concentration of protein is taken, and if different amounts of ligand are added in a titration, then the strength of any ligand-protein interaction may be estimated from measurements of the quantities of bound and unbound ligand at each point in the titration.

Some method must be provided for determining the bound and unbound fractions. If the ligand under consideration is a fluorescent probe, its distinctive spectroscopic property provides a means of achieving this goal through a simple, homogeneous assay. In other words, the enhancement of the observed fluorescent intensity and the concomitant shift in the wavelength of maximum emission which accompany binding of the fluorescent probe to the protein permit a spectroscopic resolution of the bound and unbound fractions of the probe without recourse to their physical separation.

By definition, resolution will be perfect only when the fluorescence intensity observed at the wavelength of maximum emission of the bound probe fluorescence originates entirely from this species and contains no contribution whatever from the unbound fraction, while the fluorescence recorded at the wavelength of maximum emission of the unbound fraction includes none of that due to the bound probe. Even if there is a considerable wavelength shift on binding to the protein, the weak fluorescence of the unbound probe is likely to be masked by the high wavelength edge of the bound probe fluorescence. On the other hand, if enhancement of the emitted intensity is extremely large when the probe binds protein, the signal associated with the bound fraction is unlikely to be perturbed to an appreciable degree by the much weaker fluorescence of the unbound probe. Measurements of the fluorescence intensity at the wavelength of maximum emission of the bound probe fluorescence may then be related directly to the concentration of bound probe and assuming the total concentration is known, the free fraction may be determined by subtraction.

In reality, however, the probe molecule will have an intrinsic fluorescence in aqueous solution, albeit one of a relatively low quantum yield. At high probe:protein ratios where a large proportion of the binding sites are saturated, the unbound fraction of the probe will predominate. Under these circumstances the fluorescence emitted by the high concentration of unbound probe may be quite appreciable and it would be difficult to justify neglecting its effect on the signal measured at the wavelength of emission of the bound probe fluorescence unless the two spectral peaks were completely resolved. Moreover, whether the wavelength shift on binding protein is large or small, it is highly probable that the unbound probe will be capable of reducing the fluorescence observed from the bound species by an inner-filter mechanism. The effect is largely dependent on absorption of radiation by the unbound fraction at the wavelength of excitation of the bound probe fluorescence and this is why it can be a problem even when the difference between the fluorescence emission peaks of the bound and unbound probe is large. As a result, a simple correlation between the measured fluorescence intensity and the concentration of bound probe is unlikely to hold in the presence of varying amounts of unbound probe. Since the relative proportions of bound and unbound ligand will change continuously during a binding titration, care must be taken if fluorescence intensity measurements are to be correctly interpreted in terms of the degree of binding of a fluorescent probe to a protein.

The binding of two fluorescent molecules to HSA has been examined in detail. At first attention focused on the anticoagulant warfarin. As well as being a commonly administered drug, warfarin is fluorescent and is known to exhibit a significant change in its spectral properties on binding to proteins (Chignell, 1970). Figure 3.1 shows how the fluorescence of this molecule is enhanced when it binds to human serum albumin. The

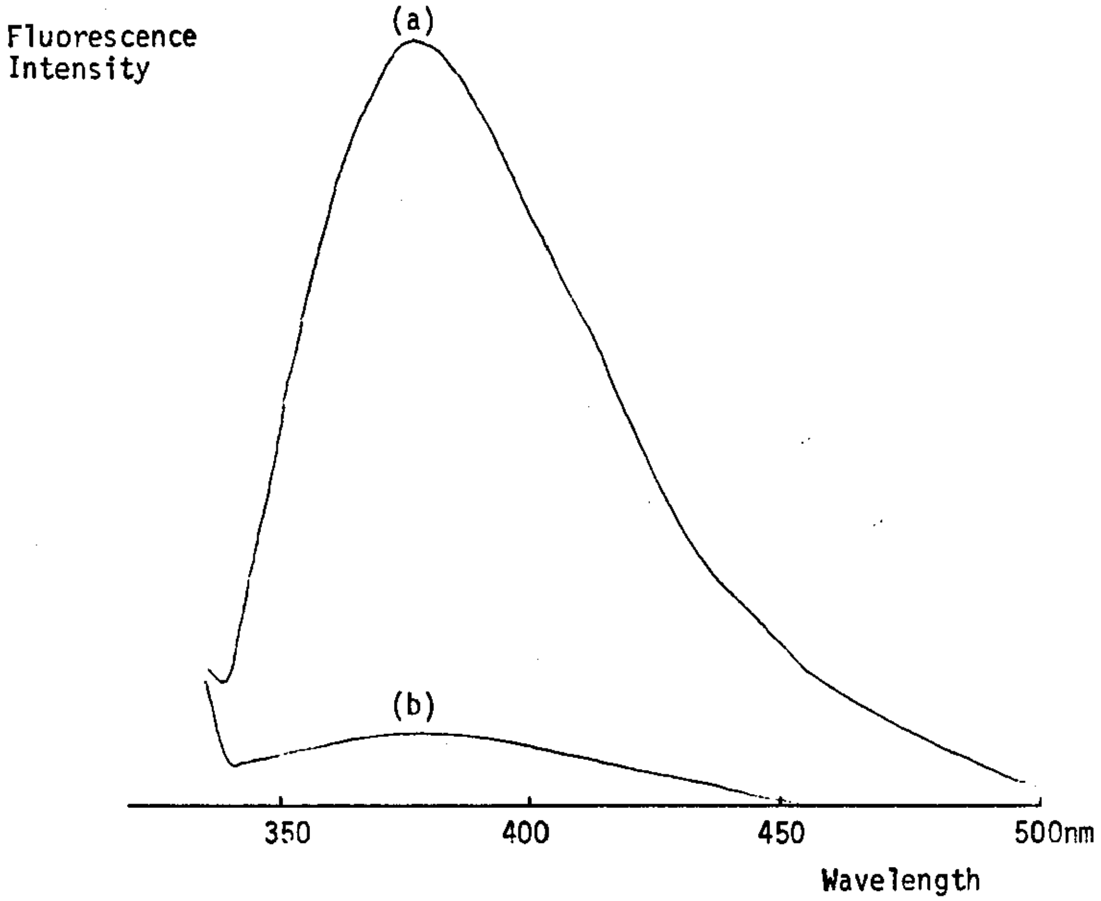

FIGURE 3.1 Corrected emission spectra of bound and free warfarin illustrating fluorescence enhancement. Wavelengths of excitation 320nm.

(a) 7.1×10^{-6}M warfarin in 0.1M Tris/HCl buffer pH 7.4 containing 5×10^{-5}M human serum albumin.

(b) 7.1×10^{-6}M warfarin in 0.1M Tris/HCl buffer pH 7.4.

concomitant blue shift in the emission maximum and the reduction of the bandwidth are illustrated in Figure 3.2.

In terms of the criteria discussed previously, however, warfarin is far from being an ideal fluorescent probe. Its quantum yield in free solution is quite appreciable and the wavelength shift on binding to albumin is too small to allow for a proper resolution of the peaks which correspond to the bound and unbound species. Indeed on binding to HSA, the fluorescence intensity observed at the wavelength of maximum emission is only about thirteen times that of the unbound probe at the same wavelength. If a sample contains protein-bound and unbound warfarin in equilibrium, any attempt to correlate the fluorescence intensity at 375nm with the concentration of bound probe will have to recognize potential interferences from the free fraction. This observation emphasizes the need to characterize the fluorescence of the probe in free solution as well as the fluorescence of the protein-bound species.

The second fluorescent molecule to be considered was the dye ANS. The dramatic enhancement of the fluorescence which accompanies binding of this probe to HSA is shown in Figure 3.3. Figure 3.4 illustrates how the wavelength of maximum emission is shifted to the blue by about 75nm when ANS binds albumin. Once again a narrowing of the emission band accompanies removal of the fluorescent probe from an aqueous environment. It should be emphasized that a much higher gain was used to record the fluorescence of the unbound probe in Figure 3.4.

The excitation spectra of warfarin and ANS are included in Figure 3.5. They have been recorded alongside the emission band of HSA to demonstrate the potential for resonance energy transfer between the protein and the fluorescent probes which bind to it. Figures 3.6 and 3.7 show how both warfarin and ANS quench the fluorescence of HSA by resonance energy transfer. The bound species of the fluorescent probes can act as acceptor molecules for the albumin fluorescence because their excitation bands overlap the emission wavelengths of the protein (Figure 3.5). Energy transfer between HSA and ANS is further illustrated in Figure 3.8 which is an excitation spectrum of bound ANS. The appearance of a strong excitation peak at about 280nm is evidence that the fluorescence recorded at 475nm is sensitized by the transfer of energy from albumin as well as by direct excitation of the bound probe fluorescence at 375nm.

The gross changes in the fluorescence spectrum of ANS which accompany its binding to HSA make this a relatively simple system to study. In marked contrast to warfarin, when ANS is used as a fluorescent

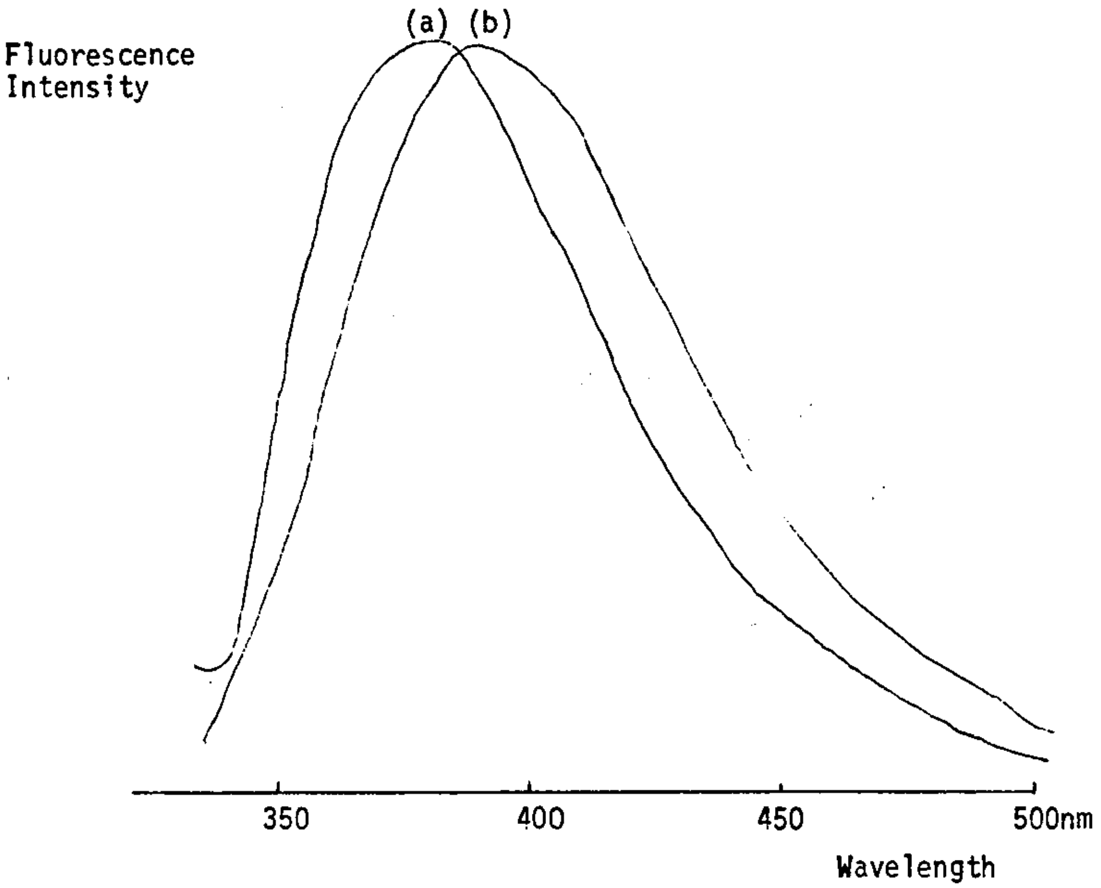

FIGURE 3.2 Corrected emission spectra of bound and free warfarin illustrating differences in peak maxima and spectral bandwidths. Wavelengths of excitation 320nm.

(a) 8 x 10^{-7}M warfarin in 0.1M Tris/HCl buffer pH 7.4 containing 5 x 10^{-6}M human serum albumin.

(b) 1 x 10^{-5}M warfarin in 0.1M Tris/HCl buffer pH 7.4.

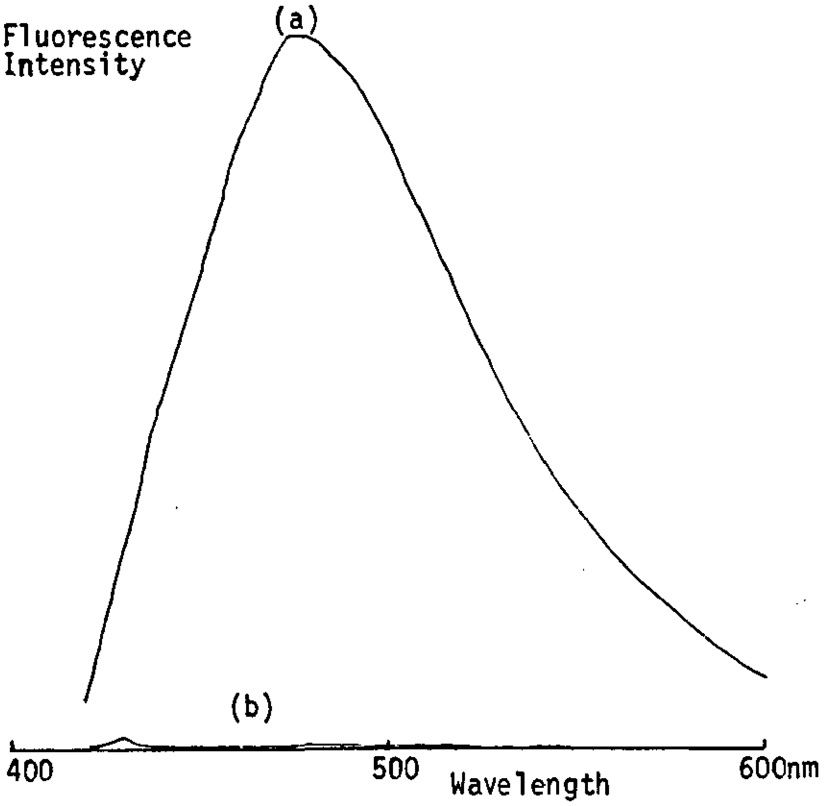

FIGURE 3.3 Corrected emission spectra of bound and free ANS illustrating fluorescence enhancement. Wavelengths of excitation 375nm.

(a) 5×10^{-7}M ANS in 0.1M Tris/HCl buffer pH 7.4 containing 1.5×10^{-5}M human serum albumin.

(b) 5×10^{-7}M ANS in 0.1M Tris/HCl buffer pH 7.4.

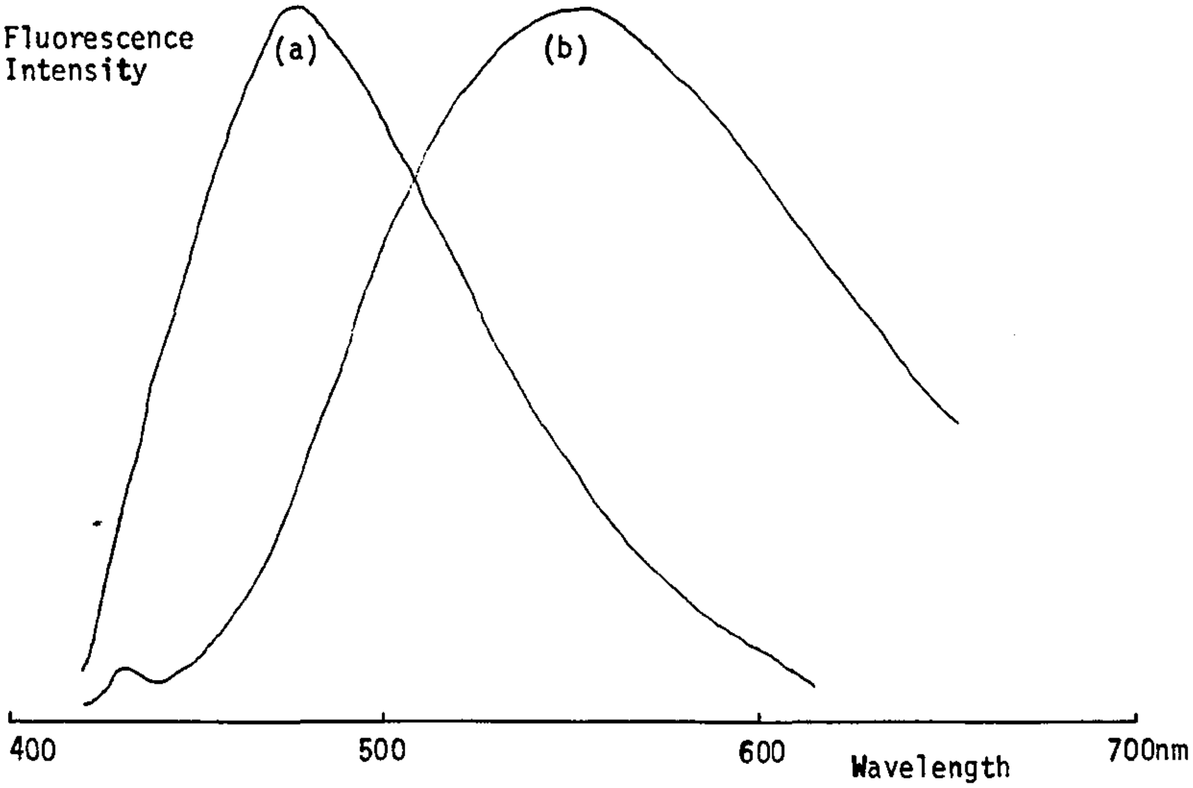

FIGURE 3.4 Corrected emission spectra of bound and free ANS illustrating differences in peak maxima and spectral bandwidths. Wavelengths of excitation 375nm.

(a) 5×10^{-7}M ANS in 0.1M Tris/HCl buffer pH 7.4 containing 1.5×10^{-5}M human serum albumin.

(b) 4×10^{-5}M ANS in 0.1M Tris/HCl buffer pH 7.4.

A much higher gain was used with spectrum (b).

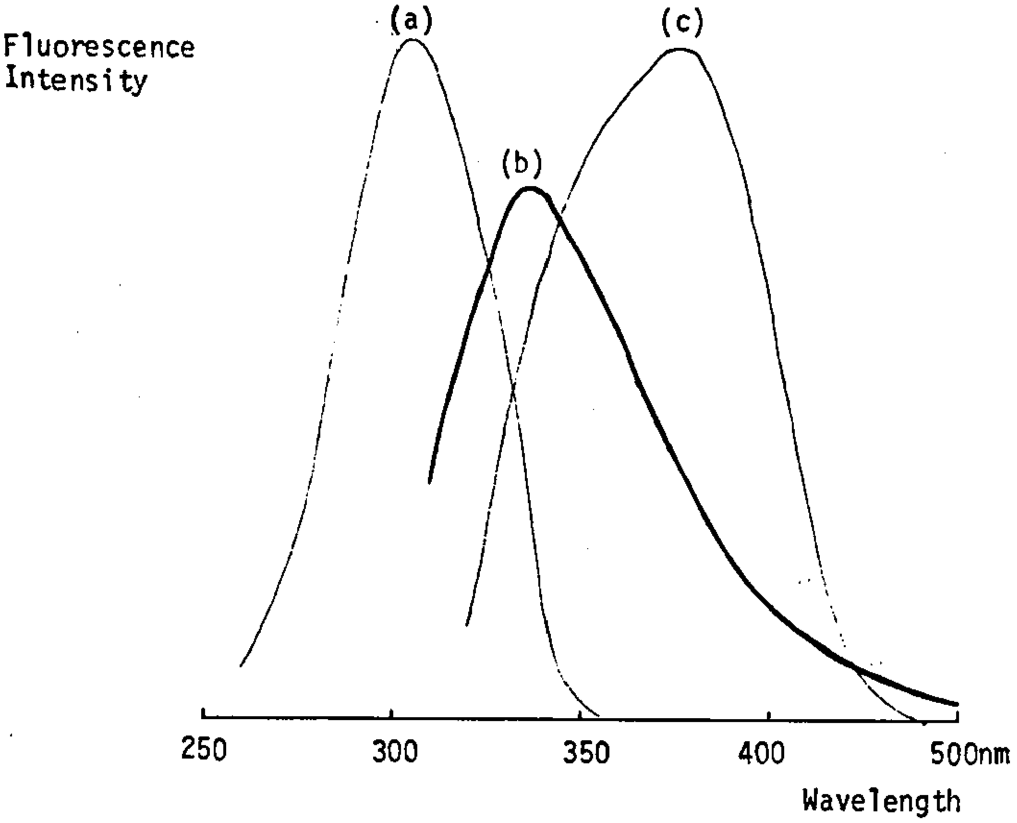

FIGURE 3.5 (a) Corrected excitation spectrum of 5 x 10^{-5}M warfarin in 0.1M Tris/HCl buffer pH 7.4. Wavelength of emission 390nm.
(b) Corrected emission spectrum of 5 x 10^{-5}M HSA in 0.1M Tris/HCl buffer pH 7.4. Wavelength of excitation 294nm.
(c) Corrected excitation spectrum of 2 x 10^{-6}M ANS in 0.1M Tris/HCl buffer pH 7.4 containing 2 x 10^{-5}M HSA. Wavelength of emission 460nm.

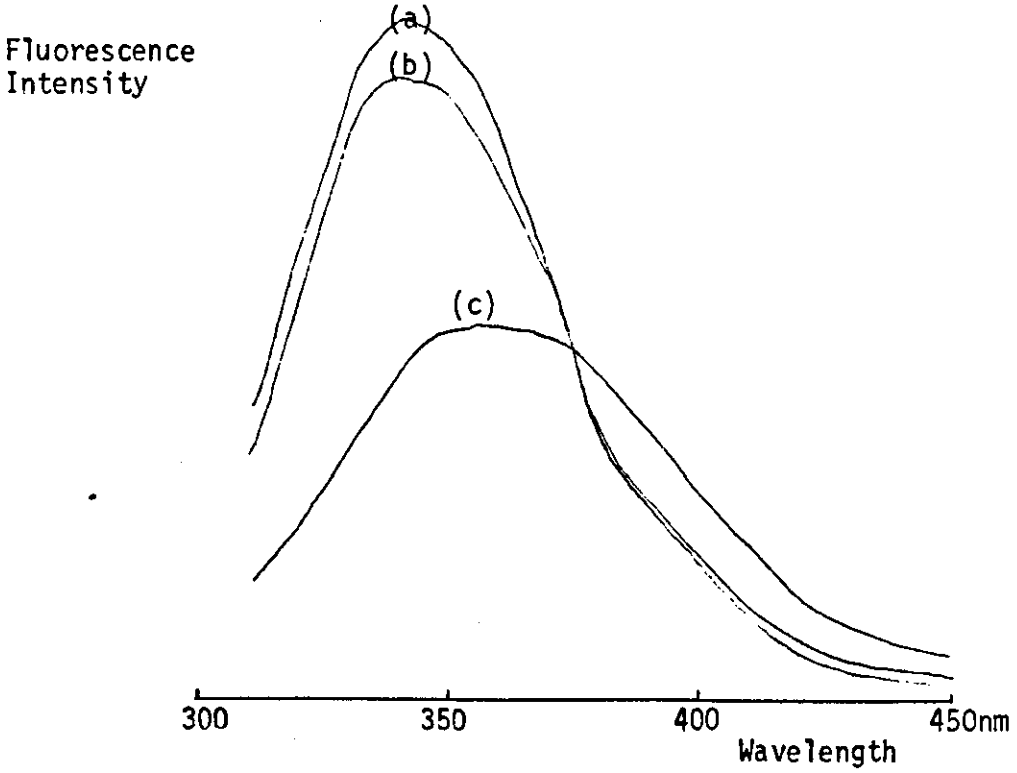

FIGURE 3.6 Emission spectra of human serum albumin illustrating resonance energy transfer to acceptor molecule (warfarin). Wavelengths of excitation 290nm.
(a) 5 x 10^{-5}M HSA in 0.1M Tris/HCl buffer pH 7.4.
(b) 5 x 10^{-5}M HSA in 0.1M Tris/HCl buffer pH 7.4 containing 1.5 x 10^{-6}M warfarin.
(c) 5 x 10^{-5}M HSA in 0.1M Tris/HCl buffer pH 7.4 containing

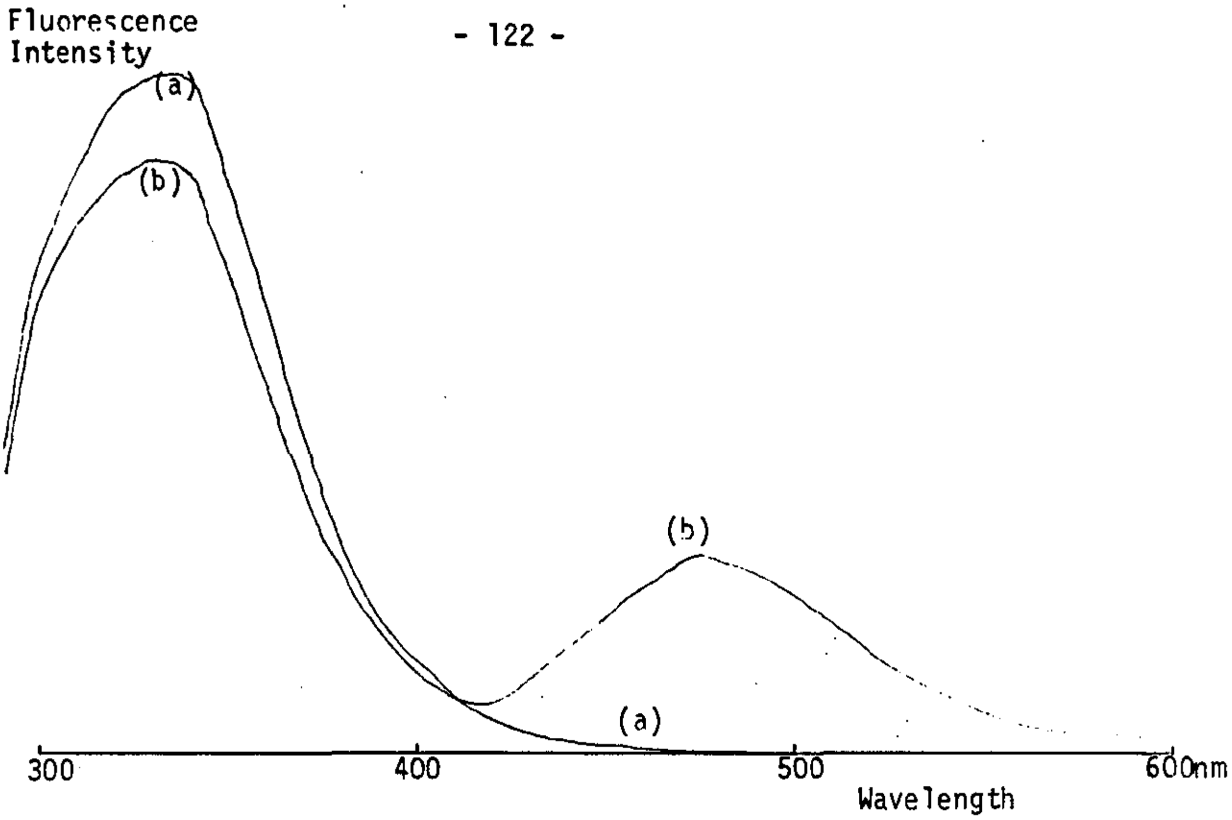

FIGURE 3.7 Corrected emission spectra of human serum albumin illustrating resonance energy transfer to acceptor molecule (ANS). Wavelengths of excitation 285nm.
(a) 2 x 10^{-5}M HSA in 0.1M Tris/HCl buffer pH 7.4.
(b) 2 x 10^{-5}M HSA in 0.1M Tris/HCl buffer pH 7.4 containing 2 x 10^{-6}M ANS.

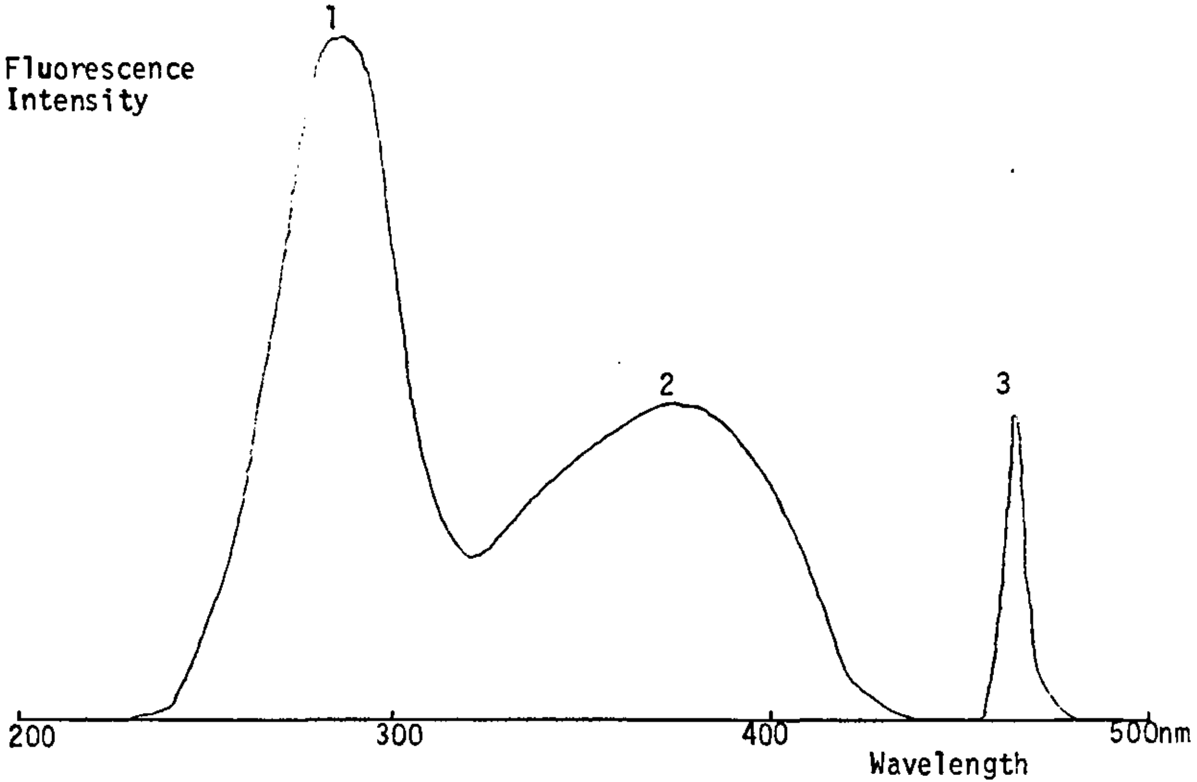

FIGURE 3.8 Corrected excitation spectrum of albumin-bound ANS. Wavelength of emission 465nm. 2 x 10^{-5}M HSA and 2 x 10^{-6}M ANS in 0.1M Tris/HCl buffer pH 7.4.
Peak 1 Excitation of albumin (Intense fluorescence measured at 465nm is due to resonance energy transfer to bound ANS
Peak 2 Direct excitation of bound ANS.
Peak 3 Rayleigh scatter peak.

probe it is possible to take a reading with the monochromators set at the wavelengths of excitation and emission of the bound probe fluorescence and, to be sure of collecting virtually no spurious signal from any ANS which is in free solution. However, the unbound fraction is still able to interfere with the measurement of the bound probe fluorescence through an inner-filter effect. Once again it will be necessary to quantify a spectroscopic property of the unbound probe when examining binding to HSA.

To produce accurate binding constants for both high and low affinity sites on a macromolecule it is important that the ligand concentration is varied over as wide a range as possible. In a fluorescence assay this means examining the intensity of the radiation emitted by protein-bound and unbound probe at both high and low concentrations. The experimental procedures used to generate the required information are described in the next section.

3.2 The Characterization of Probe Fluorescence

The work outlined in this section provided the basis on which to establish an analysis of subsequent binding curves. The role of these experiments in the overall scheme is illustrated in the flow diagram of Figure 3.9.

3.2.1 Production of a Calibration Curve for Unbound Probe

The intensity of the radiation emitted by the unbound probe was quantified by measuring the fluorescence from samples consisting of various concentrations of the probe dissolved in the assay buffer, 0.1 M Tris/HCl pH 7.40.

To prepare samples of the correct composition, microlitre quantities of a suitably concentrated stock solution of the probe were added to a fluorimeter cell containing a measured volume of the assay buffer - usually 3ml. Thorough mixing was achieved by stirring the solution with the needle of the microlitre syringe. The sample remained in the fluorimeter during the titration and its temperature was normally maintained at 23°C ± 0.2°C by means of the thermostated cell holder.

The excitation and emission monochromators were set at or very close to the wavelengths of maximum excitation and emission of the bound probe fluorescence. As far as warfarin was concerned, this meant an excitation wavelength of 320nm, and an emission wavelength of 375nm. When ANS was under examination, the corresponding settings were 375nm and 460nm. Spectra such as those in Figures 3.1, 3.3 and 3.5 were

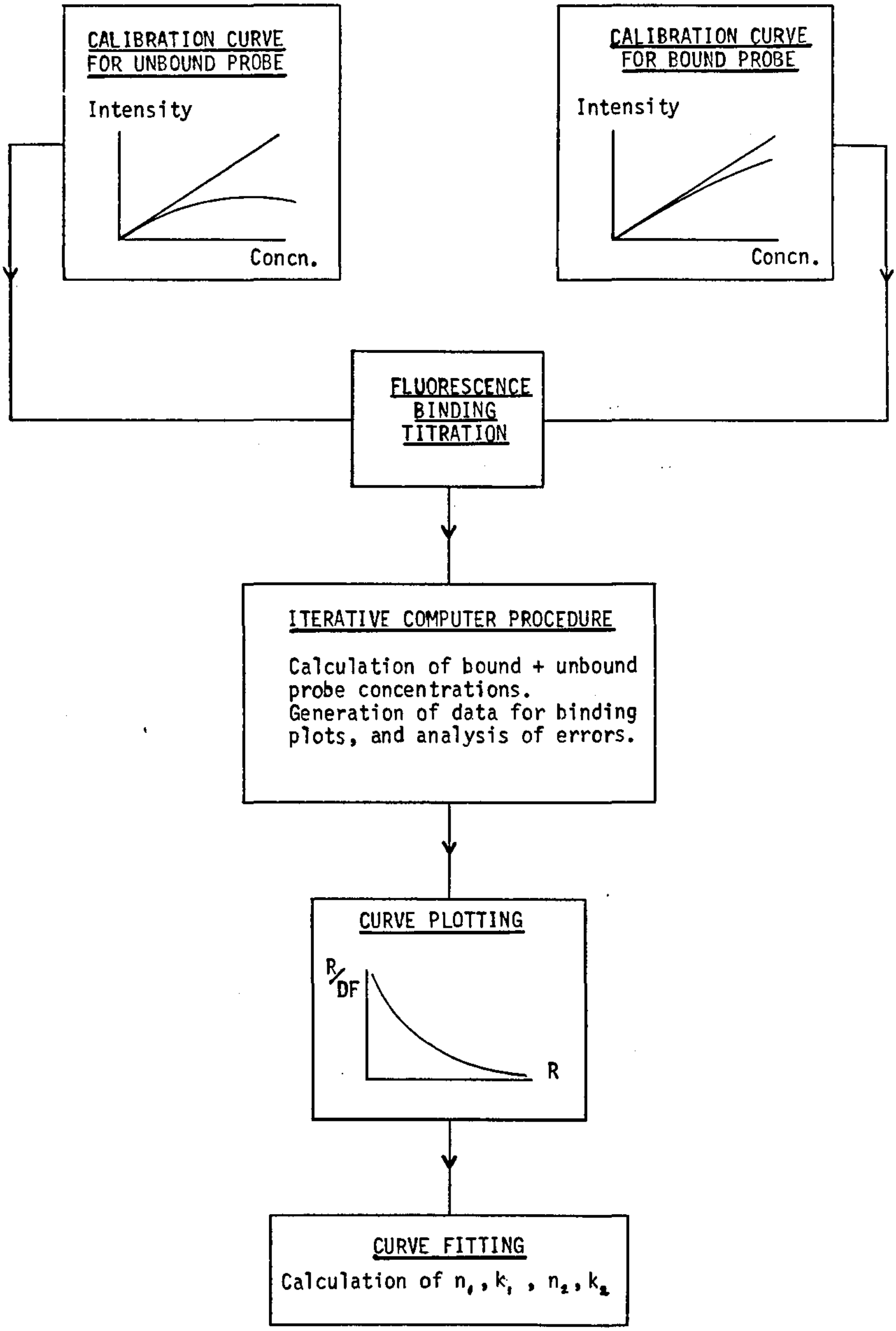
CALIBRATION CURVE FOR UNBOUND PROBE
Intensity
Concn.
CALIBRATION CURVE FOR BOUND PROBE
Intensity
Concn.
FLUORESCENCE BINDING TITRATION
ITERATIVE COMPUTER PROCEDURE
Calculation of bound + unbound probe concentrations.
Generation of data for binding plots, and analysis of errors.
CURVE PLOTTING
R/DF
R
CURVE FITTING
Calculation of n_1, k_1, n_2, k_2

FIGURE 3.9 Flow Diagram

helpful when choosing the monochromator settings.

Solutions of quinine sulphate were used to maintain the fluorimeter at a given sensitivity. This procedure ensured that instrumental drift could have no effect on the recorded fluorescence intensities.

The signal detected with only buffer in the fluorimeter cell provided a blank value which could be subtracted from the intensities obtained in the presence of fluorescent probe. Blank and sample fluorescence intensities were determimed under identical experimental conditions.

To calculate the concentration of probe at each point in the titration, an allowance had to be made for the sample dilution brought about by the repeated addition of small quantities of stock solution to the fixed volume of buffer. The blank-corrected fluorescence intensities could then be plotted against probe concentration in the form of a calibration curve. A typical example is shown in Figure 3.10. It may be regarded as a 'standard curve' and used to determine the concentration of an unknown sample.

As described above, a range of probe concentrations could be introduced into the fluorimeter cell by making serial additions of a concentrated stock solution to a measured volume of buffer. Although this method gave satisfactory results, it was quite susceptible to experimental error. This susceptibility may be appreciated from Figure 3.11(a) which shows how the sample concentration at any point is made up of contributions from all the previous additions. Since an imprecision in one pipetting step affects all the subsequent points in the titration curve, there is a likelihood of accumulating unacceptably large experimental errors in the samples of high concentration.

A second method of sample preparation was examined and found to have certain advantages. Thus, in later experiments a slightly less concentrated stock solution was taken and a number of separate dilutions prepared outside the fluorimeter cell. This is illustrated in Figure 3.11(b). Comparing the new scheme with that which involved serial additions (Figure 3.11(a)), it is obvious that the number of pipetting steps associated with each point in the titration may be reduced by preparing dilutions independently of one another. An error in dispensing one volume of reagent will now affect only a single point in the titration curve and there is no tendency to produce increasingly inaccurate samples as the concentration is raised.

When solutions were made up separately they had to be introduced

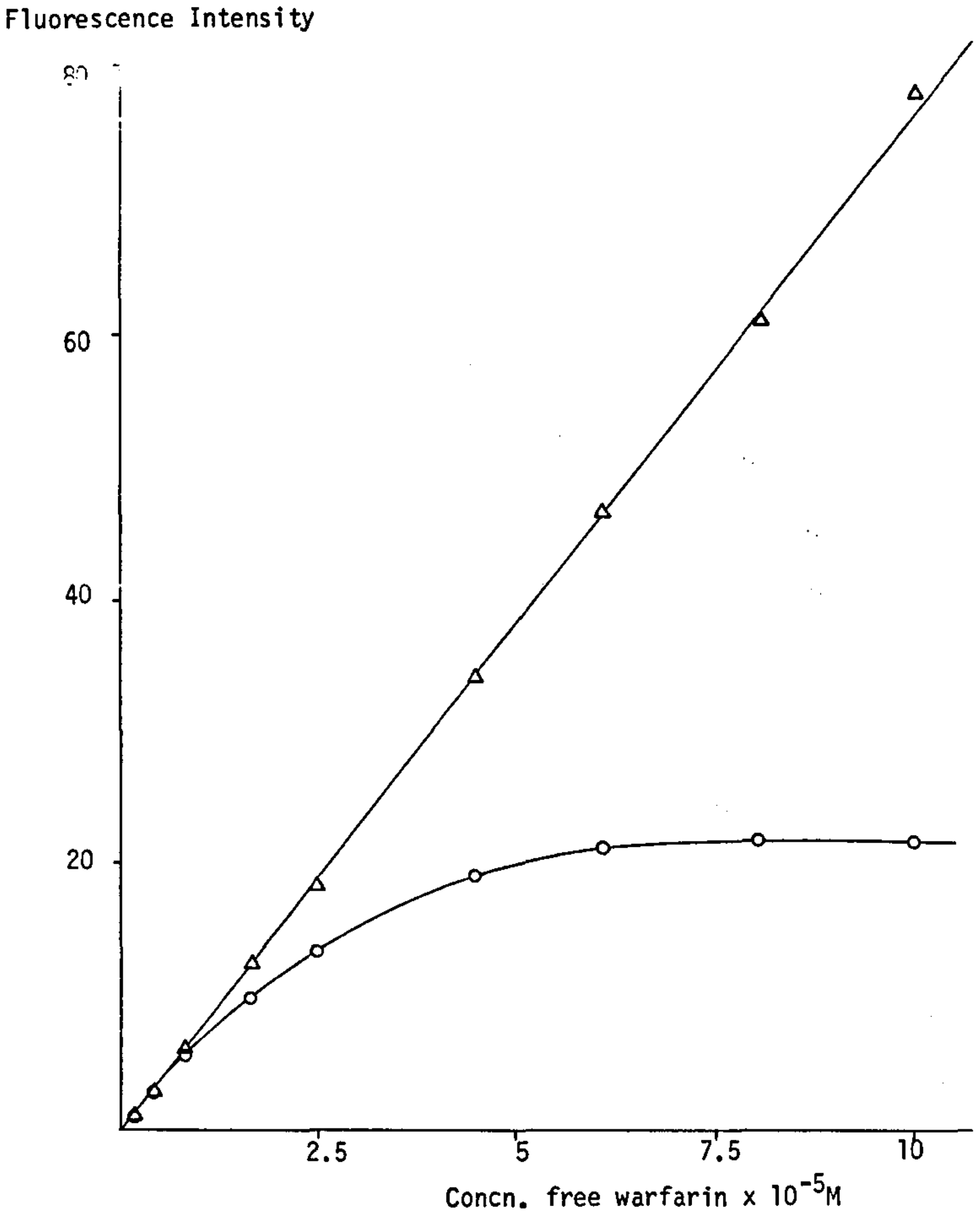

FIGURE 3.10 Calibration Curve for Unbound Fluorescent Probe (Warfarin)

o Measured fluorescence intensities from samples containing warfarin in 0.1M Tris/HCl buffer pH 7.4.

Δ Fluorescence intensities corrected for inner filter effects by determining the molar absorptivities of free warfarin at the wavelengths of excitation and emission and incorporating these values in Equation 3.5.

Solution (A) 0.1M Tris/HCl pH 7.40 containing 10^{-4}M Probe.
Solution (B) 0.1M Tris/HCl pH 7.40.

(a)

Sample No.	Preparation	No.Pipetting Steps	Probe Concn.
1	(20μl 20μl)(A)+3.0ml(B)	2	6.62x10^{-7}M
2	(20μl+20μl 40μl)(A)+3.0ml(B)	3	1.32x10^{-6}M
3	(20μl+20μl+20μl 60μl)(A)+3.0ml(B)	4	1.96x10^{-6}M
⋮	⋮ ⋮	⋮	⋮
12	(100μl+...+20μl+20μl 1.0ml)(A)+3.0ml(B)	13	2.50x10^{-5}M

(b)

Sample No.	Preparation	No.Pipetting Steps	Probe Concn.
1	20μl(A) + 2.98ml(B)	2	6.67x10^{-7}M
2	40μl(A) + 2.96ml(B)	2	1.33x10^{-6}M
3	60μl(A) + 2.94ml(B)	2	2.00x10^{-6}M
⋮	⋮ ⋮	⋮	⋮
12	1.0ml(A) + 2.00ml(B)	2	3.33x10^{-5}M

FIGURE 3.11 Scheme Showing Methods for Sample Preparation.

into the fluorimeter one after the other. This meant the fluorimeter cells had to be rinsed with the solution of next highest concentration between each measurement. However, the need to stir samples was removed and it was no longer necessary to make allowances for sample dilution when plotting results.

Due to its poor solubility in aqueous solution, it was necessary to dissolve warfarin in a small quantity of ethanol or 0.1M sodium hydroxide prior to making it up in the required volume of buffer and using as a stock solution. To demonstrate any effects these solvents may have had on the fluorescence of the probe, further experiments were required. These involved the addition of solvent to buffer solutions containing appropriate concentration of warfarin. Any alterations in the observed fluorescence were noted.

As it turned out, neither ethanol nor sodium hydroxide had any significant effect on the fluorescence of warfarin in free solution. This was true over the entire range of solvent concentrations which had been encountered in the fluorescence titrations. Consequently, the calibration curves required no solvent-correction.

3.2.2 Production of a Calibration Curve for Bound Probe

Two separate titrations were required before fluorescence intensity measurements could be translated into moles of bound probe. Both sets of results were recorded at the same temperature and with similar instrumental settings. As usual, the monochromators were adjusted to the wavelengths of maximum excitation and emission of the bound probe fluorescence.

The first of the two titrations entailed measuring the fluorescence intensity emitted by a fixed amount of probe in HSA solutions of increasing concentration. In these 'reverse titrations' the albumin concentration was raised until the probe fluorescence intensity reached a limiting maximum independent of further increases in the protein strength. Background contributions to the measured signals were accounted for by running blanks. Since the blanks were designed to include everything in the sample except the analyte, bound fluorescent probe in this case, they comprised a series of solutions containing increasing quantities of albumin. At each point in the reverse titration, therefore, it was possible to subtract scattered light and residual protein fluorescence from the total signal. However it must be emphasized that the background signals were small compared to the intense fluorescence emitted by the bound probe.

The results were plotted as illustrated in Figure 3.12. The attainment of a maximum fluorescence intensity at high protein:probe ratios suggested that all the existing probe molecules had become bound to albumin. Under these conditions it seemed reasonable to assume that the blank-corrected signal was due entirely to the fluorescence of bound probe, there being no unbound fraction to complicate matters.

Armed with information from the reverse titration, it was possible to devise a second titration in which the probe binding sites remained saturated with HSA. Tbroughout these experiments it was the albumin concentration which was held constant, or nearly so, while the amount of fluorescent probe in each sample was allowed to vary. In practice this meant selecting an appropriate concentration of albumin and dispensing a convenient volume of solution, say 3ml, into the fluorimeter cell. Small quantities of a stock solution of fluorescent probe were then added from a microsyringe the tip of which was used to stir the mixture. As with the unbound probe titration, this method of dispensing reagents was later modified so that samples of the required composition could be made up individually before inserting into the fluorimeter cell.

Whichever the method of sample preparation, titrations were carefully designed so that the final probe concentration was still low enough for there to be an excess of binding sites on the protein molecules in solution.

In this type of titration a constant background fluorescence intensity was subtracted from each of the recorded values. This signal was determined by taking the appropriate albumin solution and measuring the emission, again with the monochromators set at the wavelengths of maximum excitation and emission of the bound probe fluorescence, but doing so before any fluorescent probe had been added. The blank-corrected fluorescence intensity measurements were then plotted against the known concentration of probe in each sample. Due to the design of the experiment, this provided a calibration plot of fluorescence intensity versus bound probe concentration.

In simple terms, the calibration plot could be regarded as a standard curve for use in the determination of the concentrations of albumin-bound fluorescent probe in unknown samples. However, it would only be feasible to assay an unknown sample if it contained no fluorescent probe in free solution, or if it did, provided the fluorescence of the unbound species was negligible compared to the total signal. Obviously the first of these two provisos drastically limits the application of the calibration plot to a very narrow class of samples. On the other hand,

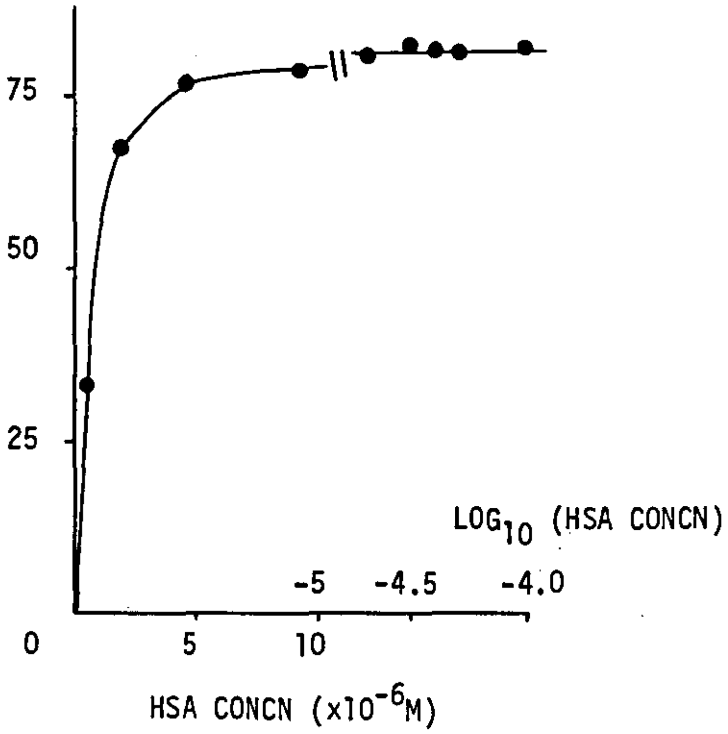

FIGURE 3.12 Reverse Titration for ANS

ANS concentration 10^{-6}M. An allowance was made for the small inner-filter effect of HSA.

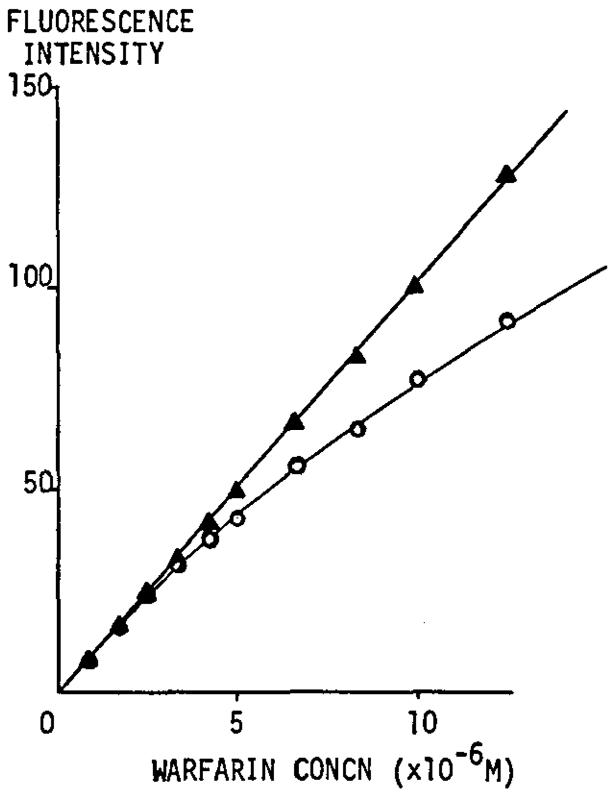

FIGURE 3.13 Calibration Curve for Bound Fluorescent Probe (Warfarin)

○ Measured fluorescence intensities from samples containing warfarin in 0.1M Tris/HCl buffer pH 7.4 containing 10^{-4}M HSA.

▲ Fluorescence intensities corrected for inner-filter effects by measuring molar absorptivities of bound warfarin and HSA. Coefficient of linear regression r=0.99986 if the fluorescence of a probe is enhanced a great many times on binding albumin, the second proviso is satisfied and a calibration curve of the type shown in Figure 3.13 can be used to determine the concentrations of bound probe in a sample which also contains fluorescent probe in free solution.

In practice, though, measurement of the signal from the bound fraction may be complicated by the presence of the unbound species even if the latter is virtually non-fluorescent. This was mentioned in section 3.1. Nevertheless, the calibration plot of fluorescence intensity versus bound probe concentration will be seen to play a central role when determining the strength of the interaction between the probe and HSA.

Zierler demonstrated in 1977 how the method outlined above for converting fluorescence intensity measurements into moles of bound fluorophor is much preferable to the most commonly used approach which involves an interpretation of the intercept of a plot of reciprocal fluorescence intensity of probe versus reciprocal protein concentration. In the graphical procedure, efforts to relate the fluorescence intensity to the concentration of bound ligand through a certain coefficient, always lead to an overestimate of the desired value (Zierler, 1977).

Additional experiments were performed in an attempt to identify how critical it was to control certain of the experimental variables. For example, the effect that a change in temperature has on the fluorescence intensity observed from a sample containing warfarin bound to HSA was monitored. The results are shown in Table 3.1. The reduction in the intensity of the fluorescence emitted by the bound probe which accompanies an increase in temperature is quite marked. Although the sensitivity of fluorescence spectra to changes in temperature has already been discussed in Section 1.6, these results emphasize the importance of maintaining strict temperature control when producing data for the protein-bound fraction of the probe.

Variations in the ionic strength of the assay buffer were found to have a less well-defined effect on the emission intensities. This may be appreciated from an inspection of the results in Table 3.2. Although small variations in the buffer strength appeared to be of little consequence, Tris/HCl buffer were always made up accurately to a concentration of 0.1M.

The effects of ethanol and 0.1M sodium hydroxide on the intensity of the fluorescence emitted by warfarin were also examined when the probe was bound to albumin. The results are analysed in the next section.

TEMPERATURE °C	OBSERVED FLUORESCENCE
14.0	85.5
16.0	81.5
18.0	77.3
20.0	75.5
21.0	74.6
21.5	74.0
22.0	73.8
22.5	73.5
22.6	73.4
22.8	73.3
23.0	73.1
23.2	73.1
23.4	72.8
23.6	72.7
23.9	72.9
28.0	67.5

TABLE 3.1 The Effect of Temperature on the Fluorescence of Albumin-Bound Warfarin.

Overall decrease in fluorescence is about 1.5% per °C. Sample composition: 1.7 x 10^{-5}M warfarin and 1.0 x 10^{-4}M human serum albumin in 0.1M Tris/HCl buffer (pH 7.4 at 20°C).

Concentration of Tris/HCl Buffer (M)	Observed Fluorescence Intensity
0.10	21.1
0.11	21.4
0.14	21.3
0.17	20.7
0.24	21.3
0.31	22.0
0.43	22.6
0.68	22.9

TABLE 3.2 The Effect of Buffer Ionic Strength on the Sample Fluorescence.

Sample : 8 x 10^{-6}M warfarin and 5 x 10^{-6}M human serum albumin in Tris/HCl buffer.

Samples were tested to see if they had been properly mixed. Samples prepared by the usual methods were subjected to further agitation using the tip of a microsyringe. No change in the recorded fluorescence intensities could be detected. Hence the rather peculiar phenomenon observed by Kolb and Weber (1975) namely, that stirring alters the results of a fluorescence binding titration, could not be reproduced and would appear to be an artefact.

The results suggest that provided reasonable regard is paid to experimental detail, the intensity of the signal emitted by a fluorescent probe may be quantified over a wide concentration range for the albumin-bound, as well as the unbound species.

3.2.3 A Detailed Examination of the Calibration Plots

To make proper use of the information contained in the calibration plots, due regard had to be paid to inner-filter, solvent and dilution effects.

It was a simple matter to make allowances for dilution of the sample. The effect arose only in titrations which required serial additions of one reagent to a fixed volume of another. Knowing the volumes involved, it was very easy to calculate the true concentrations of the sample components at each stage in the titration. For those experiments where samples were made up to the required concentrations separately and then measured one after the other in the fluorimeter, there were no dilution effects to consider and the results could be plotted directly.

Allowances for solvent effects were slightly more complicated. As mentioned earlier, it was necessary to dissolve warfarin in a small quantity of ethanol or 0.1M sodium hydroxide prior to diluting in buffer. Neither solvent appeared to have any effect whatsoever on the fluorescence emitted by the unbound fraction of the probe. However, ethanol had a considerable influence on the fluorescence of warfarin when it was bound to HSA (see Figure 3.14). The signal observed from the bound probe in the presence of ethanol was found to fit an empirical equation of the form

$$F_m = 100 \exp(-lc + mc^2) \qquad (3.1)$$

where l and m are constants, and c is the concentration of ethanol.

Using the values of l and m in Figure 3.14 provided an adequate means of correcting the bound probe calibration curve for solvent effects

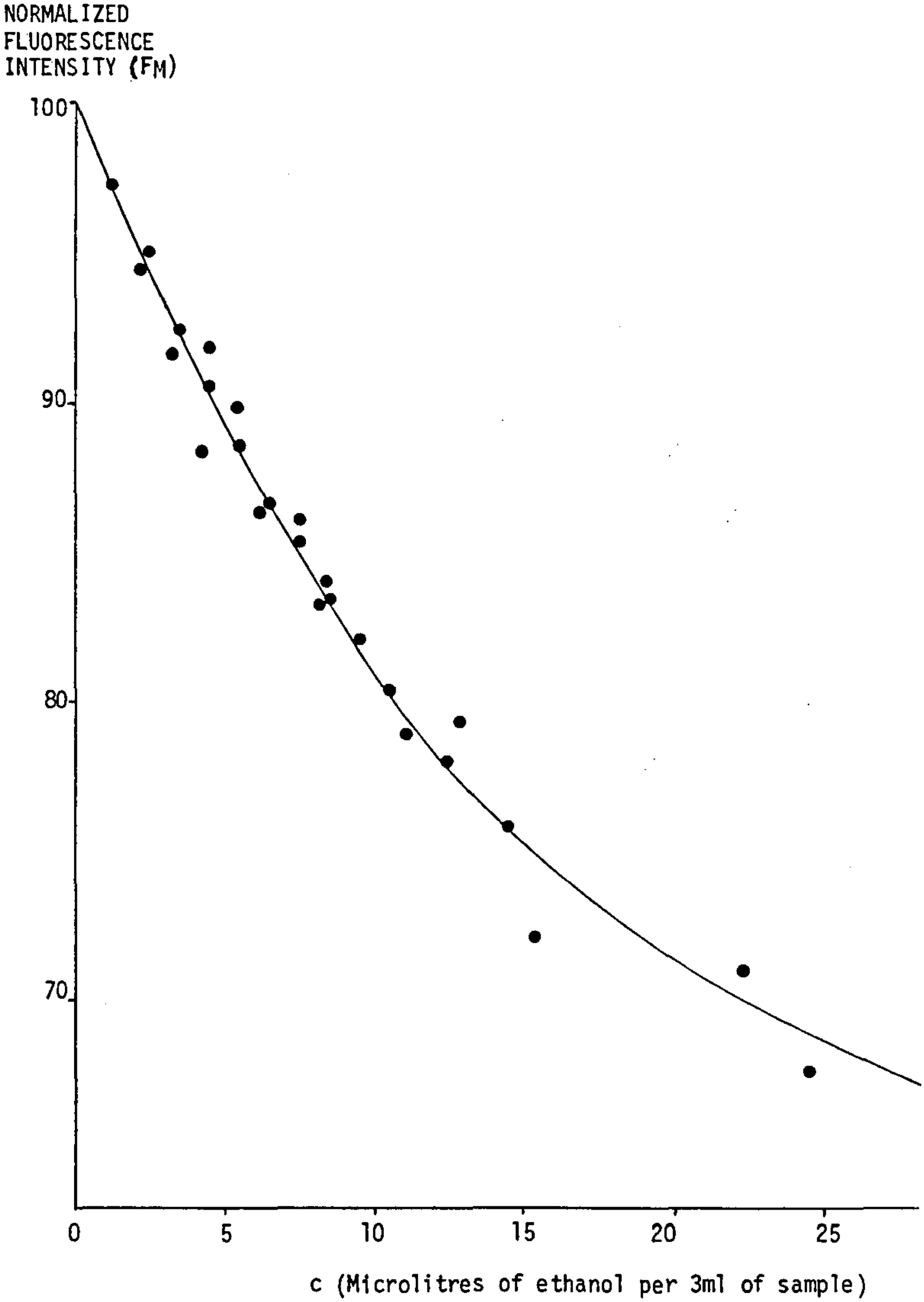

FIGURE 3.14 The Effect of Ethanol on the Fluorescence of Albumin-Bound Warfarin.

Equation of solid line is $F_M = 100 \exp(-0.025c+3.86\times10^{-4}c^2)$.

over a sufficiently wide range of ethanol concentrations.

It is obvious that during a titration in which increasing amounts of warfarin are added to HSA, the concentration of ethanol will also rise as it too is present in the stock probe solution. At the end of a titration sufficient ethanol may have accumulated to produce a considerable change in the recorded signal. Decreases of up to 15% have been observed. Consequently, it would seem advisable to avoid this solvent whenever possible, even though its perturbing effects can be suitably described in terms of Equation 3.1. Ethanol is known to denature proteins and the observed attenuation of the fluorescence emitted by the bound fraction could be due, at least partially, to an alteration of the binding site geometry and a displacement of bound fluorescent probe.

0.1M sodium hydroxide appeared to have no effect on the signal detected from the bound fraction of warfarin.

Regardless of whether corrections have been necessary for solvent or dilution effects, the calibration plots of observed fluorescence intensity versus analyte concentration were invariably non-linear. As illustrated in Figures 3.10 and 3.13 this was so for both the protein-bound and unbound fractions of the fluorescent probes. Curvature of the plots became more pronounced at high concentrations. The effects were consistent with an inner-filter mechanism, the origins of which have been discussed in Section 1.6. Attempts were made to correct the experimental data for the apparent inner-filter effects. Two approaches were used and both depended on very similar theoretical descriptions of the self-absorptive process.

Consider a fluorescent molecule or conjugate at some position (x_1, y_1) in a fluorimeter cell. As illustrated in Figure 3.15, x_1 represents the depth of sample solution through which the exciting radiation must pass before it impinges on the fluorphor. Similarly, y_1 corresponds to the depth of solution through which the emitted beam passes before emerging from the sample cell in the direction of the detector.

The intensity of the exciting radiation at any point in the fluorimeter cell depends upon the incident beam intensity attenuated by the absorption which has already taken place in the sample solution. This is best summarized in the Beer-Lambert law,

$$\log_{10} \frac{Io}{I} = abc$$

where Io is the intensity of the incident beam, I is the intensity of the radiation after the beam has passed through a depth b of solution, c is the concentration of the absorbing species and a is the molar absorbtivity of the sample. This expression may be rewritten in the form,

$$I = I_0 \exp(-2.303\, abc)$$

Thus after travelling a distance x_1 into the sample solution, the radiation which remains and is capable of exciting fluorescence has an intensity $I_0 \exp(-2.303\, a_1 x_1 c)$, where a is the molar absorbtivity of the sample at the wavelength of excitation. If there are no other absorbing species in the sample, c may be taken as the concentration of fluorphor. In the absence of an inner-filter effect, that is when $a_1 = 0$ the intensity of the incident radiation is clearly Io at every point in the sample. This means that for points at a depth x_1 into the sample, the radiation available to excite fluorescence in the presence and absence of inner-filter effects differs by the factor $\exp(-2.303\, a_1 x_1 c)$. Accordingly, if the intensity of the fluorescence emitted in the direction of the detector by a molecule centred at x_1 is labelled f in the presence of an inner-filter effect, and fo in the absence of an inner-filter effect, then

$$f = fo \exp(-2.303\, a_1 x_1 c)$$

Before reaching the detector, however, the radiation emitted by the fluorescent species may be further attenuated by self-absorption. This arises when the sample itself absorbs at the wavelength of emission. Consequently, if the fluorescence passes through a depth of solution y_1 before emerging from the sample cell in the direction of the detector, the signal which is finally measured will depend on the intensity of the radiation emitted by the fluorescent molecule modified by a second absorption term. That is,

$$fm = fo \exp(-2.303\, a_1 x_1 c) \exp(-2.303\, a_2 y_1 c)$$

or

$$fm = fo \exp(-2.303(a_1 x_1 + a_2 y_1)\, c) \qquad (3.2)$$

where fm is the fluorescence intensity measured outside the sample cell and originating at (x_1, y_1), and a_2 is the molar absorbtivity at the wavelength of emission. Again it has been assumed that no other absorbing molecules are present apart from the fluorescent species. Once more, then, c represents the concentration of fluorphor in the sample. Under these conditions it is reasonable to expect that a_2 is considerably smaller than a_1. After all, the fluorphor must absorb strongly at the wavelength of excitation for its fluorescence to be observed.

So far the signal from just one fluorescent molecule has been considered. If there were n such molecules in solution, each with coordinates (x_i, y_i), the intensity of the fluorescence that would be observed from the total population is given by

$$Fm = \sum_{i=1}^{n} fo \exp(-2.303 (a_1 x_i + a_2 y_i) c) \qquad (3.3)$$

In order to translate Equation 3.3 into a form which may be applied in practice, it is necessary to devise some method of carrying out the required summation. In Appendix A it is shown that if the conditions are those prevailing in a standard fluorimeter, the approximation that

$$Fm = Fo \exp(-2.303 (a_1 \bar{x} + a_2 \bar{y}) c) \qquad (3.4)$$

is an extremely close one. The terms $\bar{x}$ and $\bar{y}$ represent the mean values of the positions of the fluorescent molecules within the sample cell and are defined by, $\bar{x} = \sum_{i=1}^{n} \frac{x_i}{n}$ and $\bar{y} = \sum_{i=1}^{n} \frac{y_i}{n}$. Fo is the fluorescence intensity that would be registered if the sample exhibited no inner-filter effect. The error in the inner-filter correction factor is likely to be less than 1% when the above approximation is used (see Appendix A).

The first of the methods employed in the determination of inner-filter effects needed estimates of $\bar{x}$ and $\bar{y}$. As far as could be ascertained by inspection, a reasonable assumption was that the irradiated portion of the sample was disposed symmetrically about the vertical axis of the fluorimeter cell. Such an arrangement is the one shown in Figure 3.16. Under these conditions the average path lengths of the excitation and emission beams are equal. Moreover, since a 1cm cell was used, $\bar{x}$ and $\bar{y}$ were both taken to be 0.5cm. This allowed Equation 3.4 to be simplified to

$$Fm = Fo \exp(-2.303 \frac{(a_1 + a_2)}{2} c) \qquad (3.5)$$

When expressed in this form, the equation could be used to correct the fluorescence calibration plots for inner-filter effects. The only requirement was the provision of values of a_1 and a_2.

It should be noted that changes in the absorption as well as the fluorescence spectrum of a ligand may accompany binding to a macromolecule. Consequently determinations of a_1 and a_2 were necessary for both the protein-

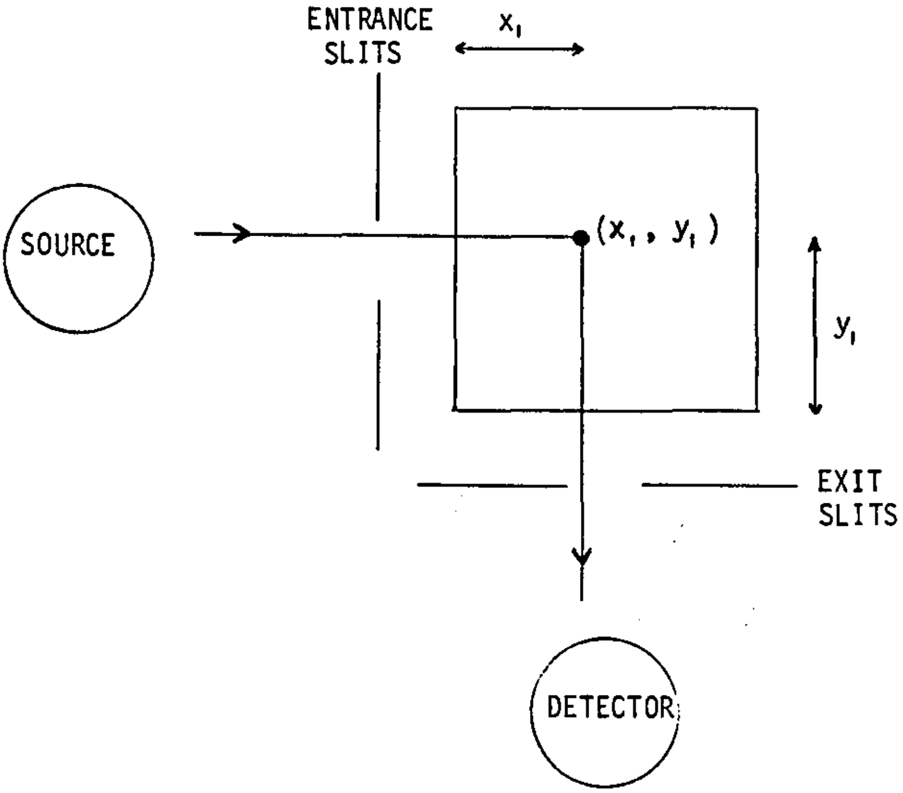
ENTRANCE SLITS
x_1
SOURCE
(x_1, y_1)
y_1
EXIT SLITS
DETECTOR

FIGURE 3.15 Diagram of Fluorescent Molecule at Some Position (x_1, y_1) in a Fluorimeter Cell.

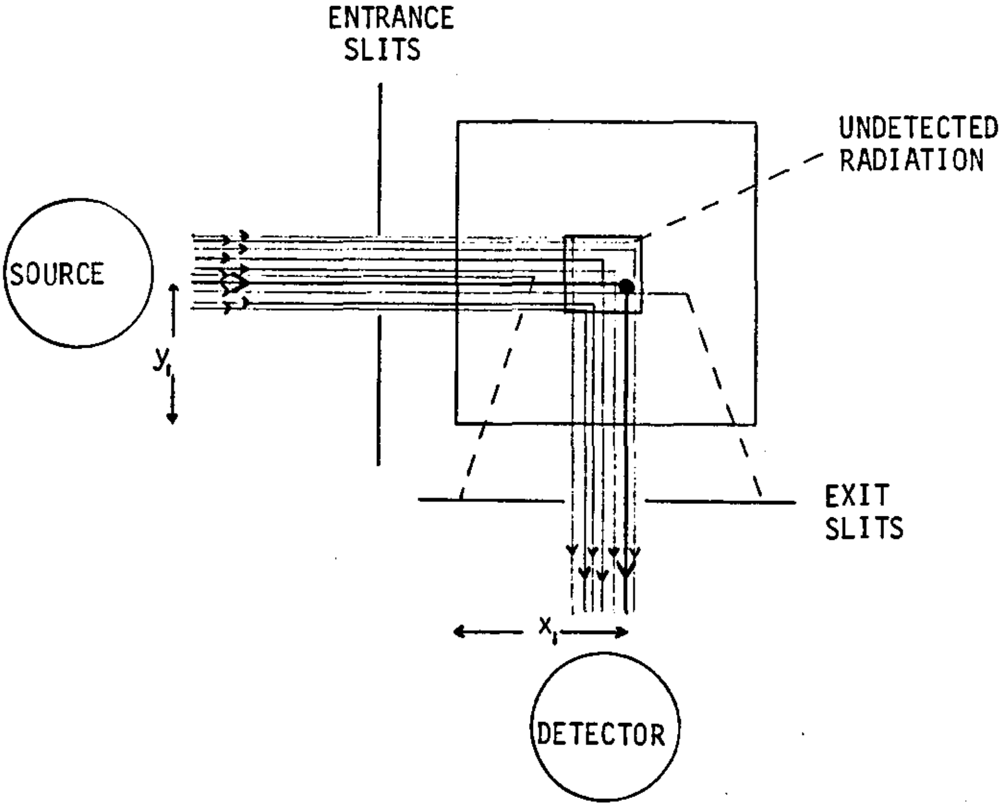
ENTRANCE SLITS
UNDETECTED RADIATION
SOURCE
y_1
EXIT SLITS
x_1
DETECTOR

FIGURE 3.16 Diagram Showing a Central Symmetric, Irradiated Portion of a Fluorimeter Cell.

bound and unbound fractions of the fluorescent probes.

For a fluorescent probe in free solution, several estimates of a_1 and a_2 were obtained by taking absorbance measurements on buffer solutions containing increasing concentrations of the probe. In each case, absorbance readings were recorded at two wavelengths. These corresponded to the excitation and emission monochromator settings used in the appropriate fluorescence titration. Knowing the concentrations of probe in each sample, it was an easy matter to find values of a_1 and a_2 from the absorbance measurements. The mean experimental values of a_1 and a_2 were calculated. Equipped with these it was possible to use Equation 3.5 to correct observed fluorescence intensities for inner-filter effects. All that was necessary was to compound the measured signals Fm with the corresponding concentrations of unbound probe, c. The 'corrected' intensities Fo were plotted against concentration to yield the inner-filter corrected calibration plot.

A typical example is shown in Figure 3.10. It is clearly linear over a wide concentrated range.

For albumin-bound fluorescent probe, absorbance measurements were again made on samples containing increasing quantities of the probe, but in these experiments a fixed concentration of albumin was present. The actual amount of HSA had been determined from a reverse titration, as described previously, and contained sufficient binding sites to accommodate all the probe molecules. As usual, absorbance measurements were recorded at the wavelengths of excitation and emission of the bound probe fluorescence. In this case, though, the protein absorbance had to be subtracted from the totals before determining a_1 and a_2. Determinations were made with a number of concentrations of the bound probe. Mean values of a_1 and a_2 were calculated from the results and along with Equation 3.5 they were sufficient to correct intensity measurements for the inner-filter effect of the bound probe itself. However, since albumin absorbs radiation in the appropriate region of the spectrum, it was shown to be capable of reducing the intensity of the fluorescence observed from the bound probe by a second inner-filter effect. (This was particularly noticeable when warfarin was being studied). To account for this effect, and in so doing to render the points in a plot of 'corrected' fluorescence intensity versus bound probe concentration independent of the protein strength, a_1 and a_2 were found for HSA. These values were used in an expanded version of Equation 3.5, as described below.

In the theory presented previously it had been assumed that the only absorbing species in the sample solution was the fluorescent molecule under examination. The assumption allowed the derivation of Equation 3.4 to be explained in a reasonably simple manner. Moreover it was valid as far as samples containing fluorescent probe in free solution were concerned. Nevertheless in experiments where there are two or more absorbing species in the sample solution, it becomes necessary to expand the exponential term in Equation 3.5 to include the molar absorbtivities and concentrations of each component. So, in general, if any number of absorbing species are present the expression takes the form,

$$Fm = Fo\ \exp\ (-2.303\left\{\frac{a_1(1) + a_2(1))}{2}c_1 + \frac{(a_1(2) + a_2(2))}{2}c_2 \ldots\ldots\right.$$
$$\left. + \frac{(a_1(r) + a_2(r)}{2}\ c_r\right\}) \qquad (3.6)$$

where c_1, c_2, ... c_r are the concentrations of the individual constituents and $a_1(1)$, $a_1(2)$, ... $a_1(r)$ and $a_2(1)$, $a_2(2)$, ... $a_2(r)$ represent the corresponding molar absorbtivities at the wavelengths of excitation and emission, respectively.

To account for the inner-filter effects of both albumin and bound probe, the appropriate version of Equation 3.6 included terms for two absorbing species. As mentioned previously, in titrations where increasing volumes of a stock solution of fluorescent probe were added to a solution of albumin in the fluorimeter cell, the protein concentration became somewhat diluted. Consequently, the inner-filter effect of the albumin was not exactly the same at each point in the titration. This was accounted for by calculating anew the concentration of HSA after each addition of fluorescent probe. Where samples had been prepared separately and the albumin concentration maintained at a steady level, the corresponding inner-filter correction was a constant factor over the whole range of the titration.

The calibration plot of bound probe concentration versus fluorescence intensity which is shown in Figure 3.13 was corrected for self-absorptive effects in the manner described. The calculated fluorescence intensities (▲) are those which would be observed from the specified concentrations of albumin-bound warfarin if neither protein nor probe exhibited an inner-filter effect. Again, the 'corrected' calibration plot is linear over a wide range of concentrations.

In contrast to the bound probe titrations, the so-called 'reverse titrations' contained fixed concentrations of fluorescent probe in the presence of increasing quantities of albumin. A reverse titration curve of observed fluorescence intensity versus protein concentration is shown in Figure 3.12. To prevent the points in this titration curve falling again at high protein concentrations an allowance was made for the increasing inner-filter effect of the albumin. Of course the correction in this instance was different at each point in the titration, being a function of the protein concentration. However it must be admitted that this adjustment for inner-filter effects was somewhat cosmetic; the intention of the reverse titration was simply to indicate the minimum protein concentration required to bind essentially all of a certain quantity of fluorescent probe. This information could be gleaned almost as easily from the uncorrected curve as from the results which had been corrected for inner-filter effects.

Although the procedure described above was highly successful in correcting experimental data for inner-filter effects, a method was developed subsequently which performed the same function but dispensed with the need to measure the molar absorbtivities of samples at the wavelengths of excitation and emission of the bound probe fluorescence. As well as cutting down on the amount of experimental work, it soon became clear that the revised procedure had important theoretical advantages. In particular, no assumption were required regarding the cell orientation or the path of the light beam through the sample. As a result, a more generally applicable procedure for the correction of inner-filter effects could be formulated.

Before describing the new method, it is worth considering some weaknesses in the present approach. As the error in assuming $\sum_{i=1}^{n} e^{(\bar{x}_i + \bar{y}_i)} = n\, e^{(\bar{x} + \bar{y})}$ has been shown to be negligible under most experimental conditions,

$$Fm = F_0 \exp(-2.303\,(a_1\bar{x} + a_2\bar{y})\,c) \qquad (3.4)$$

is a very close approximation to the general equation (3.3). Nevertheless, it may be difficult to determine $\bar{x}$ and $\bar{y}$. In the method described above it was assumed that $\bar{x} = \bar{y} = 0.5$cm. However Equation 3.4 does not require that $\bar{x}$ and $\bar{y}$ be equal, and in some experimental arrangements they are specifically designed not to be so. The equation is valid whatever portion of the sample solution is measured, be it in the centre or the corner of the fluorimeter cell, or at some intermediate location. Since no restrictions were placed on the position of the fluorescent molecule originally considered, the analysis is three-dimensional in the sense that the incident beam and the direction of the emitted radiation need not lie in the same horizontal phase. That is, the possibility that some of the fluorescent radiation can pass at a slight angle up or down into the solution and still be detected has not been discounted. Likewise, there is no requirement that the incident and emitted beams have to be arranged exactly perpendicular in the fluorimeter. Any estimates of the values of $\bar{x}$ and $\bar{y}$ must therefore include a number of assumptions about the experimental set-up and in so doing will restrict the generality of Equations 3.3 and 3.4.

The need to measure a_1 and a_2 for each absorbing species in the sample is also undesirable. Errors in determining these values may adversely affect the accuracy of the original correction procedure.

The revised method was nonetheless based on the same theoretical description of the inner-filter effect that led to Equations 3.3 and 3.4. It is clear from these expressions that the measured fluorescence intensity is dependent on some exponential function of the distances travelled by the exciting and emitted beams on passing through the sample. For a homogeneous sample solution these distances may be approximated very close to the mean values $\bar{x}$ and $\bar{y}$ or, if necessary, more complex functions can be used (see Appendix A). However they are formulated, the value of these functions depends solely on the geometry of the chosen experimental arrangement provided, of course, the sample is uniform. Furthermore, if the sample is of constant composition, and as long as the Beer-Lambert law holds, a_1 and a_2 are independent of concentration. Under these circumstances the term $(a_1\bar{x} + a_2\bar{y})$, or its more complicated equivalent, is a constant and

$$Fm = Fo \exp(-kc) \qquad (3.7)$$

where $k = 2.303\ (a_1\bar{x} + a_2\bar{y})$. If Equation 3.7 holds true for a set of measurements over a certain concentration range, it may be possible to deduce a value of k from the results and in so doing to make an allowance for inner-filter effects.

For completeness, it is worth considering how a background fluorescence signal would fit into Equation 3.7. As described before, background intensities are those emitted by the sample in the absence of fluorescent probe. Now addition of fluorescent probe produces an inner-filter effect in exactly the same manner as F_O is. The total signal which will be detected is therefore,

$$Fm = F_O \exp(-kc) + F_B \exp(-kc) = (F_O + F_B) \exp(-kc)$$

Of course, in the trivial case where there is no inner-filter effect (k = 0), the observed signal is simply the sum of the background fluorescence and the signal emitted by the fluorescent probe. From the last equation,

$$F_o = F_m \exp(kc) - F_B$$

and the inner-filter corrected fluorescence intensity for unit concentration of the probe is given by

$$F_E = F_o/c = 1/c\,\{F_m \exp(kc) - F_B\} \qquad (3.8)$$

This is simply another way of expressing F_E, the term which was defined earlier as the gradient of a plot of the 'corrected' fluorescence intensity versus probe concentration.

Since the fluorescence intensities F_m and F_B, and the concentration c are known for each point in a titration, the last equation provides a means of determining the optimum value of k for any set of results. Ideally, F_E should be constant over all values of c. In practice, of course, experimental error ensures that even if compensation for inner-filter effects is perfectly adequate, slightly different values of F_E will be obtained with each data point. Nevertheless, the best value of k may be defined as the one which produces the minimum variation in F_E over the entire range of the experiment.

The procedure was to test a trial value of k in Equation 3.8. Usually, a reasonable estimate of the 'true' value could be made, although in reality it would be possible to start with any estimate of k, however inaccurate. The initial estimate of k was used in Equation 3.8 along with the experimental values of c, Fm and F_B to complete a set of answers for F_E. The number of values obtained for F_E was equal to the number of samples measured during the titration. Typically 15 measurements were made. From the set of values of F_E, the mean and standard deviation were calculated.

If the initial estimate of k were far removed from the actual value, F_E would vary widely over the entire range of the titration. On the one hand, as increasing sample concentration were considered an underestimation of k would generate successively lower answers for F_E. Conversely, an overestimation of k would produce successively higher answers for F_E as one traversed the calibration curve. These cases are illustrated in Figure 3.17.

Nevertheless, by adjusting the estimate of k in a systematic fashion, a set of values of F_E could be found for which the standard deviation was a minimum. The value of k which corresponded to this minimum was then taken to be the optimum one for the data. The procedure may be appreciated from the results in Table 3.3. The mean of the set of values of F_E with the

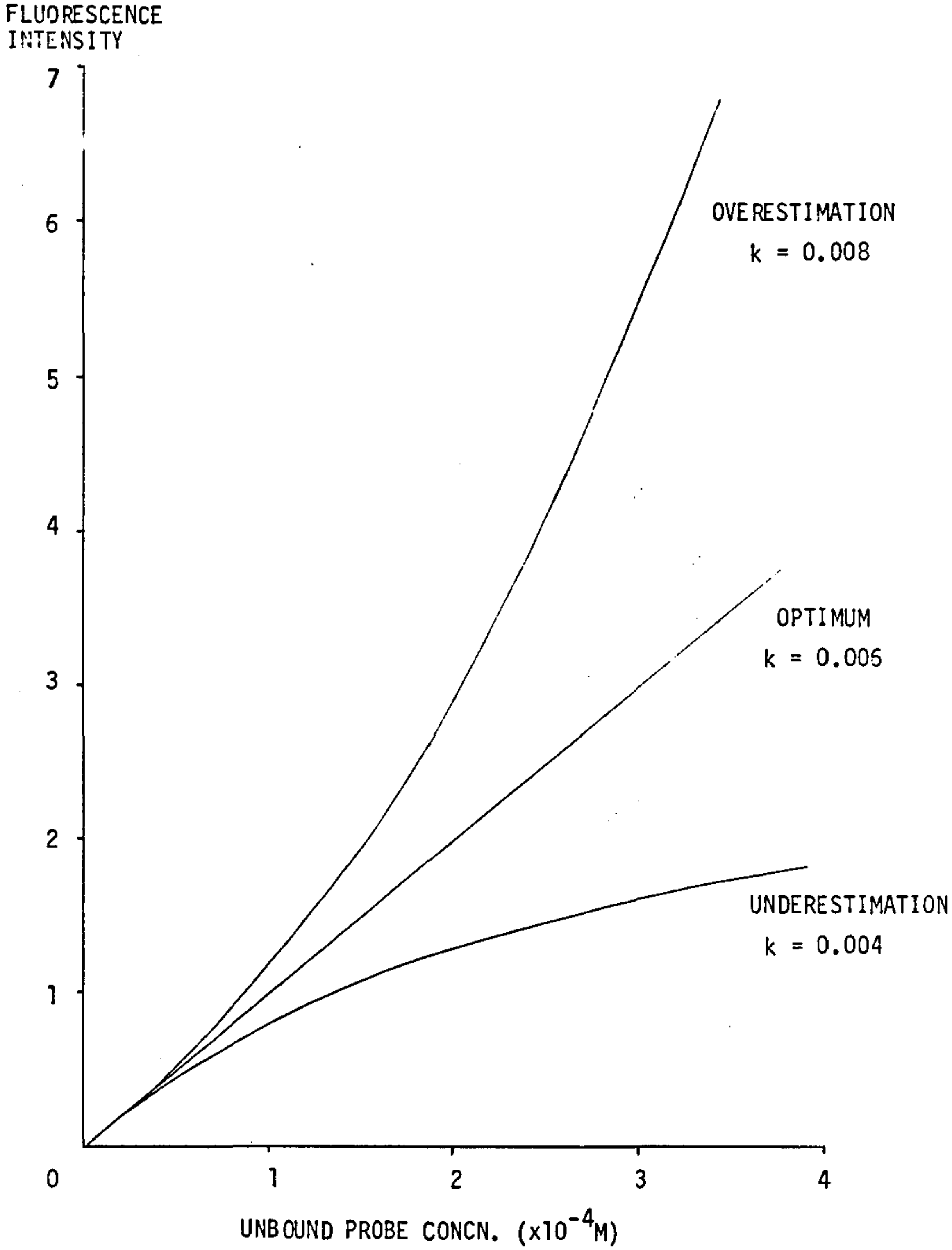

FIGURE 3.17 Illustration of Over- and Under-Estimations of k on Calibration Plots.

k	$\bar{F}_E$	sd	n
0.0056	0.9501	0.04300	14
0.0057	0.9614	0.03683	14
0.0058	0.9728	0.03145	14
0.0059	0.9845	0.02757	14
0.00598	0.9939	0.02618	14
0.00599	0.9951	0.026143	14
0.00600*	0.9963	0.026135	14
0.00601	0.9975	0.02616	14
0.00602	0.9987	0.02622	14
0.0061	1.0084	0.02781	14
0.0062	1.0207	0.03237	14

TABLE 3.3 The Optimization of k from Experimental Data.

k - inner filter correction factor (trial values)

$\bar{F}_E$ - the mean of the values of F_E obtained for each of the n data points when the appropriate value of k is used in Equation 3.8

sd - the standard deviation of the set of F_E values associated with a particular value of k

* The optimum value of k for this set of data (the corresponding sd is a minimum).

Experimental results were obtained by measuring the fluorescence emitted by samples containing ANS in 0.1M Tris/HCl buffer, pH 7.4.

minimum standard deviation was calculated and used to construct the best straight line through the inner-filter corrected flucrescence intensities. From Equation 3.8, the equation of this line is simply $F_0 = c\,F_E$. In the example shown in Figure 3.18, the best straight line through the inner-filter corrected intensities has a gradient F_E of $1.00(\pm 0.03) \times 10^4\ M^{-1}$, where the figure in brackets is the standard deviation of F_E across the curve.

Having obtained suitable values for k and F_E it is possible to construct a curve representing the fluorescence intensities which would be measured experimentally in the presence of the estimated inner-filter effects over a range of sample concentrations. If the background fluorescence is subtracted from each measurement, the curve may be defined as

$$F_m' = F_m - F_B = (cF_E + F_B)\ \exp\ (-kc) - F_B$$

which is just a restatement of Equation 3.8. In Figure 3.18 the theorectical curve can be seen to fit the experimental points over a wide concentration range. This lends support to the original statement that inner-filter effects are instrumental in distorting the linearity of calibration plots of fluorescence intensity versus concentration and that this distortion can be described adequately by a simple exponential function containing a constant k times the fluorphor concentration.

The results depicted in Figure 3.18 were obtained by measuring the fluorescence emitted from ANS in free solution. The only inner-filter effect was that of the unbound probe itself. Now, as explained before, it is necessary to consider inner-filter effects from two sources when interpreting the radiation emitted by protein-bound fluorescent probe. Consequently an extended version of Equation 3.7 is required. This expression is analogous to Equation 3.6 and in its most general form may be written as

$$F_m = F_O \exp\ (- \{k_1 c_1 + k_2 c_2 + \ldots\ldots + k_r\ c_r\ ) \qquad (3.9)$$

where k_1, k_2, k_r are the values of k for each absorbing species in the sample, and c_1, c_2, ... c_r are the corresponding concentrations.

Returning to the specific case of the bound probe fluorescence, the appropriate version of Equation 3.9 included terms for two absorbing species. Estimates of these terms were deduced separately from an examination of the result of the two titrations involved in the production of the calibration plot.

A value of k was found for HSA by considering the results of a

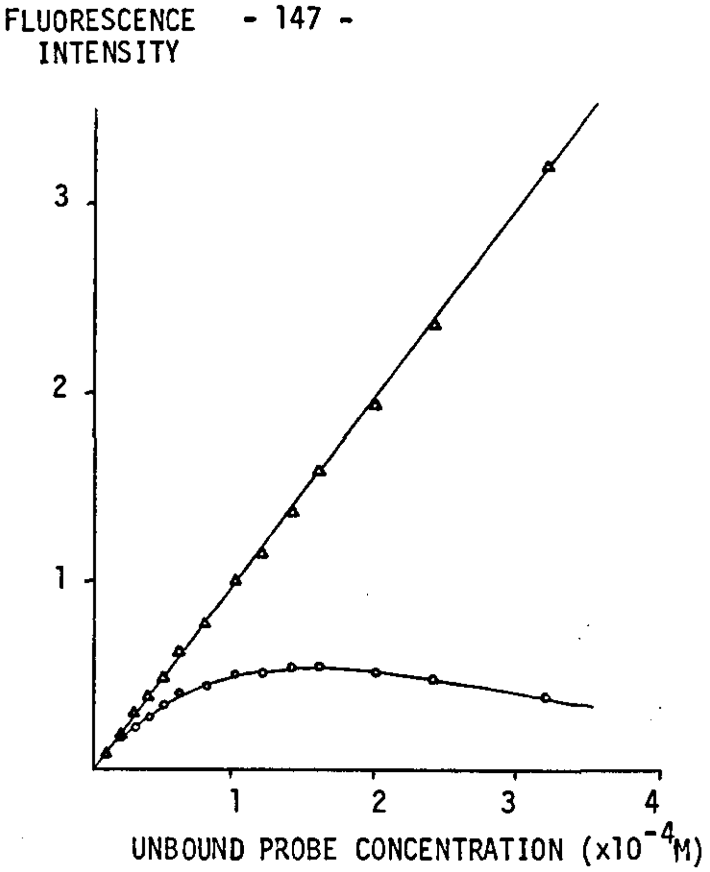

FIGURE 3.18 Calibration Plot for Unbound Fluorescent Probe (ANS)
Across whole curve, F_E=1.00(±0.03) x $10^{-4}M^{-1}$, n=14.
○ Measured fluorescence intensities.
△ Fluorescence intensities corrected for inner-filter effects by determining the optimum value of k using Equation 3.8.

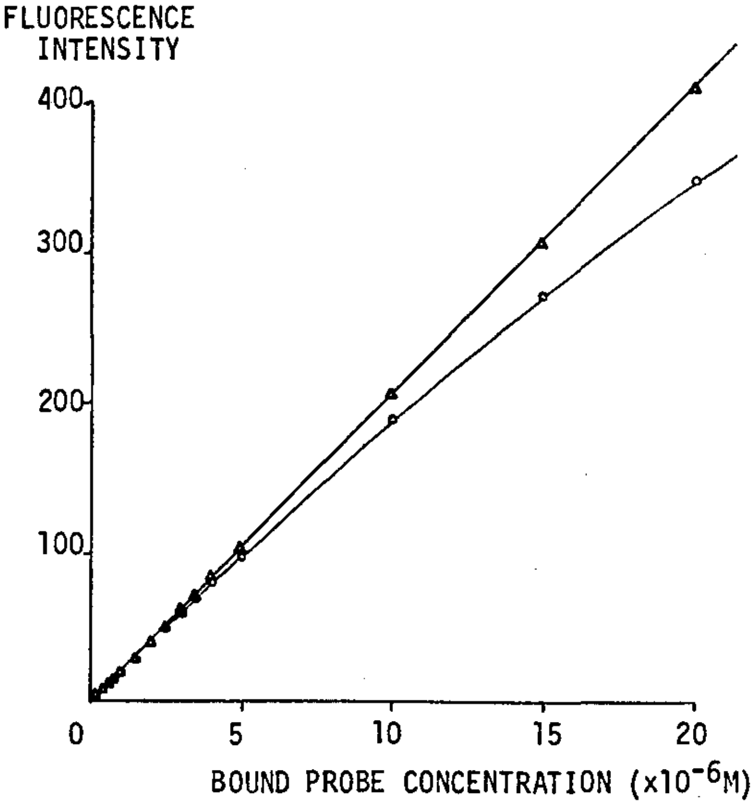

FIGURE 3.19 Calibration Plot for Bound Fluorescent Probe (ANS)
Across whole curve, F_E=2.05(±0.03) x $10^{7}M^{-1}$, n=15.
• Measured fluorescence intensities.
▲ Fluorescence intensities corrected for inner-filter effects by determining the optimum value of k using Equation 3.8.

'reverse titration'. At a certain stage in the titration sufficient albumin will be present to accommodate all the fluorescent probe in the sample. Since there is no more fluorescent probe to be bound, the signal emitted by the sample will have reached a limiting maximum which is independent of further increases in the protein concentration. However, the observed fluorescence intensity will normally start to fall again as more albumin is added because the latter exerts an inner-filter effect. A suitable allowance for the inner-filter effect of HSA must remove this anomaly so that the corrected fluorescence intensities are virtually constant at high protein concentrations.

As all the constituents in the reverse titration were invariant apart from the protein concentration, it was feasible to use an expression of the form shown in Equation 3.8 to determine the optimum value of k for albumin. In this instance F_E represented the 'corrected' fluorescence intensity attributable to unit concentration of the bound probe, and c was the concentration of HSA. The optimum value of k was defined as that which gave the minimum variation in F_E for each concentration of HSA above the critical level necessary to accommodate all the fluorescent probe.

Likewise, the second titration used in the production of a calibration plot of fluorescence intensity versus bound probe concentration involved only one variable. This was the concentration of bound fluorescent probe. Accordingly, it was possible to determine a value of k for the bound probe by taking the experimental results and applying Equation 3.8 in the normal manner.

Combining the estimates of k for the bound fluorescent probe and the albumin in the way shown in Equation 3.9 made it practicable to produce a plot of 'corrected' fluorescence intensity versus bound probe concentration whose values were independent of the protein concentration. An example is shown in Figure 3.19. Here the magnitude of F_E, which corresponds to the gradient of the straight line calibration plot, is much larger than that obtained for the same probe in free solution (Figure 3.18). Indeed, the gradients differ by a factor of more than two thousand. This is another illustration of the fluorescence enhancement which accompanies the binding of ANS to HSA.

The procedure of optimizing the value of k from the observed fluorescence intensities is easily computerized. Consequently an appraisal of the 'goodness of fit' between experiment and theory is readily available and can be used in the analysis of errors. This approach has other advantages over the previously described method for estimating inner-filter effects which are worth considering. No estimates of $\bar{x}$ and $\bar{y}$ are required as the method is independent of the geometry of the light path through the sample. In fact, inner filter corrections are possible even if the sample cell arrangement is unknown. Having performed a fluorescence titration, there is no need for further experiments to measure a_1 and a_2. This offers a saving in reagents as well as time, and reduces the level of experimental error.

A slight disadvantage of simply optimizing k to produce a mathematical fit to the data is that the correction procedure is not as physically plausible as is a direct measurement of the variables responsible for the inner-filter effect. Of course, if the assumptions about the geometry of the light path through the sample are correct and providing a_1 and a_2 are measured accurately, then the two methods of inner-filter correction will give identical results.

As shown in Figures 3.18 and 3.19, once account had been taken of solvent, dilution and inner-filter effects, it was possible to express the concentrations of bound and unbound probe as linear functions of fluorescence intensity. When in this form, the information provided the means to determine the degree of binding of a fluorescent probe to a protein over a wide concentration range.

3.3 The Production of Data for Binding Curves

The procedure was to take a convenient concentration of albumin, add various quantities of the probe and record the fluorescence emitted by the sample. The problem was to deconvolute the observed fluorescence intensities in terms of the separate contributions from the bound and unbound fractions of the ligand. By making use of the results of the previous section it was possible to achieve this and in so doing to determine the degree of binding of the fluorescent probe to HSA.

3.3.1 Practical Aspects of Binding Titrations

Initially, titrations were performed in the fluorimeter cell by adding microlitre volumes of a stock solution of probe to a known quantity of albumin. Samples were stirred with the tip of the microsyringe used to dispense the fluorescent probe. Measurements of the fluorescence intensity were recorded with the same wavelength settings and under exactly the same experimental conditions as were employed in the generation of the corresponding calibration plots. As these procedures and conditions have been described already, they will not be repeated here.

Titrations were also carried out in which a series of samples of the required composition were prepared outside the fluorimeter. The advantages of this form of sample preparation have been discussed in Section 3.2.1. Fluorescence intensities were recorded in the usual manner.

3.3.2 The Analysis of the Results of Binding Titrations

The results consisted of a series of fluorescence intensity measurements, F_m. Each measurement corresponded to a certain total concentration of fluorescent probe, C_T, the strength of the protein being constant or nearly so.

At each stage in the binding titration the concentrations of bound and unbound probe were in thermodynamic equilibrium. Since it is axiomatic that the bound probe fluorescence is far more intense than that of an equivalent quantity in free solution, the measured fluorescence intensity at any point in the titration was a unique function of the degree of binding. Thus, in the absence of inner-filter effects and background signals,

$$F_m = C_B F_E^B + C_u F_E^U \tag{3.10}$$

where F_m is the measured fluorescence, C_B and C_u are the concentrations of bound and unbound fluorescent probe; and F_E^B and F_E^u are the intrinsic fluorescence factors of bound and free fluorescent probe, respectively. Values for F_E^B and F_E^u were available from the work of the previous sections. Furthermore,

$$C_T = C_B + C_u \tag{3.11}$$

where C_T is the total concentration of fluorescent probe added to the system. Now, Equations 3.10 and 3.11 constitute two simultaneous equations containing two unknowns, C_u and C_B. In its simplest form, therefore, the problem of finding levels of bound and free ligand reduces to the solution of two simultaneous equations. Unfortunately, the observed fluorescence will nearly always be attenuated by inner-filter effects due to bound probe, free probe and protein, and may contain a contribution from albumin. These additional factors must be taken into consideration when analysing the results of a binding titration. An iterative computer procedure, FLUORB, was developed to perform this function.

Descriptions of the signals attributable to free and albumin-bound fluorescent probe were fed into the memory of the computer. As outlined previously, F_E, the fluorescence intensity corrected for inner-filter and other effects, was available for unit concentrations of bound and unbound probe from the gradients of the respective linear calibration plots. For convenience, the reciprocal values were employed. Thus, the labels FTDBC and FTDFC were given to the terms capable of converting corrected fluorescence intensities into concentrations of bound and unbound fluorescent probe. To provide a better description of the results obtained under normal experimental conditions, inner-filter correction factors for albumin, and for bound and unbound fluorescent probe were introduced in turn as AP, AB and AF. These factors were the values of the expressions $2.303\frac{(a_1 + a_2)}{2}$ or k covered in Section 3.2.3. If applicable more information concerning dilution and solvent effects was presented to the computer program.

Where necessary FLUORB had to be modified slightly to make allowances for sample dilution. In this form the program was able to calculate the total concentrations of both fluorescent probe and albumin at each point in the titration by taking regard of the slight increase in sample volume following each addition of the stock reagent. To account for solvent effects, the program had to be adapted still further. These relatively simple modifications are not shown in the listing in Figure 3.20.

Once the computer contained a description of the fluorescence intensity emitted by a wide range of concentrations of bound and unbound probe, it was programmed to accept the results of a binding titration. The process may be followed in lines 51-53 of Figure 3.20 where values of DC(I) the total concentration of probe in each sample, are fed in alongside the corresponding measured fluorescence intensities, EXF(I).

Sufficient information was then held in the memory to permit a calculation of the concentrations of the bound and unbound fractions of the probe at each point in the binding titration. However the complex nature of the calculation meant that an iterative solution was required.

Before commencing the iteration, an assumption had to be introduced in to the program. This made for rather an obvious statement. It concluded that the bound fraction of the probe was responsible for the major part of the observed fluorescence intensity over all concentrations. The assumption meant that an initial, approximate value for the bound probe concentration could be found at any point in the titration directly from the recorded fluorescence intensity EXF(I). Although not strictly true, especially at high probe:protein ratios, the assumption provided a means by which the iterative procedure could be initiated in a simple and convenient fashion. Thus in line 57 the initial estimate of the corrected emission intensity of the bound fraction CDBF(I) is set equal to the measured fluorescence signal EXF(I) for the sample under consideration. As will become clear

```
C     READ IN EXPERIMENTAL DATA
      DO 1 I=1,100
      READ(1,102,END=2)DC(I),EXF(I)
  102 FORMAT(2F10.5)
    1 CONTINUE
C     BEGIN ITERATION TO GENERATE DATA SATISFYING INPUT VALUE, EXF(I)
    2 DO 7 I=1,N
      CDBF(I)=EXF(I)
    3 DB(I)=CDBF(I)*FTDBC
      DF(I)=DC(I)-DB(I)
      CDFF(I)=DF(I)/FTDFC
      UDBF(I)=CDBF(I)*EXP(-(AB*DB(I))-(AF*DF(I))-(AP*PCONCN))
      UDFF(I)=CDFF(I)*EXP(-(AB*DB(I))-(AF*DF(I))-(AP*PCONCN))
      X=EXF(I)-(UDBF(I)+UDFF(I))
      Y=-X
      IF(X.GE.0.001) GO TO 6
      IF(Y.GE.0.001) GO TO 6
      IF(X.LE.0.001.AND.Y.LE.0.001) GO TO 4
    4 R(I)=DB(I)/PCONCN
      RONDF(I)=R(I)/DF(I)
      RINVS(I)=1/R(I)
      DFINVS(I)=1/DF(I)
      DFONR(I)=DF(I)/R(I)
      WRITE(2,103)DC(I),DB(I),R(I),RONDF(I),RINVS(I),DFINVS(I),
     1DFONR(I),DF(I)
  103 FORMAT(4(4X,F8.4,2X,F8.4))
      GO TO 7
C     ADJUST ESTIMATE OF CDBF
    6 CDBF(I)=CDBF(I)+1.5*X
      GO TO 3
    7 CONTINUE
```

FIGURE 3.20 Listing of a Segment of FLUORB

shortly, the validity of this statement is irrelevant to the proper functioning of the program.

A first approximation to the concentration of bound probe DB(1) is determined from CDBF(1) using the conversion factor FTDBC (see line 58). DF(1), the concentration of probe now supposedly remaining in free solution is found simply by subtracting DB(1) from the total concentration of fluorescent probe in the sample. In conjunction with FTDFC, DF(1) is used to obtain CDFF(1) which represents the corrected fluorescence intensity associated with this first estimate of the concentration of unbound probe. The calculation is shown in line 59. The values CDBF(1) and CDFF(1) are stored in the computer.

As well as having acess to the protein concentration, PCONCN, the program now contains estimates of the protein-bound and unbound probe concentrations. The way forward is clear. The signal that would be observed under normal experimental conditions from a sample of the proposed composition must be computed and compared with the value actually recorded. If the two quantities are in agreement, then the estimates of the concentrations of the bound and unbound fractions may be taken to be close to those existing in the sample.

The next step, therefore, is to modify the corrected fluorescence intensity due to the bound fraction, CDBF(1), so that account is made for solvent, dilution, inner-filter or other experimental artefacts. As described previously, however, experiments were usually designed so that only inner-filter phenomena were worthy of consideration. Line 61 shows how the inner-filter effects of the three absorbing species in the sample may be accounted for and how the uncorrected fluorescence intensity, UDBF(1), is determined from CDBF(1). Of course, the concentrations of the bound and unbound probe to use in this equation are the initial estimates, DB(1) and DF(1), since these make up the sample composition currently under test. At the same time and in a similar manner, it is possible to use CDFF(1) to compute the fluorescence intensity that would be observed experimentally from the unbound fraction in the presence of these inner-filter effects. Thus UDFF(1) is calculated in line 62 of the program.

The quantities UDBF(1) and UDFF(1) are summed to give the total fluorescence intensity which would be measured with the hypothetical sample of composition DF(1), DB(1), PCONCN. The result is compared with the experimental value EXF(1) in line 63. Unless the two terms agree within certain limits which are set closer together than the minimum intensity change detectable by the fluorimeter, the program adjusts the value of CDBF(1) in the appropriate direction. This adjustment may be followed in lines 63-66 and 78-79. The new value of CDBF(1) allows fresh estimates of the concentrations of bound and free fluorescent probe to be generated. Fluorescent intensities are computed again and the results compared with EXF(1). If necessary, CDBF(1) is adjusted for a second time and the cycle repeated once more. It is possible that a large number of cycles may be required before the statement in line 67 is satisfied. Fortunately, however, the oscillating iterative procedure incorporated into the program is very efficient and it can quickly reveal the sample composition responsible for the observed fluorescence intensity.

Once this has been achieved for one data point, the next value of (DC(I), EXF(I)) say (DC(2), EXF(2)) may be processed. Before doing so, though, the computer is instructed to take the concentrations of the bound and unbound probe it has just determined and, along with the protein concentration, to present the results in a form suitable for constructing binding plots. These representations are discussed in the next section and some experimental data are presented.

3.4 The Presentation of Results

The most common method for presenting the results of an in vitro binding study is in terms of one of the linearization procedures described in Chapter 1. Examples of these linear transforms are the Scatchard Plot $^{r}/Cu$ v. r (Scatchard, 1949), the double-reciprocal plot of $^{1}/r$ v. $^{1}/Cu$ (Klotz, 1946) and the plot $^{Cu}/r$ v. Cu (Klotz, 1953) in which Cu represents the concentration of unbound ligand, and r is the ratio of the concentration of bound ligand C_B to the total concentration of protein (or other macromolecule) C_p. Since the parameters of these binding equations are simple functions of the total protein concentration and the concentrations of bound and unbound ligand, it proved quite straightforward to instruct the program FLUORB to generate numerical output for binding curves. The only requirement was that the concentrations of the three species should be combined in the appropriate manner. The relevant equations are given in lines 68-73 of the program.

A subroutine was available which allowed data to be represented graphically on the lineprinter. This program was used in conjunction with FLUORB to illustrate the results of a binding titration in the form of the three plots described above.

The binding of warfarin to HSA has been studied. The results of one experiment are shown in Tables 3.4(a)-(c) and Figures 3.21-3.23. In this example, inner-filter correction factors were determined from absorbance measurements taken at the wavelengths of maximum excitation and

SUMMARY OF DATA

DC	DB	R	RONDF	RINVS	DFINVS	DFONR	DF
0.4194	0.3446	0.0675	0.9032	14.8111	13.3768	1.1072	0.0748
0.8386	0.6610	0.1295	0.7295	7.7207	5.6299	1.3714	0.1776
1.2577	0.9482	0.1858	0.6002	5.3816	3.2302	1.6661	0.3096
1.6767	1.2308	0.2412	0.5410	4.1452	2.2425	1.8485	0.4459
2.0955	1.5033	0.2947	0.4976	3.3931	1.6885	2.0095	0.5922
2.5142	1.7652	0.3461	0.4621	2.8891	1.3352	2.1639	0.7490
3.3512	2.2498	0.4413	0.4007	2.2661	0.9080	2.4958	1.1014
4.1876	2.6629	0.5225	0.3427	1.9139	0.6559	2.9181	1.5246
5.0234	3.0338	0.5955	0.2993	1.6794	0.5026	3.3413	1.9896
5.8587	3.3830	0.6642	0.2683	1.5056	0.4039	3.7273	2.4757
6.6934	3.6358	0.7141	0.2335	1.4004	0.3271	4.2818	3.0576
7.5276	3.8977	0.7658	0.2110	1.3059	0.2755	4.7403	3.6299
8.3612	4.1435	0.8143	0.1931	1.2280	0.2371	5.1795	4.2178
10.0268	4.5956	0.9038	0.1664	1.1065	0.1841	6.0094	5.4312
12.5210	4.9965	0.9836	0.1307	1.0167	0.1329	7.6499	7.5245
16.6671	5.5558	1.0955	0.0986	0.9128	0.0900	10.1426	11.1113
20.7994	5.9112	1.1675	0.0786	0.8565	0.0672	12.7520	14.8883
24.9181	6.2274	1.2320	0.0659	0.8117	0.0535	15.1708	18.6907
41.2579	7.0378	1.4015	0.0410	0.7135	0.0292	24.4162	34.2201
61.3837	7.6842	1.5428	0.0287	0.6482	0.0186	34.8065	53.6995
81.1848	8.6743	1.7558	0.0242	0.5696	0.0138	41.2987	72.5105
119.8443	11.1565	2.2946	0.0211	0.4358	0.0092	47.3668	108.6878

(a) (b) (c)

TABLE 3.4 The Data of One Binding Experiment as Represented by the Program FLUORB

DC - total concentration of warfarin (10^{-6}M)

DB - concentration of bound warfarin (10^{-6}M)

DF - concentration of free warfarin (10^{-6}M)

R - DB/PCONCN where PCONCN is the total protein concentration; in this experiment albumin concentration was 5.10 x 10^{-6}M.

RONDF - R/DF ($10^{6}M^{-1}$)

RINVS - 1/R

DFINVS - 1/DF ($10^{6}M^{-1}$)

DFONR - DF/R (10^{-6}M)

Data presented in form of

(a) Scatchard plot (Scatchard, 1949)
(b) Double reciprocal plot (Klotz, 1946)
(c) Klotz plot (Klotz, 1953)

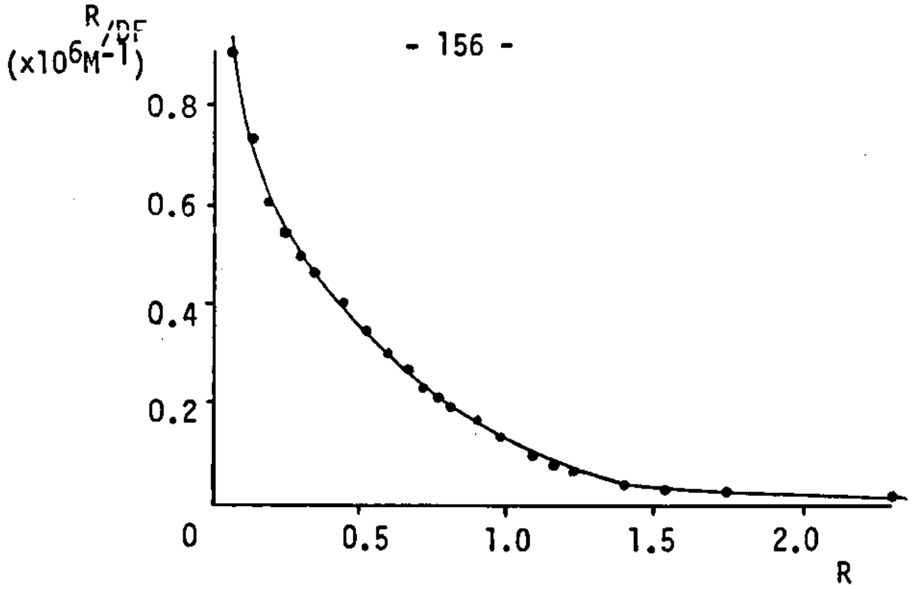

FIGURE 3.21 Scatchard Plot Representing the Binding of Warfarin to HSA.

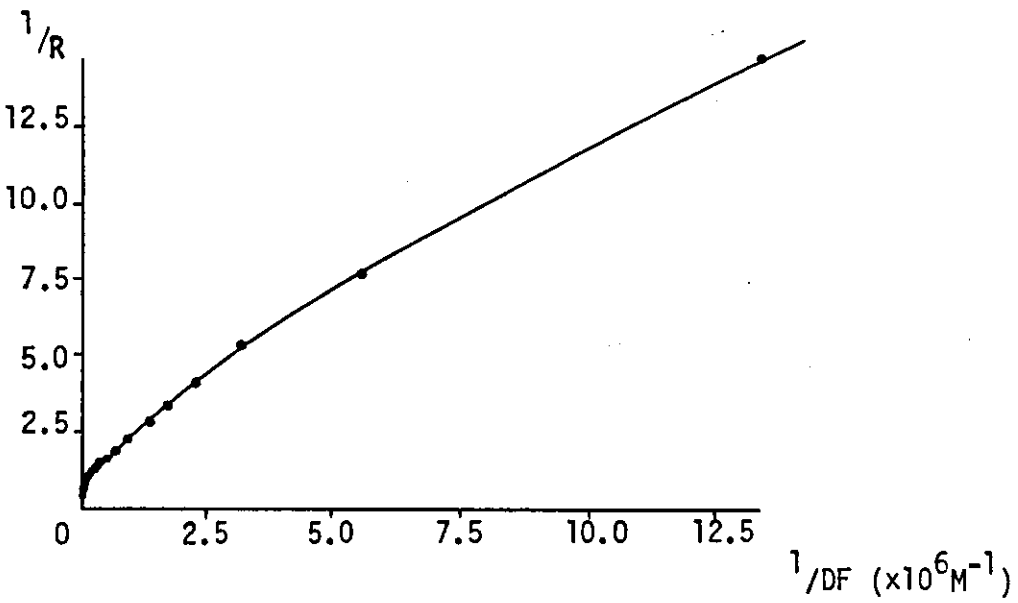

FIGURE 3.22 Double Reciprocal Plot Representing the Binding of Warfarin to HSA.

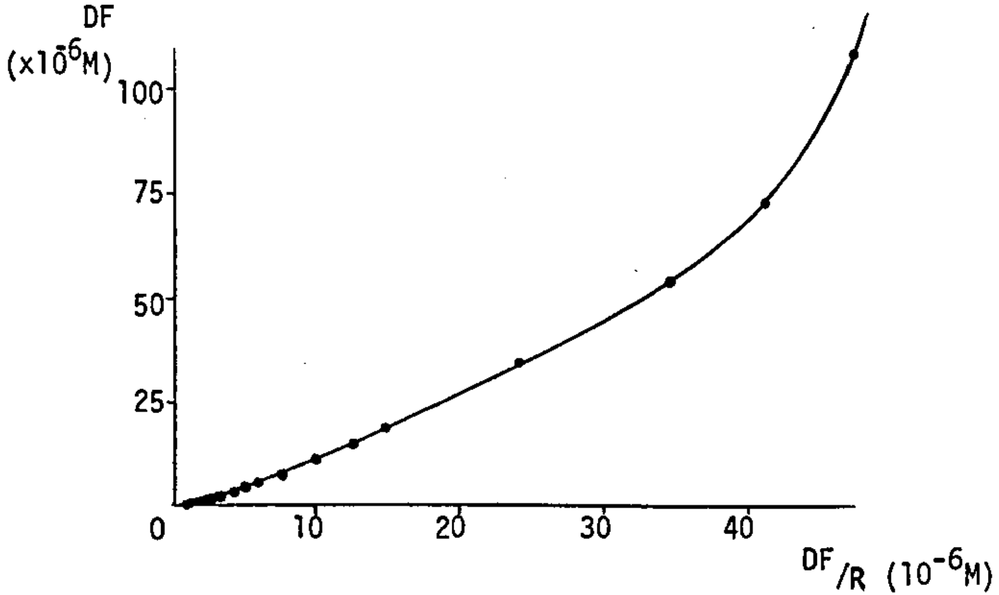

FIGURE 3.23 $^{DF}/_{R}$ Versus DF Plot Representing the Binding of Warfarin to HSA.

NB. The three graphs on this page were produced from the same set of binding data.

emission of fluorescence. Dilution effects were considered but solvent corrections were unnecessary as the stock solution of warfarin contained only a small volume of 0.1M NaOH. The units of concentration are 10^{-6}M.

A comparison of the three representations of the binding data shows how the plots of $^{1}/r$ v. $^{1}/Cu$ and $^{Cu}/r$ v. Cu tend to compress the results to one end of the graphs, while the experimental points in the Scatchard Plot are more evenly spaced. The rather cumbersome way in which the parameters of the first two transorms vary can also be appreciated by inspecting the numerical data in Tables 3.4(b) and 3.4(c). There is a temptation to draw straight lines through the points in the Klotz Plots, especially if the values obtained at the lowest probe:protein ratios are omitted. Misinterpretation of the Scatchard Plot is less easy. Furthermore, Meyer and Guttman (1968) believe the double reciprocal plot to be less widely accepted than the Scatchard representation on account of its tendency to underemphasize the results obtained at low ligand:protein ratios. These are the results which are frequently the most relevant in vivo.

Although all three portrayals of the binding data contained the same information, albeit in slightly different forms, it was concluded that the Scatchard Plot was the easiest to work with.

Now, linear plots will be obtained with the functions represented by the coordinates in Figures 3.21-3.23 only if a single class of binding sites is involved, each site being totally independent of the others. It is obvious from the results that the interaction between HSA and warfarin entails more than a single class of non-interacting sites.

Likewise, the curved Scatchard Plot in Figure 3.24 suggests that the binding of albumin to the fluorescent dye ANS is also complicated by the existence of either different classes of sites or interacting sites. In this experiment inner-filter factors were deduced directly from the calibration plots as outlined previously. There were no solvent or dilution effects to consider.

In Chapter 1 it was seen how the slopes and intercepts of linear binding plots may be used to determine the number of independent binding sites and the apparent association constants. With non-linear binding curves, which are symptomatic of more complicated interactions, Klotz and Hunston (1971) have shown that no simple relationship exists between the slopes and intercepts of these graphs and the binding constants. Under these circumstances it is necessary to employ curve-fitting procedures if anything like accurate values are required for the binding constants. Rosenthal (1967) has proposed a graphical method for the presentation and determination of binding parameters from the Scatchard plots of systems

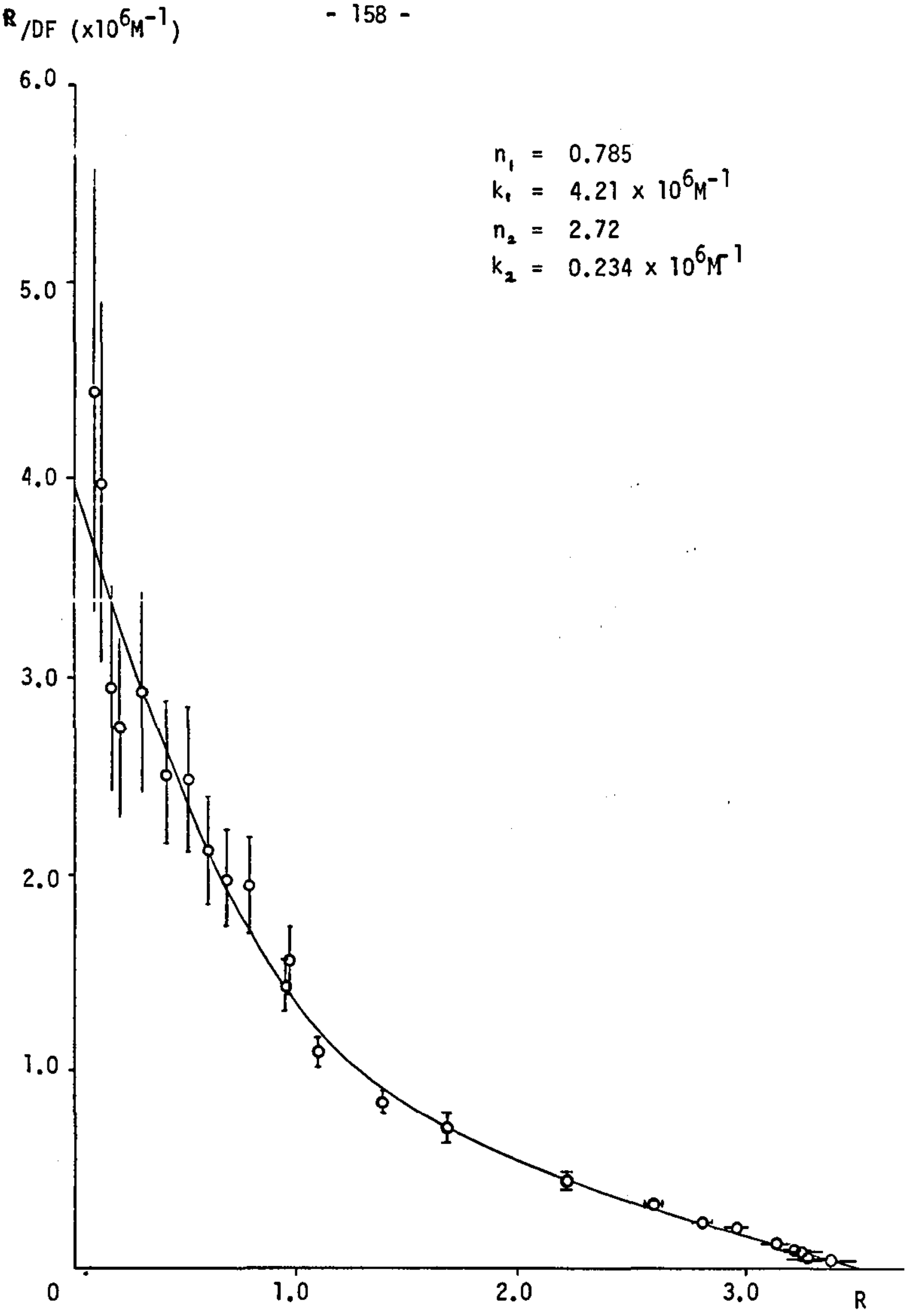

FIGURE 3.24 A Scatchard Plot Representing the Binding of ANS to HSA.

The curve and the binding constants were derived from the experimental data with the aid of the NKFIT routine. Error bars were computed as described in the text.

which involve one or more non-interacting binding sites. This method includes a trial and error procedure which has to be continued until a specified match to the experimental curve is found. Based on this approach,, Pennock (1973) has devised a simple mechanical calculator which may be used to aid in the extraction of binding parameters from experimentally determined Scatchard Plots. However, these and other manual methods suffer from their complexity and tediousness. Furthermore, a subjective decision has to be made concerning the best fit to the data.

To overcome some of these problems, a computerized curve-fitting procedure was developed which allowed for the routine analysis of binding data. The method provided a means of extracting quantitative information from the results of a binding titration. Its main features are discussed in the next section.

3.5 The Calculation of Binding Constants from Experimental Data

A computer program was written to analyse the results of a binding titration in terms of a two-site binding equation:

$$R(I) = \frac{n_1 k_1 DF(I)}{1 + k_1 DF(I)} + \frac{n_2 k_2 DF(I)}{1 + k_2 DF(I)} \qquad (3.12)$$

where $R(I)$ - moles of fluorescent probe bound per mole of protein.
$DF(I)$ - concentration of free (ie. unbound) probe.
n_1, n_2 - the number of binding sites in each class.
k_1, k_2 - the apparent association constants for these sites.
and I = 1, N where N is the number of experimental observations.

The program NKFIT finds the values of n_1, k_1, n_2, and k_2 which best satisfy Equation 3.12 for a complete set of values (R(I), DF(I). As previously described, R(I) and DF(I) may be deduced from the experimental data with the aid of FLUORB. A segment of the NKFIT routine is shown in Figure 3.25 and the following summary of its operation may be understood with reference to this listing.

By varying the binding constants n_1, k_1, n_2 and k_2 in a systematic fashion and reading in a series of DF(I) values,it is possible for the program to produce several thousand sets of results for R(I) from Equation 3.10. These are stored as the variable RR(I) in line 93. Each set of RR(I) values corresponds to a particular value of the parameters n_1, k_1, n_2 and k_2, while each member of the set is also related to a certain value of DF(I).

```
      R(I)=0.0
      RONDF(I)=0.0
      RFITDF(I)=0.0
   17 CONTINUE
C     READ IN SETS OF INPUT DATA.
      DO 7 I=1,NDATA
      READ(1,101,END=16) R(I),DF(I)
  101 FORMAT(F9,4,F10,4)
    7 CONTINUE
   16 DO 1 K=1,NI
      ONEN(K)=0.0
      DO 1 L=1,NI
      TWON(L)=0.0
      DO 1 M=1,NI
      KONE(M)=0.0
      DO 1 N=1,NI
      KTWO(N)=0.0
      SUMSQ(K,L,M,N)=0.0
    1 CONTINUE
      DO 2 I=1,101
      RFIT(I)=0.0
      ERROR(I)=0.0
      PRCENT(I)=0.0
      RR(I)=0.0
    2 CONTINUE
C     GENERATE A SERIES OF TRIAL VALUES
      DO 3 K=1,NI
      AK=K
      ONEN(K)=TONEN+(AK-1.0)*STEP/5.0
    3 CONTINUE
      DO 4 L=1,NI
      AL=L
      TWON(L)=TTWON+(AL-1.0)*STEP/5.0
    4 CONTINUE
      DO 5 M=1,NI
      AM=M
      KONE(M)=TKON+(AM-1.0)*STEP
    5 CONTINUE
      DO 6 N=1,NI
      AN=N
      KTWO(N)=TKTWO+(AN-1.0)*STEP/2.5
    6 CONTINUE
C     CALCULATE SETS OF RR USING ALL COMBINATIONS OF TRIAL VALUES
      CFMIN=SUMSQ(1,1,1,1)
    8 DO 11 K=1,NI
      DO 11 L=1,NI
      DO 11 M=1,NI
      DO 11 N=1,NI
      SSQ=0.0
      DO 9 I=1,NDATA
      RR(I)=(ONEN(K)*KONE(M)*DF(I))/(1+KONE(M)*DF(I))+
     1(TWON(L)*KTWO(N)*DF(I))/(1+KTWO(N)*DF(I))
      DIFF=(RR(I)-R(I)/R(I)
      IF(DIFF.LT.0.0) GO TO 77
      GO TO 9
   77 DIFF=-DIFF
    9 SSQ=SSQ+DIFF
      SUMSQ(K,L,M,N)=SSQ
   11 CONTINUE
C     FIND MINIMUM VALUE OF SUMSQ,CFMIN.
      CFMIN=SUMSQ(1,1,1,1)
      DO 10 K=1,NI
      DO 10 L=1,NI
      DO 10 M=1,NI
      DO 10 N=1,NI
      IF(K*L*M*N.EQ.1) GO TO 10
      IF(SUMSQ(K,L,M,N).LT.CFMIN) GO TO 15
      GO TO 10
   15 CFMIN=SUMSQ(K,L,M,N)
   10 CONTINUE
      FMIN=CFMIN/NDATA*100.0
C     SEARCH OUT VALUES OF ONEN,TWON,KONE,&KTWO WHICH GIVE CFMIN.
      IW=0
      DO 12 K=1,NI
      IW=IW+1
      IX=0
      DO 12 L=1,NI
      IX=IX+1
      IY=0
      DO 12 M=1,NI
      IY=IY+1
      IZ=0
      DO 12 N=1,NI
      IZ=IZ+1
      IF(ABS(CFMIN-SUMSQ(K,L,M,N)).LT.0.00000001) GO TO 13
   12 CONTINUE
   13 TONEN=ONEN(IW)-STEP/5.0
      TKONE=KONE(IV)-STEP
      TTWON=TWON(IX)-STEP/5.0
      TKTWO=KTWO(IZ)-STEP/2.5
      NCOUNT=NCOUNT+1
      IF(NCOUNT.GE.5) GO TO 18
      ANI=NI
      STEP=STEP/(ANI/2.0)
      NI-NI+1
      GO TO 16
   18 WRITE(2,102) ONEN(IW),KONE(IV),TWON(IX),KTWO(IZ),IW,IX,IY,
      IZ,FMIN
     1,STEP
  102 FORMAT(11X,6HONEN =,F8.5/11X,6HKONE =,F8.5/11X,6HTWON =,
      F8.5/11X,6
     1HKTWO =,F8.5/11X,4HIW =,I4/11X,4HIX =,I4/11X,4HIY =,I4/11X,
      4HIZ =,
     1I4/11X,26HAVERAGE PERCENTAGE ERROR =,F10.6/11X,12HFINAL
      STEP =,F10
     1.7///)
      WRITE(2,103)
  103 FORMAT(75H          DF               R              RFIT          ER
     1ROR PRCENT)
      SUMERR=0.0
      DO 14 I=1,NDATA
      RFIT(I)=(ONEN(IW)*KONE(IY)*DF(I))/(1+KONE(IY)*DF(I)
     1   )+(TWON(IX)*KTWO(IZ)*DF(I))/(1+KTWO(IZ)*DF(I)
     1)
      ERROR(I)=R(I)-RFIT(I)
      PRCENT(I)=((R(I)-RFIT(I))/R(I))*100.0
      RONDF(I)=R(I)/DF(I)
      RFITDF(I)=RFIT(I)/DF(I)
      SUMERR=SUMERR+(ERROR(I)*ERROR(I))
      WRITE(2,104) DF(I),R(I),RFIT(I),ERROR(I),PRCENT(I)
  104 FORMAT(5(F15.5))
   14 CONTINUE
      WRITE(2,107) SUMERR
  107 FORMAT(11X,26HSUM OF SQUARES OF ERRORS =,F10.7)
      STOP
      END
```

```
SUMMARY OF DATA

            ONEN = 0.78476
            KONE = 4.21429
            TWON = 2.72571
            KTWO = 0.23429
            IW =   8
            IX =   8
            IY =   3
            IZ =   4
            AVERAGE PERCENTAGE ERROR = 3.993513
            FINAL STEP = 0.0047619

  0.01880        0.08340        0.06956        +0.01384       +16.58984
  0.03120        0.12440        0.11097        +0.01343       +10.79273
  0.05570        0.16280        0.18430        -0.02150       -13.20808
  0.07430        0.20250        o.23377        -0.03127       -15.44044
  0.10460        0.30530        0.30530        +0.00000        +0.00141
  0.16020        0.40250        o.41489        -0.01239        -3.07716
  0.20240        0.50260        0.48465        +0.01795        +3.57207
  0.28240        0.59450        0.59559        -0.00109        -0.18336
  0.34910        0.68930        0.67328        +0.01602        +2.32431
  0.40610        0.78620        0.73214        +0.05406        +6.87647
  0.66040        0.94940        0.94254        +0.00686        +0.72206
  0.60930        0.96050        0.90529        +0.05521        +5.74761
  1.00030        1.09380        1.15180        -0.05800        -5.30287
  1.65760        1.38750        1.44893        -0.06143        -4.42745
  2.37420        1.66830        1.68770        -0.01940        -1.16270
  4.91160        2.20700        2.20696        +0.00004        +0.00185
  8.14480        2.59360        2.55101        +0.04259        +1.64203
 12.20220        2.79980        2.78914        +0.01066        +0.38061
 16.55600        2.94110        2.94071        +0.00039        +0.01339
 25.74010        3.11960        3.11561        +0.00399        +0.12786
 35.29540        3.21690        3.21117        +0.00573        +0.17799
 45.21050        3.23550        3.27124        -0.03574        -1.10477
 65.13730        3.25150        3.34000        -0.08850        -2.72189
 84.60000        3.36910        3.37737        -0.00827        -0.24537

            SUM OF SQUARES OF ERRORS = 0.0272319
```

<u>FIGURE 3.25</u> Segment of NKFIT

If the binding constants are allowed to vary over a wide range, many of the sets of results that are computed for RR(I) will be very different from the experimental set R(I). NKFIT is instructed to search through all the sets of RR(I) values it has generated and to find the one which best fits the input data. The values of n_1, k_1, n_2 and k_2 which are responsible for producing this best fit are located and displayed on the lineprinter under the labels ONEN, KONE, TWON and KTWO, respectively. These may be seen in the output presented in Figure 3.25. Once identified, these binding constants are used in Equation 3.12 along with the DF(I) values obtained by experiment to regenerate the corresponding R(I) terms. The latter are printed under the heading RFIT and for ease of comparison, they are listed alongside the R(I) values which were determined directly from the binding titration. The absolute and percentage differences between RFIT(I) and R(I) are presented under the titles ERROR and PRCENT, respectively.

To start the analysis, however, the program demands that initial trial values for the binding constants are read in. Fortunately, these do not have to be close to the 'true' values, although, of course, the time taken to construct a reasonable fit to the experimental data will be reduced if good trial values are available. Normally, inspection of the Scatchard Plot suggests reasonable initial estimates of the binding constants. Flexibility is maintained in the program by allowing the user to specify the intervals by which the trial values are to be varied and the range over which they are to extend. These parameters may be controlled separately for each binding constant.

To make the program more efficient, an iteration may be directed to ensure that the interval between the consecutive trial values becomes smaller as the fit to the experimental data gets better. This means that the most suitable binding constants can be specified very closely. For instance, in the example shown in Figure 3.25, which uses data from the Scatchard Plot of Figure 3.24, $n_1 = 0.785(0.001)$, $k_1 = 4.214(0.005)$, $n_2 = 2.726(0.001)$, $k_2 = 0.234(0.002)$ where the figures in brackets represent the final intervals between the last trial values to be tested. So, as far as NKFIT is concerned, the best fit to these results is achieved for some value of n_1 defined by the limits $0.784 \leq n_1 \leq 0.786$. Likewise, the other parameters may be specified.

Clearly, the program must be given some criterion by which it can determine the best fit to the experimental data. For all trial values of the binding constants it is possible to calculate the differences between the computed values RR(I) and the corresponding experimental quantities R(I).

As shown in line 95 of the routine, these differences may be expressed in terms of the fractional 'errors' inherent in the estimates RR(I). The criterion of best fit is that the sum of the magnitudes of these errors should be a minimum. The fitting procedure is therefore analogous to a 'least squares' method. As explained previously, the binding constants which are responsible for minimizing the defined error function are sought by the computer and eventually presented on the lineprinter.

In most cases it was possible to achieve a very good fit to the experimental data using the two-site model of Equation 3.12. An example is shown in Figure 3.26. The solid line was constructed from the optimum values of n_1, k_1, n_2 and k_2 determined by the NKFIT program. The results appear to fit the mathematical model within the limits of experimental error. (These errors are discussed in the next section).

Although the curve-fitting procedure seemed to work quite satisfactorily, it is worth pointing out that a limited variation in the binding constants about the optimum values may have only a small effect on the goodness of the fit to the experimental data. In other words, the quantities defined as 'SUM OF SQUARES OF ERRORS' and 'AVERAGE PERCENTAGE ERROR' may indicate that a reasonable fit to the results can be obtained over a restricted range of values of the binding constants, the fit perhaps being more sensitive to one binding parameter than to another. This behaviour would suggest that models based on three or more binding sites are likely to become increasingly difficult to interpret as several sets of possibly quite disparate binding constants may satisfy the input data to very similar degrees. No attempt was made to fit results to models more complicated than the two-site equation.

To determine if there is a systematic departure of the data points from the fitted curve, one may inspect the signs of the residuals (see results under ERROR heading in Figure 3.25) and ascertain whether there is an element of nonrandomness in their sequence. One sort of nonrandomness is suggested by having too few runs (or sign changes). Thus + + + + - - - - - + + + + is a sequence of signs which seems nonrandom because it has too few runs, three in this case. The theoretical distribution of the number of runs in a sequence has been calculated by Bennett and Franklin (1954) assuming that each sign is an independent random event. If required, this test could be applied to the present program. However, a visual inspection of the signs of the residuals was found to be adequate for recognizing systematic deviations between the data and the fitted binding curves.

Some effort was invested in finding an analytical solution to the determination of binding constants rather than using the trial-and-error

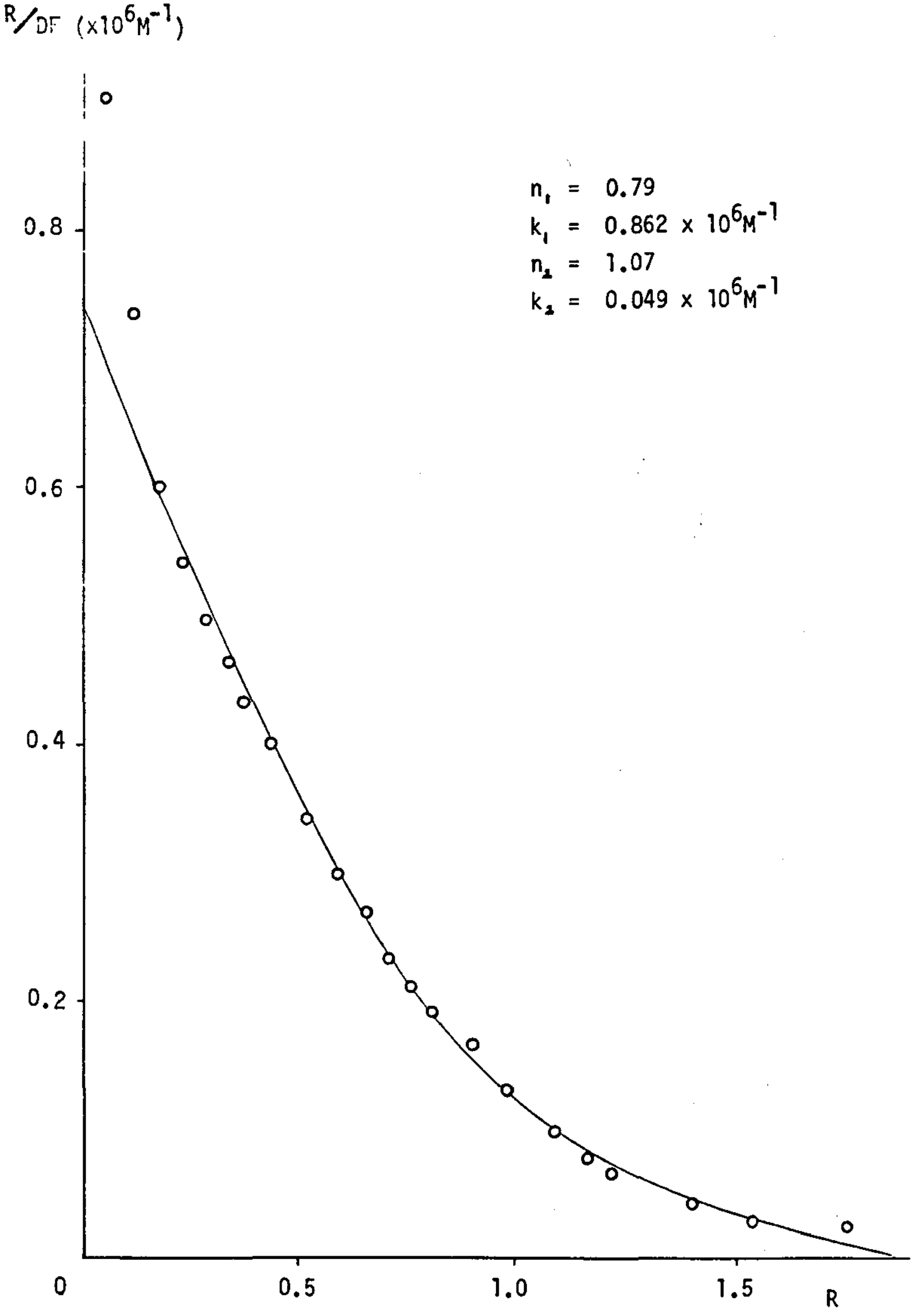

FIGURE 3.26 A Scatchard Plot Representing the Binding of Warfarin to HSA.

The curve and binding constants were derived from the experimental data with the aid of the NKFIT routine.

curve fitting procedure described above. Again only a two-site equation was considered. Since there are four unknowns, n_1, k_1, n_2 and k_2, at least four pairs of experimental values DF(I), R(I) are required to furnish answers for all the binding constants. Normally, considerably more data is available than the minimum just specified. Each pair DF(I), R(I) refers to a particular point in the binding titration. For a complete titration, then, the results associated with any four of the points may be abstracted and used to generate an estimate of n_1, n_2, k_1 and k_2. Labelling one such set of results DF(0), R(0); DF(1), R(1); DF(2), R(2); and DF(3), R(3), allows the following equations to be formulated:

$$R(0) = \frac{n_1 k_1 DF(0)}{1+k_1 DF(0)} + \frac{n_2 k_2 DF(0)}{1+k_2 DF(0)} \tag{3.13}$$

$$R(1) = \frac{n_1 k_1 DF(1)}{1+k_1 DF(1)} + \frac{n_2 k_2 DF(1)}{1+k_2 DF(1)} \tag{3.14}$$

$$R(2) = \frac{n_1 k_1 DF(2)}{1+k_1 DF(2)} + \frac{n_2 k_2 DF(2)}{1+k_2 DF(2)} \tag{3.15}$$

$$R(3) = \frac{n_1 k_1 DF(3)}{1+k_1 DF(3)} + \frac{n_2 k_2 DF(3)}{1+k_2 DF(3)} \tag{3.16}$$

Solutions are required for the binding constants n_1, k_1, n_2, k_2, in terms of the measured quantities DF(0), DF(1), DF(2), DF(3), R(0), R(1), R(2), R(3).

From Equation 3.13 it should be possible to derive an expression for k_1 which is some function of the other variables, that is

$$k_1 = F\ (n_1, n_2, k_2, DF(0), R(0))$$

Similarly, from Equation 3.14

$$k_2 = F\ (n_1, n_2, k_1, DF(1), R(1))$$

If the expression for k_1 is incorporated into the last statement, then k_2 may be written in the form

$$k_2 = F\ (n_1, n_2, DF(0), R(0), DF(1), R(1))$$

From Equation 3.15

$$n_2 = F(n_1, k_1, k_2, DF(2), R(2))$$

and substituting in the descriptions of k_1 and k_2 gives

$$n_2 = F(n_1 DF(0), R(0), DF(1), R(1), DF(2), R(2))$$

Finally, rearranging Equation 3.16 allows n_1 to be described by the function

$$n_1 = F(n_2, k_1, k_2, DF(3), R(3))$$

Inserting the appropriate expressions for n_2, k_1 and k_2 into this statement means that n_1 can be written in terms of the experimental data alone:

$$n_1 = F(DF(0), R(0), DF(1), R(1), DF(2), R(2), DF(3), R(3))$$

An estimate of n_1 is then available from the results of a binding titration. The remaining constants n_2, k_2 and k_1 are determined in sequence using the previous expressions. There are obviously several equivalent ways of solving the simultaneous equations (3.13-3.16). The route given here is just one example.

Unfortunately, when this procedure was followed it soon generated quadratic equations. Solutions to these functions were unmanageably long and included numerous terms raised to high powers. Moreover, it soon became clear that even if the solutions were much simpler, the analysis would still be complicated by the method of feeding in the results. Although any four points in the binding titration could be used to find n_1, k_1, n_2 and k_2, estimates of the binding constants would be applicable over the whole range of the experiments only if all possible permutations of the input data were considered and some mean of the estimates produced.

The unavoidable conclusion from this aspect of the work is that a curve-fitting procedure offers the best method of extracting accurate binding constants from the experimental data. The NKFIT program is more convenient than manual means of curve-fitting and, as shown in Figure 3.26 and 3.24, the intractions of warfarin and ANS with HSA appear to be consistent with a two-site binding equation.

3.6 The Analysis of Errors

Published association constants for drug-protein interactions are often in very poor agreement. To assess the accuracy of the results produced in this study, it proved useful to examine the errors generated in each stage of the procedure. Those which were critical could be identified and suitable methods of improvement suggested.

Assuming temperature, pH and buffer ionic strength did not vary from sample to sample, the main sources of error would appear to be those associated with the measurement and correction of fluorescence intensities, and with the dispensing of reagents.

Since the quality of the final binding data depends ultimately on the accuracy of the calibration curves, these will be considered first.

It is reasonable to assume that stock solutions can be made up accurately. However, as seen in Section 3.2.1, serial additions of a concentrated stock solution during a titration may eventually lead to the accumulation of quite large errors. As a remedy, the number of pipetting steps connected with each point in the titration was reduced by preparing each dilution independently of all others. Nevertheless, every sample would still differ very slightly from its intended composition due to pipetting errors.

The effects of instrumental drift were minimized by comparing sample fluorescence intensities with those emitted by quinine sulphate solutions. Unfortunately, there is a limit to how accurately the instrument can be read and at low fluorphor concentrations where a high photomultiplier gain is necessary, the noise-level may make it impossible to determine accurate fluorescence intensities. Consequently, the imprecision inherent in the measurement of the fluorescence must be compounded with the errors in dispensing reagents to define the limits of accuracy of the calibration plots.

A third factor to consider is the correction of the observed intensities for inner-filter effects. In very dilute samples where absorption of radiation by the probe is insignificant, corrections for inner-filter effects will be vanishingly small. As a result, at the low concentration end of the calibration plots the measured and corrected fluorescence intensities are very similar and errors in estimating the inner-filter correction factors a_1 and a_2 have only a marginal effect on the magnitude of the corrected values. On the other hand, when enough fluorescent probe is present to absorb a significant proportion of the incident radiation, inner-filter effects may be quite large and errors in their estimation can result in the production of highly erroneous corrected fluorescence intensities.

Having recognized the three major sources of error involved in setting up calibration plots of corrected fluorescence intensity versus probe concentration, it is worth considering how each manifests itself. An estimate of the magnitude of the different errors may then be possible.

Errors in the preparation of samples and in the measurement of fluorescence appear as a random scatter of data points about the calibration curves. As shown in Figures 3.10 and 3.13, this scatter may be observed with both corrected and uncorrected calibration plots.

One way of estimating the magnitude of the errors associated with sample preparation and intensity measurement is to make up a number of samples to supposedly the same concentration and take several measurements on each. The spread of the results may be used to judge the precision obtainable over a range of sample concentrations.

Another way of obtaining an estimate of these errors is to consider the inner-filter corrected calibration plots. In Section 3.2.3 it was shown how the optimum value of the inner-filter correction factor k would be defined as that which gave the minimum variation in F_E across the calibration plot. Obviously, if there were no errors in measuring the fluorescence intensity or in dispensing the reagents, and providing Equation 3.8 were truly applicable, the appropriate value of F_E would be a constant over the entire calibration range. In practice, of course, the different values of F_E are scattered about some mean and the degree of scatter provides an estimate of the experimental precision. A typical spread of values is illustrated in Table 3.5.

Aside from the random errors inherent in the results, a poor estimation of the inner-filter phenomenon will appear as a systematic deviation of the corrected fluorescence intensities from a linear calibration plot. When the inner-filter correction is derived from the measurements of sample absorbance at the wavelengths of fluorescence excitation and emission, some estimate of the accuracy of the allowance can be obtained from an investigation of the errors included in the absorbance readings. On the other hand, if the effect is accounted for by optimizing the inner-filter correction factor k and producing the best straight line through the data, no absorbance measurements are involved. The error in this procedure has to be estimated from the fluorescence intensity readings alone.

As described in Section 3.2.3, Equation 3.8 was employed to find the value of k which resulted in the minimum variation of F_E across the calibration plot. The mean of the least variable set of F_E values was

c	F_M	F_o	F_E
10	16.4	9.55	0.955
20	25.0	20.28	1.014
30	31.8	30.18	1.005
40	36.9	39.06	0.977
50	42.9	50.07	1.001
60	49.9	63.69	1.061
80	53.4	78.42	0.980
100	60.4	102.2	1.022
120	60.6	116.6	0.972
140	62.8	137.7	0.984
160	64.1	159.5	0.997
200	61.3	195.5	0.978
240	58.4	238.4	0.993
320	48.5	322.7	1.008

TABLE 3.5 The Variation in the Gradient of the Linear, Corrected Calibration Plot at Each Point in a Titration when the Optimum Value of k is used.

c - the concentration of ANS in 0.1M Tris/HCl buffer, pH 7.4 (10^{-6}M)

F_M - the measured fluorescence intensity

F_o - the inner-filter corrected fluorescence intensity, where

$F_o = F_M \exp(kc) - F_B$ and

$F_B = 7.9$, $k = 0.00600$ (see Table 3.3)

F_E - the gradient of the linear inner-filter corrected calibration plot, where $F_E = F_o/_c$

From the above results $\overline{F}_E = 0.996$ (sd = 0.026).

calculated and used to construct the best linear fit to the corrected fluorescence intensity measurements. Now a rearrangement of Equation 3.8 gives the following expression for k,

$$k = {}^{1}/c \ln \left(\frac{cF_E + F_B}{F_m} \right)$$

Since c, F_m and F_B are known quantities, this expression provides a means of calculating the value of k required to transpose each experimental point in the titration curve on to the linear calibration plot of gradient F_E. This is illustrated in Table 3.6 using the data shown in Figure 3.18. As expected, the mean value of k is simply that used in Equation 3.8 to determine F_E in the first place. However, a study of the variation in k across the calibration curve is useful in assessing how precisely this parameter can be defined by experiment.

In dilute solutions the inner-filter effect is very small and may be difficult to detect. The task of measuring k under such conditions is made worse by the fact that the fractional error in a recording of the fluorescence intensity increases as the sample concentration is lowered. Fortunately, as mentioned above, errors in determining the inner-filter effects of dilute samples are of little consequence. Accordingly, a 'weighted' average of the imprecision in k was found by eliminating the results obtained in very dilute solutions (say $\exp(-kc) \leq 1.05$) and calculating the standard deviation of the remaining experimental values.

For simplicity, an average value was also reported for the inaccuracy associated with dispensing the reagents and recording the fluorescence intensities. The lowest quantity of probe included in the calibration curves was well above the detection limit of the assay. Thus the error in F_E was held more or less constant over the range of concentrations examined. The variation in the estimates obtained for F_E at each point in the titration was used to define an average experimental error, dF_E (see Table 3.5).

Once reasonable estimates were available for the inaccuracies inherent in the calibration plots, it was possible to consider their effect on the interpretation of subsequent binding titrations.

The computer program FLUORB considers inner-filter effects arising from bound and unbound fluorescent probe and from albumin. So line 61 of the program may be expressed as,

$$F_O = F_M \exp(k_b c_b + k_u c_u + k_p c_p)$$

C	F_M	k
30	31.8	0.00574
40	36.9	0.00642
50	42.9	0.00591
60	49.9	0.00506
80	53.4	0.00619
100	60.4	0.00577
120	60.6	0.00619
140	62.8	0.00609
160	64.1	0.00600
200	61.3	0.00609
240	58.4	0.00601
320	48.5	0.00696

TABLE 3.6 The Value of k Required to Transpose Each Data Point on to the Linear Calibration Plot.

C - the concentration of ANS in 0.1M Tris/HCl buffer, pH 7.4 (10^{-6}M)

F_M - the measured fluorescence intensity

k - inner-filter correction factor required to transpose individual data points on to linear calibration plot;

$$k = \frac{1}{C} \ln \left(\frac{C\,F_E + F_B}{F_M} \right) \text{ where}$$

$$F_B = 7.9 \text{ and } F_E = 0.996$$

From the results $\bar{k} = 0.00600$ (sd = 0.0003).

where F_M is the observed fluorescence intensity, F_O is the inner-filter corrected intensity, k_b, k_u and k_p are the inner-filter factors for bound and unbound fluorescent probe and for albumin, and c_b, c_u and c_p are the concentrations of the corresponding absorbing species. The uncertainty in the inner-filter corrected fluorescence intensity may be related to the uncertainties in the experimentally determined parameters k_b, k_u, k_p and F_M by a partial differentiation of the previous equation. Thus, after simplification

$$\frac{|dF_O|}{F_O} = \frac{|dF_M|}{F_M} + c_b \; |dk_b| \; + \; c_u \; |dk_u| \; + \; c_p \; |dk_p|$$

where $|dF_O|$, $|dF_M|$, $|dkb|$, $|dk_u|$ and $|dk_p|$ are the absolute errors in F_O, F_M, k_b, k_u and k_p, respectively.

At any stage during a binding titration, therefore, the fractional error in the calculated inner-filter corrected fluorescence depends on the fractional error in the experimentally measured sample fluorescence. It also depends on the absolute errors in each of the estimates of the inner-filter factors multiplied by the concentrations of the corresponding absorbing species.

Now as long as the sample concentration is within the calibrated range, that is, the observed fluorescence is well above the experimental detection limit, the fractional error in F_M must be similar to that incurred in measuring fluorescence intensities for the appropriate calibration plots. Since the greater part of the sample fluorescence is due to emission from the bound probe, it is reasonable to equate $|dF_M|/F_M$ with $|dF_E|/F_E$ where the latter refers to the bound probe calibration curve. So,

$$\frac{|dF_O|}{F_O} = \frac{|dF_E|}{F_E} + C_b \; |dk_b| \; + \; C_u \; |dk_u| \; + \; C_p \; |dk_p| \qquad (3.17)$$

In practice, albumin is present at a fixed concentration and usually absorbs only a small amount of radiation at the wavelengths of excitation and emission of the bound probe fluorescence. Consequently, the value of $C_p \; |dk_p|$ is normally insignificant compared to the other terms on the right-hand side of Equation 3.17. However, since the uncertainties in measuring the inner-filter effects of the bound and unbound fractions are almost undoubtedly different, the accuracy with which the observed fluorescence can be corrected will vary depending on the degree of protein binding in the sample under investigation. In other words, as $|dk_b| \neq |dk_u|$ in Equation 3.17, $(C_b \; |dk_b| \; + \; C_u \; |dk_u|)$ will change in a non-linear fashion across the binding curve. (Had $|dk_b|$ and $|dk_u|$ been equal, the term $c_b\ |dk_b| + c_u\ |dk_u|$ would have been a linear function of the total probe concentration). Nevertheless, since both c_b and c_u get larger as more probe is added to the albumin, $\frac{|dF_o|}{F_o}$ will always increase as the total concentration of probe rises.

It is worth considering the errors in measuring the inner-filter factors of the bound and unbound fractions in more detail. At low probe: protein ratios most of the probe will be bound to albumin. Under these conditions, allowance for the extremely small inner-filter effect of the unbound probe will certainly be unimportant. In fact, at this end of the binding curve, unless the sample contains large quantities of protein, it is likely that the bound probe concentration will also be too low to exhibit an appreciable inner-filter effect. The corrected fluorescence F_o will hardly be different from the signal that is measured in practice but any small errors in allowing for inner-filter effects will be due almost entirely to uncertainties in providing for the bound probe absorption.

On the other hand, at high probe:protein ratios, there may be sufficient fluorescent probe - both bound and unbound - to generate an appreciable inner-filter effect. However, many of the binding sites on albumin will be occupied at high protein:probe ratios and the greater fraction of the ligand will be in free solution. Thus errors in characterizing the inner-filter effect of the unbound species will become of greater significance as the total probe concentration increases. Indeed, determination of this parameter will likely prove to be the limiting factor in a fluorimetric assay of the low-affinity binding sites on HSA.

Having considered the experimental errors associated with an estimation of Fo, the next step is to examine how information is extracted from this term. FLUORB retains a value of that part of the inner-filter corrected signal which is attributable to albumin-bound fluorescent probe. The program uses this value to derive an estimate for the bound probe concentration. As shown in line 58, this derivation is very simple because the inner-filter corrected fluorescence intensity is directly proportional to the fluophor concentration. That is,

$$c_B = {}^{F_o}\!/_{F_E}$$

and using partial differentiation, $\frac{|dc_B|}{c_B} = \frac{|dF_o|}{F_o} + \frac{|dF_E|}{F_E}$

The fractional error in F_o has already been described as a function of the uncertainties in the experimental determinants (see Equation 3.17). So an overall expression for the error in the estimated bound probe concentration is

$$\frac{|dc_B|}{c_B} = 2\frac{|dF_E|}{F_E} + c_B\,|dk_B| + c_u\,|dk_u| + c_p\,|dk_p| \qquad (3.18)$$

For completeness, another term would have to be included in this equation. It arises because the iterative procedure in FLUORB has to consider the contribution that the unbound probe makes to the total sample fluorescence. At high probe:protein ratios there may be sufficient probe in free solution to exhibit an appreciable fluorescence. It is conceivable that errors in estimating this signal could lead to uncertainties in determining c_B. However, it can be shown that the inclusion of an additional term in Equation 3.18 is unwarranted. The uncertainty in measuring the fluorescence of the unbound fraction would have to be very high, while, at the same time, the enhancement in the probe fluorescence on binding to albumin would have to be low. In addition, the unbound probe would need to be present in such high concentrations that uncertainties in determining the inner-filter effect would have already become unacceptable.

At any point in the binding titration, the error in the estimate of the unbound fraction may be equated with that in the bound fraction. This is so because c_u is found simply by subtracting the bound probe concentration, c_B from the total concentration, C_T (see line 59). It is reasonable to assume that the error in C_T is very small compared to the error in c_B, so $|dc_u| \simeq |dc_B|$.

Finally, the imprecision in the value obtained for the albumin concentration may be determined by taking repeated absorbance measurements on a stock solution and reporting the spread of the results. In practice, the coefficient of variation of the absorbance readings was quite low - 0.8% being a typical value.

Having assessed the experimental errors associated with the estimates of c_B, c_u and c_B, it was possible to examine their influence on the shape of the subsequent binding curves. This was quite straightforward as the parameters of the binding curves were simple functions of the total protein concentration and the equilibrium concentrations of bound and unbound ligand. The process is illustrated for the Scatchard plot of r versus r/c_u.

$$r = {}^{c_B}\!/_{c_p}$$

$$\therefore \frac{|dr|}{r} = \frac{|dc_B|}{c_B} + \frac{|dc_p|}{dp} \qquad (3.19)$$

The fractional error in r is equal to the sum of the fractional errors inherent in the calculation of the bound probe and total protein concentrations. During the course of most binding experiments only the ligand concentration is varied. Consequently, the second term on the right-hand side of Equation 3.19 will be the same for all points on the binding curve. In general, c_B cannot be determined to the same degree of accuracy irrespective of the total ligand concentration. So $\frac{|dc_B|}{c_B}$ will change across the binding curve. Above a certain ligand concentration, Equation 3.18 may be used to describe this variation for the fluorimetric assay and suggests that as r gets bigger so does the fractional error $\frac{|dr|}{r}$ (see Figure 3.24). As explained before, the problem lies in calculating inner-filter effects at high concentrations of fluorescent probe. At very low concentrations, however, a lack of sensitivity would preclude a proper measurement of the sample fluorescence, Equation 3.18 would be inapplicable and the error in r would rise again.

The other parameter in the Scatchard analysis is

$$\frac{r}{c_u} = c_B / c_p\, c_u$$

$$\therefore \left| d\left(\frac{r}{c_u}\right) \right| = \frac{1}{c_p c_u} |dc_B| + \frac{c_B}{c_p c_u^2} |dc_u| + \frac{c_B}{c_u c_p^2} |dc_p| \qquad (3.20)$$

$$\text{and, } \frac{\left|d\left(\frac{r}{c_u}\right)\right|}{r/c_u} = \frac{|dc_B|}{c_B} + \frac{|dc_u|}{c_u} + \frac{|dc_p|}{c_p} \qquad (3.21)$$

Equation 3.20 is a general expression to describe how the uncertainty in r/c_u can be related to the experimental errors. For the procedure outlined in this Chapter, the uncertainties in estimating the bound and unbound ligand concentrations are equal, and because $C_T = c_B + c_u$, a special case of Equation 3.21 is appropriate. Thus,

$$\frac{\left|d\left(\frac{r}{c_u}\right)\right|}{r/c_u} = \frac{C_T}{c_u} \frac{|dc_B|}{c_B} + \frac{|dc_p|}{c_p} \qquad (3.22)$$

At low probe:protein ratios, most of the fluorescent probe is bound to albumin and only a small fraction of the ligand remains in free solution. Under these conditions, Equation 3.22 shows that the fractional error in r/c_u will increase without bounds. That is, $\frac{d\left(r/c_u\right)}{\left(r/c_u\right)} \longrightarrow \infty$ as $c_u \longrightarrow 0$.

This explains the long error bars associated with the high values of $^r/c_u$ in Figures 3.24 and 3.26.

At the other end of the Scatchard Plot, the total ligand concentration may be sufficient to ensure that a high proportion of the fluorescent probe exists in free solution. In this context, Equation 3.22 can be used to demonstrate that as the total ligand concentration is raised, the fractional error in $^r/c_u$ will fall until it approaches that in r. Thus, as $c_u \longrightarrow C_T$,

$$\frac{\left|d\left(\frac{r}{c_u}\right)\right|}{\left(\frac{r}{c_u}\right)} \rightarrow \left|\frac{dc_B}{c_B}\right| + \left|\frac{dc_p}{c_p}\right| = \left|\frac{dr}{r}\right|$$

The marked decrease in the vertical error bars at high concentrations of fluorescent probe is apparent in Figures 3.24 and 3.26.

The general expressions 3.20 and 3.21 can be used to explain the limitations inherent in any examination of ligand-protein binding - whatever the methodology. When investigating binding to high affinity sites, $c_B >> c_u$ and the limiting factor turns out to be the inaccuracy in measuring the unbound fraction. To minimize this error, it would be preferable if the assay were one which measured cu directly. However the same equations show that in a study of binding to low affinity sites, where $c_B << c_u$, the uncertainty in determining the concentration of the protein-bound ligand is critical. It appears likely, therefore, that no one system will be ideally suited to an investigation of both high and low affinity binding sites.

In order to apply the error functions described in this Section, an updated version of the FLUORB program was prepared. It computed the uncertainties in the parameters of the Scatchard plot using actual experimental data. Equation 3.18 was required to establish the error in the estimated bound probe concentration at any point in the titration. As mentioned before, this expression was also used to describe the uncertainty in the corresponding value for the unbound probe. The uncertainties in r and $^r/c_u$ were found from Equations 3.19 and 3.22. The values of dk_u, dk_b, dk_p, dF_E and dc_p were fed in to the program as required.

A typical distribution of errors is presented for a Scatchard plot representing the binding of ANS to HSA. The variability of the results of repeated experiments has been found to agree broadly with those suggested by the error bars in Figure 3.24.

The production of these error profiles has certain practical applications. The uncertainty associated with each point in the curve allows the suitability, or otherwise, of a set of binding constants to be appreciated. For example, the solid line in Figure 3.24 is constructed from the values of n_1, k_1, n_2, k_2 shown and appears to fit the data to within the limits of experimental error.

More importantly, perhaps, the error profile emphasizes the limitations and scope of the present assay. The limitations are clear. The unbound fraction is measured indirectly - it is defined as the difference between the bound and the total ligand concentrations. At low probe: protein ratios most of the probe is in the bound fraction. Now because the absolute errors in the estimations of the bound and unbound fractions tend to be very similar, when $c_B >> c_U$ a small percentage error in the estimate of c_B will be translated into a very large percentage error in the estimate of c_U. Consequently, the procedure is not ideally suited to the measurement of binding to high affinity sites. This is manifested in the large errors in r/c_U at low concentrations of fluorescent probe. Likewise, the assay is of limited use when considering very high ligand concentrations. The problem here is in allowing for large inner-filter effects. The considerable errors in r at high probe concentrations are indicative of this limitation. However, restrictions at this end of the curve are usually unimportant because binding to low affinity sites on albumin is of less practical significance.

Nevertheless, an investigation of the distribution of errors has shown that the procedure is capable of producing accurate binding data over a very wide range of ligand concentrations. This should be borne in mind when considering the other attributes of the assay; no separation of the bound and unbound fractions is required; the experiments are simple to perform; and although processing of the results is quite complicated, the procedure is easily computerized.

3.7 Derivate and Synchronous Fluorescence Spectroscopy in the Resolution of Spectral Contributions from Bound and Free Fluorescent Probes

The purpose of the work described in this section is to identify suitable methods for differentiating more completely between the spectral contributions of free and protein-bound fluorescent probes. Once identified, such methods may lead to a simplified procedure for constructing binding isotherms. For example, the iterative procedure discussed in Section 3.3 could be avoided if there were complete discrimination between the free and bound emission peaks. Furthermore, a truly independent measure of free and bound ligand would extend the working range of most binding assays.

Two techniques were employed to amplify the differences between the emission bands of bound and free fluorescent probes. However, it should be noted that while ANS was used to examine the feasibility of applying synchronous and derivative fluorescence spectroscopy to a study of protein binding, the practical necessity to discriminate between the very weak fluorescence of the free probe and the intense fluorescence of the bound species would rarely arise. The same is not true for warfarin, of course, because the fluorescence of the unbound form can constitute a significant proportion of the total signal observed from a sample containing both bound and free fluorescent probe.

Derivative spectroscopy can be useful in resolving spectral overlap and enhancing the fine structure of most types of spectra. The technique consists of calculating the first, second or higher order of a spectrum with respect to wavelength and plotting the derivative rather than the spectrum itself. The result is an increase in structure that is generally paid for by a decrease in the signal-to-noise ratio.

Wavelength derivatives may be produced by electronic differentiation or wavelength modulation. Wavelength modulation coupled with a lock-in amplifier produces an output signal which is proportional to the derivative of intensity with respect to wavelength. An electronic signal differentiator produces an output signal which is proportional to the derivative with respect to time and uses this to simulate derivatives with respect to wavelength. Although wavelength modulation may be capable of giving superior signal-to-noise ratios in derivative absorption spectrometry, the same is not true in luminescence spectrometry where both derivative methods give similar signal-to-noise ratios (Green and O'Haver, 1974). Electronic differentiation is simpler and less expensive than wavelength modulation, it does not require a lock-in amplifier or any modification of the fluorimeter optics, and can generate the zeroth, first or other derivative time spectra simultaneously. However, the electronic method demands that the scan rate is not only constant but reproducible from scan to scan, whereas the wavelength modulation does not suffer from either of these limitations.

In this study derivative spectra were generated electronically. The technique employed is similar to that used with dual-wavelength spectroscopy (Porro, 1972), where a wavelength offset of up to several nanometers between the two optical channels produces an intensity difference which is essentially equivalent to the first derivative. With the DCSU-2 unit, however, differentiation is achieved electronically, rather than optically, through data storage and computation.

There are two main advantages of plotting the derivative of a spectral curve. Firstly, the derivative technique can be useful for resolving bands that are too close to be resolved in the original spectrum. The enhancement of resolution increases with derivative order but depends on band shape. Thus two Gaussian bands of equal height and width are just resolved in zeroth order, second derivative and fourth derivative spectra when their separations divided by their full width at half maximum is 0.85, 0.63 and 0.52, respectively (Cahill, 1980).

The second general effect of plotting the derivative of a spectrum is a discrimination in favour of its sharper features. Consequently, the influence of a broad background signal on a spectral peak may be reduced by taking the first or higher derivative. Again, discrimination against the broader band increases with derivative order (Cahill, 1980).

Fell (1978) has demonstrated the practical advantages of second derivative ultraviolet-visible spectrophotometry for the quantitative assay of drugs in formulation mixtures. Green and O'Haver (1974) suggest that derivative techniques may be especially useful in luminescence spectrometry because of the rather common occurrence of fluorescence background and band overlap problems in quantitative fluorimetric analysis.

When calculating derivatives from initial spectra, a suitable compromise must always be sought between the fidelity with which the derivative is calculated and the signal-to-noise ratio. This is so because noise, even when small, contains by far the sharpest features of a real spectrum. Noise will increasingly dominate the derivative spectrum as the derivative order is increased. The decrease in the signal-to-noise ratio can be controlled to a large degree by averaging the derivative calculation over a wavelength region that is large compared to the noise structure. This lowers the derivative signal as well as the noise level but discriminates against the latter. However, as this wavelength range is increased, the derivative becomes more and more distorted. The consequence of a finite wavelength range is therefore a decrease in the derivative signal and a decrease in resolution.

In general the optimum values of derivative order and wavelength range must be determined experimentally for each application. The attainment of an undistorted derivative is not a useful goal. The best compromise between acceptable spectral distortion and sufficiently high signal-to-noise ratios should be sought.

The first and second derivative modes of the Differential Corrected Spectra Unit-2 (DCSU-2) offer three choices of wavelength ranges which can be used in calculating alogarithms (Di Cesare and Porro, 1978). These are 2nm, 5nm and 10nm. The lowest selection, 2nm, is obviously used where resolution is necessary and signal-to-noise ratio can be sacrificed, while the highest selection, 10nm, results in the greatest signal-to-noise levels but a minimum resolution. When examining the emission spectrum of warfarin the presence of HSA, a wavelength range of 5nm gave an unacceptably noisy signal in the first derivative: an even higher noise level was observed with the second derivative mode. A satisfactory noise level was obtained for the second derivative spectrum when a 10nm wavelength offset was employed.

Figure 3.2 shows corrected emission spectra for warfarin both in free solution and in a sample containing a high molar excess of albumin. Thus Figure 3.2(b) represents the fluorescence emission spectrum of unbound warfarin. At an albumin warfarin ratio of 10:1 essentially all of the drug is bound to protein; moreover, since the fluorescence of a 5 x 10^{-5}M solution of HSA is negligible under the specified conditions, spectrum 3.2(a) is representative of the emission of the bound form of warfarin. The blue shift in the fluorescence of warfarin on binding to albumin is clear; the emission maximum of the bound form is at 376nm compared to 385nm for the unbound species. The unbound form of the drug also appears to have a slightly broader emission peak - a full width at half maximum of 78nm, as opposed to one of 67nm for the bound form.

Figure 3.27 shows the second derivatives of the spectra of Figure 3.2. As expected, the fluorescence of the unbound probe in the second derivative is shifted to a longer wavelength and its features are broader than those of the bound species. It appears that differences in the emission spectra of the bound and unbound forms of the drug are amplified in going from the zeroth order to the second derivative. Unfortunately, the increase in discrimination between the two spectra is insufficient for their complete resolution. Far too much overlap remains between the emission spectra of free and bound warfarin to allow one form to be determined in the presence of the other even with the use of derivative spectroscopy.

In comparison to warfarin a much greater blue shift accompanies the binding of ANS to human serum albumin. (The relevant spectral parameters are summarized in Table 3.7). By definition, a large separation in the emission maxima should facilitate a resolution of the bound and free fractions. However, the problem of resolving the spectra of the free and bound forms of ANS lies in the relative intensities of the emission peaks. The fluorescence of the bound species is so much more intense than the fluorescence of the free form that the latter tends to be obscured by the long wavelength tail of the former even though the emission maxima are

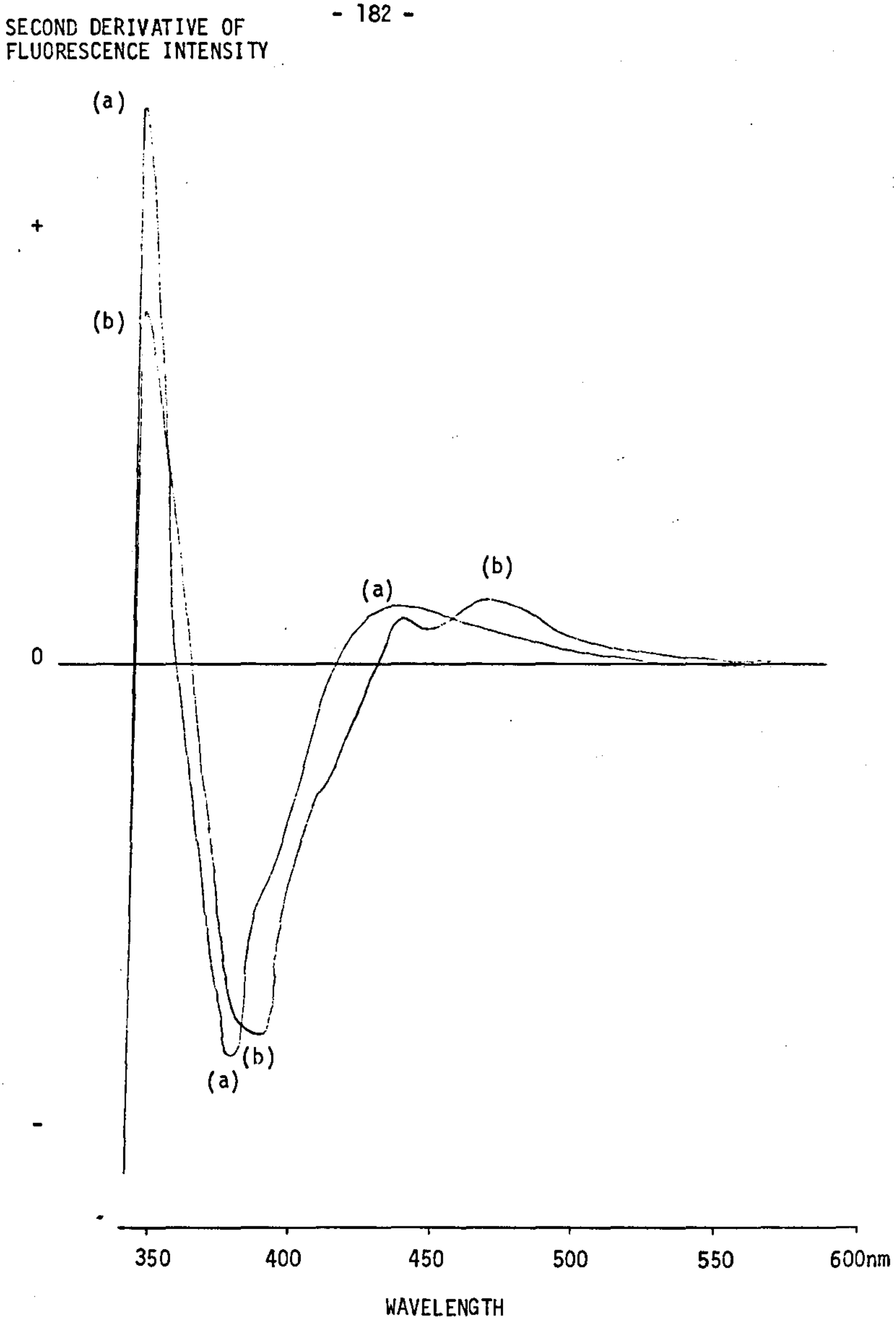

FIGURE 3.27 Derivative Spectra of Bound and Free Warfarin. Wavelengths of excitation 320nm.

(a) Sample containing 5×10^{-6}M warfarin and 5×10^{-5}M HSA in 0.1M Tris/HCl pH 7.4. Scale expansion x 2.

(b) Sample containing 5×10^{-6}M warfarin in 0.1M Tris/HCl pH 7.4. Scale expansion x 10.

The second derivative spectrum of a sample containing 5×10^{-5}M HSA was not significantly different from zero over this wavelength range.

Species		λex (nm)	λem (nm)	Stokes Shift (nm)	FWHM (nm)
Warfarin	bound	320	380	60	70
	free	320	390	70	78
ANS	bound	380	475	95	90
	free	380	530	150	150
Human serum albumin		280	340	60	75

TABLE 3.7 A Summary of the Major Features of the Fluorescence Spectra of Human Serum Albumin, Warfarin and ANS.

λex - wavelength of maximum excitation of fluorescence.
λem - wavelength of maximum emission of fluorescence.
FWHM - full width at half maximum intensity of the emission band.

separated by some 60nm. Derivative spectroscopy was incapable of producing a discrimination between the weak fluorescence due to unbound ANS and the intense fluorescence of the bound species at shorter wavelength. Because of its ability to narrow spectral band widths, synchronous fluorescence spectroscopy was viewed as a potential solution to the problem.

The idea of synchronous excitation of fluorescence emission spectra was first suggested by Lloyd in 1971. The method provides a means of increasing the sensitivity of luminescence spectrometry. Its application to the resolution of the spectra of bound and free fluorescent probes is examined below.

In conventional fluorescence spectroscopy, an emission spectrum can be generated by scanning the emission wavelength while the fluorescent compound is excited at a fixed wavelength. An excitation spectrum can be obtained by scanning the excitation wavelength while the emission is measured at a given wavelength. A third possibility consists of varying simultaneously, or synchronously, both the wavelengths of excitation and emission while maintaining a constant wavelength interval $\Delta\lambda$ between them. The result is often called a synchronously excited emission spectrum, although since it can be considered as an emission or as an excitation spectrum, Vo-Dinh (1978) simply refers to it as a synchronous signal or a synchronous spectrum. All three terms will be used interchangeably in this section.

The synchronous scanning of both excitation and emission monochromators can greatly simplify complex fluorescence spectra because the fluorescence contributed by each component is restricted to that excited at wavelengths synchronously trailing the recorded emission by a fixed value. A signal is only observed with the synchronous technique when $\Delta\lambda$ matches the interval between an absorption band and the corresponding emission band. If it is possible to select a particular $\Delta\lambda$ which matches one unique pair of absorption and emission bands, the synchronous spectrum will show only a single peak. In order to have a situation where an interval $\Delta\lambda$ can be found to match solely one pair of excitation and emission bands, it is necessary that the emission and excitation spectra consist of bands which are not separated by similar wavelength intervals.

Lloyd and Evett (1977) have shown how the characteristics of synchronous spectra can be derived quantitavely from the characteristics of the corresponding fixed excitation and emission spectra. An important attribute of synchronously excited emission spectra is their much reduced peak half-widths relative to the excitation and emission spectra from which they originate. This band-narrowing effect is a consequence of the multiplication of two intensity distribution functions - those of the excitation and emission spectra - which increase and/or decrease simultaneously. The capacity to modify the spectral band width for individual components in a mixture is an outstanding feature of the synchronous technique; it leads to a reduction in spectral overlap and an improvement in resolution.

Corrected excitation and emission spectra for the bound and free forms of warfarin are recorded in Figure 3.28. The corresponding spectra for ANS are shown in Figure 3.29. Figure 3.30 includes corrected excitation and emission spectra of HSA. The positions of the excitation and emission maxima of these species are summarized in Table 3.7.

From the data it is clear that the excitation and emission bands of warfarin are separated by roughly similar intervals when the ligand is in free solution and when it is bound to HSA. Moreover, the emission spectra of bound and free warfarin are broad peaks of comparable band-widths. Consequently, it was not possible to find an interval Δλ which would match just one of the two pairs of excitation and emission bands. Peaks due to the bound and free form of the fluorescent probe were not resolved in synchronously excited emission spectra over a wide range of Δλ values even when monochromator slits of only 2nm were used. Although of limited significance, it is worth stating that the synchronous spectrum of HSA could be readily distinguished from the signals attributable to the bound fluorescent probes for values of Δλ ranging from 30nm to 60nm.

When ANS is considered, however, it is obvious that an interval can be found which matches just the excitation and emission bands of either bound or free fluorescent probe. A synchronous spectrum of ANS in free solution is shown in Figure 3.31. The constant wavelength interval is 140nm and the band maximum is centred at an excitation wavelength of 380nm and an emission wavelength of 520nm. A synchronous spectrum of albumin-bound ANS is shown in Figure 3.32. In this case Δλ is 100nm. The band maximum corresponds to an emission wavelength of 475nm; there is no contribution from the protein in this region of the synchronous spectrum. It is interesting to note the quenching of the albumin fluorescence at 370nm (wavelength of excitation 270nm) by energy transfer to the bound fluorescent probe (Figure 3.32). Figure 3.33 illustrates the differences between the conventional and synchronous fluorescence spectra of albumin bound ANS. The narrowing of the band widths of the synchronous signal relative to the conventional emission spectrum is clear; the full widths at half maximum intensities for the synchronous and conventional spectra are 53nm and 83nm, respectively. Particular attention should be paid to the marked reduction

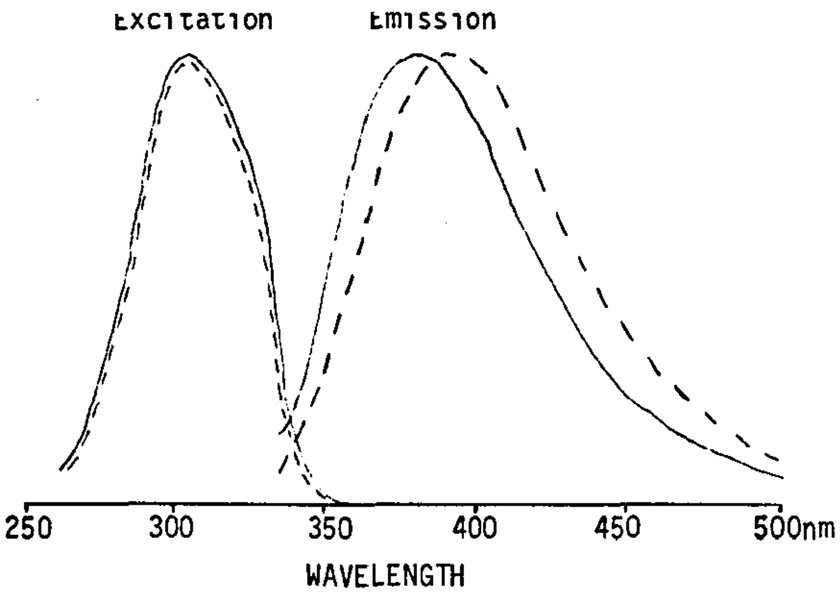

FIGURE 3.28 Corrected Excitation and Emission Spectra of Bound (-) and Free Warfarin (---).

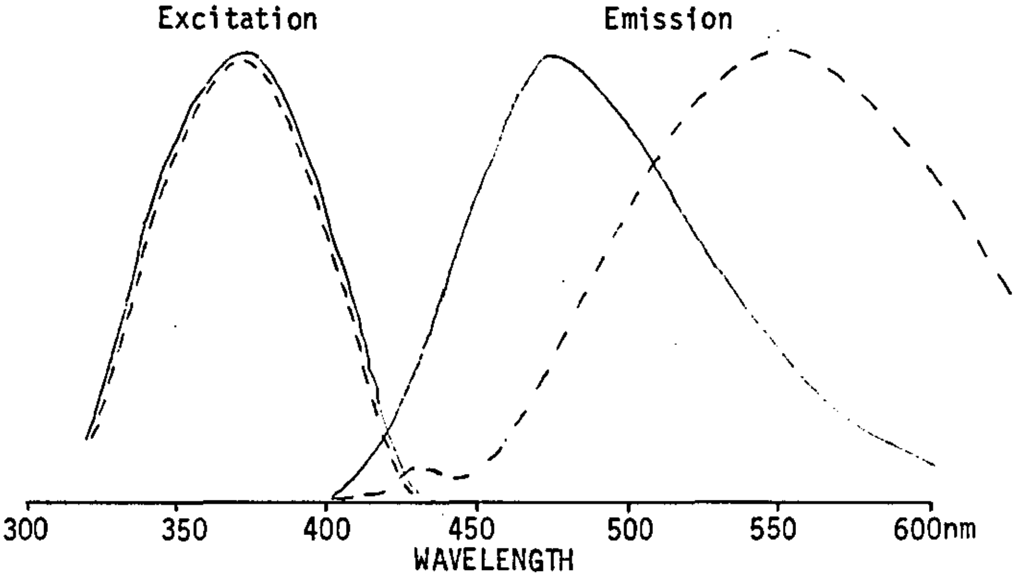

FIGURE 3.29 Corrected Excitation and Emission Spectra of Bound (-) and Free ANS (---).

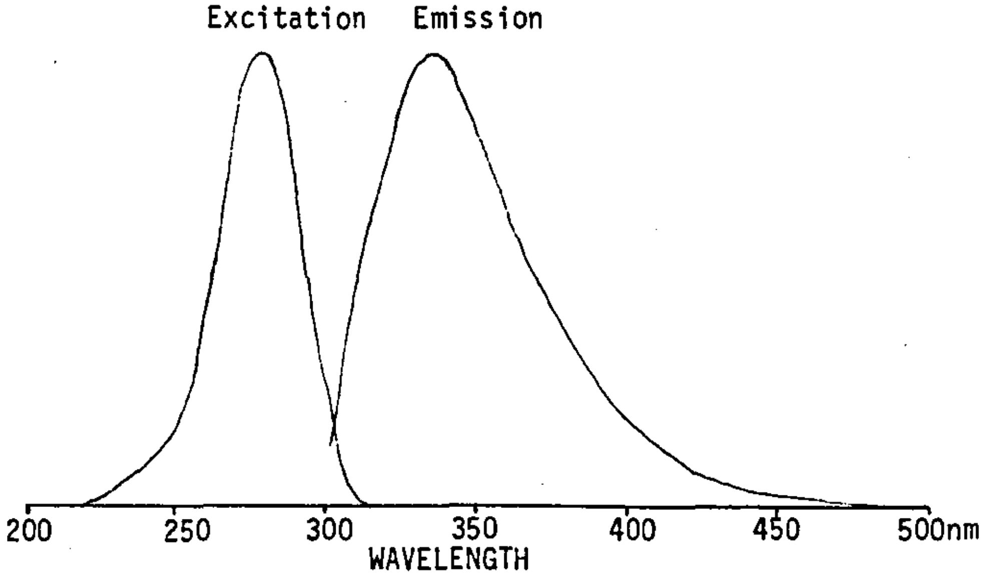

FIGURE 3.30 Corrected Excitation and Emission Spectra of Human Serum Albumin.

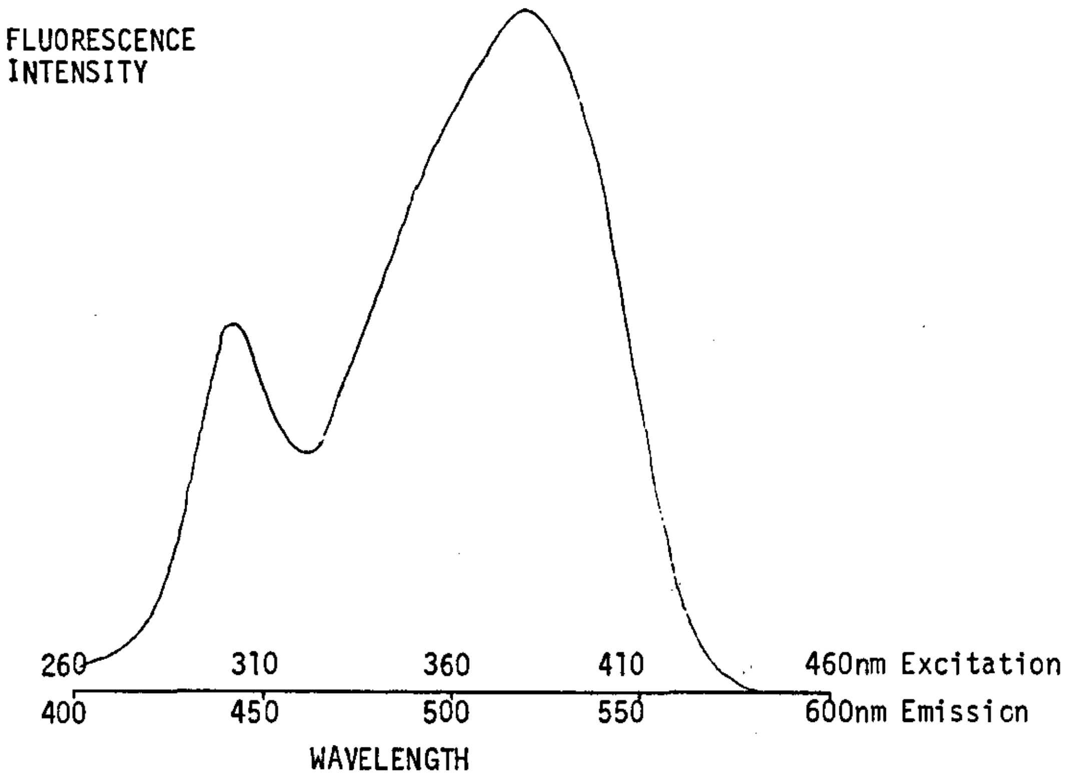

FIGURE 3.31 Synchronously Excited Emission Spectrum of ANS in Free Solution. Sample contained 10^{-4}M ANS in 0.1M Tris/HCl buffer pH 7.4.

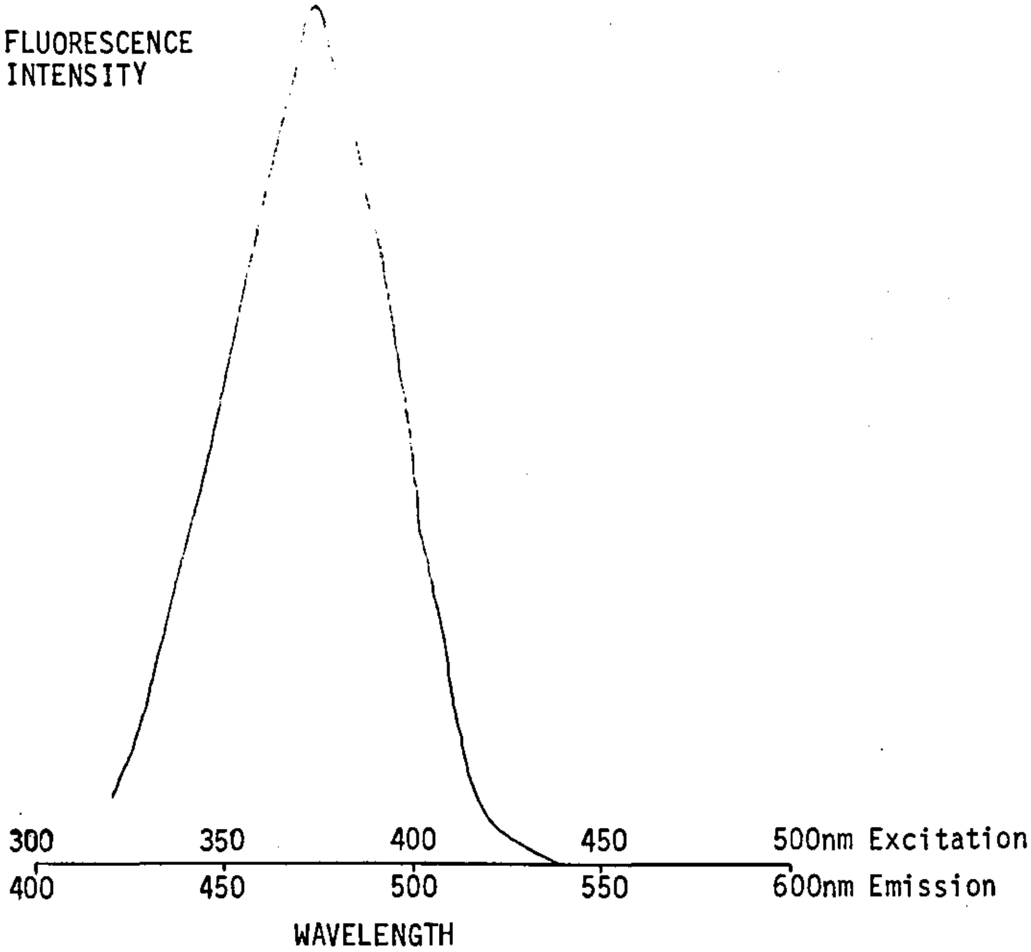

FIGURE 3.32 Synchronously Excited Emission Spectrum of Bound ANS. Sample contained 2×10^{-6}M ANS and 2×10^{-5}M HSA in 0.1M Tris/HCl buffer pH 7.4.

The ratio of the gain settings used in Figures 3.31 and 3.32 was 10:1.

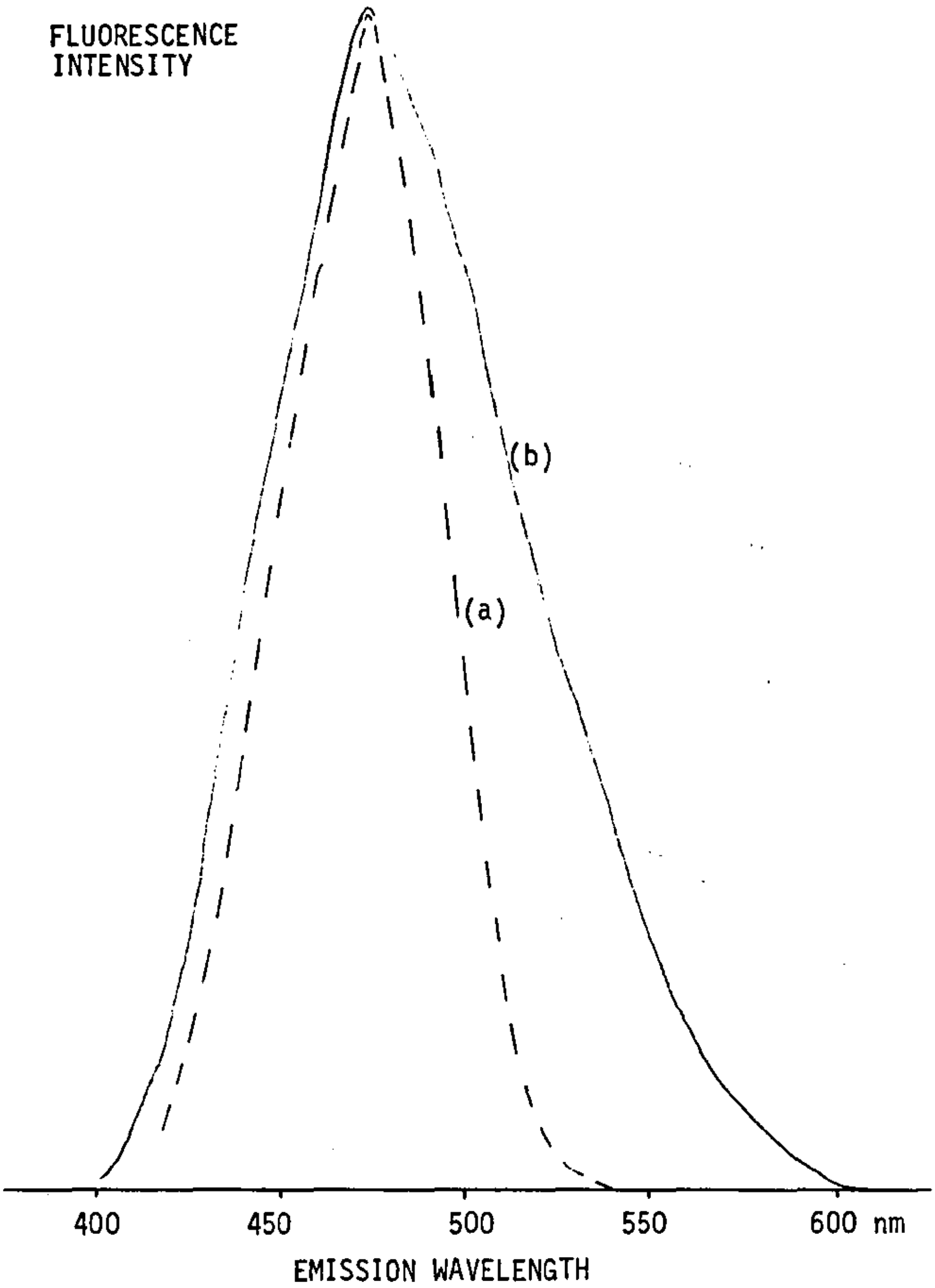

FIGURE 3.33 A Comparison of Conventional and Synchronous Fluorescence Spectra of Albumin-Bound ANS.

(a) Synchronously excited emission spectrum of sample containing 2x10^{-6}M ANS and 2x10^{-5}M HSA in 0.1M Tris/HCl buffer pH 7.4. Δλ = 100nm.
Full width at half maximum 53nm.

(b) Conventional emission spectrum of same sample.
Wavelength of excitation 375nm.
Full width at half maximum 83nm.

in the long wavelength tail of the spectral band on going from the conventional to the synchronous mode. Compared to the normal emission spectrum, the fluorescence of the bound probe in the region of 520nm is about six times lower in the synchronous spectrum. Thus, overlap between the spectra of bound and free ANS may be significantly reduced by employing the synchronous excitation of fluorescence emission rather than running normal emission spectra.

Unfortunately, it was not possible to extend the synchronous technique to the separate measurement of free and bound levels of ANS in samples containing both species. As mentioned before, the fluorescence intensity of ANS in free solution is so weak that even a small contribution from the bound probe in the region of 520nm makes quantitation impossible. While synchronous scanning of excitation and emission monochromators certainly reduced the problem of spectral interference, it was insufficient to totally eliminate the effect.

From the results presented in this section, it is possible to predict under what circumstances the derivative and synchronous techniques would be of most value. This is made easy by the fact that the fluorescent probes used in this investigation have quite different characteristics. Warfarin exhibits only a moderate enhancement in its fluorescence intensity on binding to HSA. Similarly the wavelength of maximum emission and the emission bandwidth are altered only slightly when the probe binds to albumin. Although derivative techniques can amplify differences between the emission spectra of the free and bound species, complete resolution of the peaks is not possible. Synchronous spectroscopy is also of limited use as far as warfarin is concerned because the Stokes shifts of the free and bound forms are so similar. In contrast to warfarin, the fluorescence intensity emitted by ANS increases dramatically on binding to albumin. Moreover, the wavelength of maximum emission is transferred to a much shorter wavelength. The problem here lies in discrimination between the weak fluorescence of the free forms of ANS and the intense fluorescence of the bound form. While synchronous scanning of the excitation and emission monochromators reduces the spectral band widths, complete resolution of the two signals is still not feasible.

It is clear that the class of fluorescent probes which would benefit most from derivative and synchronous techniques would exhibit moderate shifts in the wavelengths of maximum emission on binding to albumin, possibly intermediate between those of warfarin and ANS but probably similar to that of ANS, and increases in the intensity of fluorescence on binding to albumin more akin to that of warfarin than ANS.

APPENDIX A

The purpose of this appendix is to demonstrate that the approximation

$$\sum_{i=1}^{n} f_0 \exp\left(-2.303(a_1 x_i + a_2 y_i)\ c\right) \approx F_0 \exp\left(-2.303(a_1\ \bar{x} + a_2 \bar{y})c\right)$$

holds true under specified conditions.

By way of an introduction, and in order to simplify the mathematics, the hypothesis

$$\sum_{i=1}^{n} \exp\ (x_i) \approx n \exp\left[\sum_{i=1}^{n} \frac{x_i}{n}\right] \qquad \text{(A.1)}$$

will be tested.

$$e^{x_1} = 1 + x_1 + \frac{x_1^2}{2!} + \frac{x_1^3}{3!} + \ldots\ldots + \frac{x_1^r}{r!} + \ldots\ldots$$

$$e^{x_2} = 1 + x_2 + \frac{x_2^2}{2!} + \frac{x_2^3}{3!} + \ldots\ldots + \frac{x_2^r}{r!} + \ldots\ldots$$

$$e^{x_n} = 1 + x_n + \frac{x_n^2}{2!} + \frac{x_n^3}{3!} + \ldots\ldots + \frac{x}{r!} + \ldots\ldots$$

$$\therefore \sum_{i=1}^{n} e^{x_i} = e^{x_1} + e^{x_2} + \ldots\ldots + e^{x_n} = n + (x_1 + x_2 + \ldots\ldots + x_n) +$$

$$\left(\frac{x_1^2}{2!} + \frac{x_2^2}{2!} + \ldots\ldots + \frac{x_n^2}{2!}\right) + \left(\frac{x_1^3}{3!} + \frac{x_2^3}{3!} + \ldots\ldots + \frac{x_n^3}{3!}\right) + \ldots\ldots + \left(\frac{x_1^r}{r!} + \frac{x_2^r}{r!} + \ldots\ldots + \frac{x_n^r}{r!}\right) + \ldots\ldots$$

$$\therefore \sum_{i=1}^{n} e^{x_i} = n\ (1 + \bar{x} + \frac{\bar{x}^2}{2!} + \frac{\bar{x}^3}{3!} + \ldots\ldots + \frac{\bar{x}^r}{r!} + \ldots\ldots \qquad \text{(A.2)}$$

where $\bar{x} = \dfrac{(x_1 + x_2 + \ldots\ldots + x_n)}{n}$, $\bar{x}^2 = \dfrac{(x_1^2 + x_2^2 + \ldots\ldots + x_n^2)}{n}$,

$\bar{x}^r = \dfrac{(x_1^r + x_2^r + \ldots\ldots + x_n^r)}{n}$, etc. That is, $\bar{x} = \sum\limits_{i=1}^{n} \dfrac{x_i}{n}$, $\bar{x}^2 = \sum\limits_{i=1}^{n} \dfrac{x_i^2}{n}$,

$\bar{x}^r = \sum\limits_{i=1}^{n} \dfrac{x_i^r}{n}$, etc.

Now $e^{\left[\sum_{i=1}^{n} \frac{x_i}{n}\right]} = e^{\bar{x}} = 1 + \bar{x} + \dfrac{\bar{x}^2}{2!} + \dfrac{\bar{x}^3}{3!} + \ldots\ldots + \dfrac{\bar{x}^r}{r!} + \ldots\ldots$

$$\therefore\ n\, e^{\left[\sum_{i=1}^{n} \frac{x_i}{n}\right]} = n\left(1 + \bar{x} + \frac{\bar{x}^2}{2!} + \frac{\bar{x}^3}{3!} + \dots\dots + \frac{\bar{x}^r}{r!} + \dots\dots\right) \qquad (A.3)$$

The first two terms on the right-hand sides of Equations A.2 and A.3 are identical and

$$\Delta = \sum_{i=1}^{n} e^{x_i} - n\, e^{\left[\sum_{i=1}^{n} \frac{x_i}{n}\right]} = n\left\{\frac{(\overline{x^2} - \bar{x}^2)}{2!} + \frac{(\overline{x^3} - \bar{x}^3)}{3!} + \dots\dots + \frac{(\overline{x^r} - \bar{x}^r)}{r!} + \dots\dots\right\}$$

(A.4)

If the original approximation (Equation A.1) is to be acceptable, Δ must be small compared to $\sum_{i=1}^{n} e^{x_i}$

The conditions necessary to minimize Δ may be appreciated by taking Equation A.4 and examining the terms in brackets. The first term may be rewritten in the form

$$n\,\frac{(\overline{x^2} - \bar{x}^2)}{2!} = \frac{x_1}{2!}(x_1 - \bar{x}) + \frac{x_2}{2!}(x_2 - \bar{x}) + \frac{x_3}{2!}(x_3 - \bar{x}) + \dots\dots + \frac{x_r}{2!}(x_r - \bar{x}) + \dots\dots \qquad (A.5)$$

The individual components $\frac{x_i}{2!}(x_i - \bar{x})$ may be positive or negative depending on whether x_i is larger or smaller than the mean of the series. To minimize the function, however, the different values x_i should be as near to $\bar{x}$ as possible, that is $(x_i - \bar{x})$ should tend to zero.

The other functions in Equation A.4 may be expanded in a similar fashion. Again, if these terms are to be small, the variability of the series x_i should be low.

The statement $\sum_{i=1}^{n} e^{x_i} \approx n\, e^{\left[\sum_{i=1}^{n} \frac{x_i}{n}\right]}$

may be tested using an appropriate practical example. Consider a number of fluorescent molecules situated within a fluorimeter cell. Suppose a central portion of the sample is being irradiated (see Figure A.1(a)) and the molecules under examination are at depths of 0.25, 0.30, 0.35, ..., 0.75cm. So the approximation in Equation A.1 is under trial for the series $x_i = 0.25, 0.30, 0.35, \dots\dots, 0.75$. Therefore $n = 11$, $\bar{x} = 0.5$ and

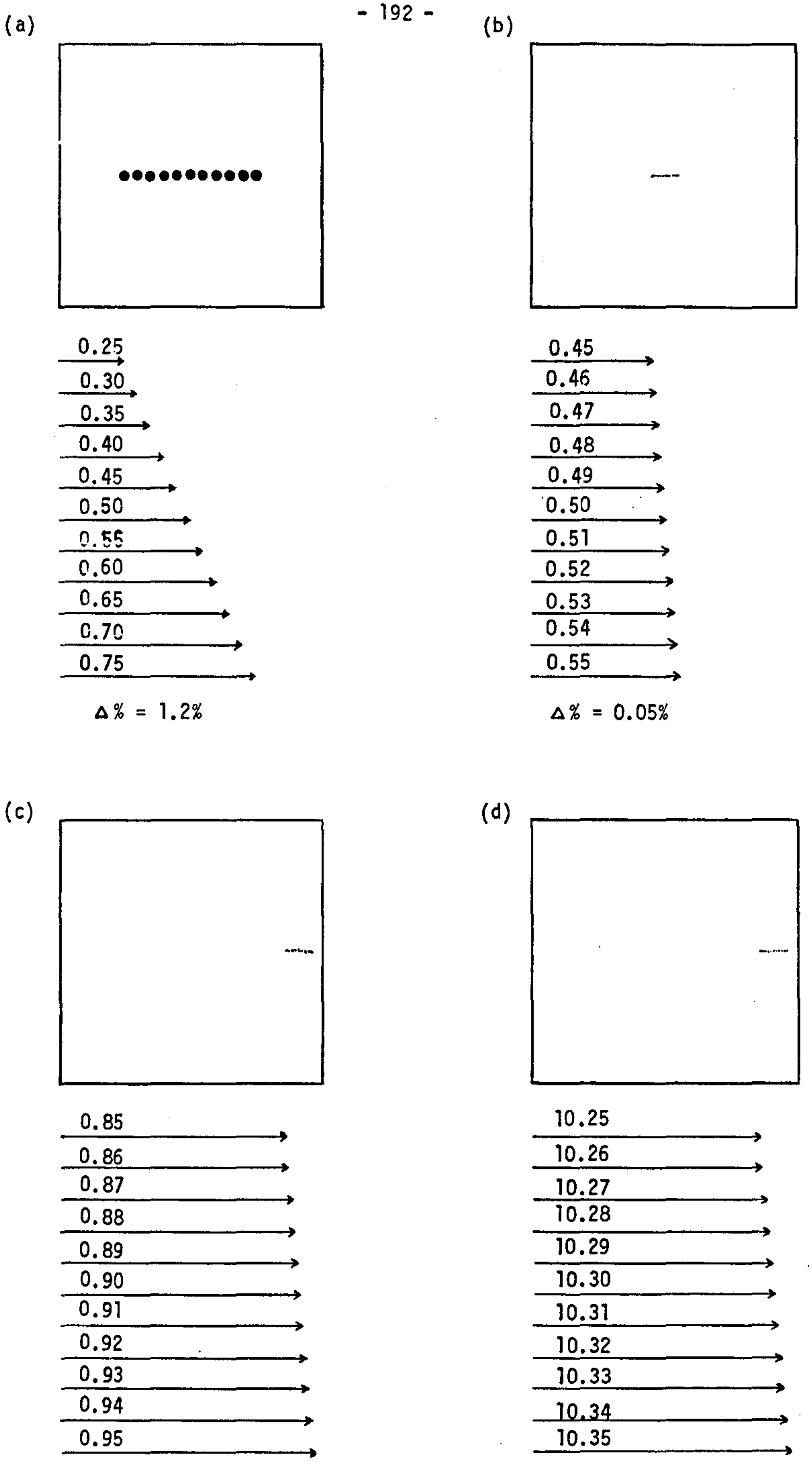
(a)
0.25
0.30
0.35
0.40
0.45
0.50
0.55
0.60
0.65
0.70
0.75
Δ% = 1.2%
(b)
0.45
0.46
0.47
0.48
0.49
0.50
0.51
0.52
0.53
0.54
0.55
Δ% = 0.05%
(c)
0.85
0.86
0.87
0.88
0.89
0.90
0.91
0.92
0.93
0.94
0.95
Δ% = 0.05%
(d)
10.25
10.26
10.27
10.28
10.29
10.30
10.31
10.32
10.33
10.34
10.35
Δ% = 0.05%

FIGURE A.1

$$\sum_{i=1}^{n} e^{x_i} = e^{0.25} + e^{0.3} + \ldots\ldots + e^{0.75} = 18.3634$$

$$n\, e^{\left[\sum_{i=1}^{n} \frac{x_i}{n}\right]} = 11\, e^{0.5} = 18.1359$$

$$\Delta = \sum_{i=1}^{n} e^{x_i} - n e^{\left[\sum_{i=1}^{n} \frac{x_i}{n}\right]} = 0.2275$$

The percentage error in using the approximation $n\, e^{\left[\sum_{i=1}^{n} \frac{x_i}{n}\right]}$ instead of $\sum_{i=1}^{n} e^{x_i}$ is $\left[\Delta \Big/ \sum_{i=1}^{n} e^{x_i}\right] \times 100\%$. In this case the error is small - about 1.2%.

The series may be used to check the validity of Equation A.4 with $\bar{x}=0.5$, $\bar{x}^2 = 0.275$, $\bar{x}^3 = 0.1011125$, etc. Evaluating the terms on the right-hand side of the equation gives

$$\Delta = 0.1375 + 0.06875 + 0.01770 + 0.00312 + 0.00043 + \ldots\ldots = 0.2275$$

which agrees with the previous result for the difference between $\sum_{i=1}^{n} e^{x_i}$ and $n\, e^{\left[\sum_{i=1}^{n} \frac{x_i}{n}\right]}$.

For a sample cell in which the irradiated portion is more restricted, the approximation becomes even better. An example is shown in Figure A.1(b) where the fluorescent molcules under consideration are located at 0.45, 0.46, 0.47, ... 0.55cm. The error in assuming that $\sum_{i=1}^{n} e^{x_i}$ can be replaced by $n\, e^{\left[\sum_{i=1}^{n} \frac{x_i}{n}\right]}$ is only 0.05%. Since the variation about the mean displacement is low, such a small discrepancy is only to be predicted (see Equation A.5). Moreover, the magnitude of Δ % is independent of the exact position of the volume under consideration. This is demonstrated in Figures A.1(c) and A.1(d); as long as the spread of x_i is constant, the percentage error associated with the approximation is invariant.

The analysis may be extended to show that

$$\sum_{i=1}^{n} \exp\,(x_i + y_i) \simeq n \exp\left[\sum_{i=1}^{n} \frac{x_i}{n} + \sum_{i=1}^{n} \frac{y_i}{n}\right] = n \exp\,(\bar{x} + \bar{y}) \qquad (A.6)$$

under certain conditions. Thus,

$$\sum_{i=1}^{n} e^{(x_i+y_i)} = n\left\{1 + (\overline{x+y}) + \frac{(\overline{x+y})^2}{2!} + \frac{(\overline{x+y})^3}{3!} + \dots \frac{(\overline{x+y})^r}{r!} + \dots\right\} \tag{A.7}$$

where $(\overline{x+y}) = \dfrac{((x_1+y_1) + (x_2+y_2) + \dots + (x_n+y_n))}{n}$,

$(\overline{x+y})^2 = \dfrac{((x_1+y_1)^2 + (x_2+y_2)^2 + \dots (x_n+y_n)^2)}{n}$,

$(\overline{x+y})^r = \dfrac{((x_1+y_1)^r + (x_2+y_2)^r + \dots (x_n+y_n)^r)}{n}$.

Now $$n\, e^{\left[\sum_{i=1}^{n} \frac{x_i}{n} + \sum_{i=1}^{n} \frac{y_i}{n}\right]} = n\, e^{(\bar{x}+\bar{y})} = n\left\{1 + (\bar{x}+\bar{y}) + \frac{(\bar{x}+\bar{y})^2}{2!} + \frac{(\bar{x}+\bar{y})^3}{3!} + \dots + \frac{(\bar{x}+\bar{y})^r}{r!} + \dots\right\} \tag{A.8}$$

The first two terms on the right-hand sides of Equations A.7 and A.8 are identical because $(\overline{x+y}) = \dfrac{((x_1+y_1) + (x_2+y_2) + \dots + (x_n+y_n))}{n} =$

$$\frac{(x_1 + x_2 + \dots + x_n)}{n} + \frac{(y_1 + y_2 + \dots + y_n)}{n} = (\bar{x}+\bar{y})$$

$$\therefore \quad \Delta = \sum_{i=1}^{n} e^{(x_i+y_i)} - n\, e^{(\bar{x}+\bar{y})} = n\left\{\frac{((\overline{x+y})^2 - (\bar{x}+\bar{y})^2)}{2!} + \frac{((\overline{x+y})^3 - (\bar{x}+\bar{y})^3)}{3!} + \dots + \frac{((\overline{x+y})^r - (\bar{x}+\bar{y})^r)}{r!} + \dots\right\} \tag{A.9}$$

If the approximation of Equation A.6 is to be acceptable, Δ must be small compared to $\sum_{i=1}^{n} e^{(x_i+y_i)}$.

The first term in Equation A.9 which contributes to Δ may be rewritten as

$$n \left\{ \frac{(\overline{x + y})^2 - (\bar{x} + \bar{y})^2}{2!} \right\} = \frac{(x_1 + y_1)}{2!} \left\{ (x_1 - \bar{x}) + (y_1 - \bar{y}) \right\} + \frac{(x_2 + y_2)}{2!}$$

$$\left\{ (x_2 - \bar{x}) + (y_2 - \bar{y}) \right\} + \ldots\ldots + \frac{(x_n + y_n)}{2!} \left\{ (x_n - \bar{x}) + (y_n - \bar{y}) \right\} \qquad (A.10)$$

If this term is to be a minimum, the values x_i and y_i should vary as little as possible from $\bar{x}$ and $\bar{y}$, respectively. The same criterion can be shown to be true for the other terms in Equation A.9.

It is now possible to consider a variable which is defined by two parameters. For example, suppose x_i and y_i represent the excitation and emission path lengths appropriate to a fluorescent molecule at some position (x_i, y_i) within a sample cell. Furthermore, suppose that in the irradiated portion of the sample solution, molecules are located at points represented by the coordinates,

i	1	2	3	4	5	6	7	8	9
x_i	0.45	0.45	0.45	0.5	0.5	0.5	0.55	0.55	0.55
y_i	0.45	0.5	0.55	0.45	0.5	0.55	0.45	0.5	0.55

This arrangement is shown diagrammatically in Figure A. 2(a). So,

$$\sum_{i=1}^{n} e^{(x_i + y_i)} = e^{0.9} + e^{0.95} + \ldots\ldots + e^{1.1} = 24.5053$$

$$9\, e^{(\bar{x} + \bar{y})} = 9\, e^{1.0} = 24.4645$$

$$\therefore \quad \Delta = 0.0408$$

The percentage error in using $n\, e^{(\bar{x} + \bar{y})}$ instead of $\sum_{i=1}^{n} e^{(x_i + y_i)}$ is 0.17% in this example. When the results are fed into Equation A. 9.

$$\begin{aligned} \Delta &= 0.015 + 0.015 + 0.00751 + 0.00251 + 0.00063 + 0.00013 + \ldots \\ &= 0.0408 \end{aligned}$$

as above.

Figures A. 2(b) and A. 2(c) show how the error in assuming the validity of the approximation is independent of the absolute values (x_i, y_i) for constant variations about the means. However, when larger volumes of the sample solution are considered, variation of the coordinates $(x_i + y_i)$ is increased and the approximation becomes less accurate. This is illustrated

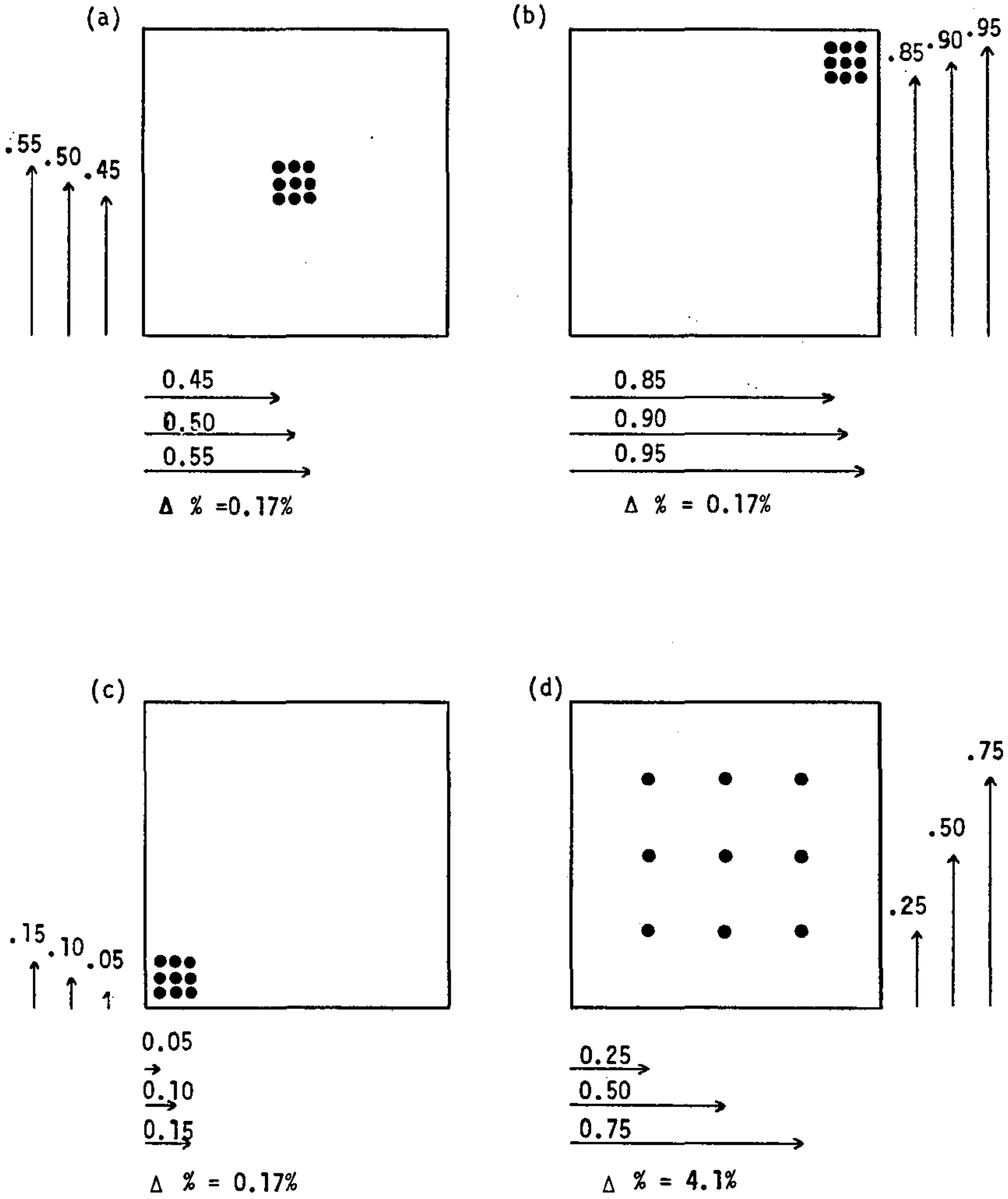
(a)
.55
.50
.45
0.45
0.50
0.55
Δ % =0.17%
(b)
.85
.90
.95
0.85
0.90
0.95
Δ % = 0.17%
(c)
.15
.10
.05
0.05
0.10
0.15
Δ % = 0.17%
(d)
.75
.50
.25
0.25
0.50
0.75
Δ % = 4.1%

FIGURE A.2

in Figure A. 2(d)

It has been shown how $\sum_{i=1}^{n} \exp(x_i + y_i) \simeq n \exp(\bar{x} + \bar{y})$ under the appropriate experimental conditions. Since the terms f_O, c, a_1 and a_2 defined in the main text are independent of x_i and y_i, the following statement must be true:

$$F_M = \sum_{i=1}^{n} f_O \exp(-2.303\,(a_1 x_i + a_2 y_i)\,c) \simeq n f_O \exp(-2.303\,(a_1 \bar{x} + a_2 \bar{y})c)$$

$$\therefore \quad F_M \simeq F_O \exp(-2.303\,(a_1 \bar{x} + a_2 \bar{y})\,c) \text{ as required.}$$

CHAPTER 4

The Application of Fluorescent Probes to a Study of Drug Binding Sites on Serum Proteins

4.1 Introduction

The development of methods for measuring the binding of fluorescent probes to HSA provided the basis from which to examine the drug-binding properties of specific sites on the albumin molecule. The procedures described in Chapter 3 were used to determine the concentrations of bound and unbound fluorescent probe in the presence and absence of potential competitor drugs. The degree of probe displacement so obtained was interpreted in terms of the affinity of the competing ligands for binding to albumin.

Evidence from Sudlow et al (1975) that warfarin and ANS bind to separate sites on albumin suggested that these compounds might serve as probes for different regions of the protein structure. Thus a number of non-fluorescent drugs were selected and tested for their ability to displace both warfarin and ANS. The first drug to be considered was phenylbutazone.

Phenylbutazone is an anti-inflammatory agent and is extensively bound to albumin (Burns et al, 1953). The interaction between this drug and warfarin is phenomenologically well established and its potentially disasterous clinical consequences are generally appreciated (O'Reilly, 1967). Aggeler et al (1967) have demonstrated the interaction in humans. As reported in the present chapter, an attempt was made to establish the degree of competition between phenylbutazone and warfarin for binding sites on albumin. The significance of this competitive binding process in the overall mechanism of the drug interaction is discussed.

The ability of the sulphonamide group of drugs to displace fluorescent probes from albumin was investigated. This group provided a series of structurally similar compounds which could be screened for the presence of common features associated with strong binding to particular sites on albumin. The binding properties of some other drugs were also examined.

While there is experimental evidence to suggest that albumin plays a major role in the binding of acidic drugs in human plasma (Tillement et al, 1981), the possibility of interactions between these drugs and other serum proteins should not be overlooked. With this possibility in mind, and in order to establish the wider applicability of the method, a number of experiments were performed using whole serum.

4.2 The Influence of Competitor Drugs on Probe Binding Curves

A procedure for studying the binding of fluorescent probes to HSA has already been described, and was discussed with regard to the subsequent generation of binding curves and constants. An obvious extension of this approach lay in a consideration of the effect of other ligands on the binding curves and affinity constants of the fluorescent probes. The purpose of the following paragraphs is to show how this was achieved for warfarin.

4.2.1 Practical Considerations

Before commencing the binding experiments it was necessary to check whether potential competitors had any effects on the analytical signal - that is, the bound probe fluorescence, other than those arising from direct displacement interactions.

Of the drugs selected for examination, none had a detectable fluorescence at the wavelength used to assay the bound fraction of warfarin. Thus on addition of the ligands, there were no spurious signals to complicate an assessment of the probe binding.

In general, the excitation peak of warfarin was centred at a considerably longer wavelength than the absorption maxima of the competing ligands. Figure 4.1 illustrates this for a number of cases. From their ultraviolet absorption spectra, it is quite clear why phenylbutazone and 2-p-(chlorophenoxy)-2-methyl propionic acid (CPMP) should be incapable of reducing the intensity of the recorded signal by a simple absorptive process. Likewise, however, the need to make allowances for the small inner-filter effects associated with the overlap of the long wavelength tail of the absorption spectra of certain sulphonamides and the excitation peak of warfarin can be equally well-appreciated. Somewhat larger corrections were required for sulphapyridine and flufenamic acid as these compounds absorb rather well around 320nm.

So when warfarin is used as a probe for albumin binding sites, there are two distinct mechanisms by which addition of a second ligand can affect a reduction in the measured signal. Firstly by a competitive or non-competitive displacement of the fluorescent probe from its binding sites. Secondly by a trivial inner-filter effect. As either, or both of these mechanisms may operate to lower the observed fluorescence, it is imperative to distinguish between the two phenomena.

An evaluation of competitor inner-filter effects was feasible by the adaptation of some of the procedures described in Chapter 3. One

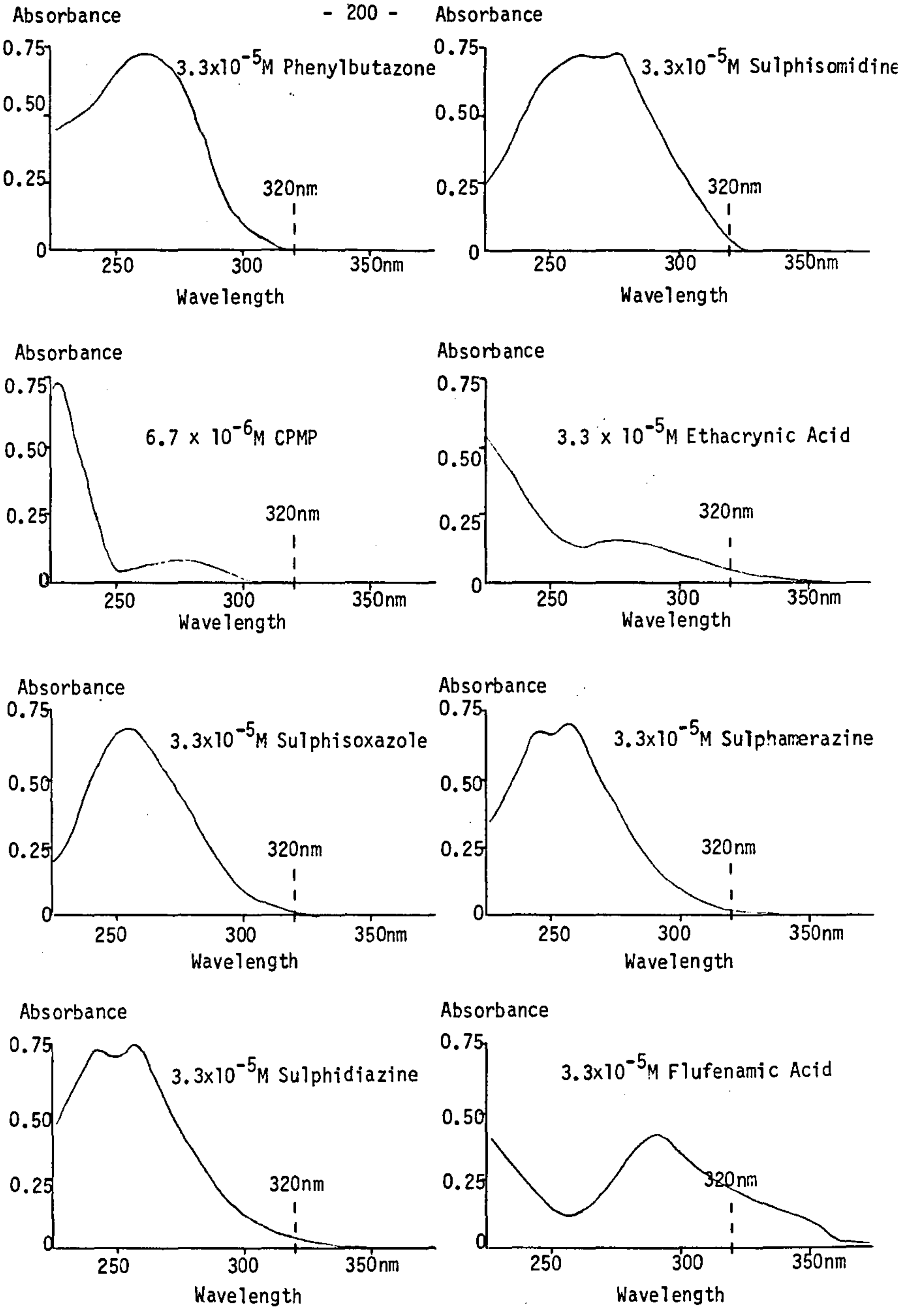

FIGURE 4.1 Absorption Spectra for Several Drugs and their Relation to the Excitation Peak of Warfarin at 320nm.

possibility was to determine the absorbance of each competitor at the wavelengths of excitation and emission of the bound probe fluorescence. The results could be used in conjunction with Equation 3.5 to correct the measured fluorescence intensity for losses due to absorption. For most of the drugs under examination however, this procedure meant that spectrophotometric readings had to be taken at wavelengths which were far removed from the main absorption peaks. Although not always of great consequence, this did tend to reduce the reliability of some of the results.

Due to its increased sensitivity, and because there are a number of theoretical as well as practical reasons for estimating inner-filter effects by a fluorimetric rather than a spectrophotometric method (see Section 3.2.3), the following procedure was routinely applied to competitive binding studies.

The potential competitor was titrated into a solution containing the fluorescent probe in free solution, but the monochromators were set at the wavelengths used to determine the bound probe fluorescence. Any changes in the emission intensity were recorded. According to Equation 3.4, a decrease in the observed fluorescence must be proportional to exp -2.303 $(a_1 \bar{x} + a_2 \bar{y})c$ where, in this instance, a_1 and a_2 are the molar absorbances of the competitor at the wavelengths of excitation and emission respectively, c is the competitor concentration, and $\bar{x}$ and $\bar{y}$ represent the mean path lengths of the excitation and emission beams. This factor may be simplified to $\exp - kc$ where $k = 2.303\ (a_1\bar{x} + a_2\bar{y})$. So,

$$F_m = F_0 \exp(-k\,c) \qquad \text{and}$$

$$k = \frac{1}{c} \ln \left(\frac{F_0}{F_m}\right) \qquad (4.1)$$

where F_m and F_0 are the fluorescent intensities observed in the presence and in the absence of competitor, respectively.

By adding known concentrations c of the ligand of interest and noting the corresponding fluorescence intensity F_m it was possible to make several determinations of the inner-filter correction factor, k . The results obtained for sulphisomidine are typical. They are presented in Table 4.1. The mean experimental values of the correction factors for several other sulphonamides are included in Table 4.2.

Once it became feasible to distinguish inner-filter from displacement effects, the production of probe binding curves in the presence of any competitor was quite straightforward. A convenient concentration of

SM Concentration $(\times 10^{-5}M)$	Observed Fluorescence (Arbitrary Units)	Inner-Filter Correction Factor, $k(\times 10^{-4})$
0.00	11.25	-
3.28	10.75	6.03
6.54	10.20	7.32
9.80	9.65	6.80
13.04	9.25	6.52
19.50	8.25	6.91
25.91	7.55	6.68
32.29	6.95	6.48
44.91	6.00	6.08
63.55	4.60	6.11

TABLE 4.1

Nine determinations of the inner-filter factor, k for sulphisomidine (SM). Warfarin concentration $4.2 \times 10^{-5}M$. Diluent buffer was 0.1M Tris/HCl pH 7.4. Wavelengths of fluorescence excitation and emission were 320nm and 375nm, respectively.

Mean value of $k = 6.55 \times 10^{-4}$

standard deviation $= 0.433 \times 10^{-4}$

coefficient of variation = 6.6%

Drug	$k \times 10^{-4}$
Sulphapyridine	45.61
Sulphisomidine	6.55
Sulphamerazine	5.83
Sulphadiazine	2.90
Sulphisoxazole	0.67

TABLE 4.2

Mean values of k for some sulphonamide drugs.
Experimental conditions as described in Table 4.1.

a potential competitor was added to an albumin solution before titrating the fluorescent probe. The program FLUORB was instructed to take account of competitor inner-filter effects before estimating the concentrations of albumin-bound and unbound fluorescent probe at each point in the titration. In practice, the main requirement was simply the provision of an appropriate inner-filter correction factor and a notification of the competitor concentration. Binding curves and constants were constructed with the aid of the usual computer programs. Alterations in the capacity of HSA to bind the fluorescent probe were revealed as changes in curve shape and modifications of binding constants.

4.2.2 Results and Observations

The effect of phenylbutazone on the binding of warfarin to HSA is illustrated in the Scatchard plots of Figure 4.2. There is clearly a dramatic reduction in the capacity of albumin for binding warfarin when phenylbutazone is present. The phenomenon is particularly noticeable at low probe-to-protein ratios when a very large proportion of the fluorescent probe appears to be displaced from its binding sites. At high warfarin concentrations the effect of phenylbutazone is less marked. These observations may be further appreciated by a study of the changes in the absolute bound probe concentrations shown in Table 4.3.

The similarity in the values of n_1 and n_2 obtained in the presence and absence of phenylbutazone (Table 4.4) suggests that this compound does not alter the number of warfarin binding sites on albumin. Coupled with the shapes of the corresponding binding curves, this provides an indication of common binding sites on albumin for phenylbutazone and warfarin. As may be expected, the downward displacement of the Scatchard plot of warfarin on addition of phenylbutazone is reflected in a large reduction in k_1 . However, the values of k_2 obtained at different competitor concentrations are little changed and suggest that the binding of warfarin to low affinity, or secondary, sites on albumin is virtually unaffected by the incorporation of phenylbutazone. From these results it seems that while phenylbutazone and warfarin share high affinity sites on HSA, competition for secondary binding sites is of little or no consequence.

However, extreme caution must be exercised at this stage. As pointed out in Section 1.7, the mechanism of the binding process need not necessarily satisfy the Scatchard assumptions even though the data are adequately fitted by the Scatchard model. The interpretation given above

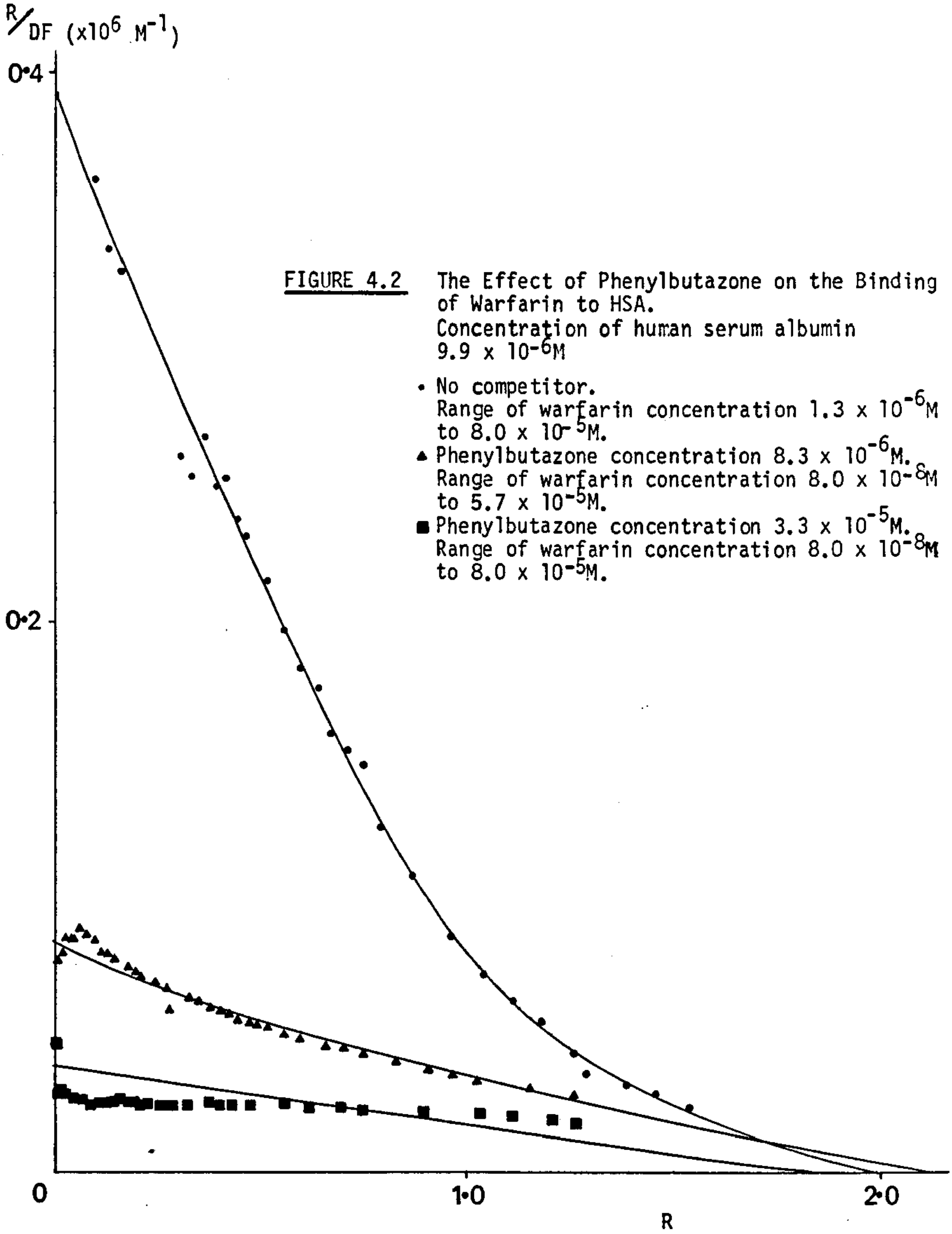

FIGURE 4.2 The Effect of Phenylbutazone on the Binding of Warfarin to HSA.
Concentration of human serum albumin 9.9×10^{-6}M

- • No competitor.
Range of warfarin concentration 1.3×10^{-6}M to 8.0×10^{-5}M.
- ▲ Phenylbutazone concentration 8.3×10^{-6}M.
Range of warfarin concentration 8.0×10^{-8}M to 5.7×10^{-5}M.
- ■ Phenylbutazone concentration 3.3×10^{-5}M.
Range of warfarin concentration 8.0×10^{-8}M to 8.0×10^{-5}M.

TABLE 4.3

The data used to construct the plots shown in Figure 4.2. Results from fluorescence titrations were processed using the FLUORB program. DC, DB and DF are the concentrations of total, bound and free fluorescent probe, respectively. R is the bound probe concentration divided by the total protein concentration. RONDF is R divided by DF. The total HSA concentration in these experiments was 9.9 x 10^{-6}M.

(a) No Competitor

DC $\times 10^{-6}$M	DB $\times 10^{-6}$M	DF $\times 10^{-6}$M	R	RONDF $\times 10^{6}$M^{-1}
1.2530	0.9788	0.2742	0.0988	0.3603
1.6704	1.2839	0.3866	0.1296	0.3353
2.0877	1.5950	0.4927	0.1611	0.3269
4.1719	3.0043	1.1675	0.3036	0.2601
4.5883	3.2768	1.3115	0.3312	0.2525
5.0046	3.6315	1.3731	0.3671	0.2674
5.4207	3.8573	1.5634	0.3900	0.2495
5.8367	4.1661	1.6706	0.4213	0.2522
6.2526	4.3816	1.8710	0.4432	0.2369
6.6684	4.6414	2.0270	0.4695	0.2316
7.4994	5.0937	2.4057	0.5155	0.2143
8.3279	5.5007	2.8292	0.5568	0.1968
9.1598	5.9014	3.2584	0.5976	0.1834
9.9892	6.7389	3.6504	0.6421	0.1759
10.8181	6.6142	4.2039	0.6702	0.1594
11.6464	7.0124	4.6340	0.7108	0.1534
12.4741	7.4018	5.0723	0.7505	0.1480
14.1280	7.8139	6.3141	0.7929	0.1256
16.6046	8.5462	8.0584	0.8680	0.1077
20.7215	9.4692	11.2522	0.9634	0.0856
24.8248	10.2332	14.5916	1.0428	0.0715
28.9145	10.9393	17.9752	1.1166	0.0621
32.9908	11.5572	21.4336	1.1816	0.0551
41.1033	12.2961	28.8072	1.2613	0.0438
49.1627	12.5380	36.6247	1.2903	0.0352
57.1697	13.4602	43.7095	1.3898	0.0318
65.1247	14.0967	51.0280	1.4602	0.0286
80.8806	14.7685	66.1122	1.5397	0.0233

TABLE 4.3 (continued)

(b) 8.3×10^{-6}M Phenylbutazone

DC $\times 10^{-6}$M	DB $\times 10^{-6}$M	DF $\times 10^{-6}$M	R	RONDF $\times 10^{6}$M^{-1}
0.0834	0.0348	0.0486	0.0035	0.0724
0.2086	0.0916	0.1170	0.0092	0.0790
0.4171	0.1837	0.2334	0.0185	0.0794
0.6256	0.2855	0.3401	0.0288	0.0847
0.8341	0.3798	0.4543	0.0383	0.0844
1.0425	0.4750	0.5676	0.0479	0.0845
1.2509	0.5885	0.6625	0.0594	0.0897
1.6676	0.7751	0.8925	0.0783	0.0877
2.0842	0.9479	1.1363	0.0957	0.0842
2.5006	1.1063	1.3944	0.1117	0.0801
2.9169	1.2678	1.6491	0.1281	0.0777
3.3331	1.4416	1.8914	0.1456	0.0770
3.7491	1.6099	2.1392	0.1627	0.0760
4.1650	1.7626	2.4023	0.1781	0.0742
4.5807	1.9182	2.6625	0.1939	0.0728
4.9963	2.0677	2.9286	0.2090	0.0714
5.8271	2.3658	3.4613	0.2393	0.0691
6.6573	2.6554	4.0019	0.2686	0.0671
7.4870	2.7267	4.7603	0.2759	0.0580
8.3161	3.2678	5.1082	0.3247	0.0636
9.1447	3.4792	5.6655	0.3523	0.0622
9.9727	3.7186	6.2541	0.3767	0.0602
10.8002	3.9667	6.8335	0.4020	0.0588
11.6271	4.1801	7.4470	0.4237	0.0569
12.4535	4.4014	8.0521	0.4463	0.0554
13.2793	4.8306	8.6487	0.4697	0.0543
14.1046	4.8683	9.2362	0.4940	0.0535
14.9293	5.0791	9.8502	0.5155	0.0523
16.5772	5.4865	11.0907	0.5572	0.0502
18.2229	5.8849	12.3380	0.5981	0.0485
20.6873	6.4546	14.2327	0.6567	0.0461
22.3275	6.8942	15.4334	0.7018	0.0455
24.7839	7.3329	17.4510	0.7472	0.0428
28.8669	8.1370	20.7300	0.8306	0.0401
32.9366	8.8618	24.0748	0.9060	0.0376
36.9930	9.4687	27.5243	0.9697	0.0352
41.0360	10.0343	31.0017	1.0293	0.0332
49.0825	11.1869	37.8956	1.1513	0.0304
57.0767	12.1596	44.9171	1.2555	0.0280

TABLE 4.3 (continued)

(c) 3.3 x 10^{-5}M Phenylbutazone

DC $\times 10^{-6}$M	DB $\times 10^{-6}$M	DF $\times 10^{-6}$M	R	RONDF $\times 10^{6}$M^{-1}
0.0830	0.0265	0.0565	0.0027	0.0473
0.2075	0.0661	0.1414	0.0067	0.0472
0.4150	0.0906	0.3245	0.0091	0.0282
0.8300	0.1834	0.6465	0.0185	0.0286
1.0374	0.2176	0.8197	0.0220	0.0268
1.2447	0.2694	0.9753	0.0272	0.0279
1.6594	0.3399	1.3195	0.0343	0.0260
2.0739	0.4294	1.6445	0.0434	0.0264
2.4882	0.5208	1.9674	0.0526	0.0267
2.9024	0.5874	2.3151	0.0593	0.0256
3.3165	0.6824	2.6341	0.0689	0.0262
4.1445	0.8143	3.3300	0.0823	0.0247
4.9715	0.9612	4.0103	0.0972	0.0242
5.7982	1.1241	4.6741	0.1137	0.0243
6.6243	1.3132	5.3111	0.1328	0.0250
7.4499	1.5004	5.9495	0.1518	0.0255
8.2749	1.6547	6.6202	0.1675	0.0253
9.0994	1.8155	7.2839	0.1838	0.0252
9.9234	1.9622	7.9612	0.1988	0.0250
10.7468	2.0831	8.6637	0.2111	0.0244
11.5696	2.2200	9.3496	0.2250	0.0241
12.3919	2.3734	10.0186	0.2407	0.0240
13.2137	2.5219	10.6918	0.2558	0.0239
14.0349	2.6760	11.3589	0.2715	0.0239
14.8556	2.8359	12.0197	0.2878	0.0239
16.4954	3.1635	13.3319	0.3213	0.0241
18.9510	3.6834	15.2676	0.3745	0.0245
20.5854	3.9594	16.6260	0.4028	0.0242
22.2176	4.2559	17.9617	0.4333	0.0241
24.6620	4.6997	19.9623	0.4789	0.0240
28.7252	5.5174	23.2078	0.5632	0.0243
32.7752	6.0829	26.6922	0.6219	0.0233
36.8119	6.8158	29.9961	0.6980	0.0233
40.8355	7.3171	33.5185	0.7506	0.0224
48.8435	8.7336	40.1099	0.8988	0.0224
56.7997	10.0439	46.7558	1.0370	0.0222
64.7045	10.8226	53.8819	1.1211	0.0208
72.5585	11.6515	60.9071	1.2108	0.0199
80.3622	12.1736	68.1886	1.2692	0.0186

TABLE 4.4

Estimated binding constants for the interaction between warfarin and HSA: the effect of phenylbutazone on these values.

Binding constants were derived from the data presented in Table 4.3 with the aid of the NKFIT program

Phenylbutazone Concn. x 10^{-6}M	n_1	k_1 x $10^5 M^{-1}$	n_2	k_2 x 10 M^{-1}
0.0	0.96	3.86	1.04	0.20
8.3	0.89	0.59	1.23	0.19
33.1	0.85	0.21	0.95	0.22

TABLE 4.5

Estimated binding constants for the interaction between warfarin and HSA: the effect of sulphisoxazole on these values.

Binding constants were derived from the data presented in Figure 4.3 with the aid of the NKFIT program.

Sulphisoxazole Concn. x 10^{-5}M	n_1	k_1 x $10^5 M^{-1}$	n_2	k_2 x $10^5 M^{-1}$
0.0	0.84	5.34	1.06	0.26
9.8	0.92	1.51	1.06	0.20
48.8	0.85	0.39	1.20	0.09

is therefore a tentative one, and is only reliable within the limits of the two-site Scatchard equation.

It is important to record that during the course of this work the observed fluorescence intensity was shown to be independent of the order in which warfarin and phenylbutazone were added to the albumin. The most obvious, and the most reasonable explanation must be that the binding of these ligands to HSA is totally reversible.

Like phenylbutazone, sulphisoxazole has a very noticeable effect on the binding of warfarin to HSA. Figure 4.3 illustrates this for two concentrations of sulphisoxazole, in experiments where the probe concentration is varied approximately two hundred-fold. Although the quantities of competitor drug are larger in this case, sulphisoxazole evidently resembles phenylbutazone in that it, too, produces a downward displacement of the warfarin binding curve.

The degree to which sulphisoxazole displaces warfarin from albumin binding is reflected in the binding constants presented in Table 4.5. These values were determined with the aid of the NKFIT program and clearly provide an excellent fit to the experimental curves of Figure 4.3. In the presence of this sulphonamide drug, the values of n_1 and n_2 are sufficiently close to those obtained with no competitor to suggest that within the limits of the binding model, warfarin and sulphisoxazole compete for identical sites on human serum albumin. Furthermore, while the undoubted reduction in k_1 demonstrates a marked increase in the affinity of HSA to bind warfarin at the primary, high affinity site, it would appear from the values of k_2 that sulphisoxazole also competes, albeit less avidly, for secondary binding sites on albumin.

Four other sulphonamide drugs were examined for their ability to displace warfarin from its albumin binding sites. According to the Scatchard plots of Figure 4.4, sulphisomidine and suphamerazine have only a very small effect on the binding of warfarin to human serum albumin. Likewise, the results presented in Figure 4.5 suggest that sulphapyridine and sulphadiázine bind very weakly, if at all, to the warfarin sites on albumin.

Using data from the experiments involving sulphapyridine and sulphadiazine, the apparent association constants for the interaction between warfarin and albumin were derived with the aid of the NKFIT program. As shown in Table 4.6 these values are very similar to those obtained in the absence of competitor and confirm that sulphapyridine and sulphadiazine have only minimal effects on the binding of warfarin to HSA.

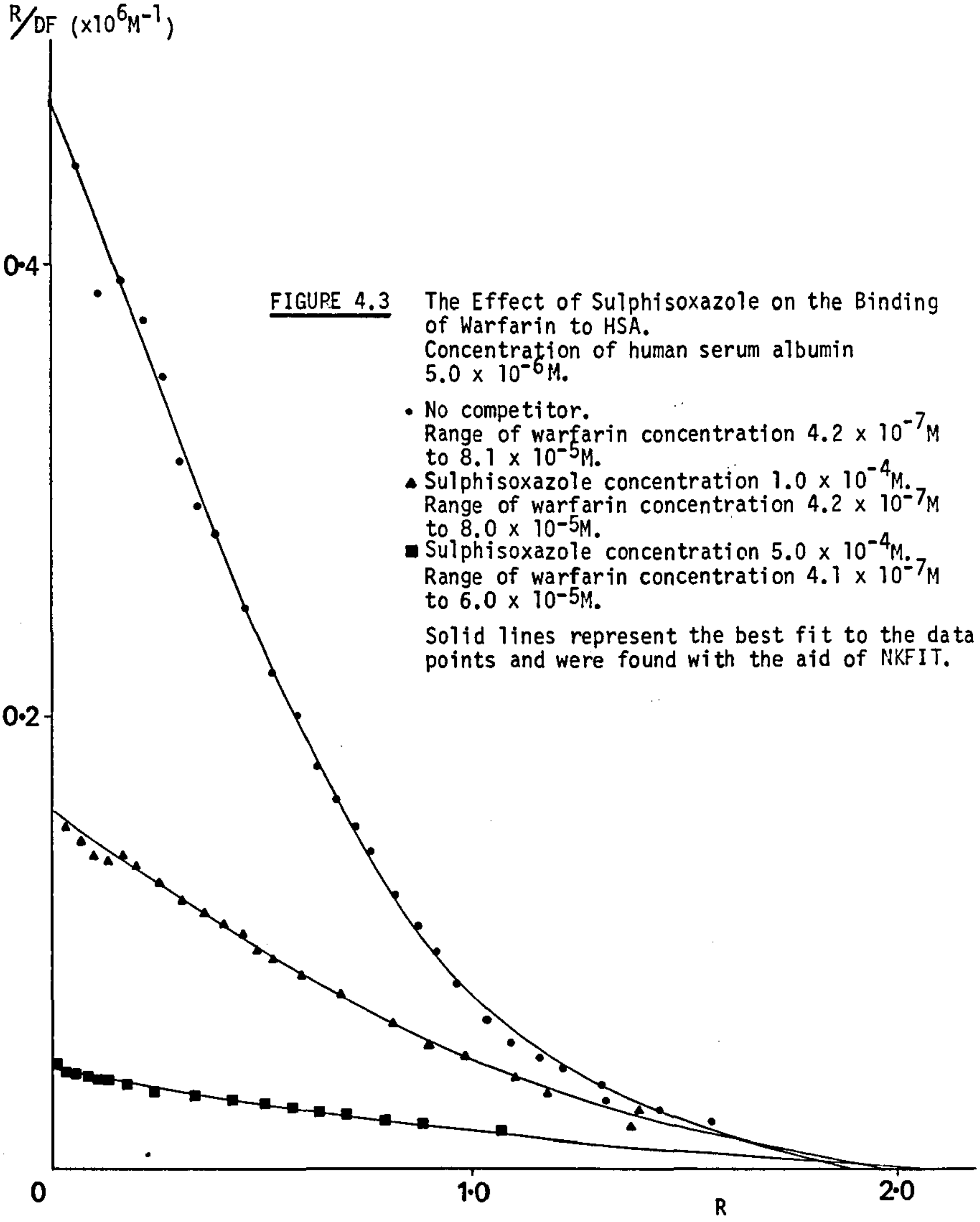

FIGURE 4.3 The Effect of Sulphisoxazole on the Binding of Warfarin to HSA.
Concentration of human serum albumin 5.0×10^{-6}M.

- ● No competitor.
Range of warfarin concentration 4.2×10^{-7}M to 8.1×10^{-5}M.
- ▲ Sulphisoxazole concentration 1.0×10^{-4}M.
Range of warfarin concentration 4.2×10^{-7}M to 8.0×10^{-5}M.
- ■ Sulphisoxazole concentration 5.0×10^{-4}M.
Range of warfarin concentration 4.1×10^{-7}M to 6.0×10^{-5}M.

Solid lines represent the best fit to the data points and were found with the aid of NKFIT.

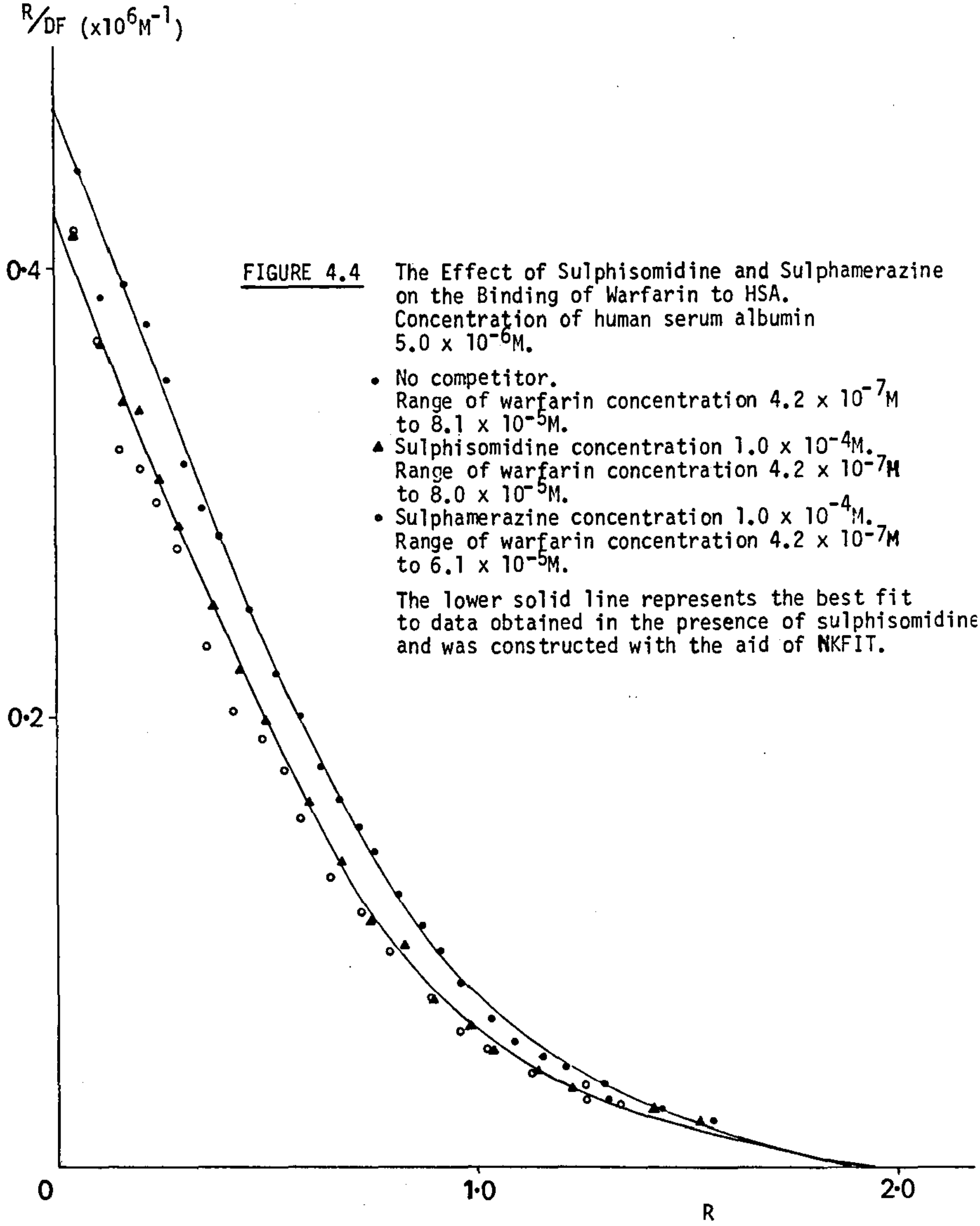

FIGURE 4.4 The Effect of Sulphisomidine and Sulphamerazine on the Binding of Warfarin to HSA. Concentration of human serum albumin 5.0×10^{-6}M.

- • No competitor. Range of warfarin concentration 4.2×10^{-7}M to 8.1×10^{-5}M.
- ▲ Sulphisomidine concentration 1.0×10^{-4}M. Range of warfarin concentration 4.2×10^{-7}M to 8.0×10^{-5}M.
- ○ Sulphamerazine concentration 1.0×10^{-4}M. Range of warfarin concentration 4.2×10^{-7}M to 6.1×10^{-5}M.

The lower solid line represents the best fit to data obtained in the presence of sulphisomidine and was constructed with the aid of NKFIT.

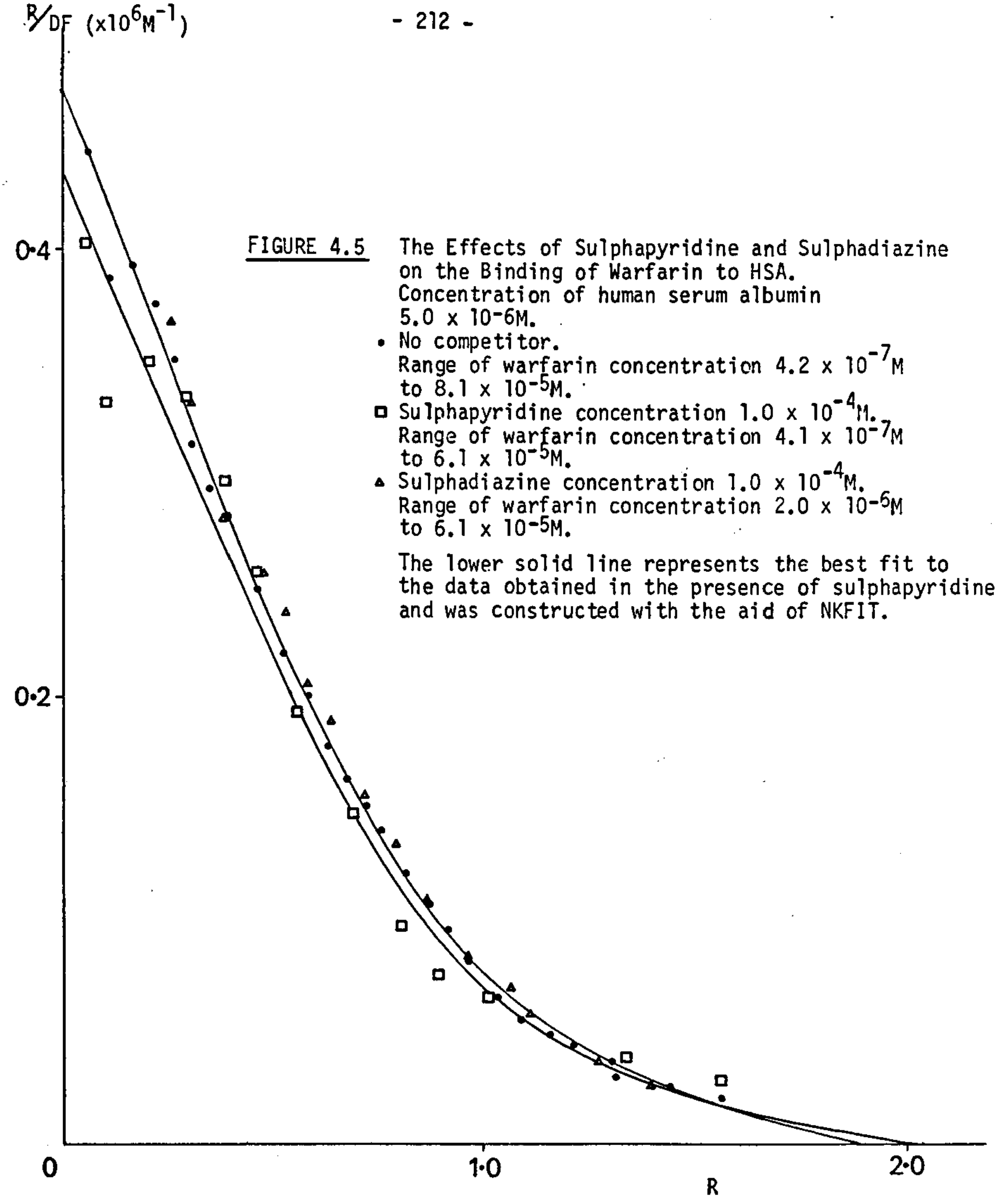

FIGURE 4.5 The Effects of Sulphapyridine and Sulphadiazine on the Binding of Warfarin to HSA. Concentration of human serum albumin 5.0 x 10-6M.

- • No competitor. Range of warfarin concentration 4.2 x 10^{-7}M to 8.1 x 10^{-5}M.
- □ Sulphapyridine concentration 1.0 x 10^{-4}M. Range of warfarin concentration 4.1 x 10^{-7}M to 6.1 x 10^{-5}M.
- ▲ Sulphadiazine concentration 1.0 x 10^{-4}M. Range of warfarin concentration 2.0 x 10^{-6}M to 6.1 x 10^{-5}M.

The lower solid line represents the best fit to the data obtained in the presence of sulphapyridine and was constructed with the aid of NKFIT.

TABLE 4.6

Estimated binding constants for the interaction between warfarin and HSA: the effect of sulphisomidine and sulphapyridine on these values.

Binding constants were derived from the data presented in Figures 4.4 and 4.5 with the aid of the NKFIT program.

Drug/Concentration	n_1	k_1 $\times 10^5 M^{-1}$	n_2	k_2 $\times 10^5 M^{-1}$
No Competitor	0.84	5.34	1.06	0.26
1.0×10^{-4}M sulphisomidine	0.81	4.92	1.13	0.20
1.0×10^{4}M sulphapyridine	0.88	4.67	1.15	0.18

So far results describing the inhibitory effects of competitor drugs on the binding of warfarin to HSA have been summarized in terms of the ability of each competitor to reduce the association constants of the probe-protein interaction. Now in theory, it should be possible to process the same experimental results but this time to determine association constants for the competitors. Klotz et al (1948) have published equations to describe the competition between two ligands for identical protein binding sites. Using this paper the following relationship was derived:

$$k_b = \frac{n\,[P]\,ka\,[DF] - ka\,[DF]\,[DB] - [DB]}{[C]\;ka[DF] - n\,[P]\;ka[DF] + ka[DF]\,[DB] + [DB]} \times \frac{ka\,[DF]}{[DB]} \qquad (4.2)$$

where k_b is the association constant for the competitor; ka is the association constant for the probe; [DF] and [DB] are concentrations of free and bound probe, respectively; [P] is the total protein concentration; [C] the total competitor concentration; and n is the number of binding sites.

The model used by Klotz et al (1948) assumes that the two ligands compete for a single class of binding sites. Since warfarin binds to at least two different sites on HSA, the Klotz model is too simple to provide a full description of its displacement by another ligand. However, at low probe to protein ratios most of the warfarin molecules will bind to the primary, high affinity site on albumin. Under these conditions the assumptions inherent in Equation 4.2 may be acceptable.

An approximate association constant was obtained for phenylbutazone using data from Table 4.3. Only estimates of bound and free warfarin obtained at low total probe concentrations were considered. When these results were fitted in to Equation 4.2 along with the appropriated binding constants, k_b turned out to be about 10^6 M^{-1}. Data from Figure 4.3 was processed in a similar manner to yield a measure of the affinity of sulphisoxazole for the major warfarin binding site on albumin. k_b for this drug was approximately 10^4 M^{-1}.

Although the estimated association constant for phenylbutazone may be slightly high (Elbary et al, 1982), the observation that it has a greater affinity than warfarin for the same class of sites on HSA agrees with the work of Solomon et al (1968). The association constant obtained for sulphisoxazole is also comparable with the literature. Hsu et al (1974), for example.

4.3 A Rapid Method for the Characterization of Drug Binding Sites on Albumin and in Whole Serum

Producing complete binding curves in the assessment of competitive binding phenomena is clearly a very useful exercise, but it can be rather time-consuming. To test large numbers of drugs for binding specific sites on albumin, more rapid procedures were devised. In their simplest form, these procedures involved the addition of potential competitors to a sample containing fluorescent probe and HSA. A reduction in the intensity of the recorded signal was taken as evidence for the competitive displacement of bound fluorescent probe.

Of course, to allow for a fuller characterization of the displacement interactions, it was necessary to have stricter control over the conditions of the experiments. Thus, the albumin concentration was normally fixed at about 5 x 10^{-6}M and the quantity of fluorescent probe was kept low so that binding was mainly to high affinity sites. After each addition of competitor, the fluorescence was measured with monochromators set at the excitation and emission wavelengths of the bound probe. Standard procedures were employed to account for light absorption by the competitor, and when more detailed information was required, the results were analysed with the aid of the FLUORB computer program. Processing the data in this way made it possible to report the quantity of fluorescent probe displaced after each addition of competitor.

The results presented in Table 4.7 demonstrate the ability of a number of ligands to displace warfarin from its binding sites on HSA. They are expressed graphically in Figures 4.6 and 4.7 over two ranges of competitor concentration.

Although the experimental points lie on smooth curves, the shape of these curves varies markedly from one competitor to the next. For example, Figure 4.6 shows that warfarin is very readily displaced from its binding sites by phenylbutazone. On the other hand, of the three sulphonamides examined, only sulphisoxazole appears to produce a significant reduction in the bound probe fraction. These observations agree with those of the previous section (Figures 4.2 to 4.5). Figure 4.6 also demonstrates that while flufenamic acid competes very strongly for warfarin binding sites and CPMP very weakly, ethacrynic acid has an affinity which is intermediate.

The results in Figure 4.7 have been extended to include higher concentrations of the competitors. They help to illustrate the huge variations in the gradients of the experimental curves and so emphasize the

TABLE 4.7

Results illustrating the competitive displacement of warfarin from HSA by increasing concentrations of a number of drugs. DC and DB are the concentrations of bound and free fluorescent probe, respectively. The percentage of fluorescent probe bound to HSA is given by %B = DB/DC x 100%. Results from experimental fluorescence titrations were processed using the FLUORB computer program. The concentration of HSA was approximately 4.7 x 10^{-6}M in all samples.

(a) Phenylbutazone

Phenylbutazone Concn x10^{-6}M	DC x10^{-6}M	DB x10^{-6}M	%B
0.00	0.833	0.556	66.8
0.83	0.832	0.493	59.2
1.67	0.831	0.431	51.9
3.33	0.830	0.333	40.1
6.64	0.827	0.211	25.5
16.43	0.819	0.092	11.2
32.32	0.806	0.060	7.5
47.71	0.793	0.043	5.4

(b) Sulphisoxazole

Sulphisoxazole Concn x10^{-6}M	DC x10^{-6}M	DB x10^{-6}M	%B
0.00	0.833	0.581	69.8
4.17	0.832	0.547	65.7
8.33	0.831	0.527	63.4
16.64	0.830	0.480	57.9
41.40	0.826	0.382	46.3
82.11	0.819	0.289	35.3
161.6	0.806	0.193	24.0

TABLE 4.7 (Contd)

(c) Sulphamerazine

Sulphamerazme Concn x10^{-6}M	DC x10^{-6}M	DB x10^{-6}M	%B
0.00	0.840	0.545	64.9
16.68	0.838	0.529	63.1
33.31	0.837	0.505	60.4
66.39	0.834	0.482	57.8
164.4	0.826	0.439	53.2
323.4	0.812	0.387	47.6

(d) Sulphisomidine

Sulphisomidine Concn x10^{-6}M	DC x10^{-6}M	DB x10^{-6}M	%B
0.00	0.840	0.588	70.0
16.67	0.838	0.568	67.7
33.44	0.837	0.552	65.9
66.66	0.834	0.542	65.0
165.0	0.826	0.512	62.0
324.7	0.812	0.477	58.7

(e) Flufenamic Acid

Flufenamic Acid Concn x10^{-6}M	DC x10^{-6}M	DB x10^{-6}M	%B
0.00	0.840	0.571	68.0
1.67	0.838	0.537	64.1
3.33	0.837	0.502	60.0
6.64	0.834	0.393	47.1
16.43	0.826	0.161	19.4
32.32	0.812	0.048	5.9

TABLE 4.7 (Contd)

(f) Ethacrynic Acid

Ethacrynic Acid Concn $\times 10^{-6}$M	DC $\times 10^{-6}$M	DB $\times 10^{-6}$M	%B
0.00	0.834	0.529	63.5
1.67	0.833	0.491	59.0
3.34	0.831	0.472	56.7
6.65	0.828	0.438	52.8
16.47	0.820	0.361	44.0
32.40	0.807	0.261	32.3

(g) 2-(p-chlorophenoxy)-2 methyl proprionic acid (CPMP)

CPMP Concentration $\times 10^{-6}$M	DC $\times 10^{-6}$M	DB $\times 10^{-6}$M	%B
0.00	0.834	0.589	70.6
3.35	0.831	0.589	70.8
16.52	0.820	0.554	67.5
32.50	0.807	0.509	63.1

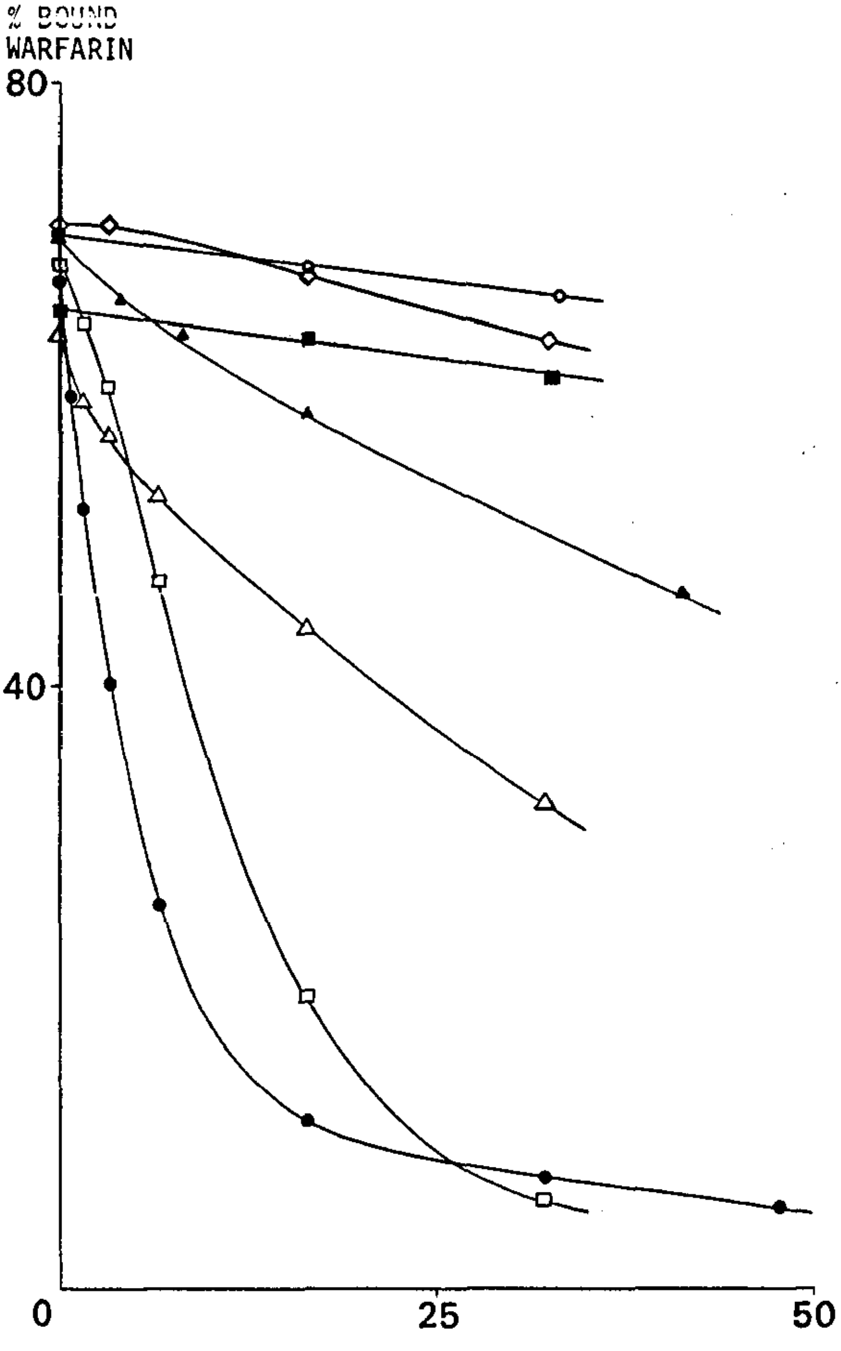

FIGURE 4.6 The Effect of a Number of Drugs on the Degree of Binding of Warfarin to HSA.
● Phenylbutazone, ▲ Sulphisoxazole, ○ Sulphisomidine,
□ Flufenamic Acid, △ Ethacrynic Acid, ◇ CPMP, ■ Sulphamerazine.

Initial total concentrations of warfarin were 8.3 x 10^{-7}M.

The concentration of human serum albumin was 4.8 x 10^{-6}M.

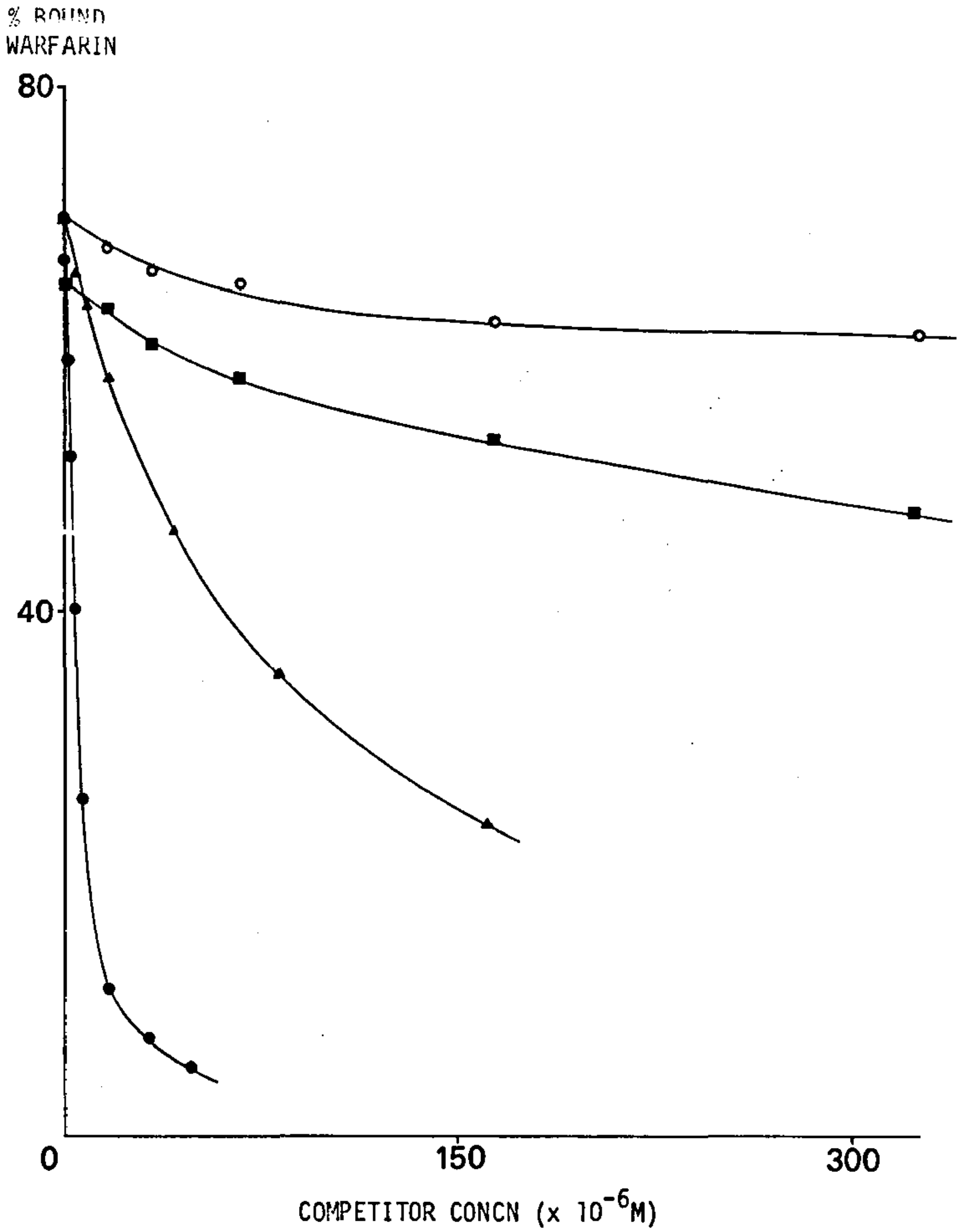

FIGURE 4.7 The Effect of a Number of Drugs on the Degree of Binding of Warfarin to HSA over an Extended Concentration Range.

● Phenylbutazone, ▲ Sulphisoxazole, ■ Sulphamerazine, ○ Sulphisomidine.

Initial total concentrations of warfarin were 8.3 x 10^{-7}M. The concentration of human serum albumin was 4.8 x 10^{-6}M.

underlying differences in the abilities of the various competitors to displace bound fluorescent probe. The initial gradients of the curves for phenylbutazone and sulphisomidine differ by a factor of sixty five. Continuing the results to include higher concentrations of the competitors also allows for a better classification of ligands which bind only weakly to the probe binding sites. Thus the results in Figure 4.7 suggest that sulphamerazine has a slightly higher affinity for the warfarin binding sites than does sulphisomidine.

Unfortunately, the displacement of warfarin by ANS was not susceptible to assessment by the normal fluorimetric procedure. Although a marked reduction in the sample fluorescence at 375nm accompanied the addition of ANS to a solution containing warfarin and albumin, the decrease in the recorded signal could not be related directly to a competitive displacement interaction. The problem appeared to lie with the occurrence of resonance energy transfer from warfarin to ANS. There were two reasons for supposing this to be so. Firstly, both fluorescent probes had been shown to bind strongly to HSA (see Chapter 3). When attached to the albumin molecule it is highly likely that their mean separation would be within the range normally available to the energy transfer process. The maximum distance over which energy transfer can take place is generally accepted to be about 70Å (Förster, 1951).

The second important point to note was the fact that the fluorescence emission spectrum of warfarin overlaps the excitation spectrum of ANS. This may be appreciated from a study of the spectrum shown in Section 3.1. Indeed, the two bands appear to have their maxima at virtually the same wavelength. This clearly makes for a very efficient transfer of energy.

An experiment was performed to confirm that the observed effects were the result of resonance energy transfer rather than displacement phenomena. A sample solution containing warfarin and HSA was prepared. As usual, the bound probe fluorescence was excited at 320nm. The addition of ANS to this sample produced an obvious decrease in the warfarin fluorescence centred at 385nm (see Figure 4.8). Tests showed that this decrease was far too large to be the result of a simple inner-filter mechanism. Furthermore, when the same wavelength of excitation was used and warfarin added to a solution containing ANS and HSA, there was a noticeable increase in the intensity of the ANS fluorescence at 475nm. The effect is shown in the corrected spectra of Figure 4.9. Enhancement of the ANS fluorescence could not be demonstrated in the absence of HSA and must have been due to a short range energy transfer process.

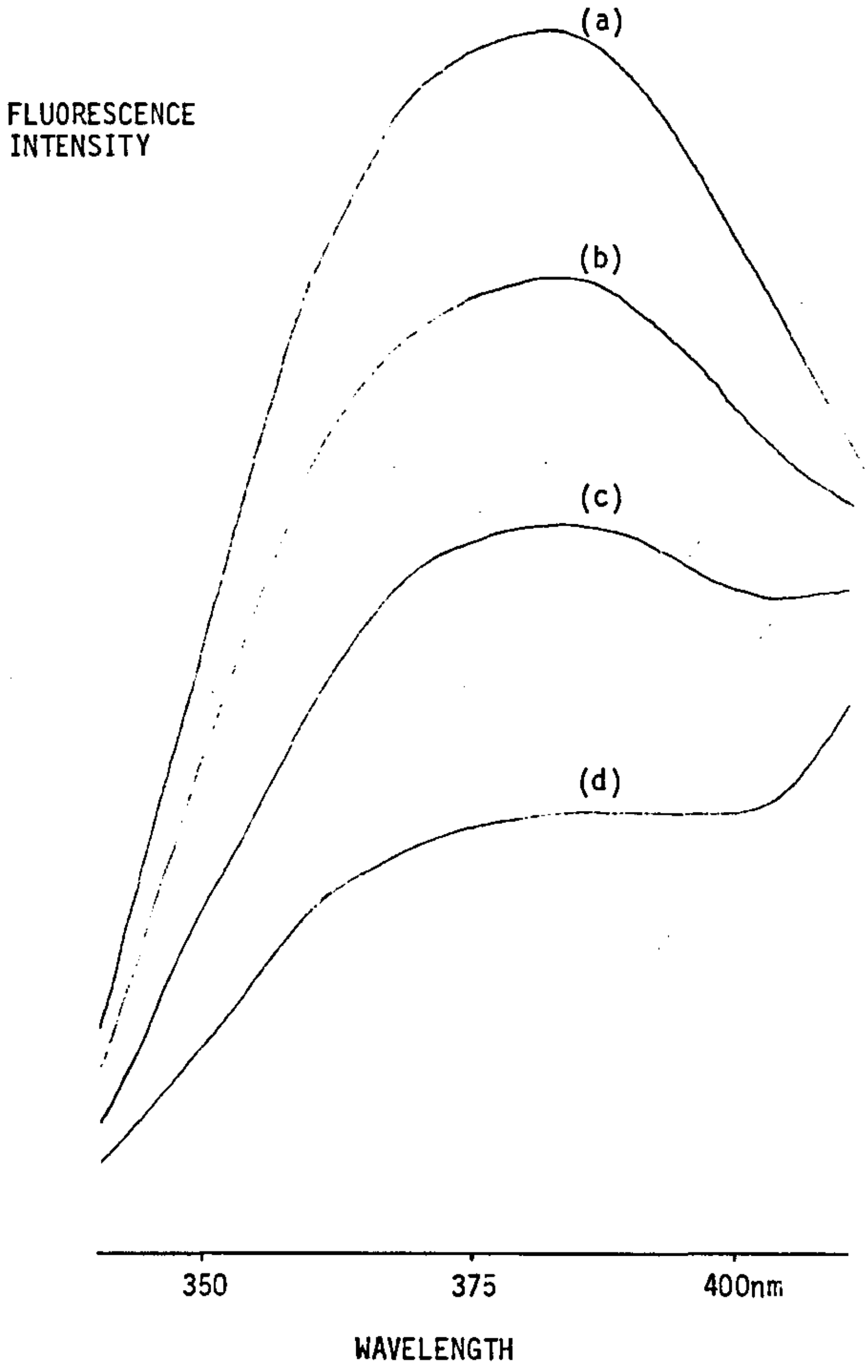

FIGURE 4.8 The Decrease in the Fluorescence of Albumin-Bound Warfarin on Addition of ANS.

Corrected emission spectra recorded with an excitation wavelength of 320nm. Warfarin concentration 1.33 x 10^{-6}M, HSA concentration 4.31 x 10^{-6}M.

(a) No ANS
(b) 1.69 x 10^{-6}M ANS
(c) 3.37 x 10^{-6}M ANS
(d) 6.72 x 10^{-6}M ANS

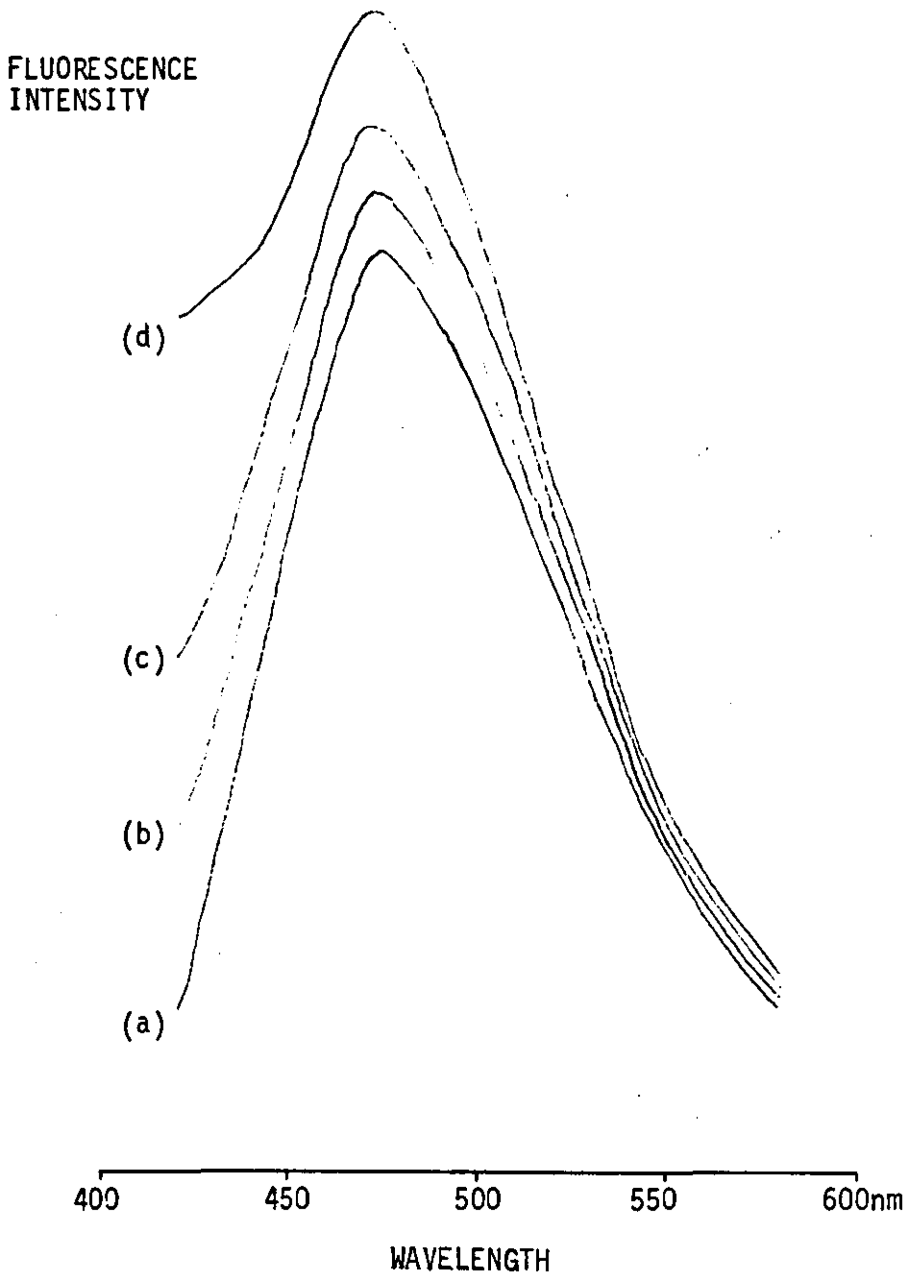

FIGURE 4.9 The Increase in the Fluorescence of Albumin-Bound ANS on Addition of Warfarin.

Corrected emission spectra recorded with an excitation wavelength of 320nm. The enhanced ANS fluorescence centred at 475nm is due to resonance energy transfer with warfarin as donor. ANS concentration 6.77×10^{-7}M, HSA concentration 4.31×10^{-6}M.

(a) No warfarin
(b) 3.34×10^{-7}M warfarin
(c) 6.67×10^{-7}M warfarin
(d) 1.33×10^{-6}M warfarin

Since the excitation and emission spectra of ANS are centred at longer wavelengths than those of warfarin, studies concerned with the displacement of ANS were not complicated by inner-filter or energy transfer processes.

A number of drugs were examined for their ability to influence the binding of ANS to albumin. The effects of increasing concentrations of several of these potential competitors are shown in Figure 4.10. CPMP, ethacrynic acid and flufenamic acid in particular compete quite strongly with ANS. Phenylbutazone displaces very little fluorescent probe and warfarin practically none at all. In fact the last result suggests that ANS and warfarin bind to completely different sites on the albumin molecule. To emphasize the point, the primary binding sites of warfarin and ANS were labelled sites I and II respectively. This is in line with the notation of Sudlow et al (1975).

An inspection of the data in Figures 4.6 and 4.10 reveals that flufenamic acid is able to displace both ANS and warfarin from their albumin binding sites. To a slightly lesser degree this is also true of ethacrynic acid. A further set of experiments were devised to test the contention that these two ligands compete for both ANS and warfarin binding sites on albumin.

In these experiments two different ligands were introduced into a sample containing HSA and ANS. The first was one which bound preferentially to site I on albumin so even after adding a large quantity of it to the sample, only a very small proportion of the fluorescent probe would be displaced from site II. The second ligand was supposed to bind to both sites I and II. As such, it was expected to compete with ANS at site II and with the first ligand at site I.

From measurements of the fluorescence intensity at 470nm it was possible to calculate the concentrations of bound and unbound probe at each stage in the procedure. Results for one experiments are presented in Table 4.8. They show the degree to which ANS was displaced when flufenamic acid was added to a sample containing HSA, ANS and sulphisoxazole.

Table 4.9 is a summary of the results of several experiments of this kind. As demonstrated on previous occasions it is clear that flufenamic acid displaces ANS from albumin binding sites. However, Table 4.9 also illustrates a definite enhancement of this effect in the presence of a number of drugs.

Intensification of the competition between flufenamic acid and ANS may be explained in a fairly simple manner. The drugs listed in Table 4.9 appear to bind to site I on albumin (see Figure 4.6). So, supposedly, does

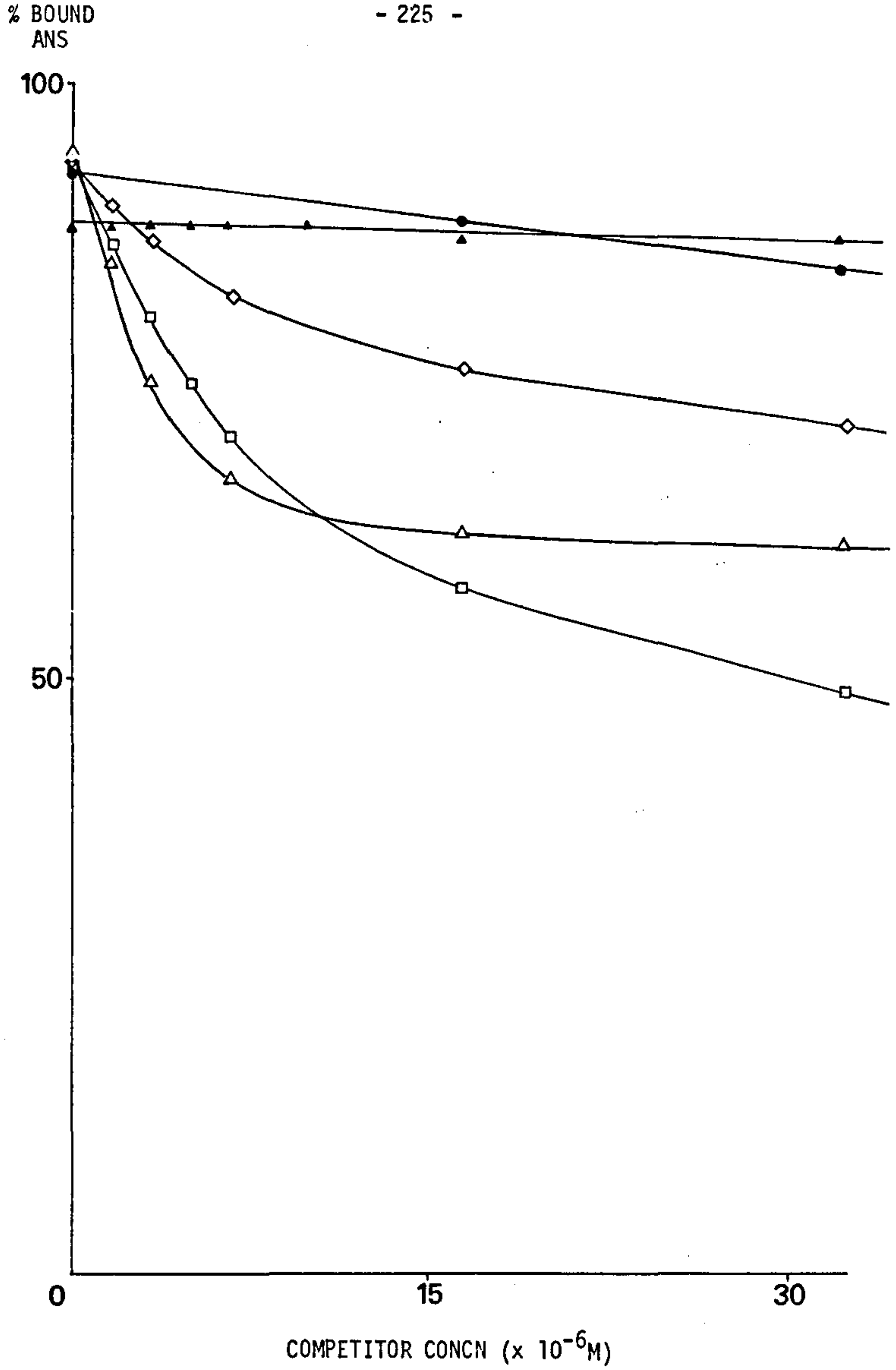

FIGURE 4.10 The Effect of a Number of Drugs on the Degree of Binding of ANS to HSA.

▲ Warfarin, □ Flufenamic Acid, ● Phenylbutazone, △ Ethacrynic Acid, ◇ CPMP.

Initial total concentrations of ANS were 3.3×10^{-6}M. The concentration of human serum albumin was 4.8×10^{-6}M.

TABLE 4.8

The displacement of ANS from HSA by flufenamic acid in the presence of sulphisoxazole. The bound probe fluorescence was measured with excitation and emission monochromators set at 375nm and 470nm, respectively. The albumin concentration was 5.0 x 10^{-6}M. Results were analysed using FLUORB. DC, DB and DF are the concentrations of total, bound and unbound ANS. % displacement is the percentage of bound fluorescent probe displaced on addition of flufenamic acid to a sample of ANS, HSA and sulphisoxazole.

DC x10^{-6}M	DB x10^{-6}M	DF x10^{-6}M	Sulphisoxazole Concentration x10^{-4}M	Flufenamic Acid Concentration x10^{-6}M	% Displacement
3.35	3.31	0.04	0.04	0.00	-
3.29	3.18	0.11	1.64	0.00	-
3.29	2.75	0.54	1.64	1.64	13.76
3.28	2.38	0.90	1.63	3.27	24.90

TABLE 4.9

The displacement of ANS from HSA by flufenamic acid in the presence of a number of ligands. Experimental conditions and nomenclature as in Table 4.8.

RATIO is defined as,

$$\frac{\text{percentage of bound ANS displaced by flufenamic acid in the presence of the named second drug}}{\text{percentage of bound ANS displaced by the same concentration of flufenamic acid only}}$$

Concn. of flufenamic acid x 10^{-6}M	Second Drug	Concentration of Second Drug x 10^{-4}M	% Displacement	RATIO
1.66	-	-	7.23	1.00
1.64	SM	1.64	7.95	1.10
1.64	SMZ	1.64	8.75	1.21
1.64	SF	1.64	13.76	1.90
1.65	PB	1.64	14.23	1.97
1.61	WF	1.61	16.06	2.22
3.32	-	-	13.68	1.00
3.28	SM	1.64	15.87	1.16
3.28	SMZ	1.63	17.25	1.26
3.27	SF	1.63	24.90	1.82
3.28	PB	1.64	25.08	1.83
3.23	WF	1.61	30.19	2.21

SM - sulphisomidine SMZ - sulphamerazine SF - sulphisoxazole
PB - phenylbutazone WF - warfarin

flufenamic acid. Competition for binding between flufenamic acid and one of the other drugs will result in the mutual displacement of both ligands to a degree which depends firstly on their relative binding affinities for this class of sites and secondly on their concentrations. Hence, in the presence of a drug which binds to site I, the resultant shift in equilibrium means that more flufenamic acid is free to compete with the ANS bound at site II. The concentration of the bound fluorescent probe is then diminished still further due to the enhanced competitive interaction. Since this increase in the capacity of flufenamic acid to displace ANS depends in the first instance on the ability of the site I drug to compete with flufenamic acid, those drugs with the highest site I binding affinities may be expected to produce the largest elevation in the concentration of unbound probe. From Table 4.9 this is seen to be so. The drugs, ranked in decreasing order of their ability to affect the binding of ANS to HSA in the presence of flufenamic acid, are warfarin > phenylbutazone > sulphisoxazole >> sulphamerazine > sulphisomidine. This ranking reflects the site I binding strengths of these ligands as demonstrated by their tendency to displace warfarin from albumin (Figures 4.6 and 4.7).

Although it binds very avidly to site I, mediation of phenylbutazone in the displacement of ANS by flufenamic acid appears to be somewhat less than expected. This is probably due to the fact that phenylbutazone can also bind to site II albeit very weakly (see Figure 4.10). Competition between phenylbutazone and flufenamic acid at both site I and II would mean that more complicated equilibria prevail with this combination of drugs than with the others in Table 4.9. Nonetheless, the results of these experiments are unequivocal and are consistent with binding of flufenamic acid to both sites I and II.

The displacement processes involving flufenamic acid, ANS and the other ligands were reversible. That is, for a fixed total concentration of ANS, the amount which remained bound to albumin was independent of the order in which the other reagents were added.

Competitive binding involving ANS and ethacynic acid was also examined in more detail. The results in Table 4.10 show how the presence of warfarin and sulphisomidine influence the displacement of ANS by ehtacrynic acid. Intensification of the displacement effect was obviously much greater with warfarin than with sulphisomidine. This was so for each of three concentrations of ethacrynic acid and further emphasized the difference in the affinities of the drugs for site I. The results were also consistent with binding of ethacrynic acid to both site I and site II on albumin.

TABLE 4.10

The displacement of ANS from HSA by ethacrynic acid in the presence of sulphisomidine and warfarin. The albumin concentration was 4.9 x 10^{-6}M.

% displacement is the percentage of bound fluorescent probe displaced on addition of ethacrynic acid to a sample of ANS, HSA and second drug.

RATIO is defined as,

$$\frac{\text{percentage of bound ANS displaced by ethacrynic acid in the presence of the named second drug}}{\text{percentage of bound ANS displaced by the same concentration of ethacrynic acid}}$$

Concn of ethacrynic acid, x 10^{-6}M	Second Drug	Concentration of Second Drug, x 10^{-4}M	% Displacement	RATIO
1.66	-	-	11.11	1.00
1.64	SM	1.64	11.62	1.04
1.64	WF	1.64	13.01	1.17
3.32	-	-	20.72	1.00
3.27	SM	1.64	20.44	0.99
3.27	WF	1.63	26.12	1.26
16.40	-	-	32.64	1.00
16.14	SM	1.62	32.23	0.99
16.14	WF	1.61	43.30	1.32

SM - sulphisomidine

WF - warfarin

A comparison of Tables 4.9 and 4.10 shows that similar concentrations of warfarin and sulphisomidine have a greater influence on the displacement of ANS by flufenamic acid than they have on the displacement of ANS by ethacrynic acid. This is a consequence of the different affinities of ethacrynic acid and flufenamic acid for sites I and II.

So far, only the displacement of fluorescent probes from binding sites on HSA has been reported. However, experiments were also performed using whole serum. 10ml volumes of blood were taken from three healthy adult male volunteers. The blood was allowed to stand at room temperature for several hours until clotting was complete. The clots were removed and the samples spun at 4000rpm for 30 minutes. The supernatants were decanted and centrifuged again. 2ml aliquots of the clear sera were stored at -20°C.

Small volumes of serum (sample 1) were thawed and diluted 100-fold in Tris/HCl buffer 0.1M pH 7.40. The displacement of ANS from its serum binding sites was investigated by monitoring the probe fluorescence in the absence and in the presence of various competitor drugs. An ANS concentration of 5 x 10^{-6}M was used in these studies. The reagent concentrations were such that the serum background fluorescence was extremely small - just 0.14% of the signal recorded in the absence of competitor. Some results are presented in Table 4.11 (a). The low serum fluorescence contributed to the attainment of a high precision. Very similar results were obtained when a second serum sample was used (see Table 4.11 (b)).

By way of a comparision, Table 4.12 shows the extent to which ANS is displaced from albumin, rather than from serum binding sites. With the concentration of albumin set at 6.0 x 10^{-6}M, the results suggest that flufenamic acid and ethacrynic acid displace ANS slightly more readily in this medium than in diluted whole serum. However, the HSA concentration in serum sample 1 was determined by the standard method of electroimmunodiffusion and found to be 6.72 x 10^{-6}M, that is, 44.6g/l. This figure lies within the generally accepted 'normal' range of 35-50g/l (Peters, 1977). When values of bound probe concentration/HSA concentration were calculated for ANS in the presence of flufenamic acid and ethacrynic acid in the diluted serum and in the albumin solution, the earlier discrepancies disappeared. This was not so for sulphisomidine, though. While it may compete only very weakly with ANS, sulphisomidine appears to displace a significantly larger proportion of the bound probe in the diluted serum than in a solution containing a similar concentration of albumin.

Experiments were also performed to examine the displacement of warfarin from its serum binding sites. As before, a 100-fold dilution of

TABLE 4.11

(a) Displacement of ANS in human serum by a number of ligands. Serum sample I was diluted 100-fold in 0.1M Tris/HCl pH 7.40. The ANS concentration was 5.0 x 10^{-6}M. Figures in brackets (s) were calculated from

$$s = \sqrt{s_1^2 + s_2^2}$$

where s_1 and s_2 refer to the standard deviations of the fluorescence intensities obtained in the prescence and in the absence of competitor.

Drug	Concentration x10^{-5}M	% Displacement of bound ANS
Flufanamic Acid	5.0	40.22 (0.16)
Flufenamic Acid	5.0	41.60 (0.21)
Ethacrynic Acid	5.0	26.84 (0.14)
Ethacrynic Acid	5.0	28.71 (0.21)
CPMP	5.0	17.50 (0.15)
Warfarin	5.0	7.58 (0.21)
Sulphisoxazole	5.0	2.84 (0.12)
Sulphisomidine	5.0	2.53 (0.12)
Sulphisomidine	5.0	2.58 (0.23)

(b) Displacement of ANS in human serum. Serum sample II was diluted 100-fold in 0.1M Tris/HCl pH 7.40. The ANS concentration was 5.0 x 10^{-6}M.

Drug	Concentration x10^{-5}M	% Displacement of bound ANS
Flufenamic Acid	5.0	40.74 (0.12)
Ethacrynic Acid	5.0	28.86 (0.20)
Sulphisoxazole	5.0	1.73 (0.20)

TABLE 4.12

Displacement of ANS from albumin binding sites. The concnetrations of HSA and ANS were 6.0 x 10^{-6}M and 5.0 x 10^{-6}M, respectively. Figures in brackets were calculated from the standard deviations of the fluorescence intensities obtained in the prescence and in the absence of competitor.

Drug	Concentration x10^{-5}M	% Displacement of bound ANS
Flufenamic Acid	5.0	44.04 (0.20)
Ethacrynic Acid	5.0	33.11 (0.11)
Sulphisomidine	5.0	0.75 (0.14)

TABLE 4.13

Displacement of warfarin from HSA and serum binding sites. Figures in brackets were derived from the standard deviations of the fluorescence intensities obtained in the presence and in the absence of competitor. Serum sample I was diluted 100-fold in 0.1M Tris/HCl pH 7.40. The HSA concentration was 6.7 x 10^{-6}M.

Drug	Concentration x10^{-5}M	% Displacement of bound warfarin	
		Serum Sample I	HSA
Sulphamerazine	1.0	6.16 (0.87)	5.71 (0.53)
CPMP	1.0	6.28 (0.59)	6.02 (0.50)
Sulphisomidine	1.0	11.46 (0.66)	5.55 (0.53)
Sulphisoxazole	1.0	7.39 (0.64)	8.26 (0.59)
Ethacrynic Acid	1.0	29.26 (0.62)	26.47 (0.52)
Flufenamic Acid	1.0	26.13 (0.65)	27.24 (0.96)
Phenylbutazone	1.0	60.78 (0.60)	55.96 (0.50)

serum sample 1 was employed and the results compared with those obtained in solutions of 6.7 x 10^{-6}M HSA. The serum background fluorescence was about 11% of the total signal observed in the absence of competitor. The corresponding figure for the albumin fluorescence was about 5.5%. Inner-filter effects were considered for each competitor drug and the normal allowances made. Except for flufenamic acid, the necessary corrections were very small - about 1%, or less.

An examination of the results in Table 4.13 shows that there is a good correlation between the ability of sulphamerazine, CPMP, sulphisoxazole, ethacrynic acid, flufenamic acid and phenylbutazone to displace warfarin from binding sites in human serum and in HSA preparations where the albumin concentrations are similar. However, under these experimental conditions sulphisomidine appears to displace twice as much warfarin in whole serum as it does in a solution of HSA.

4.4 Discussion of Methods and Results

Some general features of the procedures described in this chapter are worthy of further consideration. Positive aspects include the capacity to study binding over a wide range of ligand concentrations; the ability to examine the binding properties of non-fluorescent drugs which may be difficult to assay directly; and the potential to apply the methods to almost any ligand/fluorescent probe combination: these points are discussed separately in the following paragraphs. Possible limitations are covered later.

The binding of fluorescent probes to albumin was expressed most conveniently in the form of Scatchard plots. The ability to extend these plots over a wide range of probe concentrations is extremely important, particularly if the effect of adding potential competitors is to be assessed. Now the series of curves shown in Figures 4.2 and 4.3 were obtained in the presence of phenylbutazone and sulphisoxazole, respectively. The curves are clearly of a similar shape and tend towards common intercepts on the R axes. This concurrence is reflected in the corresponding values derived using the curve-fitting procedure. Unfortunately, in the past many studies have not been extended to low values of R /DF. Aarons et al (1979) have shown that this practice can lead to an apparent decrease in the values of the intercepts on the R axis in the presence of increasing concentrations of competitor. The problem is particularly severe if the Scatchard plots are curved when the effect may be wrongly assigned to a decrease in the number of binding sites available to the fluorescent probe. Because the present method allows measurements to be taken at low as well as high R/DF values, it is much harder to misinterpret the results. Thus an inspection of Figures 4.2 and 4.3 immediately shows how phenylbutazone and sulphisoxazole compete strongly with warfarin for binding to albumin without reducing the number of potential sites per protein molecule.

The procedures used in this chapter take the form of competitive binding assays. As such, they allow the binding properties of ligands to be examined in terms of their ability to compete with fluorescent probes for specific sites on albumin. Now ligands which are capable of displacing bound fluorescent probe may be difficult to measure themselves. For example, if the ligand is a non-fluorescent drug, a direct assessment of its binding to HSA may be impossible. Displacement studies like those described above offer a convenient way of demonstrating the affinity of any ligand for particular sites on HSA.

Although results have been presented for only two fluorescent probes and a limited number of competitors, the methods could easily be used to study the binding and displacement of any number of fluorescent probes. The availability of several suitably designed fluorescent molecules could lead to a fuller characterization of drug binding sites on HSA. Eventually, it may even be possible to describe the structural features which are necessary for a ligand to bind to a particular region of the albumin molecule.

The scope of the method used to examine the influence of competitor drugs on probe binding curves was limited by two factors. Firstly, it would rarely allow for an accurate determination of the association constant of the competitor; very approximate values are the best that can be hoped for when more than one binding site is involved in the displacement interaction. This limitation is a general one and is not restricted to the present experimental approach. The second, perhaps less important limitation is the time required to produce full binding curves.

The procedures outlined in Section 4.3, on the other hand, made for a very rapid assessment of ligand binding. Furthermore, while the experiments discussed in Section 4.2 were concerned with the influence of fixed quantities of potential competitors on the association constants and binding curves of fluorescent probes, the displacement studies of Section 4.3 were more suited to an examination of the effects of varying the competitor concentration. The complimentary nature of the two approaches proved very useful when seeking clarification of the behaviour of certain drugs in binding albumin.

Before assessing the clinical significance of particular results, it is important to consider some problems associated with the extrapolation of data from in vitro binding experiments. Most of the non-methodological problems are related to the albumin used in the experiments - its source and fatty acid content, and the concentration at which it is employed.

Free, that is, unesterified fatty acid, the form in which fat is released from the adipose tissue storage deposits, is one of the most important metabolites transported by plasma albumin. Although the plasma free fatty acid concentration is quite variable, the molar ratio of free fatty acid to albumin is usually in the range 0.5 to 3.0 (see Miller et al, 1982. Not surprisingly, it has been known for many years that serum albumin preparations also contain variable amounts of lipid impurity (Kendal, 1941) and the bulk of this impurity appears to consist of free fatty acids. Recently, Birkett et al (1978) have examined the fatty acid content of 13 commercial HSA preparations. The figures varied from 0.03 to 9 moles of fatty acid per mole of albumin. According to the survey, the Hoechst preparations used in this work contains about 1.2 mole fatty acid/mole albumin.

As discussed in Chapter 1, there is ample evidence to suggest that free fatty acids can alter the binding of drugs and endogenous ligands to HSA. Indeed, there may even be a significant effect for changes in free fatty acid concentration within the physiological range (Spector et al, 1973). Because of this, some workers employ a charcoal treatment based on that of Chen (1967) to strip free fatty acids from albumin before commencing binding studies. While, if the procedure were widely adopted, it might be useful in allowing for a better cross-correlation of laboratory results, native HSA does contain bound fatty acids and it may be more appropriate to study ligand binding to the albumin molecule as found in vivo. With this point in mind, no attempt was made to produce defatted albumin. The strategy is probably further justified by the findings of Birkett, et al (1978) which suggests that the fatty acid content of the Hoechst material is within the limits normally found in plasma.

Chen and Koester (1980) examined the fluorescence characteristics of several commercial samples of HSA before and after treatment to remove bound impurities. The emission spectra of the untreated samples varied in shape, and the relative quantum yields differed widely. Dialysis and charcoal treatment minimized the spectral differences, although the quantum yields still varied. It appears that fluorescent impurities were present in some samples, while nonfluorescent quenching contaminants were present in others. The authors discuss various factors which may contribute to differences between commercial sources of HSA.

To make certain of obtaining consistent results, all experiments reported here were carried out using the same batch of albumin.

There are a number of accounts in the literature concerning the effects of albumin concentration on the results of binding experiments (Bowmer and Lindup, 1978; Boobis and Chignell, 1979). Suggestions why the apparent association constants and the number of binding sites should be dependent upon the experimental protein concentration have been put forward by these authors. The maintenance of fixed quantities of albumin throughout each series of experiments should have avoided these complications. Furthermore, because the albumin concentration was kept low, dimer-formation would have been minimized. This concentration-dependent polymerization process, which can undoubtedly affect the binding of ligands to HSA, has been investigated by Zini et al (1981).

Comparing the suitability of ANS and warfarin as fluorescent probes for albumin binding sites, it is clear that there are certain practical advantages to be gained by employing the former. Its fluorescence excitation and emission peaks are centred at longer wavelengths than those of warfarin and this renders it less susceptible to inner-filter effects arising in the ultraviolet region of the spectrum when potential competitors are added. On binding to albumin, the fluorescence of ANS is much more intense than that of warfarin, while in free solution it has a much lower quantum yield; measurement of the bound fraction in the presence of the free is much easier with ANS. Furthermore, because the ANS fluorescence is at a longer wavelength than the warfarin fluorescence, interference from serum constitutes is much reduced. Nevertheless, as well as being a fluorescent molecule, warfarin does have the advantage of being a commonly adminstered drug: displacement of this fluorescent probe is certain to involve an important drug binding site on albumin.

It is useful to consider the results obtained in this chapter in relation to what is already known about drug binding sites on albumin and to highlight those of possible clinical significance.

While results showed unequivocally that warfarin, phenylbutazone and sulphisoxazole compete avidly for similar sites on HSA, none of these ligands exhibited a tendency to displace ANS from albumin binding sites. The conclusion that warfarin and ANS bind different sites on HSA is in accord with that of Sudlow et al (1975).

Ranking drugs in order of their tendency to displace warfarin and ANS made it easier to appreciate the different affinities of these compounds for the two probe binding sites. Thus it became clear that the sulphonamide drugs competed with warfarin for sites on albumin but had no effect on the binding of ANS. Furthermore, the binding affinities of these antibacterial agents seemed to be highly dependent upon their side-chain substituents. Unfortunately, it is usually very difficult to relate binding affinities to specific structural features of the interacting molecules. Such rationalization normally requires information about the environment and geometry of the binding site on the macromolecule and needs to be supported by an extensive review of the binding of large numbers of ligands. Nevertheless there has been some speculation in the literature concerning the relationship between the structure of sulphonamide drugs and their binding to albumin.

Hsu et al (1974) investigated the binding of 11 sulphonamide derivatives to bovine serum albumin and showed that binding affinities were enhanced by hydrophobic side-chain substitutions and decreased by hydrophilic side-chain substitutions in the parent molecule. The same authors claimed that methyl groups on pyrimidine ring of certain sulphonamide drugs increased the phenomenon of protein binding. This effect has also been reported for the binding of sulphonamides to HSA (Agren et al, 1971). It is interesting to note that results in Figure 4.7 of this chapter suggest that sulphamerazine binds more strongly to HSA than does sulphadiazine; the only difference between the drugs is the methyl group on the pyrimidine ring of sulphamerazine.

Hsu et al (1974) also found that the methoxazole ring in oxacillins seems to give these compounds greater binding affinities than the group of penicillins at large. This substituent is also present in sulphisoxazole, and may account for its unusually high affinity for albumin binding sites (see Figure 4.3).

Evidence for the relative importance of the binding forces involved in sulphonamide-albumin interactions is still rather contradictory. While the opinion of Scholtan (1968) that most of the energy of sulphonamide-albumin binding is due to hydrophobic forces has received increasing support, other experimental evidence has suggested an important role for electrostatic interactions between the sulphonamide anion and positive charges on the protein surface.

Moriguichi et al (1968) for example, evaluated the binding of 19 sulphonamides to bovine serum albumin and showed that the binding correlated with the pKa of the N' nitrogen of the sulphonamides. They proposed that their findings gave support to the view of Klotz (1953) that electrostatic forces are dominant in the binding of such anions to serum albumin. Agren et al (1971) investigated the binding of 13 sulphonamide drugs to HSA. For these drugs, a marked elevation in binding was observed on increasing the pH from the acidic to the basic side of the pKa value. Thus the anionic form of a sulphonamide drug appears to be more extensively bound than the uncharged species. The authors concluded that the major determinant in sulphonamide binding is electrostatic, and speculated on the involvement of an attraction between the sulphonamide anion and the positively charged amino acids on either side of the single tryptophan residue in HSA. This region of the albumin molecule has been proposed as a primary drug binding site by Swaney and Klotz (1970) and has been discussed in some detail in Chapter 1. Bearing in mind the competition between sulphonamide drugs and warfarin for binding albumin (see Figure 4.7), it is interesting to note that Fehske et al (1979) have identified the lone tryplophan residue as part of the warfarin binding site on HSA.

As well as considering electrostatic forces, Agren et al (1971) also found a direct relationship between lipophilicity and binding of the 13 sulphonamides to HSA. However, a secondary role was attributed to hydrophobic binding. Nonetheless, Jardetzky and Wade-Jardetzky (1965) have used nuclear magnetic resonance to show that the hydrophobic part of the sulphonamide structure, probably the p-aminobenzene moiety, participates in binding.

It seems clear then, that both electrostatic and hydrophobic forces are involved in the binding of sulphonamide drugs to HSA. The problem of data interpretation lies in the proper resolution of the various physiochemical effects involved in the interactions between these drugs and albumin.

From results presented in this chapter it appears sulphisoxazole and warfarin bind strongly to the same class of sites on albumin. Now, displacement from HSA can be expected to have serious consequences for highly bound drugs that have a narrow therapeutic range and a low volume of distribution. The oral anticoagulants including warfarin fall into this category. However, despite the theoretical possibilities of an interaction between the sulphonamides and the oral anticoagulants, there is no evidence as yet to suggest that such an interaction has any clinical significance whatever (Stockley, 1974). The importance of distinguishing between potential and actual drug interactions should not be overlooked.

The observation that long-acting sulphonamide drugs are liable to displacement from albumin in vivo by more highly bound acidic agents such as phenylbutazone (Anton, 1960) is not surprising; it has been shown in this chapter that sulphonamide drugs and phenylbutazone bind to the same class of sites on HSA. The clinical significance of this interaction has yet to be established.

The ease with which phenylbutazone displaced warfarin from HSA and from whole serum was consistent with the results of other studies (O'Reilly, 1973; Solomon et al, 1968; McElnay and D'Arcy, 1980b). Indeed addition of phenylbutazone to the appropriate samples produced such a large increase in the unbound fraction of the fluorescent probe that it is tempting to assume that this displacement mechanism is the most important process contributing to the warfarin anti-inflammatory drug interactions observed in man. However, as well as operating via the displacement of a drug from plasma protein binding sites, drug interactions may involve other processes such as modified absorption, metabolism, excretion and receptor-site response, and competition for tissue binding sites (see Section 1.2). Thus the tendency to attribute most drug interactions to only one of several theoretically possible mechanisms is probably unrealistic.

Although considerable time and effort has been invested in studies of the binding of warfarin to HSA and its displacement by phenylbutazone a full understanding of the mechanisms involved in the interaction of these drugs has still to be achieved. Since these agents can produce potentially hazardous pharmacological effects when co-administered, comprehensive studies in humans have not been attempted. Recently, however, a thorough investigation of the effects of phenylbutazone on warfarin pharmacokinetics and anticoagulant activity has been carried out in rats by Yacobi et al (1980). The interaction between these drugs was found to involve at least three processes: an inhibition of warfarin biotransformation (deceased intrinsic clearance); displacement of warfarin from plasma protein binding sites; and an apparent potentiation of the anticoagulant action produced by a given plasma warfarin concentration. The latter may have been caused, at least in part, by a direct anticoagulant effect of phenylbutazone.

Results from the paper of Yacobi et al (1980) showed that phenylbutazone displaces more warfarin in vivo than it does in vitro. It appears likely that the displacement of warfarin in vivo is due not only to phenylbutazone but also to one or more of its metabolites. In fact, one of the major phenylbutazone metabolites - oxyphenylbutazone, is known to bind strongly to albumin (Chignell, 1968) and probably competes with warfarin for albumin binding sites (Wosilait and Ryan, 1979).

Theoretically, the more pronounced phenylbutazone displacing effect in vivo could be due to the accumulation of warfarin metabolites capable of competing with warfarin for albumin binding sites. Thus, inhibition of the metabolism and elimination of the S-isomer of warfarin by phenylbutazone has been suggested as an alternative mechanism for the increased anticoagulation observed in humans (Lewis et al, 1974). The point that drugs which are capable of competing with each other for albumin binding sites might also compete for elimination and metabolic pathways was emphasized by Gillette (1973).

In 1981 O'Reilly and Goulart attempted a study of certain aspects of the interaction between phenylbutazone and racemic warfarin in humans. In agreement with the work of Yacobi et al (1980) on rats, the interaction in humans appeared to be complex and multifactorial.

It seems likely that other important drug interactions will be the result of several processes. So the effort required to elucidate fully the mechanism of a drug interaction can be enormous. On the other hand, because drugs that displace one another from albumin binding sites may also compete for elimination pathways, a study of competition for binding at the plasma protein level may have a role in the prediction of drug involvement in the unrelated elimination interaction mechanism.

Results from this chapter also suggested that flufenamic acid could compete strongly for albumin binding sites with both warfarin and ANS. To a lesser degree, this behaviour was also exhibited by ethacrynic acid. A series of experiments involving the addition of two competitor drugs to a sample comprising fluorescent probe bound to albumin provided a neat confirmation of these findings. Further support for the results may be found in the microcalorimetric investigation by Otagiri et al (1978) which shows that more than one site contributes to the heat evolved when flufenamic acid binds to HSA. According to Chignell (1969b), flufenamic acid may bind to three very high affinity sites on HSA.

The experiments used to confirm the existence of two separate binding sites on albumin for flufenamic acid and for ethacrynic acid involved a number of simultaneous binding equilibria. It is likely that further studies concerned with multiple binding equilibria will help in the interpretation of other, perhaps rather anomalous, experimental data. For instance, should a drug be bound to albumin at a certain class of binding sites and addition of a second drug, which is known to bind to a different class of sites, cause displacement of the first, the presence of a third ligand bound reversibly to both sites may be implicated. Of course, if no such ligand can be identified, it may be necessary to check that the second drug does not bring about a displacement of the first simply by inducing a conformational change in the protein.

There are also strong implications stemming from this part of the work for some in vivo studies. A drug may be shown by measurements in vitro to bind to a certain class of albumin binding sites. Circular dichroism experiments may subsequently reveal that on binding the small molecule, the protein suffers no marked changes in its three-dimensional conformation. Nevertheless, administration of this drug to a patient receiving multiple drug-therapy may well result in the displacement of drugs from chemically distinct and apparently unrelated classes of binding sites. Quite possibly, this would be due to the existence of other drugs or endogenous ligands which bind strongly at more than one class of binding site. Any shift in the equilibrium concentrations of these albumin-bound molecules could produce unexpected increases in the unbound fractions of certain drugs. Since these are the pharmacologically active fractions, a toxic response may ensue. To predict accurately such responses would require a comprehensive knowledge of the concentrations and binding characteristics of all the drugs and ligands involved. Although there may never be sufficient information to allow a foolproof prognosis, a better understanding of these more complex interactions would surely result from a fuller characterization of both primary and secondary binding sites on HSA.

The use of serum samples in the study of fluorescent probe and drug binding produced no problems over and above those encountered in the use of HSA solutions. With fresh serum samples the background fluorescence was quite acceptable. This rendered pretreatment of sera unnecessary.

When a number of ligands were allowed to compete for binding sites with two fluorescent probes in whole serum and in suitably concentrated albumin solutions, the degree of displacement was found to be the same in both media. This supports the idea that the binding sites for acidic drugs in human serum are mainly or exclusively those on albumin (Tillement et al, 1981). While it is still conceivable that acidic drugs can bind to other plasma proteins, these sites will undoubtedly have relatively low binding affinities.

In the case of sulphisomidine, considerably more fluorescent probe was displaced from serum than from albumin binding sites. Until further information is available, any explanation of the seemingly higher affinity of sulphisomidine for whole serum must be rather speculative.

Despite its usefulness, there is a major objection to the employment of fluorescence spectroscopy in a study of binding phenomena. Although this objection could apply equally well to other spectroscopic techniques, it is one which should not be overlooked. The possibility exists that a drug or other ligand may cause a change in the spectroscopic properties of a probe, in particular a change in the emission spectrum; by modifying the protein conformation and hence the environment of the fluorescent probe, rather than by displacing the molecule from a specific class of binding sites.

To verify some of the results obtained using fluorescence spectroscopy, the binding and displacement of fluorescent probes were examined by a separate technique, that is, equilibrium dialysis. Unlike the homogeneous fluorescence assay, the equilibrium dialysis procedure depended upon the physical separation of the bound and free fractions of the probe. More importantly, however, the analytical signal did not rely on any modifications in the spectroscopic properties of the fluorescent probe on binding to albumin.

Some equilibrium dialysis experiments are discussed in the next chapter.

CHAPTER 5

Equilibrium Dialysis : A Classical Technique for Studying Drug-Protein Binding

5.1 Principle of the Method

Dialysis is a separation process that depends on the differential transport of solutes of dissimilar sizes across a porous barrier separating two liquids when the only driving force is a concentration gradient. The technique is normally used to separate solutes which are too large to cross the barrier from those small enough to diffuse freely through it.

Dialysis is very easily accomplished. The minimum requirements for simple dialysis are met when a semi-permeable membrane is used to stabilize a concentration gradient between a solution on one side and pure solvent on the other. The kinetic movement of the solute molecules will tend to drive them spontaneously through the membrane in the direction of lower concentration. At the same time solvent molecules will move in the opposite direction in response to the osmotic pressure difference. The ability of the solute molecules to traverse the membrane depends on their size and shape.

This concept of dialysis was first proposed by Graham in 1861 who used the process to separate solutes of widely differing sizes. Since then, the method has been refined to allow a higher degree of selectivity and adapted to give rise to a number of related techniques. The most important theoretical and practical aspects of dialysis have been covered by Craig (1965 and 1968).

Equilibrium dialysis - as its name implies - is based on the attainment of an equilibrium across the dialysis membrane. This equilibrium is achieved by the net transfer of dialysable molecules in response to an initial concentration gradient across the membrane. The more concentrated solution is called the retentate and the more dilute solution the diffusate.

Equilbrium dialysis represents a very powerful experimental tool for studying the interactions between low molecular weight ligands and biological macromolecules. The method is founded on the reversibility of such interactions and permits the measurement of the distribution of the ligand between the bound and free forms. Its use in characterizing antibody-hapten binding has been reviewed by Karush and Karush (1971).

In practice, equilibrium dialysis is carried out in a unit comprising two half cells or chambers separated by a semi-permeable membrane. Initially, diluent buffer is placed in one half-cell and known quantities of ligand and macromolecule, say protein, are added to the other. Alternatively, the ligand and protein may be placed on opposite sides of the membrane. The solvent system, sample volume, pH and ionic strength should be identical in both half-cells. The two solutions are stirred continuously to allow them to stay in contact through the membrane until equilibrium is reached. The feasibility of the method arises because the dialysis membrane is impermeable for the macromolecule but allows the ready diffusion of all other solutes. While attainment of diffusion equilibrium across the membrane normally requires several hours, the chemical equilibrium for the binding reaction can be reached within a fraction of a second.

After a pre-determined equilibrium period, the ligand concentration in the protein-free chamber is measured using an appropriate analytical method. If a true equilibrium has been achieved, this value must equal the concentration of unbound ligand in the chamber containing protein: the bound form is too large to cross the membrane. Knowing the total ligand concentration in the dialysis unit, the bound ligand concentration can be found by subtraction. It is sometimes possible to measure the equilibrium concentration of ligand in both half-cells. A knowledge of the total quantity of ligand added to the system is then unnecessary for a calculation of the bound fraction.

The characteristics of the membrane are obviously very important in equilibrium dialysis work. It must have a well-defined pore diameter to prevent diffusion of the macromolecule. Adsorption of ligand and macromolecule on to the membrane should be as small as possible. The mechanical strength must be sufficient to avoid rupture but the membrane must not be too thick; the thinner the membrane the less the non-specific adsorption and the shorter the dialysis time. Fortunately, a very suitable, commercially available material exists in the form of extruded cellulose casing (Visking Tubing). This extremely reproducible casing has been used widely for preparative dialysis in biochemical work.

A good preparation of the membrane will help to reduce blanks. Blanks may arise when membrane impurities perturb spectroscopic or other measurements of the free ligand. Thus, it is common practice to wash membranes several times before use. Once a membrane has been wetted, however, it should never be permitted to dry out again as this can alter its porosity.

Materials used to construct cells for equilibrium dialysis should have little or no tendency to adsorb any of the solutes under examination. Half-cells must fit tightly as any leakage of the dialysing solutions would lead to erroneous results. Some useful information on the design of equilibrium dialysing systems is presented in a paper by Weder et al, (1971).

The diffusion of ligand across the membrane clearly represents the most important aspect of the equilibrium dialysis procedure. A good understanding of this process is essential if the method is to be fully exploited.

The rate of diffusion of any single solute through a membrane depends on a number of factors, some of which are interdependent. They include the solute, the solvent and the temperature as well as the choice of membrane and the cell design. Nonetheless, under properly controlled conditions, and for an ideal, pure solute, the overall rate of diffusion across the membrane can be described by an equation which is analogous to Fick's law for diffusion in free solution. This can be written as:

$$\text{Rate of diffusion} = - DA\frac{dc}{dx} \qquad (5.1)$$

where D is the diffusion constant, A is the area of the membrane, and $\frac{dc}{dx}$ is the concentration gradient.

If the rate of diffusion for a given solute and membrane is proportional only to the concentration gradient across the membrane, Fick's law is obeyed and the process is analogous to first order reaction kinetics. A plot of the logarithm of the concentration in the retentate against time should give a straight line. When a linear escape plot is produced experimentally, it suggests that the solute is behaving ideally over the range of concentration examined and is homogeneous with respect to size within the limits of discrimination of the membrane.

Not all pure solutes give straight line escape plots. In these circumstances the results can be interpreted in terms of association, dissociation, or slow conformational rearrangement of the dialysable molecule. More often than not, however, a deviation from linearity is an indication of an impurity in the preparation. Escape patterns and their interpretation are discussed more fully elsewhere (Craig, 1965). Escape plots are particularly valuable in the design of equilibrium dialysis experiments because they allow the approach to equilibrium to be fully characterized.

According to Fick's law, the rate of diffusion depends on the membrane surface area. The consequences of providing the maximum area for dialysis are at once obvious from equation 5.1. Thus in equilibrium dialysis, the dialysing volumes should be small enough so that they can form a thin film over the whole membrane surface. This is best achieved by continuously stirring the solutions on both sides of the membrane in a completely reproducible manner: the simplest procedure involves the slow rotation of the cells.

It is important to control the temperature during dialysis runs because the rate of diffusion is directly proportional to the absolute temperature. This follows from the Stokes-Einstein equation:

$$D = RT / 6\Pi\zeta\, rN \qquad (5.2)$$

where D is the diffusion coefficient, ζ is the viscosity, r is the radius of the molecule and N is Avogadro's constant.

Equation 5.2 also shows how the rate of diffusion decreases with increasing solvent viscosity. The solvent can also influence the rate of dialysis by solvation, by conformational effects on the solute and by changing the state of association of certain dialysable molecules. As the role of the solvent in dialysis is quite complicated, equilibrium times should be re-examined whenever the solvent composition is changed.

Since protein molecules constitute non-diffusable charged species, in many binding studies the distribution of diffusable ionic species between the half-cells is subject to the Gibbs-Donnan effect. If experiments involving albumin are performed at pH 7.4 Garn and Kimbel (1961) regard this to be acceptable although the isoelectric point is at a pH of about 4.9. In practice, moreover, the Gibbs-Donnan effect can be reduced to a negligible value for charged ligands by including a sufficient concentration of inorganic ions in the solvent (Edsall and Wyman, 1958). An ionic strength of 0.1 is generally adequate to render the effect insignificant.

Although it is feasible to control most of the experimental and environmental variables associated with the diffusion of ligand across the membrane, the approach to equilibrium in dialysis studies can be influenced by the very parameter that is being measured; that is, the distribution of the ligand between the bound and free forms.

It is common practice to establish the time to equilibrium in a buffer versus buffer system. A solution of the ligand is dialysed against the diluent buffer. The concentrations in the retentate and in the diffusate are followed until there is a uniform distribution of the ligand across the dialysis membrane. The equilibrium period is then fixed and adhered to during subsequent binding studies. Unfortunately, as the extent of binding varies, so does the time to equilibrium. If the protein binds a substantial fraction of the total ligand, a longer equilibration period is required. To avoid potentially serious errors, it is important to establish that the reported values of free ligand concentration are the true equilibrium values for all bound fractions.

5.2 Design of Dialysis Cells and Performance Tests

Special dialysis cells were designed for use in drug-protein binding studies. They were made from Teflon (polymethacrylate), a material which shows a low non-specific adsorption of proteins (Weder et al, 1971). A unit consisting of two half-cells is illustrated in Figure 5.1.

The two halves of the cell were readily coupled by means of a single nickel screw which passed through a hollow, threaded column in the centre of each unit. When a dialysis membrane was trapped between the half-cells, two separate compartments were formed. Sample solutions were injected into these compartments via small entry ports in the walls of the cells. The ports were sealed with plastic screws.

The total volume in each half-cell compartment was 2.8ml. This meant that with a sample of 2ml, a sufficiently large 'active' membrane area remained.

Thorough mixing of samples and hence reasonable dialysing times were achieved by rotation of the complete cells. A device was produced which would accept and rotate a number of cells. The equipment consisted of two parallel rollers, one of which was driven by an electric motor. The other roller was free to rotate and positioned at a slightly higher level than the first. The roller bars were also displaced horizontally so as to take a hollow glass tube of specific internal diameter. Tests showed that the motion of the driven roller was faithfully transferred to the glass tube it supported; there was no tendency for the latter to slip. Moreover, because the dialysis cells fitted tightly into the hollow tube they could be guaranteed to rotate as one.

When placed in the rotation assembly, the membranes in the dialysis cells were in the vertical position and at right-angles to the rotational axis. The motion of the cells meant that sample solutions came into contact with the whole area of the membrane. The rate of rotation could be adjusted at will by regulating the power supplied to the electric motor driving the assembly.

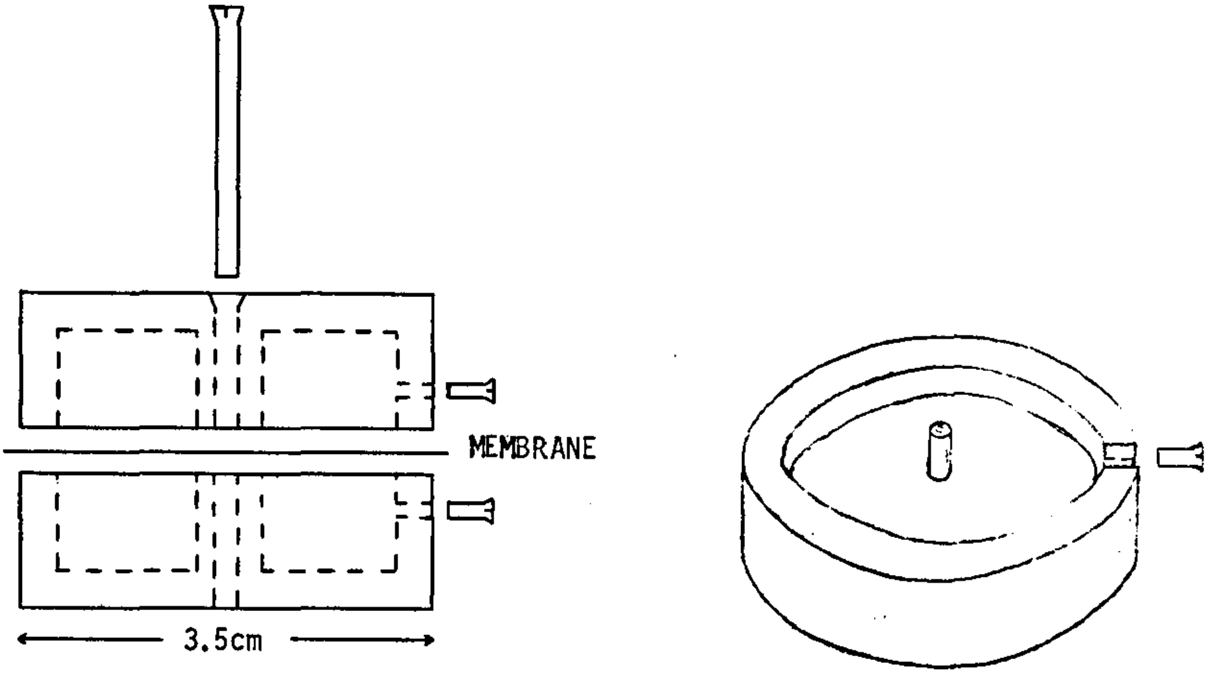

CROSS-SECTION OF DIALYSIS CELL

HALF-CELL

FIGURE 5.1 An Illustration of a Dialysis Cell Used in this Study.

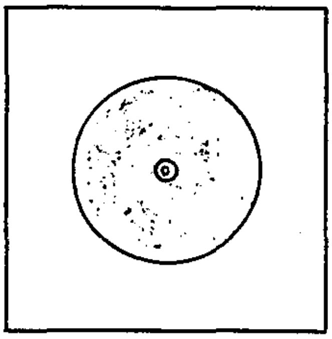

FIGURE 5.2 The Pattern of Membrane Oxidation Following Dialysis of a Potassium Permanganate Solution.

Visking tubing (Scientific Instrument Centre Ltd) was used as the dialysis membrane. Pieces of a convenient size were cut from the tubing and soaked in concentrated sodium carbonate solutions at 100°C for about 16 hours. The membranes were then washed several times in boiling distilled water to remove any remaining soluble components. Treated membranes were stored at 4°C in distilled water. To avoid altering sample volumes, drops of water were removed from the membranes with adsorbent tissue prior to their insertion in the dialysis cells. However, membranes were never allowed to dry out.

Before commencing on drug binding studies, the performance of the equilibrium dialysis equipment was examined thoroughly. Experiments were carried out to test for leakage of sample solutions and efforts were made to detect any spurious fluorescence signals arising from membrane contaminants or from molecules leaching out of the cell walls. The dialysing time for a low molecular weight ligand was also determined and the degree of solute adsorption on cell walls and membranes was investigated. Brief descriptions of the trials carried out with the new dialysing system are given below.

The tightness of fit of the half-cells was tested using a coloured solution. A small quantity of potassium permanganate was dissolved in distilled water. Dialysis cells containing this solution were spun overnight at room temperature. Subsequent inspection of the membranes showed that the oxidized portions were stained brown and easily identifiable. The extremely sharp pattern of membrane oxidation illustrated in Figure 5.2 demonstrates quite clearly that there was no leakage of solution from the sample compartments.

Several attempts were made to detect spurious signals caused by the removal of fluorescent substances from the dialysis membrane or the cell walls. Even after rotating a buffer solution in the sealed dialysis unit for up to 24 hours, there was no increase in the background fluorescence at any wavelength.

The time required to reach equilibrium was found for a sample containing warfarin. 2ml aliquots of a solution of warfarin in 0.1M Tris/HCl buffer, pH 7.4 were dispensed into several half-cells. An equal volume of unspiked buffer was then added to the other half of each of the dialysis cells. So, initially drug was only present on one side of the membranes.

The loaded cells were placed on the rotation assembly and spun at a constant rate of 17 revolutions per minute. At specified times units were removed and the quantities of drug on either side of the membrane were assayed. To do this, measured volumes of solution were extracted from each of the half-cells and placed in the fluorimeter. Fluorescence intensities were recorded using the wavelengths of maximum excitation and emission for warfarin in free solution. With the aid of the non-linear calibration curve shown in Figure 5.3, the data were analysed in terms of the concentrations of warfarin on either side of the membrane after the various dialysing times. The results are presented in Figure 5.4 and illustrate the approach to equilibrium across the cell.

To check for the adsorption of ligand on to the Teflon walls of the dialysis cells or on to the membrane itself, the total concentration of warfarin recovered from each cell was plotted against time. As may be appreciated from the results shown in Figure 5.4, no significant decrease in the recovery of drug could be detected for periods of rotation up to 28 hours. It may be concluded that there is no non-specific adsorption of warfarin within the dialysis cell.

5.3 Application of Dialysing System to Drug-Protein Binding Studies

5.3.1 Control of Fluid Shifts and Other Factors

Preliminary performance tests in buffer versus buffer systems are essential if dialysis cells are to be applied properly to more complex systems. Nevertheless, careful thought is required when directing this information to the design of future experiments. Some simple theoretical arguments are useful in this context. Before introducing these ideas, however, it is worth examining the practical consequences of establishing an osmotic pressure gradient across the dialysis membrane.

When equilibrium dialysis is used to determine the free ligand fraction in drug-protein binding studies, the results may be subject to large errors because of fluid shifts within the test system (Moll and Rosenfield, 1978). These shifts can effect the volumes of solution on both sides of the membrane making interpretation of the data quite difficult. The phenomenon is obviously due to the osmotic activity of the protein molecules and so is more marked at high concentrations. Its effect may be lessened by increasing the rigidity of the dialysis membrane or by applying a compensating pressure within the protein-containing compartment (Kurz et al, 1977).

Although the cells used in this study had been designed to resist changes in the volumes of the liquid samples initially added to either side of the membrane, it was important to test their effectiveness under the appropriate experimental conditions.

Blue Dextran is a dye with a molecular weight of over two million. Molecules of this polymeric material are far too large to pass through the

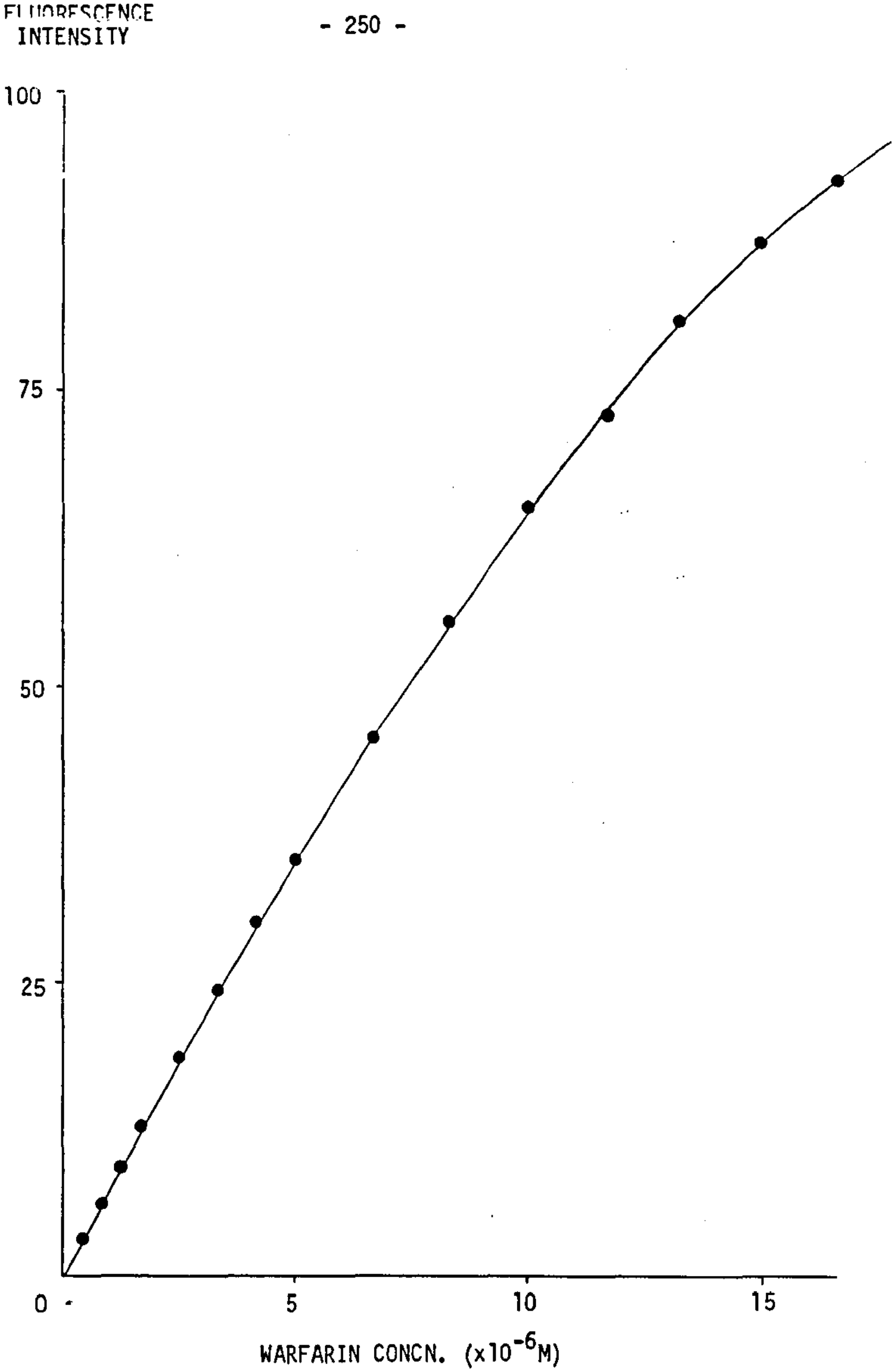

FIGURE 5.3 Calibration Curve for Warfarin in Free Solution.

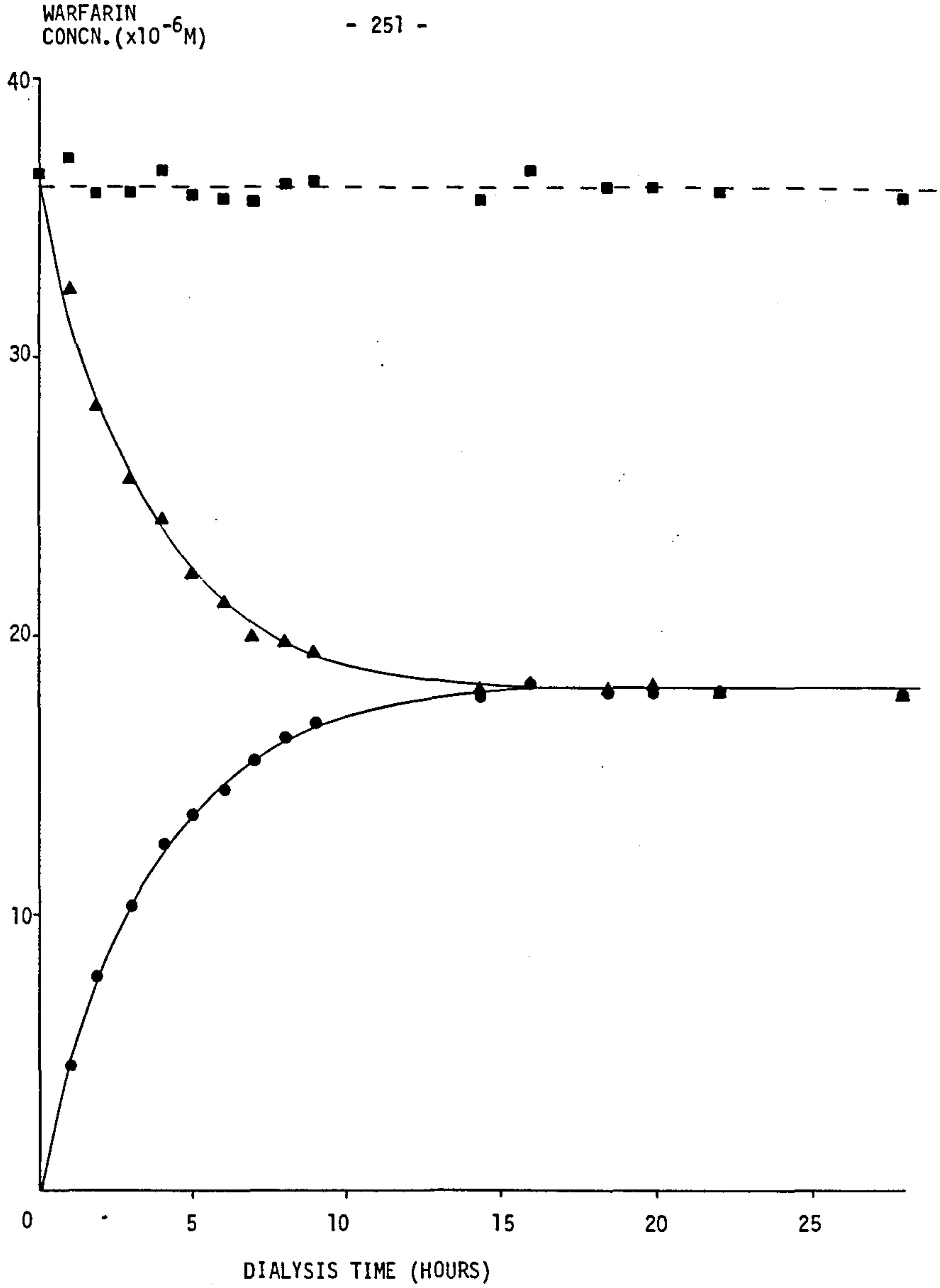

FIGURE 5.4 The Equilibration of Warfarin Across the Dialysis Membrane.

■ Total recovery of ligand.
▲ Retentate concentration.
● Diffusate concentration.

pores of a dialysis membrane. The dye was employed as a marker to monitor volume changes in the cell compartments. Two solutions containing Blue Dextran were prepared; a third containing warfarin was also used:

Solution A	0.1M Tris/HCl pH 7.4 / 0.04% Blue Dextran
Solution B	" " / 5 x 10^{-6}M HSA
Solution C	" / 2.5 x 10^{-3}M Warfarin

2ml of Solution A were added to both compartments of several dialysis cells. The loaded units were rotated at room temperature for 24 hours. After dialysing, the absorbances of the solutions in the half-cells were recorded at 630nm. The same procedure was followed for Solution B, although slightly higher readings were obtained because of a small contribution from the HSA. These control experiments were not subject to fluid shifts since the same solutions were present on both sides of the semi-permeable membranes; they simply provided a means of converting absorbance measurements obtained in spiked buffer and protein solutions directly into mg/ml of Blue Dextran. Consequently, when 2ml of Solution A were dialysed against 2ml of Solution B under the specified conditions, the final concentrations of Blue Dextran were readily available (see Table 5.1).

Clearly, there had been no significant change in the concentrations of Blue Dextran originally present in the buffer- and protein-containing compartments even though a gradient of osmotic activity had existed across the membrane. In other words, no volume changes had been detected. Furthermore, when 200 μl of Solution C was added to 2ml of Solution B before dialysing against 2ml of Solution A, the results showed that the initial discrepancy between the sample volumes on either side of the membrane had been maintained.

Dialysing System	Blue Dextran Concn. (mg/ml)			
	Buffer Compartment		Protein Compartment	
	Before Dialysis	After Dialysis	Before Dialysis	After Dialysis
2ml Solution A v 2ml Solution B	0.400	0.395	0.400	0.392
2ml Solution A v 2ml Solution B + 0.2ml Solution C	0.400	0.397	0.360	0.361

Table 5.1

The ability of the cells to halt the flow of water into the protein compartment depends on a fairly simple mechanism. This is the tendency of the air above the sample solutions on either side of the membrane to oppose any volume changes prevailed upon it.

Immediately after a dialysis unit has been loaded and sealed, the air-pocket in each half-cell is at atmospheric pressure. If a protein solution is present in one half-cell and diluent buffer in the other, the osmotic flow of water across the membrane will increase the quantity of liquid in the protein compartment. Assuming the membrane is rigid, this flow will reduce the volume of the air above the protein solution while expanding the volume above the buffer solution. Thus as osmosis continues, an increasing back-pressure develops across the membrane opposing the movement of water into the protein compartment.

When the flow of water across the membrane is counterbalanced by the back-pressure, then by definition the latter is the osmotic pressure of the solution. Now, osmotic pressure is a colligative property of solutions: it is a function of the number of solute molecules per unit volume. This is normally expressed as $\pi = {}^{c}/_{M}\,RT$, where M is the molecular weight, c is the concentration in g l^{-1}, R is the gas constant (0.0821 l-atm mol^{-1} K^{-1}), T is the absolute temperature and π is the osmotic pressure in atmospheres. So, a 5 x 10^{-6}M solution of HSA at 23°C gives an osmotic pressure of 1.21 x 10^{-4} atmospheres. In this instance the counterbalancing force required in the dialysis cell is extremely small compared to the atmospheric pressure already present above the sample solutions. In fact, assuming the usual 0.8ml of air exists in both half-cells, and knowing that pressure is inversely proportional to volume, it is easy to show that a fluid shift of only a fraction of a microlitre is needed to produce the required pressure differential. This change is much too small to detect.

It is also easy to understand why the introduction of ligand molecules into the dialysis cells had no effect on the net osmotic flow. At equilibrium, the same quantities of unbound ligand will reside on either side of the membrane. Furthermore, the bound fraction will not change the number of non-diffusable solutes per unit volume in the protein compartment; so the osmotic pressure, being a colligative property, is also unchanged. Fluid shifts should not be a problem when these dialysis cells are used for drug-protein binding studies.

When warfarin was dialysed in a buffer versus buffer system, results showed that approximately 16 hours were required to establish equilibrium between the diffusate and the retentate (see Figure 5.4). All other diffusable ligands under examination had molecular weights which were similar or slightly lower than that of warfarin. Hence 16 hours probably represents the longest dialysing time likely to be encountered.

In protein binding studies, however, the approach to equilibrium is affected not only by the rate at which the ligand crosses the membrane, but also depends on the concentration of the unbound fraction and the side of the membrane to which the ligand is first added. While it is easy to appreciate how these factors can influence the time needed to reach equilibrium, their potential to introduce serious errors into binding data has rarely been considered. Very recently, however, the approach to equilibrium in dialysis systems has been studied in detail by Øie and Guentert (1982) and by McNamara and Bogardus (1982). Their methods of analysis are worthy of consideration because they make way for a critical examination of the design of the drug-protein binding experiments described in this section.

According to Øie and Guentert, when drug is initially added to the protein-containing compartment of the equilibrium dialysis cell, the concentration on the buffer side of the membrane at any time t is given by

$$C_B = \frac{Co\alpha}{(1+\alpha)} \left(1 - e^{-K_T (1+\alpha) t}\right) \qquad (5.3)$$

where Co is the initial drug concentration and K_T is the rate constant governing the transfer of drug across the membrane. The term α is the unbound fraction in the protein compartment: a value of $\alpha = 0.01$, for example, indicates that 1% of the drug is in the unbound form.

When drug is initially added to the buffer side a similar equation is obtained:

$$C_B = \frac{Co}{1+\alpha} \left(\alpha + e^{-K_T(1+\alpha) t}\right) \qquad (5.4)$$

Although the actual concentration on the buffer side of the membrane is the variable of interest, in order to examine the influence of α on equilibration times it is better to express C_B in relative terms. A fraction away from the true equilibrium concentration of drug in the buffer compartment is defined as

$$\delta = \frac{\text{Absolute Value } (C_B^{\infty} - C_B)}{C_B^{\infty}} \qquad (5.5)$$

where C_B^{∞} is the value of C_B as t tends to infinity.

Equations (5.3) and (5.4) show that $C_B^{\infty} = Co\ \alpha/(1+\alpha)$ for both protein and buffer spiked samples. So in a form which is analogous to Equation (5.3), the time course of this fraction when drug is initially on the protein side is

$$\delta_p = e^{-K_T\ (1+\alpha)\ t} \qquad (5.6)$$

When drug is initially placed on the buffer side of the membrane (see Equation 5.4), the time course of δ is described by:

$$\delta_B = \frac{e^{-K_T\ (1+\alpha)\ t}}{\alpha} \qquad (5.7)$$

The last two equations provide a ready means of finding K_T from experimental data obtained in buffer versus buffer systems. Under these conditions, $\alpha = 1$ and $\ln \delta = -2K_T\ t$. Consequently, if the logarithm of δ is plotted against time for an ideal solute, a straight line of slope $-2K_T$ should result. The information contained in Figure 5.4 has been processed in this way and the escape plot is shown in Figure 5.5.

The graph is clearly linear for dialysing times of 9 hours or less. (For longer dialysing times, the error in δ becomes unacceptable as near-equilibrium conditions prevail). As outlined in Section 5.1, the linear relationship indicates that the rate of dialysis depends simply on the concentration gradient across the membrane. It also shows that the solute has no tendency to associate or dissociate during the period of dialysis.

The gradient of the straight line drawn in Figure 5.5 was found by regression analysis. It gives the value of K_T as 0.147 hr^{-1}. The importance of this term lies in its ability to test the approach to equilibrium under different experimental conditions.

Consider first the buffer versus buffer system. The time to reach some fraction δ from the true equilibrium concentration is given by $t = {}^{-\ln\delta}/2K_T$. Using the value of K_T determined by experiment, it is possible to find how close the system is to equilibrium at any stage. An idea of the approach to equilibrium is presented in Table 5.2. For this simple system it is not essential to calculate K_T: the same information can be obtained by inspection of the raw experimental data (Figure 5.4). With more complicated systems, however, a knowledge of K_T is invaluable for predicting suitable equilibration times.

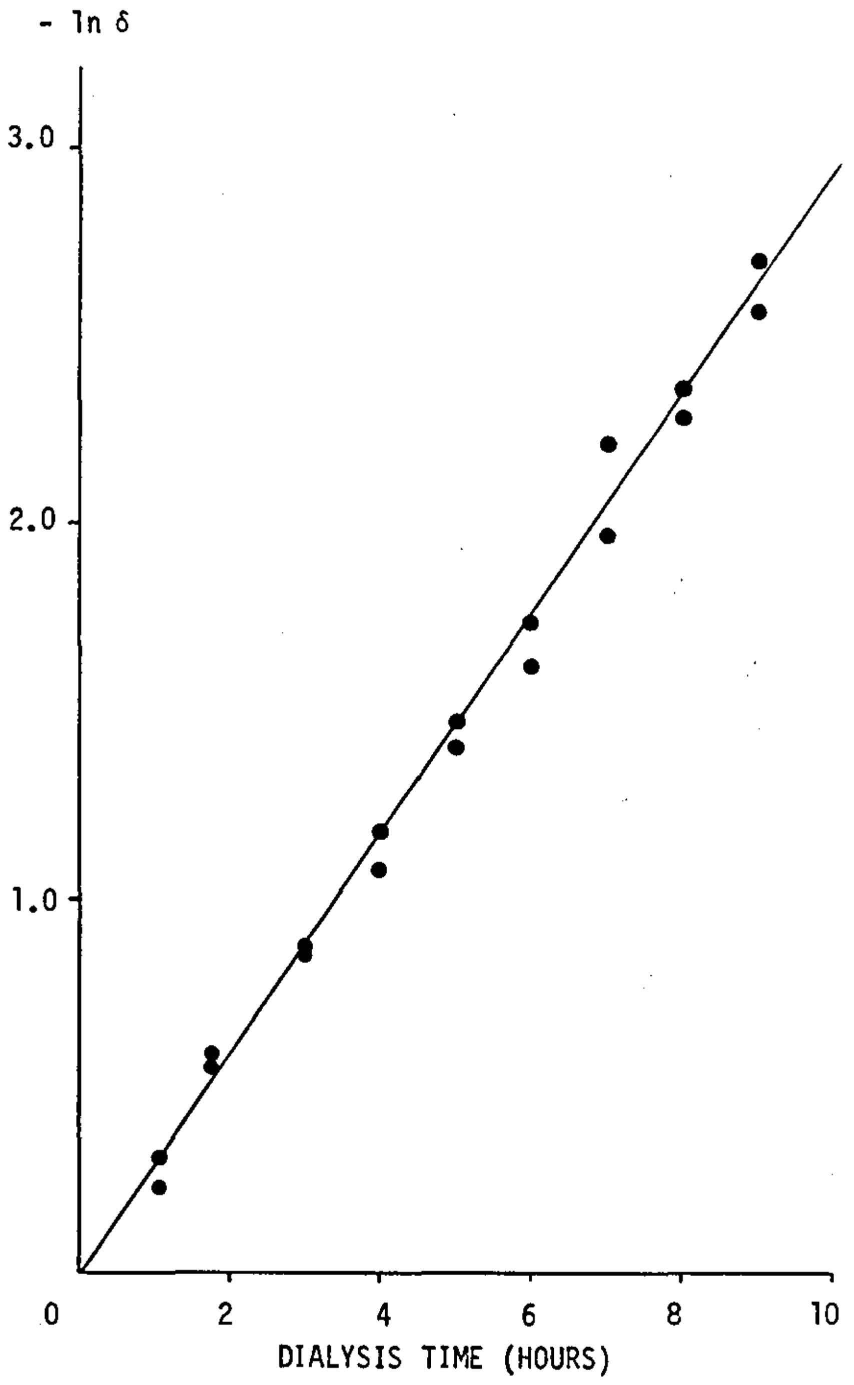

FIGURE 5.5 Escape Plot for Warfarin Using Data of Figure 5.4.

Coefficient of linear regression for fitted line, $r = 0.996$.
Gradient of straight line plot is $-2K_T$.

Deviation from true equilibrium (%)	Time of dialysis t (hr)
50	2.36
10	7.86
5	10.19
2	13.31
1	15.66

Table 5.2

Approach to equilibrium in dialysis cell. Ligand is warfarin.

When the different time courses exhibited by buffer and protein spiked samples are examined, it soon becomes clear that the former requires more time to reach comparable δ values as a greater quantity of drug must be transported across the membrane. For example, if 1% of a drug is in the unbound fraction ($\alpha = 0.01$), 99% of the initial mass present in a buffer spiked sample must cross the membrane to reach equilibrium. In a comparable protein spiked system, only 1% of the initial mass of drug must diffuse to the buffer side at equilibrium.

A comparison of the two systems benefits from a consideration of the dialysis times required to reach a given value of δ. Rearrangement of Equation (5.6) for the protein spiked system produces

$$tp = \frac{-\ln \delta p}{K_T\,(1+\alpha)} \qquad (5.8)$$

where tp is the time to reach some fraction δ_p from the true equilibrium concentration when the drug is initially added to the protein side. So as the unbound fraction becomes smaller, tp reaches a limiting value $\frac{-\ln\delta p}{K_T}$ which is twice that of a buffer versus buffer system.

On the other hand, when the buffer is spiked, the value of t_B given by Equation (5.7) is

$$t_B = -\frac{(\ln \delta_B + \ln \alpha)}{K_T\,(1+\alpha)} \qquad (5.9)$$

Instead of reaching a limiting value as α decreases, t_B continues to increase without bounds.

Wherever possible then, drug should be added on the protein side of the membrane. This minimizes equilibration times and reduces potential problems such as drug degradation, microbial growth and protein denaturation. All drug-protein binding studies described in this chapter were performed using protein spiked samples.

Table 5.3 emphasizes the importance of the initial experimental conditions by comparing the time to reach concentrations 1% and 5% from the true equilibrium value for both buffer and protein spiked samples. Sine K_T was taken to be 0.147 hr^{-1}, the figures are applicable to warfarin binding studies. The practical advantage of initially placing the drug on the protein side of the membrane is obvious throughout the range of α, but becomes more obvious as α decreases.

	α	t_B(hr)	t_P(hr)	t_B/t_P
$\delta = 0.05$	1.0	10.2	10.2	1.00
	0.5	16.7	13.6	1.23
	0.1	32.8	18.5	1.77
	0.05	38.8	19.4	2.00
	0.01	51.2	20.2	2.54
	0.005	56.2	20.3	2.77
	0.001	67.3	20.4	3.31
$\delta = 0.01$	1.0	15.7	15.7	1.00
	0.5	24.0	20.9	1.15
	0.1	42.7	28.5	1.50
	0.05	49.2	29.8	1.65
	0.01	62.0	31.0	2.00
	0.005	67.0	31.2	2.15
	0.001	78.2	31.3	2.50

Table 5.3

Influence of initial conditions and fraction unbound (α) on the time to reach a fraction δ away from the equilibrium concentration.

$K_T = 0.147\ hr^{-1}$

Table 5.3 illustrates a second important point: the extent of ligand binding controls the approach to dialysis equilibrium in binding studies. Although the time to equilibrium is usually established in buffer versus buffer systems, it should really be found for the system with the smallest expected α value. All the results presented in Section 5.4 have been checked to ensure that acceptably low values of δ hold whatever the unbound fraction.

5.3.2 Experimental Procedures

The binding of warfarin to HSA was studied using the apparatus described earlier in this chapter. A number of cells were fitted with dialysis membranes and sample solutions were introduced into the half-cells via the entry ports. 2ml volumes of a 5×10^{-6}M solution of HSA were dispensed in to one set of half-cells followed by very small amounts of a concentrated warfarin solution. The diluent buffer used for both drug and protein was 0.1M Tris/HCl pH 7.4. Across the membranes from the spiked protein samples, the matching half-cells contained 2ml of the diluent buffer.

Once loaded, the dialysis cells were placed on the rotation assembly and installed in a thermostated cage set at 23°C. The samples were rotated for 18 hours at a constant rate of 17 revolutions per minute. During the dialysis runs, a maximum-minimum thermometer showed that the temperature variation about the mean was ± 0.2°C.

After dialysis, the concentration of free drug was determined from measurements of the warfarin fluorescence in the buffer compartment of each cell. As explained previously, this may be accomplished with the aid of a suitable calibration curve (see Figure 5.3). To perform the analysis automatically, a computer program called DIALB was devised.

Simple experiments were carried out to test for possible background signals arising in the dialysis cells. It is conceivable that fluorescent species weakly bound to albumin can dissociate during dialysis and these could traverse the membrane to interfere with the assay of unbound ligand in the buffer compartment. However, no spurious signals could be detected in buffer samples dialysed against HSA for 18 hours.

As fluid shifts had been shown to be negligible during the course of dialysis, the DIALB program assumed that initial discrepancies between the volumes of solution in each half-cell were maintained. This meant that any differences in the volumes of solution on either side of the membrane could be taken into account when the program went on to calculate the concentrations of total, free and bound ligand in the protein compartment.

Now the bound ligand fraction being confined to the protein compartment was found by recalling the total quantity of ligand dispensed into the cell and subtracting the amounts of free ligand distributed between both the protein and the buffer compartments. At equilibrium, the concentrations of unbound ligand are the same on either side of the dialysis membrane and so the situation is described by

$$C_B V_P = T_L - C_U V_B - C_U V_P$$

where C_B and C_U are the equilibrium concentrations of bound and unbound ligand respectively, V_P and V_B are the volumes of solution in the protein and buffer compartments rspectively, and T_L is the total amount of ligand added to the system. Thus having determined C_U, an equation of the form

$$C_B = \frac{1}{V_P} (T_L - C_U (V_B + V_P))$$

allowed the computer program to establish the concentration of bound ligand in the protein compartment under the conditions specified by V_P, V_B and T_L. The routine finally presented the data in terms of the parameters of some commonly used binding curves including the Scatchard representation (Scatchard, 1949).

Equilibrium dialysis was used to study competition between ligands for specific binding sites on HSA. As usual warfarin and HSA were added to one compartment of the dialysis cell and diluent buffer to the other. After equilibrium had been reached across the membrane, the unbound fraction of the fluorescent probe was measured in the buffer compartment. During competitive binding studies, however, small quantities of other ligands were dispensed into the protein compartments of some of the dialysis cells already containing warfarin and HSA. Following dialysis, increased levels of fluorescent probe in the buffer compartments were taken as evidence for competitive displacement from albumin binding sites. Because a fluorimetric assay was employed, it was sometimes necessary to take account of inner-filter effects arising from the presence of competitor in the buffer compartment.

When equilibrium dialysis was used to examine the binding of sulphonamide drugs to HSA, the ligand concentrations on both sides of the membrane were determined spectrophotometrically. In these studies, drug and albumin were added to one half-cell and diluent buffer to the other. After equilibrium had been established across the membrane, samples were extracted from each half-cell and the sulphonamide concentrations estimated by the method of Bratton and Marshall (1939). This procedure is based upon a coupling reaction which is carried out under acid conditions to produce a diazonium salt. The concentrations of the coloured product may be determined by measuring the sample absorbance at 545 nm.

Experiments on spiked samples showed that the colourimetric assay was not restricted to buffer samples but could be used to determine the concentration of sulphonamide in a solution of HSA; the only complication was the subtraction of a small protein blank. It appeared that the acidic conditions used in the Bratton and Marshall coupling reaction were sufficiently extreme to denature the protein and to render any bound ligand available for diazotization. Thus two pieces of information were obtained from each dialysis cell; the concentration of unbound sulphonamide in the buffer compartment, and the total concentration of sulphonamide in the protein compartment. From the data it was a simple matter to calculate the concentration of bound ligand in each cell and to analyse the results in terms of Scatchard plots. There was no need to recall the quantities of sulphonamide originally added to each cell - except, perhaps, to check the total amount of drug recovered after dialysis.

5.4 Equilibrium Dialysis Results

The smallest quantity of warfarin which could be measured in the buffer compartment was dependent upon the detection system and the experimental design. An approximate value for this quantity was found by inspection of the data used to construct the calibration plot shown in Figure 5.3. Using standard methods of data processing, the limit of detection turned out to be about 4×10^{-8} mol l^{-1} warfarin. This figure was useful when checking the validity of points in the high-affinity region of the binding curve. For example, the lowest value of unbound warfarin in the curve of Figure 5.6 is 8½ times that of the limit of detection and clearly falls well within the domain of the calibration curve.

At the other end of the curve the bound ligand fraction should not be too low. This is so because the bound ligand is calculated as the difference between the total ligand and the free ligand. If this difference is small, the bound fraction can not be determined accurately. The smallest bound fraction included in the Scatchard plot was therefore restricted to about one quarter of the total ligand in the protein compartment.

As explained in Section 5.3.1, it is desirable to estimate the time to equilibrium for the sample containing smallest unbound fraction α. This is the sample for which the approach to equilibrium is slowest. For the data presented in Figure 5.6, the lowest value of α is about 0.3. With the rate constant determined for warfarin, Equation (5.6) shows that in this case 97% of the free ligand has equilibrated after 18 hours. With the highest value of α included in Figure 5.6, it can be demonstrated that 99% of the unbound fraction will have reached equilibrium during the same period. Under the specified conditions, and over the range of values covered by the binding curve, the effect of α on the deviation from true equilibrium was therefore extremely small. No corrections were made to the binding curve.

The Scatchard plots describing the binding of warfarin to HSA as measured by equilibrium and fluorescence enhancement are shown in Figure 5.6 and appear to be in reasonable agreement. While the curves themselves are very similar, particularly at high values of r, discrepancies between the

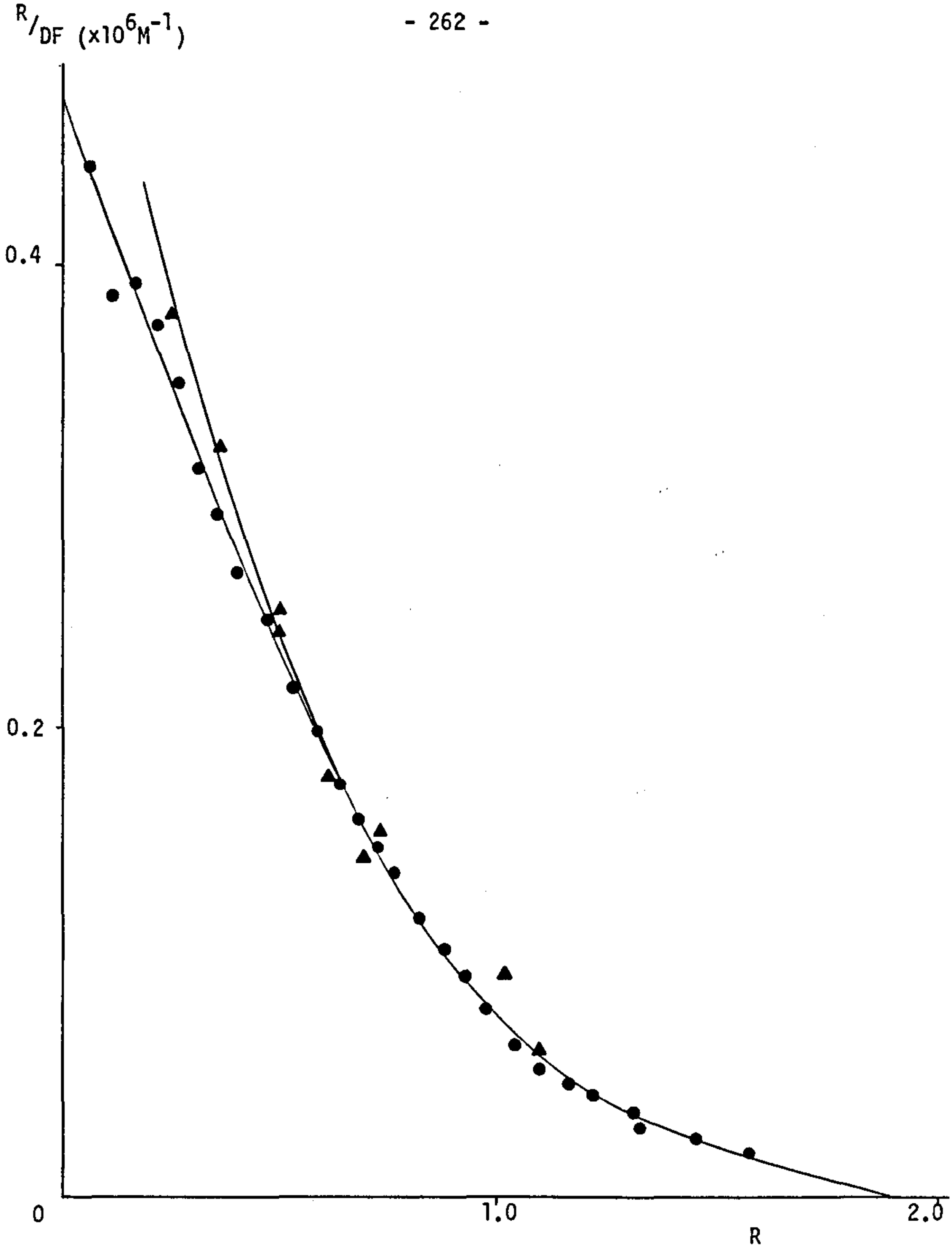

FIGURE 5.6 Scatchard Plots Describing the Binding of Warfarin to Human Serum Albumin.

▲ Equilibrium Dialysis.
● Fluorimetric Titration.

Binding constants derived from data with the aid of the NKFIT program:
Equilibrium dialysis $n_1 = 0.61$, $k_1 = 0.91 \times 10^6 M^{-1}$, $n_2 = 1.29$, $k_2 = 0.041 \times 10^6 M^{-1}$.
Fluorimetric titration $n_1 = 0.84$, $k_1 = 0.53 \times 10^6 M^{-1}$, $n_2 = 1.06$, $k_2 = 0.026 \times 10^6 M^{-1}$.
The solid lines drawn in the figure were constructed using the above binding constants.

binding constants are more apparent. It may be that too few data points were obtained in the equilibrium dialysis experiment to derive meaningful binding constants.

Even over the proper working range of the assay, the results yielded by the equilibrium dialysis technique were of somewhat poorer precision than those obtained in the corresponding fluorimetric titrations. An attempt was made to identify the major sources of imprecision in the equilibrium dialysis procedure.

Whenever warfarin was assayed in buffer versus buffer systems the results tended to exhibit very low coefficients of variation. For example, when 2.5 x 10^{-8} moles of warfarin were equilibrated across the dialysis membrane, the coefficient of variation was about 0.6%. Indeed, for a given concentration, the sample-to-sample variation was no greater than the variation between repeated measurements on individual samples. This suggested that the limiting error in buffer versus buffer dialysis systems was associated with the recording of fluorescence intensities rather than with the loading and operation of the cells.

As noted earlier, there was no adsorption of the drug to the dialysis membrane and cell surfaces. Similarly, it has already been demonstrated how the addition of protein to one half-cell resulted in a negligible fluid shift across the membrane. Only very rarely did membranes contain imperfections or split to give erroneous results. Furthermore, if dialysable compounds dissociated from albumin, they were non-fluorescent and did not interfere with the measurement of unbound ligand. The pH and buffer ionic strength should have been sufficient to eliminate the need for Donnan corrections (Garn and Kimbel, 1961; Edsall and Wyman, 1958).

It is possible that a partial denaturation of the albumin occured during the period of dialysis. Although not demonstrated experimentally, this would appear to be a potential source of error in the binding assay.

Results obtained using the equilibrium dialysis technique and demonstrating the displacement of warfarin from its albumin binding sites are given in Table 5.4. They show quite clearly that the ability to displace the fluorescent probe increases from sulphisomidine to sulphisoxazole to phenylbutazone. This observation agrees with the findings of the fluorescence enhancement work.

When equilibruim dialysis was used to study the displacement of ANS from HSA, no increase in the unbound fraction was produced by addition of warfarin to the protein compartment. Again this result may have been predicted from previous fluorescence enhancement work.

Competitor	Competitor Concn ($\times 10^{-6}$M)	Total Warfarin Concn. in Protein Compartment ($\times 10^{-6}$M)	% Displacement
Phenylbutazone	24.8	5.41	65.0
Sulphisoxazole	25.0	6.26	13.7
Sulphisomidine	24.8	6.54	2.5
Sulphisoxazole	25.1	1.59	24.5
Sulphisomidine	24.9	1.71	4.0

Table 5.4 The displacement of warfarin from HSA as determined by equilibrium dialysis.

However, while the fluorimetric procedure allowed the total protein, probe and competitor concentrations to be selected at will, the equilibrium dialysis studies of competitive binding were harder to control. Although any initial concentrations of albumin, probe and competitor could be placed in the protein compartment of the dialysis unit, the equilibrium concentration of both ligand were dependent upon their distribution across the membrane and hence on their protein-binding characteristics. This made it very difficult to achieve the same conditions in equilibrium dialysis and in fluorescence enhancement experiments. Results from the two techniques may be compared qualitatively but the figures relating to the percentage of probe displaced by a particular competitor are valid only under the specified conditions.

A number of samples containing known quantities of sulphonamide drug were determined using the Bratton and Marshall procedure. A standard curve for sulphisomidine is plotted in Figure 5.7 and is linear over a wide concentration range. The log-log representation is simply for convenience.

Although the extinction coefficient of the coloured product varies from drug to drug, linear standard curves were also obtained for sulphisoxazole and sulphadiazine.

The standard curves were used to estimate sulphonamide concentrations in both buffer and protein compartments after dialysing spiked solutions of HSA against diluent buffer. To ensure that absorbance readings were high enough to fall within the working range of the standard curve yet still allow free drug to be determined at low sulphonamide:albumin

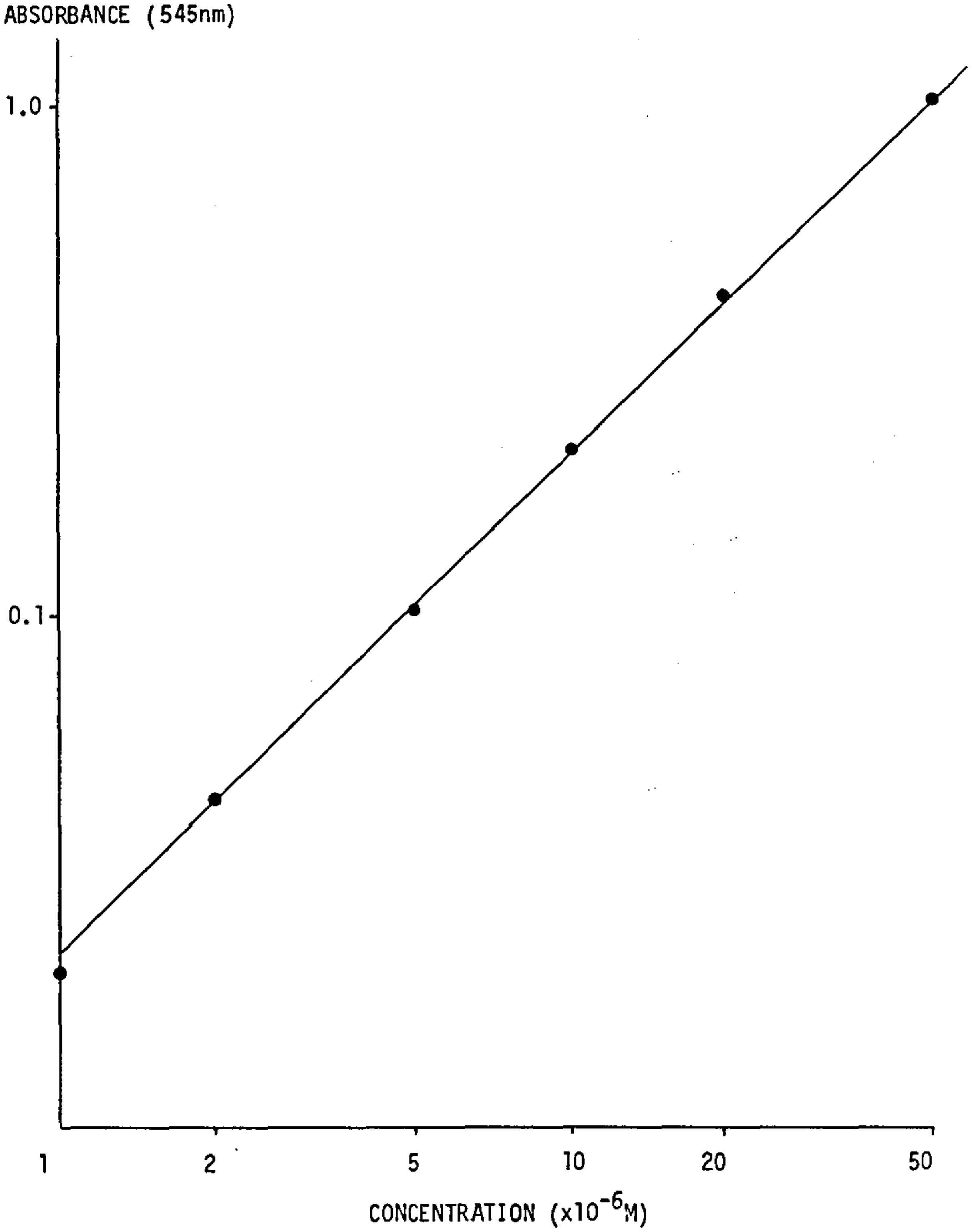

FIGURE 5.7 Calibration Plot for Sulphisomidine.

Coefficient of linear regression for fitted line, r = 0.99995.

ratios, the concentration of HSA in the protein compartment was raised to 10^{-4}M. This concentration of albumin was still too low to produce a detectable fluid shift across the membrane. (Theoretical fluid shift $<$ 0.02%). Furthermore, the absorbance of HSA at 545 nm remained far too small to interfere with measurements of the total sulphonamide in the protein compartment.

As shown in Figure 5.8, linear Scatchard plots were obtained for sulphisoxazole and sulphisomidine. This suggests that these drugs bind to a single class of sites on albumin. The binding of sulphadiazine was so low that a categorical statement of curve shape is impossible. However, it seems most reasonable to assume that this Scatchard plot is also linear.

Values for the binding constants were derived from the slopes and intercepts of the graphs in Figure 5.8. Sulphisoxazole clearly has the highest affinity for albumin binding sites. Thus a rank order correlation has been demonstrated between the binding affinities of the three sulphonamides and their capacities to displace warfarin from HSA (see Figures 4.5 and 4.7 and Table 5.4).

It is worth recalling that an approximate value for the association constant of sulphisoxazole was obtained by measuring its ability to displace warfarin in a fluorimetric titration. The conclusion that k was roughly 10^4 M^{-1} agrees with the findings of the corresponding equilibrium dialysis experiment.

5.5 Comparison of the Fluorimetric and Equilibrium Dialysis Methods for Studying Drug-Protein Binding

Equilibrium dialysis provided a theoretically sound and unambiguous experimental method for studying the binding of drugs to HSA. However, the principle application of this conventional technique was to test the validity of results obtained using the homogeneous fluorimetric procedure.

The significance of the apparent agreement between the two techniques is best appreciated by a comparative evaluation of the methodologies. The most important features are summarized in Table 5.5.

In the context of this study, certain aspects of the procedures are worthy of elaboration. For instance, consider the uncertainties inherent in estimates of the unbound ligand. After equilibrium has been reached across the dialysis membrane the concentration of free ligand is measured directly in the buffer compartment. As long as an assay of sufficient sensitivity is available, small quantities of unbound ligand can be determined with

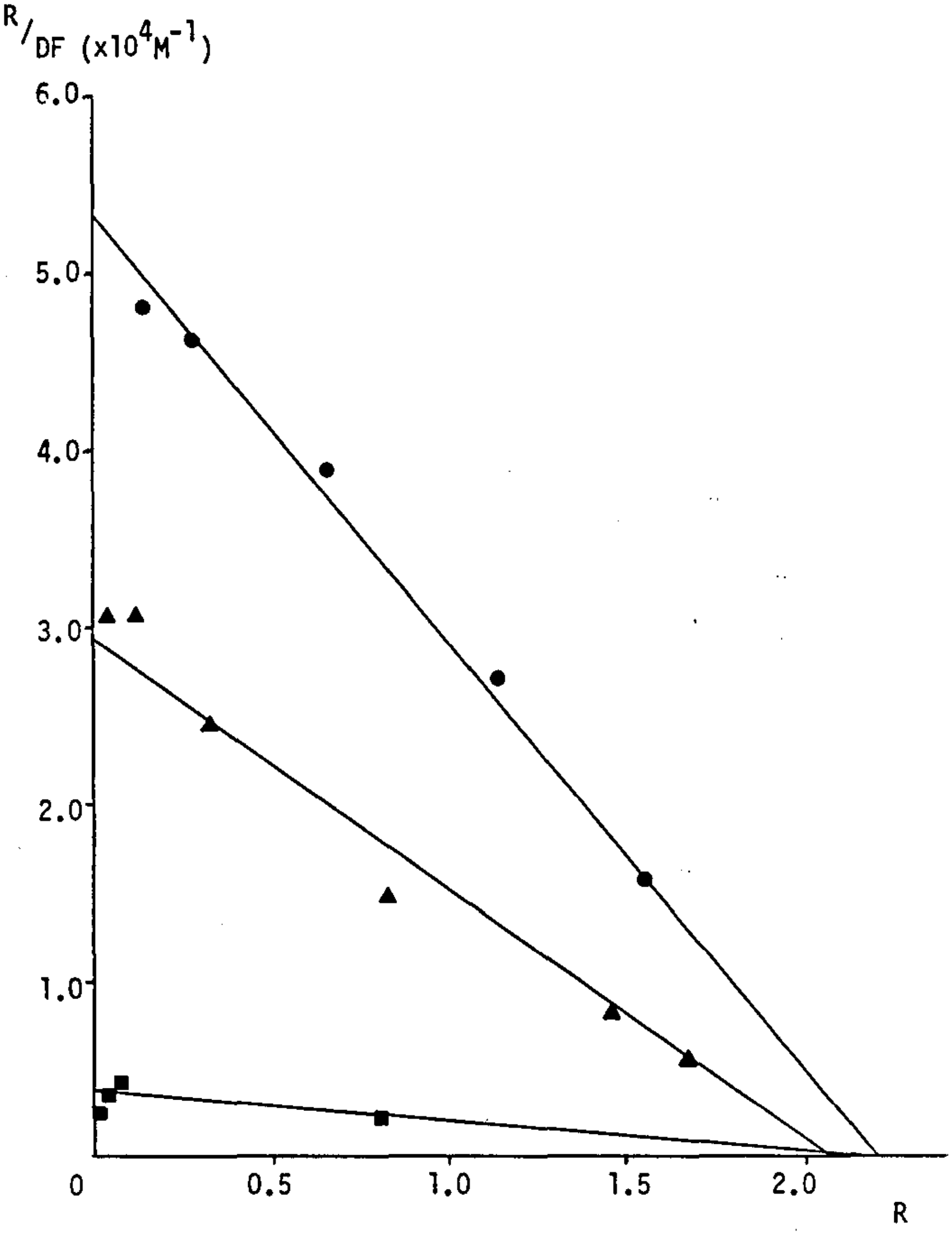

FIGURE 5.8 The Binding of Three Sulphonamide Drugs to HSA as Determined by Equilibrium Dialysis.

- ● Sulphisoxazole ; from Scatchard plot n=2.2, k=2.4x10^{4}M^{-1}.
- ▲ Sulphisomidine ; from Scatchard plot n=2.1, k=1.3x10^{4}M^{-1}.
- ■ Sulphadiazine ; from Scatchard plot n=2.1, k=1.7x10^{3}M^{-1}.

Table 5.5

Equilibrium dialysis	
Advantages:	1. Direct measurement of unbound fraction. 2. Easy interpretation of data. 3. Flexible - there are a large number of techniques available for measuring unbound ligand.
Disadvantages:	1. Tedious and time-consuming. 2. May be complicated by fluid shifts, Donnan effects, instability of reagents, and by non-specific binding of solutes to membranes and cell surfaces. 3. High consumption of reagents. 4. Ligands must be small enough to diffuse readily through membrane. 5. Time to equilibrium dependent on unbound fraction. 6. Limited use in deriving structural information regarding nature of binding sites.
Fluorescent probes	
Advantages:	1. Rapid titrations possible. 2. Low consumption of reagents. 3. Ligands need not be dialysable. 4. May be used over wide concentration range.
Disadvantages:	1. Indirect method for determing free fraction. 2. Attenuation of signal by inner-filter effects, scattered light and background fluorescence. 3. Interpretation of data is complicated. 4. Limited number of suitable fluorescent probes.

precision. The homogeneous fluorimetric procedure on the other hand relies on an indirect measurement of the free fluorescent probe: the bound probe is determined first and the free fraction calculated as the difference between this value and the total probe added. When most of the ligand is bound, the free fraction is perceived as a small difference between two relatively large numbers. Considerable uncertainties may therefore arise in the indirect estimation of small concentrations of free fluorescent probe.

If equilibrium dialysis is more suited to the measurement of small quantities of free ligand, the fluorimetric procedure is better adapted to an estimation of small quantities of bound ligand. With equilibrium dialysis the bound ligand is calculated as the difference between total and free ligand. The fractional error in the measurement of these quantities will be amplified in the bound ligand if the latter is relatively small. So as the bound fraction decreases, results obtained with equilibrium dialysis will become progressively less reliable. With the fluorimetric procedure, the bound probe is higly fluorescent and small quantities can normally be measured with precision.

It is imperative that binding curves obtained using equilibrium dialysis and fluorimetric methods are compared only over the appropriate ranges of free and bound ligand, and that the precision of the results in different regions of the curves is properly appreciated. Any significant disagreements between the two sets of data can then be properly assessed.

The choice of a suitable technique for measuring the unbound ligand in a dialysis cell clearly depends upon the system under study and the quantities of reagents employed.

Although the colourimetric assay of Bratton and Marshall (1939) is of limited sensitivity, it proved adequate for a study of weakly bound and moderately bound sulphonamide drugs. To examine strongly bound sulphonamides, or to permit the use of lower albumin concentrations, it would probably be necessary to produce fluorescent rather than coloured sulphonamide derivatives (Sturgeon and Schulman, 1975).

If equilibrium dialysis is used to study systems in which ligand is very extensively bound - for example, when high affinity antibodies are present - it is necessary to use a very sensitive assay, perhaps involving radioactively labelled ligands of high specific activity. Although this is undoubtedly a very powerful technique and one that has been applied to drug-protein binding studies, there are a number of problems associated with the use of radio-labelled ligands (see Chapter 1).

As far as equilibrium dialysis studies are concerned, it is most convenient if the unbound ligand has some intrinsic property which can be measured directly. For instance, if the free ligand is moderately fluorescent in aqueous buffer it can be determined accurately and simply. This is the case with warfarin. In comparison, ANS is a more 'ideal' fluorescent probe: it is highly fluorescent when bound to proteins but only weakly fluorescent in aqueous solution. Consequently, a straightforward fluorimetric determination of free ANS is not particularly sensitive. Nonetheless, if it is important to measure very small quantities of this ligand resort can be made to a more sensitive assay which involves extracting the ANS into a non-polar solvent and measuring the enhanced fluorescence.

The equilibrium dialysis technique is obviously very flexible. As long as there is some way of measuring the free ligand, it can be applied to virtually any binding study. There are only comparatively few suitable fluorescent probes with which to characterize protein binding sites.

Apart from its general applicability, the widespread use of equilibrium dialysis in drug-protein binding studies and in therapeutic drug monitoring owes much to the clinical significance of the unbound fraction. While other techniques can measure free drug levels, equilibrium dialysis provides the most reliable and often the most sensitive method for determining this important parameter.

In general, the information supplied by equilibrium dialysis experiments is very simple to interpret. This means it is easy to apply the procedure to a quantitative study of drug-protein binding. Nevertheless, its use in the derivation of structural information regarding the nature of the binding sites is very limited. The reverse is often true with fluorescent probes: data interpretation can be quite complicated but valuable information can be obtained about the binding sites themselves. For example, the polarity of the amino acids in the vicinity of the binding site, or the proximity of fluorescent residues such as tryptophan may be revealed.

Equilibrium dialysis is a somewhat tedious and time-consuming technique. Unlike the method of fluorescence enhancement, equilibrium dialysis is unable to exploit the extreme rapidity with which drugs and proteins interact. Equilibrium times of the order of hours are required in spite of the fact that the binding interaction is practically instantaneous. Furthermore, because it is essentially a single-point method, equilibrium dialysis needs numerous separate experiments to complete a binding curve. In comparision, fluorimetric titrations are more rapid to execute and tend to demand less reagent.

Micro-cells have been developed for equilibrium dialysis (Eisen, 1971) and these allow small quantities of material to be tested. They also offer the advantage of shorter equilibration times than those encountered with standard equipment because of the thinner liquid layers. However, extremely sensitive detection systems are necessary because of the small sample volumes.

As well as being inconvenient, long time courses can pose severe practical difficulties in equilibrium dialysis work. Denaturation of the protein is often the most serious problem, but degredation of unstable ligands may also occur. Microbiological growth can interfere with the measurement of free ligand. Fortunately, the drugs and fluorescent probes used in this study appeared to be reasonably stable over long periods. The linear escape curve for warfarin (Figure 5.5) confirmed there was no degredation during the course of dialysis. All the same, it is conceivable that HSA is not entirely stable when rotated for long periods in the dialysis cells.

Other complicating factors associated with equilibrium dialysis are listed in Table 5.5. With the specially designed cells, fluid shifts were shown to be negligible over a wide range of protein concentrations. Non-specific binding of reactants to the dialysis membrane and the cell walls was not encountered, and precautions were taken to minimize Donnan effects. While much elementary considerations are frequently neglected in equilibrium dialysis work (Bridges and Wilson, 1976), the effect of α on the time to equilibrium is rarely mentioned at all in binding studies. If results are to be trusted, it is important to check that equilibrium conditions hold for all values of the unbound fraction.

The dissociation of weakly bound species from albumin during dialysis may be a potential problem. If these are dialysable components they may influence the analytical data. Should fatty acids or other endogenous ligands be removed, this could affect the availability of drug binding sites. Such phenomena may occasionally account for differences between the equilibrium dialysis and spectroscopic assessments of drug-protein binding.

Practical difficulties associated with the fluorimetric titrations have been discussed at length in previous chapters. They include the sensitivity of the bound probe fluorescence to inner-filter effects, and the contributions of unbound probe and total protein to the recorded signal. The relative importance of the interfering factors depends on the choice of fluorescent probe.

The major problem encountered with the fluorimetric assay is in assessing the physical significance of the results. For instance, when a drug binds to albumin it may induce a conformational change in the protein.

Should this structural modification be sufficient to change the spectroscopic properties of a fluorescent probe already bound to albumin, it would be wrong to conclude that there had been a direct displacement interaction involving a specific binding site. However, the good agreement between the results of the equilibrium dialysis and the spectroscopic methods, suggests that the latter provides a valid technique for measuring drug-protein binding.

CHAPTER 6

The Automation of Binding Studies Based on the Principle of Flow Injection Analysis

6.1 Theoretical and Practical Aspects of Continuous Flow Analysis

Over the last 20 years, there has been an increasing demand to use automated methods in chemical analysis. In 1957 Skeggs introduced the idea of air-segmented continuous flow systems to medical laboratory analysis, and equipment based on this principle is now available in most clinical chemistry laboratories. A recent estimate suggests that more than 50,000 continuous flow units are currently in use (Holy, 1982).

For many years following the work of Skeggs (1957), it was assumed that air segmentation of the flowing streams and attainment of a steady-state signal were essential for continuous flow analysis. Lately much interest has focused on a more radical approach which dispenses with the need to mix the sample and reagent intimately and bases analysis on the dispersion patterns produced under laminar flow conditions. The feasibility of this technique was demonstrated independently by Růžička and Hansen (1975), and Stewart et al (1974). They performed similar experiments by injecting samples directly into the carrier stream and have proved that analysis without air segmentation is not only possible but also advantageous. Růžička and Hansen have called the technique flow injection analysis (FIA).

The renewed interest in flow-stream systems using non-segmented analysis is reflected in the expanding literature on FIA. There are a number of excellent reviews of the technique by Růžička and Hansen (1978), Betteridge (1978), Růžička and Hansen (1979b), Růžička and Hansen (1980), Ranger (1981) and Rocks and Riley (1982). A textbook on the subject has also been published (Růžička and Hansen, 1981). Only the essential features of FIA will be covered in this section; more comprehensive treatise are available in the literature.

In FIA a small precise volume of sample is injected into a non-segmented carrier stream of a reagent which moves in a laminar flow towards and through a suitable detector. The simplest flow injection system (Figure 6.1(a)) consists of a pump P which is used to propel a carrier stream of reagent R through a thin tube; an injection port, by means of which a well-defined volume of a sample solution S is injected into the

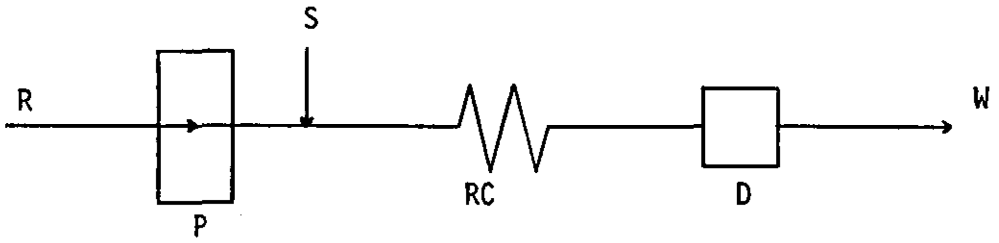

(a) Simple FIA System.

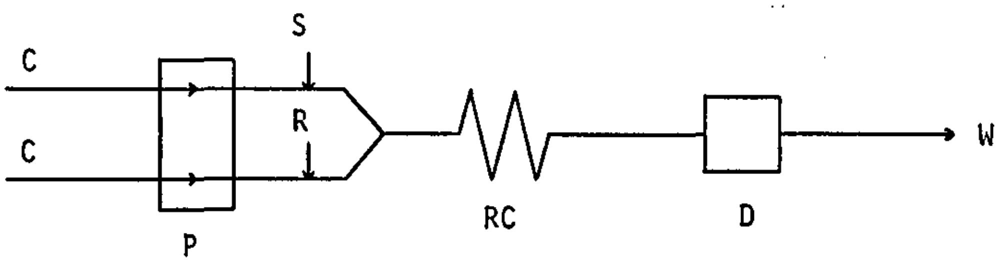

(b) Synchronous Merging Zone FIA System.

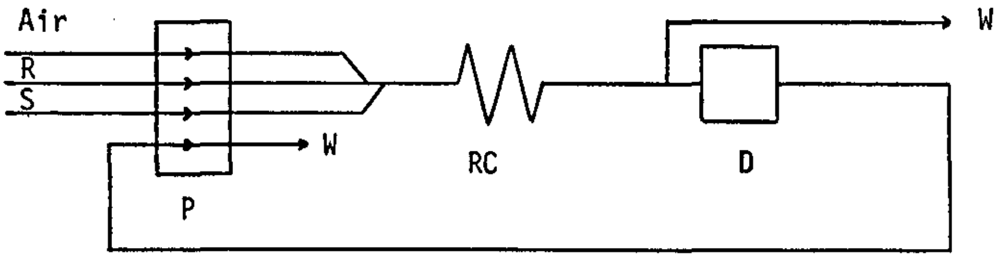
Air
W
R
S
W
RC
D
P

(c) Simple Gas Segmented System

FIGURE 6.1 Configurations of Different Continuous Flow Systems

S - sample, R - reagent, P - pump, RC - reaction coil, D - detector, W - waste, C - inert carrier.

carrier; a reaction coil RC in which the sample zone disperses and reacts with the components of the carrier stream; and a flow-through detector from which the measured stream passes to waste W.

In practice the technique is founded on a combination of three principles: precise sample injection, controllable sample dispersion and reproducible timing. However, the most important feature of FIA, and the one which distinguishes it from other forms of continuous flow analysis, is the presence of a sample-carrier interface over which concentration gradients develop during the course of analysis. The conditions governing the dispersion of the sample zone in the flowing carrier stream are considered below: manipulation of the dispersion allows particular analytical requirements to be satisfied.

When water flows slowly and steadily through a pipe the frictional forces between the layers of moving liquid establish a longitudinal velocity profile. Under such conditions of laminar flow the velocity at the walls is zero, and that at the centre is twice the mean (Taylor, 1953). This gives rise to a parabolic velocity profile (Figure 6.2(a)). In the absence of molecular diffusion, a sample placed into a moving stream would take up the shape shown in Figure 6.2(b). Under these theoretical conditions, the sample would have an infinitely long tail by the time it reached the detector and there would be an unacceptable carry over between samples. Fortunately, because of molecular diffusion, this case does not arise. Diffusion of molecules between the carrier and sample plug serves to limit the convective dispersion and effectively mixes sample and reagent. This process is illustrated in Figure 6.2(b). A molecule (A) placed centrally in the plug will tend to diffuse into a region of lower concentration; by so doing there is a high probability that it will move into a layer of liquid moving at a slower longitudinal velocity. Thus radial diffusion (diffusion perpendicular to the direction of flow) modifies the shape of the leading edge of the sample plug. A molecule originally in position B likewise diffuses into the carrier solution; in this case it encounters a layer of faster moving liquid which carries it towards the centre of the sample zone. So sample and carrier molecules, the latter including reagent, are mixed. Of course longitudinal diffusion of the sample molecules also occurs. However, Taylor (1953) showed that dispersion by longitudinal diffusion can be ignored relative to that caused by the main flow pattern, whereas radial diffusion is always important in narrow tubes and at low flow rates it may even be the major mechanism for sample dispersion. The moderating effect of diffusion-induced dispersion on the longitudinal dispersion caused by

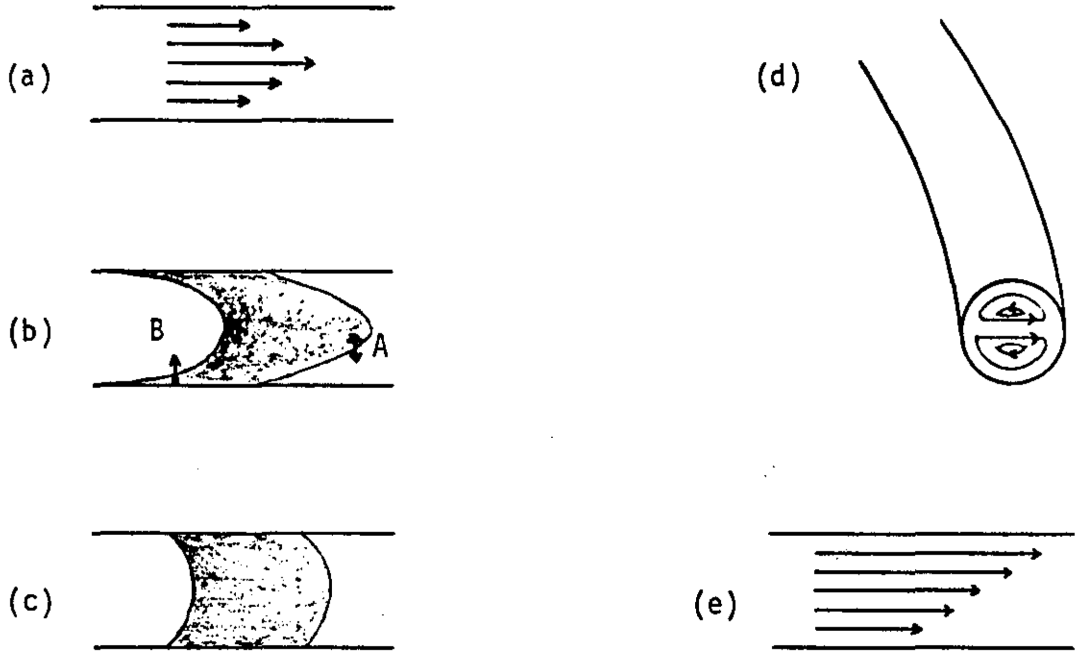

FIGURE 6.2 Velocity Profiles and Shapes of Injected Sample Zones.

(a) Laminar flow, parabolic velocity profile.
(b) Sample dispersion caused by laminar flow without diffusion.
(c) Sample shape resulting from laminar flow with molecular diffusion.
(d) Secondary flow pattern in cross-section of tightly coiled tube at high velocity.
(e) Velocity profile in coiled tubes at high flow velocity.

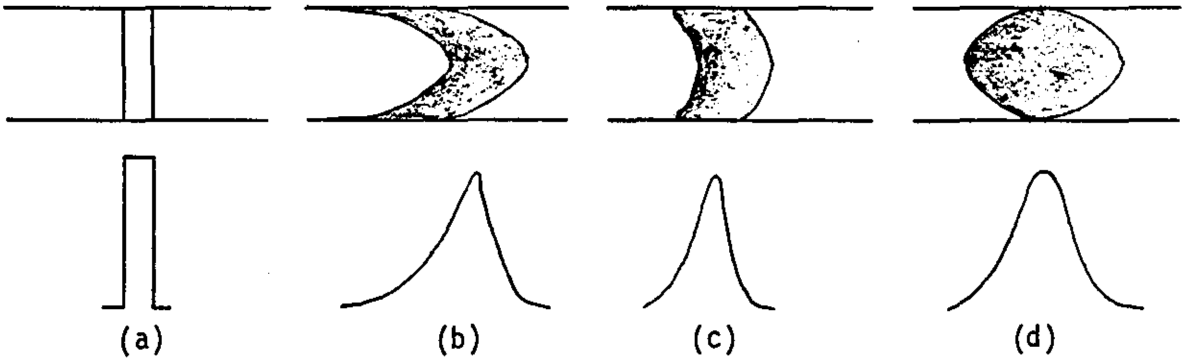

FIGURE 6.3 Diagrammatic Representation of Effects of Convection and Radial Diffusion on Concentration Profiles of Samples Monitored at a Suitable Distance Downstream from Injection.

(a) No dispersion.
(b) Dispersion predominantly by convection.
(c) Dispersion by convection and diffusion.
(d) Dispersion predominantly by diffusion.

the carrier flow is shown in Figure 6.2(c) and explains the low carryover and high sample throughput possible with FIA.

Originally the low carryover of FIA was attributed to turbulent flow (Růžička and Hansen, 1975). A set of key experiments by Betteridge and Růžička (1976) suggested that the mixing process was diffusion controlled and this was strengthened by the discovery of Taylor's paper. It is now recognized that FIA operates effectively only under conditions of laminar flow (Betteridge, 1978) and the misconception that turbulent flow is essential has been dispelled.

While Taylor (1953) derived a mathematical description of dispersion related to convective flow and molecular diffusion, Růžička and Hansen (1978) borrowed the chemical engineering model of 'tanks-in-series' to explain dispersion and concentration profiles in FIA systems and to identify the main variables that can be manipulated to achieve the desired degree of mixing. Reijn et al (1980) have also presented some theoretical aspects of FIA. Only the practical implications of these studies will be considered here.

The physical dispersion of the sample cone between the points of injection and detection is reflected in the peaks recorded by the flow-through detector (Figure 6.3). The relative importance of the dispersive processes depends upon the choice of experimental parameters. Changes in the flow rate, tube diameter, injected volume, line length, diffusion coefficient of the analyte, or any combination of these factors can alter the dispersion of the sample in the carrier stream as seen by the detector.

Sample size is a very important analytical parameter and has a marked effect on peak shape. Růžička and Hansen (1981) have considered the effect of sample size on dispersion separately from that due to the flow. They showed that if increasing volumes of dyed solution are injected into a flow stream, the height of individual peaks will increase until an upper limit or steady state has been reached. At this stage the recorded signal will correspond very closely to the concentration of undiluted dye and the dispersion D will be virtually unity. If $S_{\frac{1}{2}}$ is the volume of sample required to reach 50% of the steady state signal, injecting two $S_{\frac{1}{2}}$ volumes gives 75% of the maximum signal corresponding to D=1.33, and so on. So D=1 can never truly be reached in FIA. For a limited dispersion of the sample zone, approximately two $S_{\frac{1}{2}}$ volumes are required; in other applications less than one $S_{\frac{1}{2}}$ will suffice. The effects of sample size are considered in Section 6.2.

It is clear that the peak shape will also be influenced by the sample and carrier matrices because the whole of the plug, matrix and sample is diffusing into the carrier. The higher the viscosity of a particular sample, the lower its dispersion (Betteridge and Růžička, 1976); therefore a more viscous sample zone will be less effectively mixed with the carrier stream. This may be an important consideration when dealing with serum samples.

To give large signals and a high throughput with minimum carryover, longitudinal dispersion of the sample zone should be kept as small as possible. Coiled tubes are useful in this context because they are better than straight tubes at limiting this type of dispersion. At high flow velocities in tightly coiled narrow-bore tubes, centrifugal forces generate a secondary flow perpendicular to the main axial flow (Figure 6.2(d)). Axial flow velocity being greatest near the centre of the tube, centrifugal forces will cause fluid near the centre to be forced towards the outer wall. This modifies the parabolic velocity profile and produces an approximately linear profile (Figure 6.2(e)) which limits sample dispersion and permits a very high sample throughput.

There are other factors to control when maximizing throughput. The smallest sample size consistent with adequate sensitivity should be selected, and both the line length (distance between the points of sample injection and detection) and the tube diameter should be small. The line length is an important variable in controlling throughput because the sample dispersion increases as the square root of the distance travelled. In theory, it is even more appropriate to limit dispersion by reducing the bore of the tubing. Tubes with internal diameters of more than about 1.0mm are unsuitable because of excessive carryover. On the other hand, practical considerations exclude the use of very narrow tubes. For instance, reaction tubes of less than 0.3mm internal diameter are easily blocked and at lengths greater than 1 or 2m they may cause sufficient back pressure to prevent the maintenance of a reasonable flow rate. Furthermore, as the most commonly used detector - the spectrophotometer - requires an optical path length of at least 0.5mm, narrower manifold tubing can cause non-uniformity of flow just in the region where the sample is measured. The choice of tube diameters is therefore rather restricted in FIA; 0.3mm to 0.8mm covers the range of acceptable internal diameters.

Between the points of injection and detection the sample plug will have been physically dispersed to a degree which is governed by the flow conditions. In addition, some chemical reactions may have taken place at the sample-carrier interface. The recorded signal will reflect both processes.

The analytical readout in FIA is usually obtained from the peak height, which in turn is related to sample concentration. Růžička and Hansen (1978) define dispersion D as the ratio of the concentration of the sample solution before and after the dispersive process has taken place. This provides a simple practical method of measuring dispersion and allows one set of flow conditions to be compared with another. Dispersion can be classified as limited (D=1-3), medium (D=3-15) and large (D>15). The different degrees of dispersion can be employed in the following ways.

If the original composition of the sample solution is to be measured, dispersion in the flow stream should be limited so that the readout obtained at the centre of the sample zone is not affected by any mixing with the carrier molecules. Hence, with limited dispersion the sample integrity is maintained to a high degree. This is ideal when little or no dilution of the sample is required and the flow injection system is simply serving as a delivery system for the introduction of samples into measuring devices. As the samples undergo little dispersion, very high throughputs are possible.

Medium dispersion is of prime importance in this study. It encompasses numerous analytical applications in which the sample zone is mixed with the carrier stream, or perhaps with several reagents in sequence, to produce a reaction product that can be measured by a flow-through detector. The centre of the sample zone must be mixed effectively with the reagent molecules and so for many systems the extent and rate of chemical interactions have to be taken into account when designing suitable flow conditions. Not only must sufficient mixing take place between the sample zone and reagent, but the residence time must be long enough to allow adequate formation of the products before the detector is reached. In this work a suitable compromise is sought between the requirements of mixing and reaction time on the one hand and maximum acceptable broadening of the sample zone on the other because an increase in zone width lowers the sampling frequency. For slow reactions, then, the residence time should be extended by decreasing the velocity of the carrier stream, not by increasing the line length. The latter would tend to increase dispersion and produce band broadening. To cater for slow chemical reactions it is often best to select flow conditions where the reaction is incomplete but reproducible. This is possible with FIA since the high reproducibility of mixing and timing in the non-segmented stream produces a valid analytical result without the need to reach equilibrium.

Large dispersion may be exploited to obtain a suitable sample dilution or to produce a concentration gradient which is stretched over a longer period of time. A sample which is too concentrated for assay can be injected into a manifold designed to give a high dispersion and so be effectively diluted. Very highly dispersed patterns, best produced by including a mixing chamber between the injection port and the detector, have been used to perform flow injection titrations.

As mentioned previously, reproducible timing is an important feature of FIA. Clearly, the time which elapses between the introduction of the sample into the carrier stream and its arrival at the detector depends upon the flow rate. Since there are no compressible gas bubbles in flow-injection manifolds, even extremely short residence times can be maintained reproducibily. Nonetheless, if the signal is to be read on the rapidly ascending part of the response curve, it is essential to check that the timing is well-controlled; any fluctuations in flow rate that affect the residence time of the sample in the system will result in imprecise peak heights. There are several ways of achieving the constant steady flow of fluids necessary for quantitative FIA.

Peristaltic pumps are commonly used to propel the carrier stream in flow injection systems. The main drawback of the peristaltic pump is that the stream is never completely pulse-free. Well-designed pumps with many closely spaced rollers are often acceptable because they tend to generate a pulsation of high frequency but low amplitude. Sometimes, however, damping devices are required with peristatic pumps in order to reduce pulsation of the carrier stream. Constant pressure-head devices, on the other hand, provide pulse-free flow patterns but they are not as versatile as peristaltic pumps. For simple flow-injection experiments, a pressurized gas will give a uniform flow.

Once a steady flow has been established by the pumping system, it should not be disrupted by other units connected to the manifold. Avoiding perturbation of the carrier stream is of prime concern when designing the sample injection valve. Ideally the injection process should place a well-defined sample zone of precise volume and short duration into the continuously moving carrier stream without disturbing the latter at all.

The first of the inlet systems to gain widespread acceptance was the simple flap valve shown in Figure 6.4(a) and devised by Růžička and Hansen (1975). Its main shortcoming is its reliance on the skill of the operator; the volume of the sample is controlled by the position of the plunger and the form of the injected plug depends on the speed with which the plunger is depressed. When disposable plastic syringes are used, the minimum reproducible sample volume may be rather large for routine work.

In comparison to flap valves, rotary injection valves offer a more practical way of introducing precise sample volumes into the carrier stream. With this system two independent flow systems are used. The rotary valve shown in Figure 6.4(b) consists of a moveable core furnished with a volumetric cavity for containing the sample, and a bypass which allows the carrier stream to flow uninterupted while the volumetric cavity is in the "fill" position. The filling may be done with a syringe or by aspiration with a pump. When the valve is turned into the inject position, the sample plug is swept directly into the carrier stream because the bypass is adjusted to have a higher hydrodynamic resistance than the volumetric cavity. After a specified time, the valve is returned to its initial position where it is washed and filled with another sample while the analysis proceeds. This injection system produces minimal disruption of the carrier stream and allows small volumes to be dispensed very precisely.

Turbulence in the flow stream can also be minimized by ensuring that connections between the various components of the manifild have a low dead volume. It is particularly important to avoid turbulent flow in the detector. Coils and connecting lengths of tubing should be well attached on a solid support so that the flow path remains unchanged during each set of experiments. If loose pieces of tubing are moved and the radius of bent sections altered inadvertantly, flow patterns and hence peak shapes may be affected.

The technique described so far consists of a single flowing reagent carrier stream into which is injected a sample of precise volume. The resulting product is measured downstream (see Figure 6.1(a)). A number of refinements to this basic technique have extended the scope of the method. Since they proved useful in the present study, two important developments are discussed below.

The stopped-flow technique allows reaction kinetics to be examined. By a carefully controlled intermittant pumping, the sample zone can be moved through the flow line until the reagent and sample have mixed to the required degree. Stopping the carrier stream so that the reaction proceeds in the flow cell permits rate measurements to be made. Of course, such a reaction rate measurement will only be successful if the movement of the carrier stream is brought to a complete standstill so that the same section of the sample zone is held within the flow cell during the course of the reaction. Indeed FIA theory shows that when the carrier stream is held stationary, dispersion of the sample zone will cease - except for a negligible contribution from molecular diffusion - and remain constant irrespective of the period of residence in the flow cell (Růžička and Hansen, 1979a).

Another reason for operating a flow-injection system in the stopped-flow mode is to increase the sensitivity of measurement. This is applicable if an extension of the residence time improves the yield of detectable product. Thus Lim et al (1980) increased the sensitivity of an automated immunoassay procedure by stopping the flow in a heated reaction coil and allowing sufficient reaction products to develop before pumping the sample zone through the detector.

The second refinement to the conventional flow injection technique avoids the relatively high reagent consumption which is the main disadvantage of all continuous flow systems. This is the method of merging zones first described by Bergamin et al (1978) and illustrated diagramatically in Figure 6.1(b). Unlike the basic technique which consumes reagent continuously even when no sample is present in the apparatus, the principle of merging zones is based on the injection of sample and reagent plugs into separate inert carrier streams which are synchronized so that the sample and reagent met and mix in a reproducible manner. Distilled water or dilute buffer may be used as a carrier in both streams. Thus only very small quantities of reagent are required per test and no reagent is used during start-up or shut-down.

A novel method of dealing with concentrated samples based on the merging zone principle was developed by Mindegaard (1979). Sample and reagent were injected slightly out of synchrony so that the reagent just overlapped the dilute tail of the sample zone. By this method, serum albumin was measured in undiluted samples. Braithwaite and Miller (1979) have also applied flow injection analysis to the determination of albumin in whole serum.

Rather surprisingly, while FIA has proved useful in fields as diverse as water and environmental control, and agricultural and pharmaceutical analysis, relatively few clinical chemists have so far exploited this new concept (Rocks and Riley, 1982). Nonetheless, FIA appeared to offer the best means for automation of the drug-protein binding studies described in earlier chapters and, as outlined below, the technique had a number of important advantages over gas-segmented flow analysis.

Conventional continuous flow analysers are based on the use of air-segmented streams. The purpose of segmentation is to prevent sample carryover and to assist in mixing. In such analysers the samples are successively aspirated from individual wells into a tube and forwarded through a pump where the flowing stream is regularly segmented by air bubbles delivered by another pump. Further downstream a reagent is added to all individual segments which then pass through a reaction coil. Before signals are recorded the air segmentation has to be removed in a debubbler. To allow for the introduction and removal of air from the liquid stream, gas-segmented flow analysers tend to be relatively complicated. As shown in Figure 6.1(c), even the simplest chemistry requires a four-channel pump; the corresponding flow injection system needs only one channel (Figure 6.1(a)).

The compressibility of the bubbles in air segmented streams leads to a pulsating flow. The uneven flow, coupled with the fact that the sample has to travel through the pump, means that exact timing is not possible in segmented continuous flow analysers. To minimize the effects of irregularities in the sampling time, bubble-segmented systems are designed to attain at least 95% of the steady state signal. Besides reducing the throughput, this requires larger sample volumes than are used in FIA. Since the movement of a segmented carrier stream can not be stopped and restarted nearly as exactly as a nonsegmented stream, continuous kinetic analysis is not possible in gas segmented flow systems.

Both types of continuous flow analyser are known to give a similar reproducibility of measurement. However, while wash cycles are necessary in gas-segmented analysis to prevent sample carryover, they are not required in FIA.

So there were clearly a number of technical reasons for favouring FIA over conventional continuous flow analysis: these included a higher sampling rate, a more rapid readout and a smaller sample volume. The flow injection system was also much cheaper and simpler to construct in the laboratory. Most importantly, though, dispersion of the sample zone could be controlled in FIA and this offered a more flexible approach to the automation of the drug-protein binding studies.

Although there is an obvious need for automation in analytical and clinical chemistry, there are no other reports in the literature concerning the application of FIA to the study of drug-protein interactions.

6.2 The Application of FIA to a Study of Drug-Protein Binding using Fluorimetric Detection

The feasibility of applying single channel conventional FIA to a study of the binding of ligands to HSA was assessed in a series of preliminary experiments. The marked increase in fluorescence exhibited by ANS on binding to albumin offered a simple means of monitoring the course of the interaction in the flow stream. The effects of line length, flow rate, sample volume and residence time were examined in an attempt to produce acceptable peak heights and sampling frequencies.

A simple septum or flap injection valve, similar to the one depicted in Figure 6.4(a), was used in the initial studies. Tubing having an internal diameter of 0.76mm ran between the injection valve and a silica flow-cell positioned centrally in the sample compartment of the fluorimeter (Baird Atomic Fluoripoint Spectrofluorimeter). The carrier stream was propelled by a peristaltic pump (Mini-S type, Ismatec, Zurich) or by a constant head device. The fewest possible connections were employed between the flow line and the other components of the manifold. In a further effort to preserve the laminar flow of the carrier, care was taken to avoid dead volumes at junction points. ANS was used as the carrier reagent and small volumes of a solution of HSA were injected manually through the flap valve. Peak profiles were recorded by measuring the fluorescence in the flow cell using wavelengths corresponding to the excitation and emission maxima of albumin-bound ANS.

Suitable flow rates were readily established with the peristaltic pump. Unfortunately, the peaks suffered considerable distortion due to pulsation of the carrier stream. Pulsing was reduced by including a coiled tube between the pump and the sample injection port. Nonetheless, even very long lengths of tubing were incapable of totally suppressing pulsation of the carrier stream. A constant pressure head in the form of a Mariotte flask (Pharmacia Uppsala, Sweden) was used to propel the carrier stream. This simple method produced completely pulse-free flow patterns and was used routinely in the flow injection studies.

The effect of various parameters on peak shape and height were investigated using a flow rate of 1.1 ml min^{-1} and a line length of 60cm. The concentration of ANS in the carrier stream was 5 x 10^{-6}M, and the injected sample comprised a 5 x 10^{-6}M solution of HSA. The diluent for both carrier and reagent was 0.1M Tris/HCl pH 7.4.

When 50μl sample volumes were used reproducible signals were obtained but these tended to be in the form of double peaks. Clearly, en route to the detector there had been insufficient dispersion to allow effective mixing and subsequent interaction between the centre of the sample zone and the carrier stream. While albumin at the leading and tailing edges of the sample

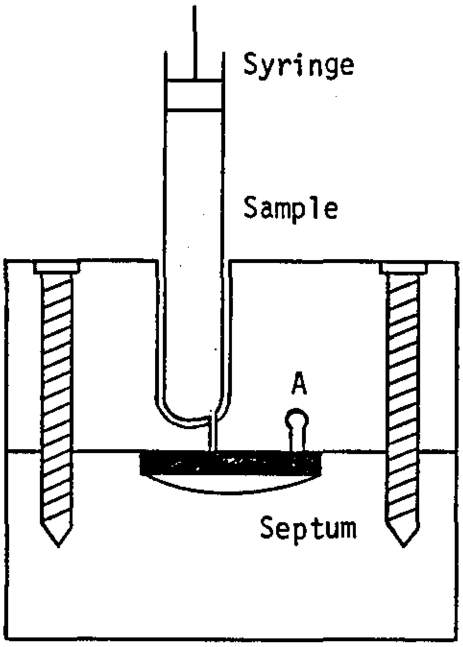

(a) Sample Flap Injection Valve

Cross-section of flap valve. Carrier flows through A. On depression of syringe, septum is forced down and sample occupies resulting depression. Septum regains original position and forces sample into carrier stream.

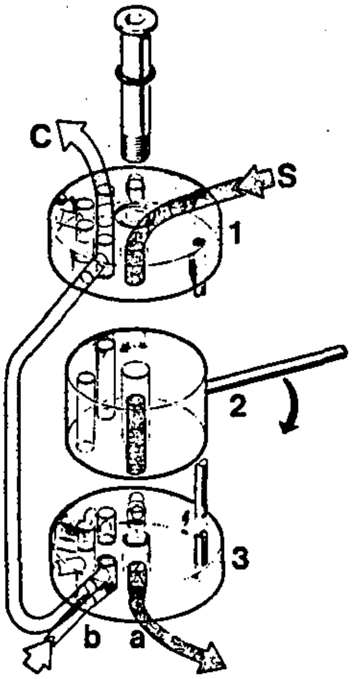

(b) Rotary injection valve.

Multi-injection valve consisting of a rotor(2) sandwiched between two stators (1 and 3), the whole being clamped together by a bolt. The rotor has three volumetric bores of which one is shown filled by sample solution S, the excess of which is drained through the bottom stator at (a). In the rotor position shown, the carrier stream C bypasses the rotor via a shunt, entering the valve through the bottom stator at (b). After turning the rotor in the direction indicated the sample zone is swept by the carrier stream into the system because the bypass conduit has a higher hydrodynamic flow resistance.

FIGURE 6.4 Injection Valves.

plug had reacted with ANS to give measureable quantities of the highly fluorescent product, the central segment was largely devoid of the bound species and produced a trough in the output signal.

Experiments using the stopped-flow technique showed that these double peaks could be transformed into single peaks of higher intensity. A delay of one minute was found to be sufficient to allow almost complete binding of sample and reagent under the specified conditions.

As expected, an increased dispersion of the sample zone in the flowing reagent stream also resulted in single peaks. This was achieved by inserting a coil between the injection port and the detector. The increased dispersion produced broadening of the samples peaks and so reduced the maximum sampling rate.

Without stopping the carrier stream or inserting a coiled tube in the flow line, the consequences of lowering the sample size were noted. Under these conditions of low total dispersion, decreasing the volume of HSA injected from 50 to 20μl had no effect on peak height. For premixed samples this would correspond to a steady-state signal. However, with a 20μl sample volume, thorough mixing was achieved in the flow stream; single peaks were observed and the height of the response curves could not be increased by stopping the flow. Below 20μl, the peak heights decreased with sample volume and below about 10μl the signal was proportional to the injected volume. So, in order to exhibit the necessary degree of dispersion, the flow system demanded a sample volume of 20μl or less.

Employing the simple single-channel arrangement, using a flow rate of 1.1ml min^{-1}, a line length of 60cm and injecting 20μl sample volumes, preliminary observations were made on the displacement of ANS from HSA by flufenamic acid. While the displacement interaction was clearly demonstrated (see Figure 6.5), the equipment fell short of the requirements necessary for a routine quantitative study of drug-protein binding. The shortcomings of the flap injection valve were severe, particularly when such small sample volumes were required; peak heights were of poor reproducibility and depended to a large degree on the technique of the operator. A more sophisticated system was required to exploit the potential of the flow injection technique.

A commercially available double-injection valve and modular FIA system (Bifok, Sollentuna, Sweden) offered a number of advantages over the conventional single channel arrangement. The Bifok rotary injection valve allowed the sampling procedure to be partially automated. This meant that small samples could be injected precisely without disrupting the carrier

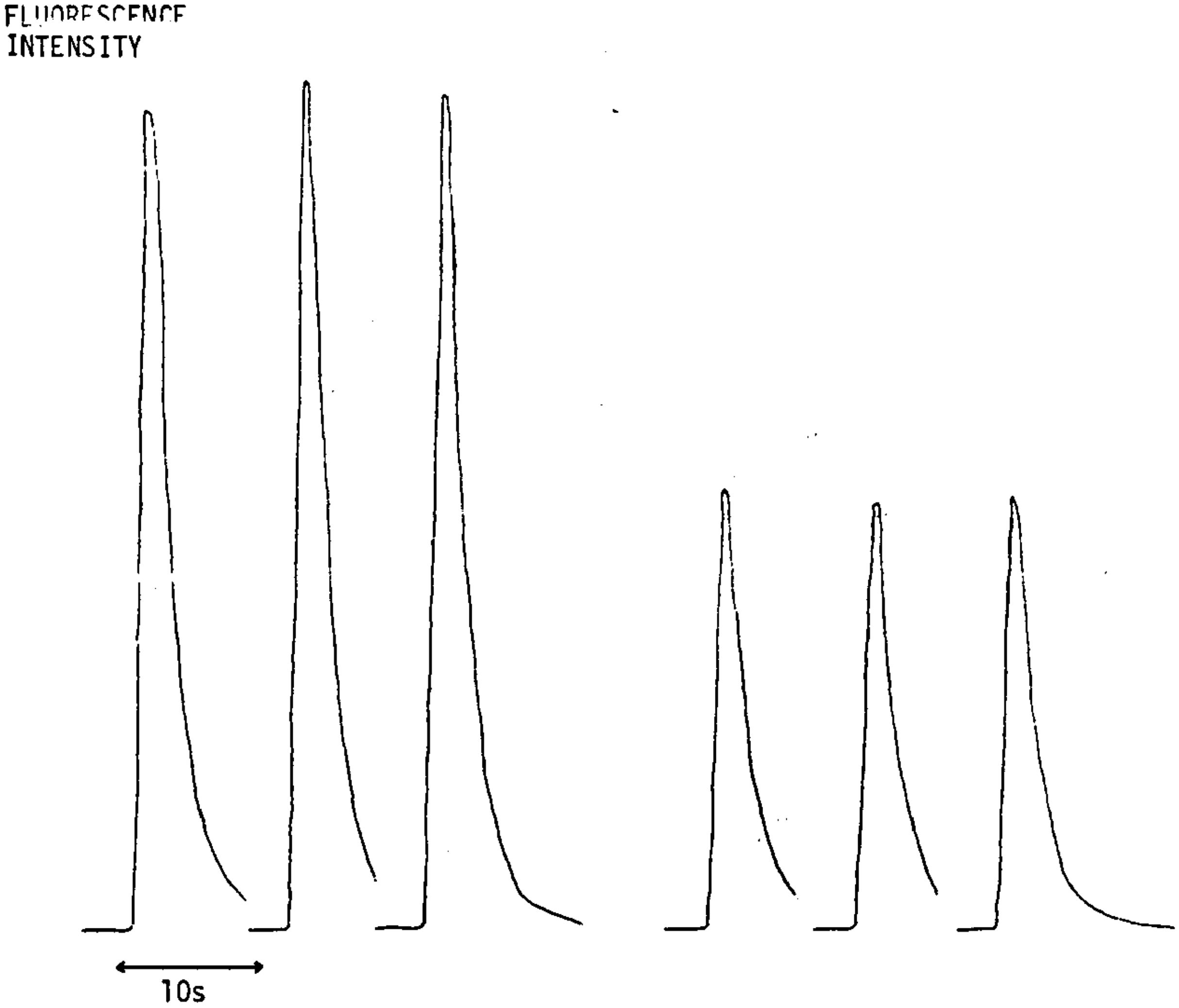

FIGURE 6.5 The Displacement of ANS from Human Serum Albumin by Flufenamic Acid; Conventional FIA Technique.

20µl sample volumes were injected via the flap valve into a carrier stream containing 5 x 10^{-6}M ANS. In the first series of peaks the samples were aliquots of a 5 x 10^{-6}M HSA solution in the second series, albumin samples contained 2 x 10^{-5}M flufenamic acid.

stream. The manifold components in the system could be arranged in any desired sequence and were designed to fit together with the minimum dead volume. Standard HPLC connections between the manifold tubes also helped to suppress the creation of turbulent flow. The modular design of this system and the double-injection facility gave a far greater flexibility of operation than had been possible with the simple equipment.

The double-injection valve was particularly suited to the technique of merging zones. This refinement allowed binding studies to be performed with even greater economy of reagents. Drug and protein solutions were made up in 0.1M Tris/HCl pH 7.4 and the same buffer was used as the carrier stream. The sample (HSA) and reagent (ANS) solutions were injected into separate carrier streams (see Figure 6.1(b)). The inert buffer carrier streams were synchronized so that the reagent and sample zones merged and partially mixed. For further mixing the reagent/sample zone was passed through a short length of coiled tubing before it entered the flow cell in the fluorimeter.

To check that the two zones arrived simultaneously at the confluence of the separate buffer streams, air bubbles were injected into both lines. Since the peristallic pump again produced unacceptable pulsing, Mariotte flasks were set up on both carrier streams in symmetrical fashion. For fine adjustments to the merging of the bubbles, the vertical heights of the flasks could be altered slightly. As a further test of the accuracy of merging, and to ensure that viscosity differences between the sample and the reagent did not significantly change their flow rate, solutions were visualized with bromophenol blue. The dye was not present during the binding studies.

An electronic timing device was used routinely with the rotary injection valve. This device controls the length of the injection period when sample is being swept from the volumetric cavity into the carrier stream. It is possible to inject all the sample contained in the cavity by allowing a long clearance time. If prefered, however, the tail of the sample zone may be restricted by letting the motor return the rotor to the load position before all the sample has been cleared. In practice, there was no need to reduce tailing and a convenient sample volume could be obtained by injecting all of the material contained in the volumetric cavity. Furthermore, a lower reproducibility of injection is probably obtained when only partial sample clearance is allowed (Růžička and Hansen, 1981).

To monitor the clearance of material from the volumetric cavities of the double-injection valve, albumin and ANS were injected simultaneously into the two carrier streams and the fluorescent product was measured downstream. For a given flow rate, the peak heights showed an initial increase with the clearance time. However, when sufficient time had been allocated to allow removal of all the sample and reagent from the injection manifold, the peak heights reached a limiting maximum which was independent of further increases in the clearance time. Thus the correct setting for the electronic timer was established for the appropriate flow rate.

Merging zone FIA was employed successfully in two separate studies. The first involved an assessment of the capacity of a number of drugs to displace warfarin and ANS from both albumin and serum binding sites. The second application demonstrated the feasibility of producing complete binding curves using flow injection analysis.

The displacement of ANS from HSA was performed under controlled conditions. The flow rate in these experiments was 1.4ml min^{-1} and the timer on the injection valve was set at 3.0s. This meant that 35µl of sample (HSA) and reagent (ANS) were consumed for each operation of the valve. The internal diameter of the tubing was 0.76mm. The volume of the silica flow cell was 45µl. The time lapse between the merging of the sample and reagent zones, and the arrival of material in the fluorimeter flow-cell was 15s, corresponding to a line length of 45cm. Peak heights were measured with the excitation and emission monochromators set at 375mm and 470mm, respectively. Under the given flow conditions, and with the specified amounts of material, the reaction between HSA and ANS appeared to have reached completion before passing through the fluorimeter; stopping the carrier flow and hence increasing the incubation period had no effect on peak heights. Sampling rates of 60 samples hr^{-1} were possible without incurring carryover.

The sample and reagent concentrations were selected so that the bound probe fraction was large. This ensured that subsequent displacement interactions were concerned mainly with primary binding sites. Hence solutions of 10^{-5}M HSA and 10^{-5}M ANS were injected into the separate carrier streams. At least five peaks were recorded. Immediately afterwards, the same concentrations of albumin and fluorescent probe were injected, but the latter contained either 10^{-4} or 10^{-5}M quantities of a competitor drug. Again several consecutive signals were recorded.

When solutions containing albumin and ANS were injected separately into the carrier stream, no fluorescence could be detected at the analytical wavelength. The inner-filter effects were also shown to be negligible. Consequently, the signals recorded after merging of the sample and reagent zones were dependent only upon the concentration of bound fluorescent probe. None of the competitor drugs had measurable inner-filter effects. Any decrease in the recorded signal was therefore interpreted as a displacement of the bound fluorescent probe from HSA.

The displacement of ANS from serum binding sites was studied using the same merging zone FIA system. Serum samples were diluted 50-fold in Tris/HCl buffer prior to assay. A very small background signal was detected from the serum itself but this did not complicate interpretation of the results.

A similar flow injection procedure was followed when studying the effect of a number of drugs on the binding of warfarin to HSA. Here, 6×10^{-5}M HSA and 1×10^{-5}M warfarin solutions were injected simultaneously into the separate carrier streams. The effects of incorporating different drugs into the warfarin solution were recorded as changes in the peak heights. The ratio of albumin to warfarin was chosen so that the high affinity sites on the protein molecule were unsaturated. The absolute quantities of the reactants provided sufficient sensitivity for the accurate measurement of peak signals, but the albumin concentration was kept low enough to avoid the problems encountered with viscous samples.

While warfarin itself had a negligible inner-filter effect, the blanks in the assay were not zero. A small signal was detected from both the albumin and the free fraction of the fluorescent probe. Consequently there was not a truly linear relationship between the peak height recorded by the fluorimeter and the concentration of bound fluorescent probe. Nevertheless, because the bound probe contributed by far the greater part of the signal, the error in calculating the fraction displaced directly from the peak height was small. Furthermore, this discrepancy could be completely rectified by recalling the degree to which the fluorescence of warfarin was enhanced on binding to albumin.

Of the potential competitor drugs investigated, only flufenamic acid had a significant inner-filter effect. At the higher concentration tested, it reduced the measured signal by 1.5%. This small attenuation of the fluorescence was taken into consideration when calculating the quantity of warfarin displaced by flufenamic acid.

The second major application of the merging zone technique concerned the production of a complete Scatchard plot. The aim was to describe the binding of ANS to HSA over a wide concentration range. To give adequate sensitivity, the Perkin-Elmer model MPF 44B fluorescence spectrometer was used as the detector. Preliminary work confirmed that this instrument was powerful enough to record signals from the most dilute samples. No other changes were made to the merging zone flow injection system already described.

As usual, solutions were made up in 0.1M Tris/HCl pH 7.4 and the same buffer was employed as the carrier. A flow rate of 3.0ml min^{-1} was employed. Using a clearance time of 5s, 35μl volumes of ANS and HSA solutions were released simultaneously into the separate carrier streams from the double injection valve. Injections were performed at one minute intervals. Fluorescence intensities were measured at 460nm using an excitation wavelength of 375nm and a spectral bandwidth of 20nm. HSA and ANS solutions were maintained at 23°C ± 0.5°C immediately prior to injection.

The fluorescence intensity of unit concentration of bound probe was determined by measuring peak heights obtained with HSA:ANS ratios of greater than 10:1. Under these conditions, the albumin was able to accommodate essentially all of the injected fluorescent probe. However the stopped-flow technique was used to check that the binding interaction had reached completion before the sample zone passed through the detector.

Variations in detector response or carrier flow patterns were monitored by measuring the fluorescence emitted by quinine sulphate solutions injected into the buffer stream. This was done before each sample measurement and formed a series of useful reference peaks.

Over an appropriate range of concentrations, no signals could be detected when HSA or ANS alone were released into the carrier stream. The linearity of the response of the detector to bound fluorescent probe was established by plotting peak heights against concentration of bound probe. In addition, inner-filter effects were shown to be negligible. Hence when a 5×10^{-5}M solution of HSA was injected into one carrier stream and increasing quantities of ANS into the other, it was a simple matter to convert intensity measurements into concentrations of bound fluorescent probe. A knowledge of the total concentration of ANS in each injected plug allowed the unbound concentrations to be found by difference.

To determine the absolute concentration of HSA at the point of detection, it was necessary to measure the extent to which the sample had been dispersed during its passage along the flow line. A solution containing known concentrations of albumin and ANS was placed in the flow cell and the steady-state signal recorded. The same concentrations of protein and fluorescent probe were injected into the synchronized carrier streams and following the standard procedure, the product was measured in the flow cell. The ratio of the steady-state signal to the FIA peak heights gave an accurate estimation of the dispersion within the flow system. Sufficient information had then been accumulated to allow for the construction of a complete Scatchard plot.

6.3 Results Obtained using the Flow System

The peaks presented in Figure 6.5 show how a conventional flow injection system can be used to demonstrate competitive binding phenomena. The ability of flufenamic acid to displace ANS from human serum albumin is registered as a decrease in the output signal. The ratio of the recorded peak heights suggests that the specified concentration of flufenamic acid displaces approximately 44% of the bound fluorescent probe. This result corresponds closely to the value obtained using the static method (see Table 4.11). From the width of the flow injection peaks it is clear that a maximum throughput of about 240 samples hr^{-1} is possible with this arrangement. However because a single channel system was employed, the flow rate of 1.1ml min^{-1} meant that a minimum of 275μl of reagent was consumed for each measurement.

Amongst other things, the method of merging zones offered a more efficient use of reagent than had been possible with the conventional technique. Results obtained with this method and depicting the competition for albumin binding sites between ANS and a number of acidic drugs are shown in Figure 6.6. Only 35μl volumes of sample and reagent were required for each measurement. The maximum sampling rate of 60 samples hr^{-1} may be deduced from the peak profiles.

Table 6.1 is a summary of the results of several merging zone experiments in which ANS and acid drugs were competing for binding sites on albumin. An attempt has been made to compare these results with others obtained under the equivalent static conditions. It is worth considering the basis of this comparison.

When sample and reagent met and mix in the merging zone technique, there is a dilution of the reactants. If equal volumes are injected on both lines and if mixing of the zones is instantaneous and complete, there will be an immediate halving of the concentrations of the various components in the merging streams. In reality there is always a short delay before merging of the zones is complete. However, as long as the mixing process is reproducible, this delay is of no practical significance. Furthermore, diffusion-induced dispersion of sample, reagent and product becomes the dominant mixing process as material is carried towards the detector. Despite the complexity of the dispersion pattern involved, flow injection theory (Růžička and Hansen, 1978) shows that the concentration ratio of reagent: sample will always remain constant in the case of merging zones - except, of course, for the consumption in the required chemical reaction - regardless

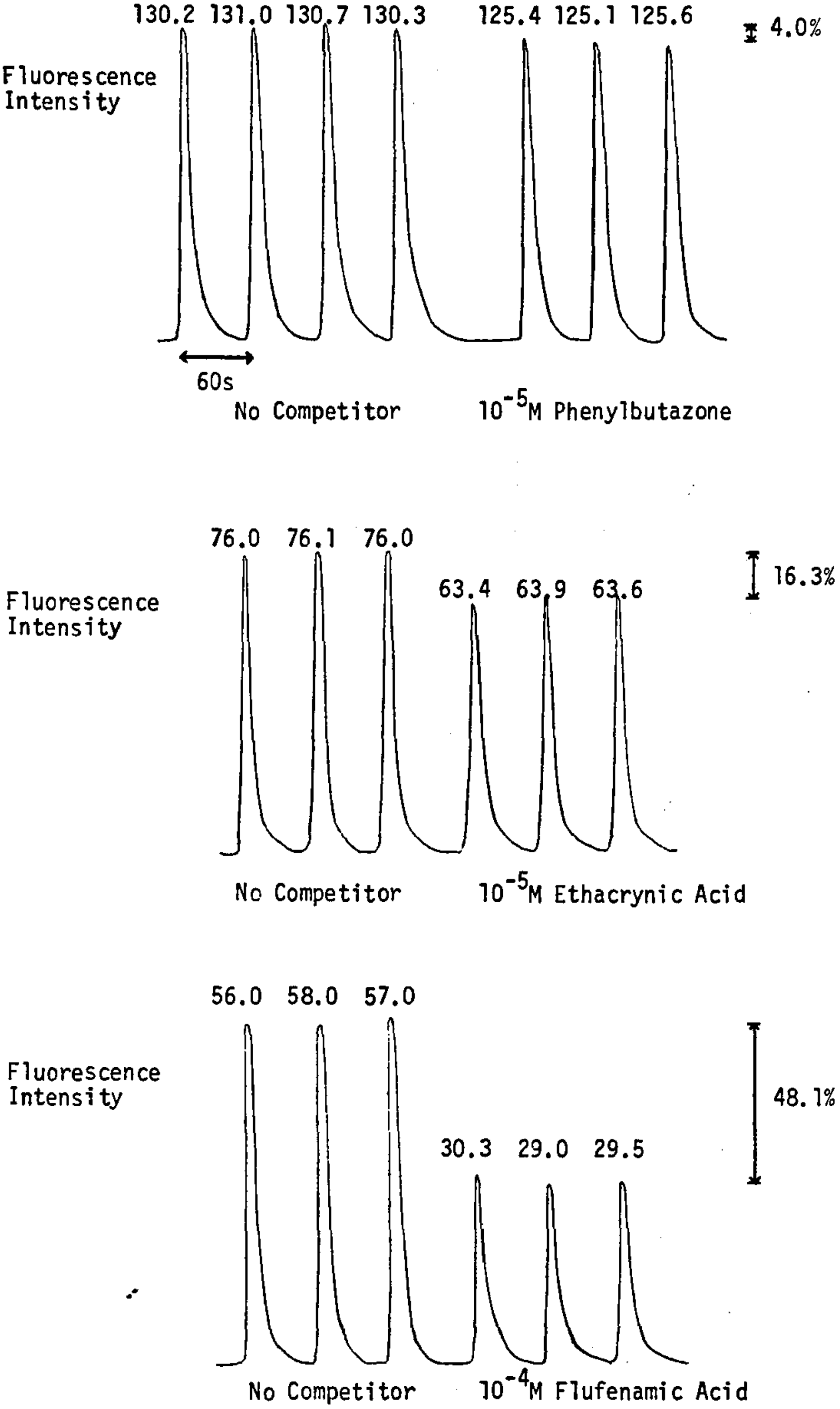

FIGURE 6.6 The Displacement of ANS from Human Serum Albumin by a Number of Acidic Drugs: Merging Zone FIA Technique.

35µl volumes of 10^{-5}M HSA and 10^{-5}M ANS solutions were injected into synchronized buffer carrier streams flowing at 1.4ml min^{-1}. Potential competitor drugs were then included in the solutions of fluorescent probe.

Drug	Concentration	% Displacement of bound ANS	
		FIA	Static
Flufenamic acid	10^{-4}M	44.6 + 2.8	53.82 + 0.16
	10^{-4}M	48.1 + 2.1	
	10^{-4}M	47.5 + 2.2	
	5×10^{-5}M	40.7*	40.9*
	10^{-5}M	19.8 + 2.8	16.13 + 0.20
	10^{-5}M	21.6 + 1.6	
	10^{-5}M	17.8 + 2.4	
Ethacrynic acid	10^{-4}M	30.3 + 0.6	37.62 + 0.80
	10^{-4}M	30.5 + 0.7	
	10^{-4}M	31.1 + 1.0	
	5×10^{-5}M	28.9*	27.8*
	10^{-5}M	16.6 + 0.8	13.74 + 0.14
	10^{-5}M	16.3 + 0.3	
2-p-(chlorophenoxy) -2-methyl proprionic acid	10^{-4}M	14.7 + 0.5	17.92 + 0.45
	10^{-4}M	15.9 + 0.7	
	10^{-5}M	4.5 + 0.8	5.38 + 0.14
	10^{-5}M	4.6 + 0.6	
Phenylbutazone	10^{-4}M	18.2 + 1.4	19.06 + 0.26
	10^{-4}M	20.2 + 0.7	
	10^{-5}M	4.0 + 0.3	4.19 + 0.18
	10^{-5}M	3.5 + 0.7	
Warfarin	10^{-4}M	8.3 + 0.7	9.46 + 0.14
	10^{-4}M	7.4 + 0.8	
	10^{-4}M	8.3 + 0.9	
	10^{-5}M	0.7 + 1.7	3.15 + 0.12
	10^{-5}M	1.2 + 0.5	
Sulphisoxazole	10^{-4}M	4.5 + 0.8	3.57 + 0.14
	10^{-4}M	5.0 + 0.5	
	10^{-4}M	4.7 + 0.6	
	5×10^{-5}M	1.7*	2.8*
	10^{-5}M	1.8 + 0.5	0.99 + 0.17
Sulphisomidine	10^{-4}M	1.1 + 1.2	1.84 + 0.10
	10^{-5}M	0.5 + 1.2	0.26 + 0.12

TABLE 6.1 The Displacement of ANS from its albumin binding sites by acidic drugs. FIA and static results.

* Results of experiments using 50-fold diluted normal human serum; in other cases the sample was 10^{-5}M human serum albumin.

ANS concentration 5 x 10^{-6}M - 10^{-5}M.

Results ± standard deviation; typically 10 readings.

of how far the zones have travelled. Consequently a direct comparison with static methods is usually possible. To achieve this in practice, the same concentration ratios of HSA, fluorescent probe and competitor were added to a 1cm fluorimeter cell as had been injected into the merging carrier streams. The normal static procedure was employed and the results were analysed using the FLUORB program.

As shown in Table 6.1, agreement between the two methods was generally good. Nonetheless, there were some initial differences, particularly with flufenamic and ethacrynic acids. Both drugs appeared to displace ANS more readily in the flow injection experiments. Evidence was produced to show that such discrepancies were due to kinetic aspects of the binding interaction. The merging zone experiments were repeated but delays of one minute or more were introduced by stopping the flow. In the absence of a competitor, this process had no effect on peak heights. When flufenamic acid was present, intensity changes of about 30% were observed after stopping the flow. An allowance for kinetic effects produced a better agreement between the results of the flow injection and static techniques.

Table 6.1 also shows that the method of merging zones can be used to study whole serum samples. Again, the results suggest an excellent agreement between the flow injection and the static procedures.

A summary of the results of the flow injection work on warfarin displacement is given in Table 6.2. A small part of the original data used to compile this table is shown in Figure 6.7. The relative capacity of a number of drugs to displace the fluorescent probe from binding sites on HSA confirms the findings of earlier, static work.

A Scatchard plot representing the binding of ANS to HSA and constructed with data from one of the titrations described in Chapter 3 is shown in Figure 6.8. For comparison, the results obtained using the merging zone flow injection technique are included in the same graph. There is an excellent agreement between the two sets of data. As indicated, the degree of dispersion in the flow line ensured that the albumin concentration at the point of detection was quite similar to that used in the static procedure.

Typical flow injection peaks, made up of replicate measurements on a single sample, are included alongside the Scatchard plots. The peaks are quite sharp and the separation of their maxima reflects the sampling rate of 60 samples hr^{-1}. The mean of these peak heights was calculated and used to specify one of the points in the binding curve. The coefficient of variation of the replicate measurements was 1.85% and gives some idea of the precision obtainable with the flow injection method.

Drug	Concentration	% Displacement of bound warfarin
Phenylbutazone	10^{-5}M	15.9 + 1.3
	10^{-5}M	18.0 + 0.5
	10^{-5}M	15.1 + 1.1
	10^{-4}M	39.4 + 2.5
	10^{-4}M	35.1 + 1.6
	2×10^{-4}M	61.7 + 1.2
	2×10^{-4}M	60.9 + 1.2
	2×10^{-4}M	61.2 + 1.2
Flufenamic acid	10^{-4}M	42.1 + 1.5
	10^{-4}M	41.6 + 1.5
	10^{-4}M	39.2 + 1.4
	2×10^{-4}M	59.8 + 1.8
	2×10^{-4}M	61.2 + 1.7
Ethacrynic acid	10^{-4}M	24.2 + 0.9
	10^{-4}M	25.7 + 1.2
	10^{-4}M	25.7 + 0.6
	10^{-4}M	24.6 + 1.3
	2×10^{-4}M	35.6 + 1.7
	2×10^{-4}M	35.9 + 1.2
	2×10^{-4}M	35.7 + 0.2
Sulphisoxazole	10^{-5}M	1.3 + 2.2
	10^{-4}M	9.1 + 0.5
	10^{-4}M	11.6 + 0.4
	2×10^{-4}M	20.8 + 1.7
	2×10^{-4}M	21.3 + 1.4
2-p-(chlorophenoxy)-2-methyl propionic acid	10^{-4}M	5.7 + 1.7
	10^{-4}M	2.9 + 1.3
	10^{-4}M	4.3 + 0.7
	2×10^{-4}M	10.2 + 1.4
	2×10^{-4}M	11.9 + 1.0
Sulphisomidine	10^{-4}M	0.8 + 1.7
	10^{-4}M	1.8 + 0.9
	2×10^{-4}M	5.4 + 1.4
	2×10^{-4}M	3.7 + 0.8

TABLE 6.2 The displacement of warfarin from its albumin binding sites by acidic drugs as measured by FIA.

Concentration of human serum albumin samples 6×10^{-5}M.

Concentration of warfarin 10^{-5}M.

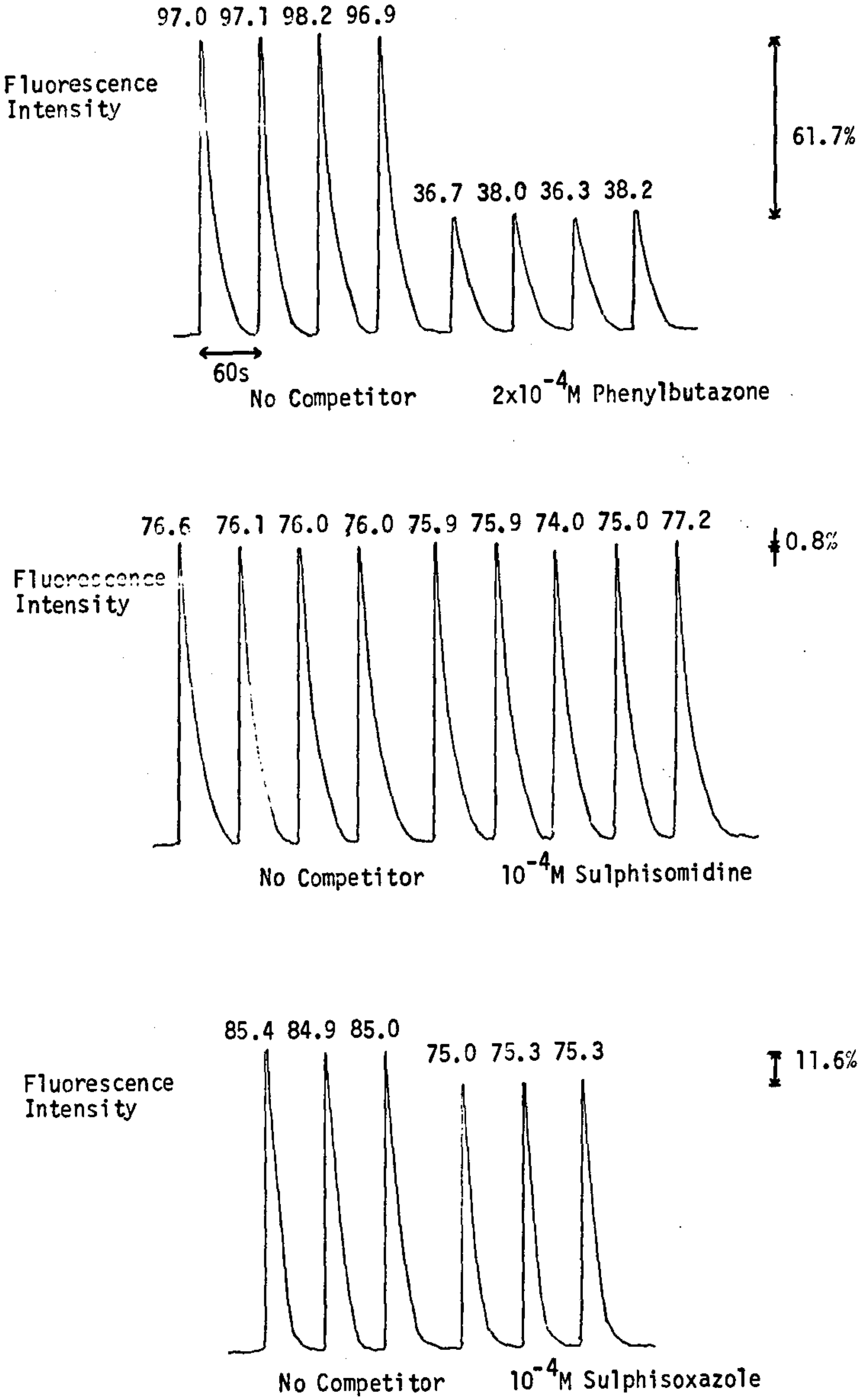

FIGURE 6.7 The Displacement of Warfarin from Human Serum Albumin by a Number of Acidic Drugs: Merging Zone FIA Technique.

35μl volumes of 6x10^{-5}M HSA and 1x10^{-5}M warfarin solutions were injected into synchronized buffer carrier streams flowing at 1.4ml min^{-1}. Potential competitor drugs were then included in the solutions of fluorescent probe.

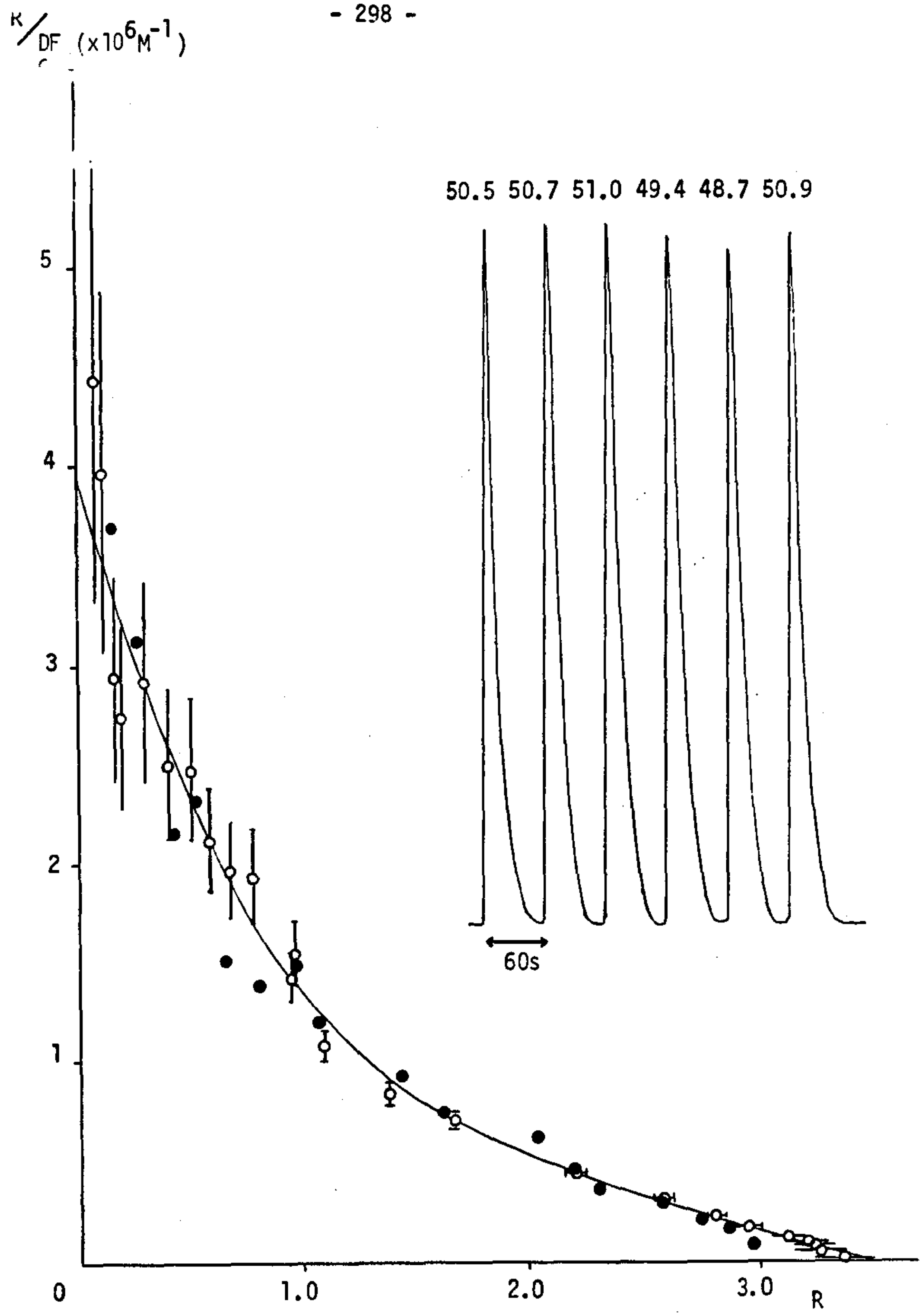

FIGURE 6.8 The Binding of ANS to HSA as Measured by Fluorescence Titration (○) and Merging Zone FIA (●).

Typical flow-injection peaks are illustrated.

6.4 Discussion of Methods and Findings

Flow injection analysis has been applied successfully to a study of drug-protein binding. The method has a number of advantages over the more conventional procedures described in previous chapters. The flow-injection system was readily automated, results could be generated quickly and only very small sample volumes were required. A further economy was made by using the merging zone technique to minimize reagent consumption.

The short path length across the flow cell meant that inner-filter effects were reduced ten-fold compared to those encountered with the standard 1cm fluorimeter cell. Consequently, calibration plots of fluorescence intensity versus concentration were linear over much wider ranges in the flow injection experiments. This resulted in a considerable simplification in the analysis of results.

The avoidance of troublesome inner-filter effects was particularly valuable when assessing the ability of several drugs to displace fluorescent probes from albumin and serum binding sites. If, as then, a number of absorbing species are present in solution, allowing for their combined inner-filter effects can be quite difficult. Hence in this application the flow injection system was able to exploit the benefits of fluorimetric detection while avoiding some of the problems associated with inner-filter phenomena.

Unlike many other methods of studying drug-protein binding, FIA can be used to examine reaction kinetics. For instance, measuring signals under non-equilibrium conditions can increase the displacement effect that is observed in competitive binding studies: a 30% increase was encountered with flufenamic acid in serum. This amplification could provide additional analytical information with which to characterize drug-protein interactions.

While a greater flexibility of operation can be achieved with the flow injection system, the method was less sensitive than the equivalent static procedure. Although dispersion of the sample zone could be controlled to give an acceptable signal, another variable which influences peak heights - the flow cell diameter - was severely restricted because turbulence had to be avoided. The necessarily short path length of the flow through detector generally means that fluorescence measurements in FIA are of limited intensity: if samples of similar composition are included in a 1cm cuvette and in a flow cell of path length 1.2mm, the former emits a correspondingly stronger signal.

To compensate for this fact, a higher gain is normally required when the fluorimeter is used as a flow-through detector. This invariably reduces the signal:noise ratio and can adversely affect the reproducibility of the assay. It is clear from the results in Table 6.1 that some loss of precision was encountered on going from a static to a flow injection procedure.

Interpretation of the results of the flow injection experiments required an understanding of the effects of reaction kinetics and sample dispersion. Armed with this information, a surprisingly good agreement has been demonstrated between the flow injection and static methods of assessing displacement phenomena. The flow injection system was used satisfactorily with diluted serum as well as with pure albumin solutions. The relatively high degree of dispersion within the manifold ensured that differences in viscosity between serum and albumin samples were negligible. If undiluted sera are used in low dispersion manifolds, viscosity differences may influence the results.

The data shown in Figure 6.8 represent the first attempt to construct a complete drug-protein binding curve using FIA. The agreement with the static method is excellent. Although there were no reports of such work in the literature, these results suggested that merging zone flow injection analysis could be used successfully in quantitative binding studies. Recently, Abdullahi et al (1983) have extended the FIA work to investigate the binding of basic drugs to α - acid glycoprotein.

As an aid to future drug-protein binding studies, it might be useful to convey data directly from the fluorimeter to a microcomputer. The routines used to analyse the binding data and perform curve-fitting routines could be programmed into the microcomputer. In this way, binding constants would be generated rapidly and conveniently from the flow injection results. The introduction of microprocessors to control the injection procedure and the carrier flow velocity would make for a more precise and robust assay. Optimization of the experimental variables would also be easier.

Given the significant advantages of FIA over conventional continuous flow systems, it is rather surprising how little use has been made of the technique in the field of clinical chemistry. Rocks and Riley (1982) have summarized the clinically relevant species so far determined by FIA. However, many of the assays developed to measure these substances must be regarded as feasibility studies only. The work of Lim et al (1980) in which the combined techniques of merging zones and stopped-flow were used in a homogeneous energy-transfer fluoroimmunoassay of albumin clearly shows the potential of the flow injection approach. It appears that the major obstacle to the adoption of FIA into routine clinical chemistry laboratories is the absence of a suitable, commercially available, fully automated flow injection analyser.

CHAPTER 7

Discussion

An accurate procedure for the assessment of the degree of binding of fluorescent probes to proteins has been developed. Unlike earlier methods, the procedure takes account of the contribution of the free fluorescent probe to the total signal. This refinement leads to a more reliable determination of association constants, particularly for fluorescent molecules which exhibit only a moderate change in their spectroscopic properties on binding to proteins. The procedure was used to examine the binding of two fluorescent probes to human serum albumin. There appears to be only one other case in which an attempt has been made to account for the fluorescence of the unbound ligand when analysing binding data (Maes et al, 1982).

Once the intensity of the signals emitted by the protein-bound and unbound forms of a fluorescent probe had been established, no physical separation of the bound and free fractions in unknown samples was required. Inner-filter effects and background signals were fully accounted for during the resolution of the analytical signal into contributions from free and bound fluorescent probe. Computer programs were written to carry out the necessary data processing and to generate binding curves and constants. In the absence of these programs, it would have been extremely tedious to consider the separate factors comprising the total signal; moreover, the introduction of simplifying assumptions would have led to conclusions of questionable validity.

The methods of correcting fluorescence intensity measurements for inner-filter effects were discussed in some detail. The ability of the recommended correction procedure to account for the distortion of the calibration curves was examined in theoretical as well as in practical terms. Inner-filter effects are a common problem in analytical fluorimetry and may be worthy of further attention.

Binding constants for the interactions between warfarin and HSA, and between ANS and HSA were determined by fitting data to the two-site Scatchard model. An objective measure of the goodness of fit was used. This is clearly a more satisfactory approach than the simple visual means of curve-fitting which are sometimes employed; subjective influences on the visual decomposition of binding curves are notorious.

Whenever additional parameters are introduced into a binding equation, the goodness of fit to a given set of results will increase. This is simply a consequence of the additional flexibility of the model. Ultimately, if as many parameters are present as data points, the curve may pass through every point. A compromise must be sought between adding new parameters and improving the goodness of fit. Within the limits of experimental error, the binding of warfarin and ANS to HSA was adequately described by a two-site Scatchard model. While it would have been a simple task to extend the analysis to a three-site binding equation, interpreting the meaning of a very small change in the goodness of fit would have been more difficult. It would have involved the construction of several binding curves, each containing a large number of data points, and the application of a statistical test to discern whether the increase of the goodness of fit on including additional parameters in the model was significantly more than could be expected on the basis of chance alone (Munson and Robard, 1980). This process would have had to be repeated for each binding curve, including those obtained in the presence of competitor drugs.

The limitations of the different mathematical models of ligand-protein binding were discussed in Section 1.7. The binding constants derived for the interaction between the two fluorescent probes and HSA must therefore be understood in the context of the two-site Scatchard model. The fact that the Scatchard plots have negative slopes over their entire ranges means that the results can be fitted to the Scatchard model. Although the absence of positive slopes in these curves indicates that positive cooperativity is not apparent in the binding processes under examination, it is not possible to deduce from this that all the assumptions inherent in the generalised Scatchard model are satisfied. In other words, the existence of other allosteric phenomena in the binding of warfarin and ANS to HSA cannot be ruled out.

The procedures for measuring free and bound levels cf fluorescent probes were used to assess the affinities of various drugs for specific sites on HSA. By examining the effect of drugs on the binding curves of a fluorescent probe it was possible to identify those ligands which competed for common sites on albumin. Drugs which produced a large reduction in the bound fraction of a fluorescent probe were taken as having a high affinity for that particular binding site.

It appears from the results of Chapter 4 that warfarin and ANS bind to separate regions of the albumin molecule. Thus while warfarin, phenylbutazone and some sulphonamide drugs were shown to compete for the same class of sites on HSA, these compounds did not affect the binding of ANS.

Certain other drugs were shown to bind avidly to both the warfarin and ANS binding sites of albumin, that is, to sites I and II respectively. The distribution of these drugs between two high-affinity sites of HSA was confirmed by studies of the binding equilibria between three ligands and albumin. The possible clinical consequences of the administration of drugs which can bind avidly to more than one class of binding sites on HSA were discussed.

The crystal structure and molecular conformation of the fluorescent probes warfarin and ANS have been determined using X-ray crystallographic techniques (Valente et al, 1975; Cody and Hazel, 1976). Unfortunately, a full understanding of the ability of these molecules to bind to different sites on the albumin molecule may only be available when the complete three-dimensional structure of the protein is revealed.

The competition between fluorescent probes and drugs for protein binding was examined using whole sera as well as purified albumin solutions. No pretreatment of serum samples was required. Almost all of the drugs under examination displaced the same quantities of fluorescent probe irrespective of whether binding was to total serum proteins or to albumin alone. The results were consistent with the view that albumin is the major binding protein for acidic drugs in human serum.

The observed displacement interactions involving fluorescent probes and drugs supported the common-site model. This proposes that only a finite number of ligand binding sites exist on albumin and drug displacement interactions are a result of direct competition for common binding sites. However, the view that non-competitive mechanisms may have had a role in at least some of the observed displacement interactions cannot be dismissed out of hand. Certainly the cooperative viewpoint of displacement phenomena has a number of advocates, for example Madsen and Ellis (1981), and Weber (1975). Moreover, the ability of many ligands to induce conformational changes in the albumin molecule is well-known, although in some cases the changes may be small and restricted to the immediate environment of the binding site. On the other hand, recent progress has been made in the identification of specific regions of the albumin molecule which are involved in the binding of drugs. Current evidence concerning the location of the major drug binding sites of HSA has been examined in Section 1.4.2; so far only three important drug binding sites have been identified. It would seem reasonable to suppose, therefore, that direct competition for individual binding sites is a real effect, but its importance relative to non-competitive mechanisms in displacement interactions has yet to be resolved and will surely be dependent upon the drugs involved.

Recognising the fact that changes in the spectroscopic properties of an albumin-bound fluorescent probe may not be the result of a displacement interaction at all, but could be due simply to a slight rearrangement of the immediate environment when a second ligand binds to the same protein molecule, equilibrium dialysis was used to check the findings of the fluorescence titrations. As demonstrated in Chapter 5, there was a good agreement between the results of the spectroscopic and equilibrium dialysis techniques. This would appear to validate the use of the homogeneous fluorescence assay in the assessment of drug-protein binding. The importance of considering the effect of the unbound fraction on the time to dialysis equilibrium was stressed. Thus, as well as examining the results of the two techniques, the comparative evaluation included an assessment of practical aspects of the fluorimetric and equilibrium dialysis procedures.

Flow injection analysis (FIA) was identified as the most promising means of automating the ligand-binding assays. A high sample throughput and a low consumption of reagents were achieved using the merging zone flow injection technique. The semi-automated system could handle diluted whole serum as well as pure albumin solutions. A complete binding curve was constructed using the results of flow-injection experiments. The procedure also illustrated some kinetic aspects of the displacement of fluorescent probes from albumin.

The agreement between the results of the flow injection and 'static' methods was very good. Hence, flow injection analysis should provide the opportunity to examine the binding properties of large numbers of drugs and fluorescent probes, and would allow numerous serum samples to be handled routinely and effeciently.

The advantages of FIA in automated analysis have been questioned even recently (Holy, 1982). However, these criticisms may be coloured by a commercial interest in the promotion of segmented continuous flow analysers. Moreover, the arguments in favour of flow injection analysis are compelling (Hansen and Ruzicka, 1982; Stewart, 1982) and should help to dispel any remaining doubts as to the potential of this technique in clinical chemistry and other fields of analysis.

The procedures outlined in Chapter 3 were concerned with measuring levels of free and bound fluorescent probe in a mixture. The principle technique required that the fluorescence intensities of the free and protein-bound forms of the probe were first determined and then used to interpret the signal emitted by a sample containing both species into components from the bound and free fluorescent probe. In its simplest representation, this involved the solution of two simultaneous equations. In the context of this work, efforts were also made to achieve the spectral resolution of the emission bands of the free and protein-bound fluoresccent probes. The technique of derivative and synchronous fluorescence spectroscopy were of some use in improving the discrimination between the peaks of interest. However, the resolution was insufficient to permit direct quantitative measurements of bound and free levels of warfarin and ANS. Nonetheless, it was possible to identify the class of fluorescent probes which could benefit most from the application of the derivative and synchronous techniques to the resolution of the overlapping peaks of bound and free ligand.

Recently, differences in fluorescence polarization have been used to resolve the overlapping spectra of free and bound fluophors (Roemelt et al, 1980). This is an interesting technique but it is of fairly limited sensitivity. In spite of this, a procedure for measuring total drug levels in serum has been developed (TDx System, Abbot Laboratories Ltd) which is based upon a competitive binding immunoassay and uses the principle of fluorescence polarization to measure tracer-antibody binding directly. The need for the physical separation of free and antibody-bound tracer is eliminated.

The clinical implications of some of the drug displacement interactions encountered in this study were discussed in Section 4.4. Caution was stressed in attributing too much emphasis to the role of plasma protein binding displacement in drug interactions. Drugs which are likely to be involved in clinically important displacement interactions will be highly bound to plasma proteins at normal dosing levels, have a small apparent volume of distribution and display a relatively narrow range of therapeutic concentration at their sites of action. This should be borne in mind when attempting to predict the clinical significance of the competition between drugs for albumin binding sites.

The coumarin anticoagulants, in particular, are known to be involved in hazardous drug interactions. Hence the choice of warfarin as a fluorescent probe for monitoring drug displacement interactions is especially relevant. Of course, it should be appreciated that drug interactions involving warfarin are likely to be dependent upon several factors, only one of which is displacement from plasma protein binding sites.

While plasma protein binding displacement is only very occasionally a major underlying mechanism of drug interactions, the study of protein binding and displacement may still assist in the identification of potentially dangerous combinations of drugs. Drugs which compete for plasma protein binding sites may also compete for elimination and metabolic pathways and for tissue binding sites. Further studies of drug-albumin binding may also provide a better understanding of the molecular aspects of drug-protein and drug-receptor interactions.

The importance of plasma protein binding on the distribution, metabolism, elimination and pharmacological activity of drugs has been discussed in Section 1.1. As the free drug concentration in plasma reflects the expected pharmacological effect, it is certainly prudent to consider this fraction for drug plasma level monitoring rather than the total concentration, particularly when a drug is highly bound at therapeutic levels.

Under most physiological conditions there is relatively little interindividual difference in protein binding of drugs and so the free drug concentration is a fairly constant percentage of the total. However, in patients with renal and hepatic diseases, or when hypoalbuminemia is present, the free drug concentration may be substantially increased so that toxic effects can occur when the total drug concentration is within the usual therapeutic range. In such circumstances the free drug should be measured. Similarly, if drug displacement is likely to accompany the co-administration of highly protein-bound drugs, the monitoring of free drug levels is clearly indicated.

Unfortunately, it is normal practice to determine total drug levels in the blood rather than free drug levels, even for highly bound drugs. It is hardly surprising that the measurement of total blood levels frequently gives poor correlations with therapeutic or toxicological effects. In clinical situations that are known or assumed to be associated with significant changes in plasma protein binding, the use of total drug measurements may lead to serious errors in estimating dosage requirements.

In the past drug monitoring has usually been concerned with the total drug in plasma and not just the free fraction. This has been due to difficulties in separating the bound and free fractions and in determining the frequently very low levels of unbound drug. The recent introduction of disposable ultrafilters may have only partially alleviated the problem (Ruprah et al, 1981).

The development of new methods for resolving bound and free drug should lead to a better assessment of the relationship between drug levels and therapeutic activity. Moreover, compared to total drug measurements, this approach will provide a more satisfactory foundation on which to base any adjustments of drug administration. The new methods may depend upon the concept of free ligand assays introduced by Midgley and Wilkins (1982). Free drug levels could be monitored by measuring the competition between fluorescent probes and drugs for binding to specific antibodies or other proteins mixed with patient serum samples. The fluorescent probe would be chosen to bind strongly to the added specific binder (which also binds the drug), but to have little or no affinity for binding to native drug binders such as albumin in the biological fluid. Only a small quantity of the fluorescent molecule would be added so as not to disturb the binding equilibrium of the drug. The major obstacle to the development of such drugs is likely to be the synthesis of suitable fluorescent compounds.

An obvious extension to the work of this study is an investigation of the binding of acidic drugs to blood proteins other than albumin - possibly α_1-acid glycoprotein and α -fetoprotein (AFP). It would be particularly interesting to compare the drug binding properties of human serum albumin and AFP in the light of the probable homology of their amino sequences and primary structures. In addition an examination of the binding of drugs to AFP may give a better understanding of the relationship between the binding capacities of maternal and fetal plasma.

Fluorescent probes are already proving useful in the characterization of the plasma protein binding of basic drugs. The synthesis of new site-specific fluorescent probes should give a further impetus to this work.

Advances in tissue techniques may make it easier to obtain samples for drug binding studies. The displacement of drugs from tissue binding sites has a high potential for adverse effects, and fluorescent probes may be increasingly important in investigations of drug interactions at tissue binding sites.

The continued use of fluorescent probes in drug-protein binding studies is assured. It is to be hoped, however, that many of the contradictions and discrepancies which have appeared in the literature on the binding of drugs to human serum albumin will be avoided in the future. This will only occur if there is a better understanding of the analytical methods employed and a fuller appreciation of the limitations of the available binding models.

REFERENCES

The abbreviated titles of journals are those which appear in current volumes of Index Medicus. The abbreviation listing may be found in the Cummulated Index Medicus Volume 12 (1971).

Aarons, L.J. (1981) : Kinetics of drug-drug interactions. Pharmacol Ther 14 (3), 321-344.

Aarons, L.J. and Rowland, M. (1981) : Kinetics of drug displacement interactions. J Pharmacokinetics Biopharm 9 (2), 181-190.

Aarons, L.J., Schary, W.L. and Rowland, M. (1979) : An in vitro study of drug displacement interactions : warfarin-salicylate and warfarin-phenylbutazone. J Pharm Pharmacol 31, 322-330.

Abdullahi, G.L., Miller, J.N., Sturley, H.N. and Bridges, J.W. (1983) : Studies of drug-protein binding interactions by flow injection analysis with fluorimetric detection. Anal Chim Acta 145, 109-116.

Adir, J., Miller, A.K. and Vestal, R.E. (1982) : Effects of total plasma concentration and age on tolbutamide plasma protein binding. Clin Pharmacol Ther 31 (4), 488-493.

Aggeler, P.M., O'Reilly, R.A., Leong, L. and Kowitz, P.E. (1967) : Potentiation of anticoagulant effect of warfarin by phenyulbutazone. N Engl J Med 276, 496-501.

Ågren, A., Elofsson, R. and Nilsson, S.O. (1971) : Some physico-chemical factors influencing the binding of sulfonamides to human albumin in vitro. Acta Pharmacol Toxicol (Suppl) (Kbh) 29 (3), 48-56.

Ahlfors, C.E., Shwer, M.L. and Ford, K.B. (1982) : Bilirubin-albumin binding in neonatal salicylate intoxication. Dev Pharmacol Ther 4, 47-60.

Anderson, S.R. and Weber, G. (1969) : Fluorescence polarization of the complexes of 1-anilino-8-naphthalenesulfonate with bovine serum albumin. Evidence for preferential orientation of the ligand. Biochemistry 8 (1), 371-377.

Anton, A.H. (1960) : The relation between the binding of sulfonamides to albumin and their antibacterial activity. J Pharmacol Exp Ther 129, 282-290.

Anton, A.H. (1973) : Increasing activity of sulfonamides with displacing agents : a review. Ann NY Acad Sci 226, 273-292.

Anton, A.H. and Boyle, J.J. (1964) : Alteration of the acetylation of sulfonamides by protein binding, sulfinpyrazone and suramin. Can J Physiol Pharmacol 42, 809-

Anton, A.H. and Solomon, H.M. (eds) (1973) : Drug protein binding. Ann NY Acad Sci 226.

Ashbrook, J.D., Spector, A.A., Santos, E.C. and Fletcher, J.E. (1975) : Long chain fatty acid binding to human plasma albumin. J Biol Chem 250 (6), 2333-2338.

Atkins, P.W. (1970) : Molecular Quantum Mechanics. Oxford University Press.

Becker, R.S. (1969) : Theory and Interpretation of Fluorescence and Phosphorescence. Wiley Interscience.

Behrens, P.Q., Spiekerman, A.M. and Brown, J.R. (1975) : Structure of human serum albumin. Fed Proc 34, 591.

Bennet, C.A. and Franklin, N.L. (1954) : Statistical analysis and the chemical industry. pp668-677, Wiley, New York.

Bergamin, H., Zagatto, E., Krug, F. and Reis, B.F. (1978) : Merging zones in FIA. Part 1. Double proportional injector and reagent consumption. Anal Chim Acta 101, 17-23.

Betteridge, D. (1978) : Flow injection analysis. Anal Chem 50 (9), 832A-846A.

Betteridge, D. and Ruzicka, J. (1976) : The determination of glycerol in water by flow-injection analysis. A novel way of measuring viscosity. Talanta 23, 409-410.

Bird, A.E. and Marshall, A.C. (1967) : Correlation of serum binding of penicillins with partition coefficients. Biochem Pharmacol 16, 2275-2290.

Birkett, D.J., Myers, S.P. and Sudlow, G. (1977) : Effect of fatty acids on two specific drug binding sites on human serum albumin. Mol Pharmacol 13, 987-992.

Birkett, D.J., Myers, S.P. and Sudlow, G. (1978) : The fatty acid content and drug binding characteristics of commercial albumin preparations. Clin Chim Acta 85, 253-258.

Bjornsson, T.D., Brown, J.E. and Tschanz, C. (1981) : Importance of radiochemical purity of radiolabelled drugs used for determining plasma protein binding of drugs. J Pharm Sci 70 (12), 1372-1373.

Bloomfield, V. (1966) : The structure of bovine serum albumin at low pH. Biochemistry 5 (2), 684-689.

Boobis, S.W. (1977) : Alteration of plasma albumin in relation to decreased drug binding in uremia. Clin Pharmacol Ther 22 (2), 147-153.

Boobis, S.W. and Chignell, C.F. (1979) : Effect of protein concentration in the binding of drugs to human serum albumin-sulphadiazine, salicylate and phenylbutazone. Biochem Pharmacol 28, 751-756.

Bowen, E. and Woker, F. (1953) : Fluorescence of Solutions. Longman, Green and Co (London).

Bowman, W.C. and Rand, M.J. (1980) : Textbook of Pharmacology, 2nd edition. Blackwell Scientific Publications Ltd.

Bowmer, C.J. and Lindup, W.E. (1978) : Binding of phenytoin, L-tryptophan and O methyl red to albumin. Unexpected effect of albumin concentration on the binding of phenytion and L-tryptophan. Biochem Pharmacol 27, 937-942.

Bowmer, C.J. and Lindup, W.E. (1982) : Decreased drug binding in uraemia: effect of indoxyl sulphate and other endogenous substances on the binding of drugs and dyes to human albumin. Biochem Pharmacol 31 (3), 319-323.

Braithwaite, J.L. and Miller, J.N. (1979) : Flow injection analysis with a fluorimetric detector for determinations of glycine and albumin. Anal Chim Acta 106, 395-399.

Brand, L. and Gohlke, J.R. (1971) : Nanosecond time-resolved fluorescence spectra of a protein-dye complex. J Biol Chem 246 (7), 2317-2324.

Brand, L. and Gohlke, J.R. (1972) : Fluorescence probes for structure. Annu Rev Biochem 41, 843-868.

Bratton, A.C. and Marshall, E.K.,Jr. (1939) : A new coupling component for sulfanilamide determination. J Biol Chem 128, 537-550.

Bridges, J.W. and Wilson, A.G.E. (1976) : Drug-serum protein interactions and their biological significance. In : Progress in Drug Metabolism 1 pp193-247, ed. by Bridges, J.W. and Chasseaud, L.F. : John Wiley and Sons.

Brinkschulte, M. and Breyer-Pfaff, U. (1980) : The contribution of α_1-acid glycoprotein, lipoproteins, and albumin to the plasma binding of perazine, amitriptyline, and nortriptyline in healthy man. (1980) Nauyn-Schmiedebergs Arch Pharmacol 314, 61-66.

Brodersen, R. (1974) : Competitive binding of bilirubin and drugs to human albumin studied by enzymatic oxidation. J Clin Invest 54, 1353-1364.

Brodersen, R. (1980) : Binding of bilirubin to albumin. CRC Crit Rev Clin Lab Sci 11 (4), 305-399.

Brodersen R., Sjödin, T. and Sjöholm, I. (1977) : Independent binding of ligands to human serum albumin. J Biol Chem 252 (14), 5067-5072.

Brodie, B.B. (1965) : Displacement of one drug by another from carrier or receptor sites. Proc R Soc Med 58, 946-955.

Brown, J.R. (1974) : Structure of serum albumin : disulfide bridges. Fed Proc 33, 1389.

Brown, J.R. (1975) : Structure of bovine serum albumin. Fed Proc 34, 591.

Brown, J.R. (1978) : Structure and evolution of serum albumin. In : Albumin : Structure, Biosynthesis, Function. FEBS 11th Meeting, Copenhagen, 1977 ed. by Peters, T. and Sjöholm, I., Pergamon Press, Oxford.

Brown, N.A., Jahnchen, E., Müller, W.E. and Wollert, U. (1977) : Optical studies on the mechanism of the interaction of the enantiomers of the anticoagulant drugs phenprocoumon and warfarin with human serum albumin. Mol Pharmacol 13 (1), 70-79.

Brown, N.A., Wilson, A.G.E. and Bridges, J.W. (1982) : Chain length dependency of fatty acid and carbamate binding to serum albumin. Biochem Pharmacol 31 (24), 4019-4029.

Bruderlein, H. and Bernstein, J. (1979) : An investigation of the L-tryptophan binding site on serum albumin, using cyclic analogs and fluorescent probes. J Biol Chem 254 (22), 11570-11576.

Burns, J.J., Rose, R.K., Chenkin, T., Goldman, A., Schulert, A. and Brodie, B.B. (1953) J Pharmacol Exp Ther 109, 346-357.

Bush, M.T. and Alvin, J.D. (1973) : Characterization of drug-protein interactions by classic methods. Ann NY Acad Sci 226, 36-43.

Cahill, J.E. (1980) : Derivative spectroscopy: understanding its application. International Laboratory 10 (1), 64-72.

Calvo, R., Carlos, R. and Erill, S. (1982) : Effects of carbamylation of plasma proteins and competitive displacers on drug binding in uremia. Pharmacology 24, 248-252.

Chakrabarti, S.K. (1978) : Cooperativity of warfarin binding with human serum albumin induced by free fatty acid anion. Biochem Pharmacol 27, 739-743.

Cham, B.E., Bochner, F., Imhoff, D.M., Byrne, G. and Gunsberg, M. (1982) : In vivo and in vitro studies on the binding of salicylate to human plasma proteins: evidence for one type of binding site. J Pharmacol Exp Ther 220 (3), 648-653.

Chen, R.F. (1967) : Removal of fatty acids from serum albumin by charcoal treatment. J Biol Chem 242 (2), 173-181.

Chen, R.F. (1973) : In : Practical Fluorescence - Theory, Methods and Techniques. ed. by Guilbault, G.G., Marcel Dekker, New York.

Chen, R.F. and Koester, J. (1980) : Fluorescence properties of human serum albumin : effect of dialysis and charcoal treatment. Anal Biochem 105, 348-353.

Chignell, C.F. (1968) : Circular dichroism studies of drug-protein complexes. Life Sci (II) 7, 1181-1186.

Chignell, C.F. (1969a) : Optical studies of drug-protein complexes. II. Interaction of phenylbutazone and its analogs with human serum albumin. Mol Pharmacol 5, 244-252.

Chignell, C.F. (1969b) : Optical studies of drug-protein complexes. III. Interaction of flufenamic acid and other N-arylanthranilates with serum albumin. Mol Pharmacol 5, 455-462.

Chignell, C.F. (1970) : Optical studies of drug-protein complexex. IV. The interaction of dicoumarol and warfarin with human serum albumin. Mol Pharmacol 6, 1-12.

Chignell, C.F. (1971) : Physical methods for studying drug-protein binding. Chapter 9 in Concepts in Biochemical Pharmacology, Part 1, ed. by Brodie, B.B. and Gillette, J.R. : Springer, New York.

Chignell, C.F. (1972) : Fluorescence spectroscopy - a tool for studying drug interactions with biological systems. Chapter 2 in Methods in Pharmacology, Vol. 2 pp33-61. Appelton-Century-Crofts, New York.

Chignell, C.F. (1974) : Fluorescence spectroscopy as a tool for monitoring drug-albumin interactions. In : Drug Interactions, pp111-122, ed. by Morselli, P.L., Garattini, S. and Cohen, S.N. : Raven Press, New York.

Christensen, L,K., Hansen, J.M. and Kristensen, M. (1963) : Sulphapherazole-induced hypoglycaemic attacks in tolbutamide-treated diabetics. Lancet 2, 1298-1301.

Christmann, D.R., Crouch, S.R., Holland, J.F. and Timnick, A. (1980) : Correction of right-angle molecular fluorescence measurements for absorption of fluorescence radiation. Anal Chem 52, 291-295.

Churchich, J.E. (1972) : L-kynurenine: a fluorescent probe of serum albumins. Biochem Biophy Acta 285, 91-98.

Coassolo, P., Briand, C., Bourdeaux, M. and Sari, J.C. (1978) : Microcalorimetric method to determine competitive binding. Action of a psychotropic drugs (dipotassium chlorazepate) on L-tryptophan·human serum albumin complex. Biochim Biophys Acta 538, 512-520.

Cody, V. and Hazel, J. (1976) : Crystal and molecular conformation of the fluorescent probe, 8 -anilino-1-naphthalenesulfonic acid (ANS). Biochem Biophys Res Commun 68 (2), 425-429.

Colowick, S.P. and Womack, F.C. (1969) : Binding of diffusable molecules by macromolecules : rapid measurements by rate of dialysis. J Biol Chem 244 (3), 774-779.

Coulson, C.J. and Smith, V.J. (1980) : Correlation of hydrophobicity with protein binding for clorobiocin analogs. J Pharm Sci 69 (7), 799-801.

Courtice, F.C. (1971) : Lymph and plasma proteins : barriers to their movement throughout the extracellular fluid. Lymphology 4, 9-17.

Craig, L.C. (1965) : Differential dialysis. In : Advances in Analytical Chemistry and Instrumentation 4 pp35-74, ed. by Reilley, C.N. : John Wiley and Sons.

Craig, L.C. (1968) : Dialysis and ultrafiltration. Chapter 8 in Methods in Immunology and Immunochemistry 2 pp119-133, ed. by Williams, C.A. and Chase, M.W. : Academic Press, New York and London.

Dabrowiak, J.C. (1983) : Minireview : sequence specificity of drug-DNA interactions. Life Sci 32 (26), 2915-2931.

Dale, R.E. and Brand, L. (1975) : Protein luminescence. Photochem Photobiol 21, 459-463.

Daniel, E. and Weber, G. (1966) : Cooperative effects in binding by bovine serum albumin. I. The binding of 1-anilino-8-naphthalene-sulfonate. Fluorimetric titrations. Biochemistry 5 (6), 1893-1900.

D'Arcy, P.F. and McElnay, J.C. (1982) : Drug interactions involving the displacement of drugs from plasma protein and tissue binding sites. Pharmacol Ther 17, 211-220.

Davis, B.D. (1943) : The binding of sulphonamide drugs by plasma proteins. A factor in determining the distribution of drugs in the body. J Clin Invest 22, 753.

DiCesare, J.L. and Porro, T.J. (1978) : Use of a microprocessor for obtaining corrected, difference, derivative and polarization fluorescence spectra. Trends in fluorescence 1 (2), 16-21.

Dodd, G.H. and Radda, G.K. (1969) : 1-anilinonaphthalene-8-sulphonate, a fluorescent conformational probe for glutamate dehydrogenase. Biochem J 114, 407-417.

Doody, M.C., Gotto, A.M.Jr., and Smith, L.C. (1982) : 5-(dimethylamino) naphthalene-1-sulfonic acid, a fluorescent probe of the medium chain fatty acid binding site of serum albumin. Biochemistry 21 (1), 28-33.

Edsall, J.T. and Wyman, J. (1958) : Biophysical Chemistry Vol. I. Academic Press, New York.

Ehrnebo, M., Agurell, S., Boréus, L.O., Gordon, E. and Lönroth, U. (1974) : Pentazocine binding to blood cells and plasma proteins. Clin Pharmacol Ther 16 (3), 424-429.

Eisen, H.N. (1971) : Equilibrium dialysis. Microtechnique. In : Methods in Immunology and Immunochemistry 3 pp393-394, ed. by Williams, C.A. and Chase, M.W. Academic Press, New York and London.

Ekman, B., Sjödin, T. and Sjöholm, I. (1980) : Binding of drugs to human serum albumin -XV. Characterization and identification of the binding sites of indomethacin. Biochem Pharmacol 29, 1759-1765.

Elbary, A.A., Vallner, J.J. and Whitworth, C.W. (1982) : Effect of albumin conformation on the binding of phenylbutazone and oxyphenbutazone to human serum albumin. J Pharm Sci 71 (2), 241-244.

El-Gamal, S., Wollert, U. and Müller, W.E. (1983) : Binding of several phenothiazine neuroleptics to a common binding site of α_1-acid glycoprotein, orosomucoid. J Pharm Sci 72 (2), 202-205.

El-Nimr, A., Hardee, G.E. and Perrin, J.H. (1981) : A fluorimetric investigation of the binding of drugs to lysozyme. J Pharm Pharmacol 33, 117-118.

Ewing, G.W. (1970) : Molecular luminescence : fluorescence and phosphorescence. Chapter 4 in Instrumental Methods of Chemical Analysis. McGraw-Hill Book Company.

Faed, E.M. (1981) : Protein binding of drugs in plasma, interstitial fluid and tissues : effect on pharmacokinetics. Eur J Clin Pharmacol 21, 77-81.

Fang, S.C. and Lindstrom, F.T. (1980) : In vitro binding of ^{14}C-labelled acidic compounds to serum albumin and their tissue distribution in the rat. J Pharmacokin Biopharm 8 (6), 583-597.

Feely, J., Stevenson, I.H. and Crooks, J. (1981) : Altered plasma protein binding of drugs in thyroid disease. Clin Pharmacokin 6, 298-305.

Fehske, K.J., Müller, W.E. and Wollert, U. (1978) : The modification of the lone tryptophan residue in human serum albumin by 2-hydroxy-5-nitrobenzyl bromide. Hoppe Seylers Z Physiol Chem 359 (6), 709-717.

Fehske, K.J., Müller, W.E. and Wöllert, U. (1979a) : A highly reactive tyrosine residue as part of the indole and benzodiazepine binding site of human serum albumin. Biochim Biophys Acta 577, 346-359.

Fehske, K.J., Müller, W.E. and Wollert, U. (1981) : The location of drug binding sites in human serum albumin. Biochem Pharmacol 30 (7), 687-692.

Fehske, K.J., Müller, W.E., Wollert, U. and Velden, L.M. (1979b) : The lone tryptophan residue of human serum albumin as part of the specific warfarin binding site. Mol Pharmacol 16, 778-789.

Fehske, K.J., Schläfer, U., Wöllert, U. and Müller, W.E. (1982) : Characterization of an important drug binding area on human serum albumin including the high-affinity binding sites of warfarin and azapropazone. Mol Pharmacol 21, 387-393.

Feldman, H.A. (1972) : Mathematical theory of complex ligand-binding systems at equilibrium : some methods of parameter fitting. Anal Biochem 48 (2), 317-338.

Fell, A.F. (1978) : Analysis of dosage forms by second derivative ultraviolet-visible spectrophotometry. Proc Analyt Div Chem Soc 15 (9), 260-267.

Fletcher, J.E., Ashbrook, J.D. and Spector, A.A. (1973) : Computer analysis of drug-protein binding data. Ann NY Acad Sci 226, 69-81.

Fletcher, J.E., Spector, A.A. and Ashbrook, J.D. (1970) : Analysis of macromolecule-ligand binding by determination of stepwise equilibrium constants. Biochemistry 9 (23), 4580-4587.

Förster, T. (1951) : In : Fluoreszenz Organischer Verbindungen, S. pp83-86. Vandenhoek and Rupprecht, Göttingen.

Foster, J.F. (1960) : Plasma albumin. In : The Plasma Proteins 1 pp179-239, ed. by Putnam, F.W. : Academic Press, New York.

Fremstad, D., Bergerud, K., Haffner, J.F.W. and Lunde, P.K.M. (1976) : Increased binding of quinidine after surgery : a preliminary report. Eur J Clin Pharmacol 10, 441-444.

Freundlich, H. (1907) Z. Physik Chem 57, 385.

Frohlich, J., Pudek, M.R., Cormode, E.J., Sellers, E.M. and Abel, J.G. (1981) : Further studies on plasma proteins, lipids and dye-and drug-binding in a child with analbuminemia. Clin Chem 27 (7), 1213-1216.

Galley, W.C. and Milton, J.G. (1979) : Protein Emission. Photochem Photobiol 29, 179-184.

Gambhir, K.K. and McMenamy, R.H. (1973) : Location of the indole binding site in human serum albumin. Characterization of major cyanogen bromide fragments with respect to affinity labelling positions. J Biol Chem 248 (6), 1956-1960.

Garn, F.W. and Kimbel, K.H. (1961) : (Fate and excretion of depot sulfonamides. I. Binding on plasma proteins). Arzneimittelforsch 11, 701-707.

Geisow, M. (1977) : Serum albumin structure and function. Nature 270, 476-477.

Genazzani, E. and Pagnini, G. (1963) : Binding capability of various sulphonamides to serums of different animal species. Am J Vet Res 24, 1212-1216.

Gibson, R.E. and Levin, S.A. (1977) : Distinctions between the two-state and sequential models for cooperative ligand binding. Proc Natl Acad Sci USA 74 (1), 139-143.

Gifford, L. (1981) : Spectrophotometry and fluorimetry. Chapter 5 in Therapeutic Drug Monitoring ed. by Richens, A. and Marks, V. : Churchill Livingstone.

Gillette, J.R. (1973) : Overview of drug-protein binding. Ann NY Acad Sci 226, 6-17.

Giuliani, A., Hassan, H.J., Casalbore, P., Marini, L., Orlando, M. and Tentori, L. (1981) : Structural or functional heterogeneity of normal human serum albumin, alloalbumin, bisalbumin. Clin Chim Acta 113, 43-49.

Glasson, S., Zini, R., D'Athis, P., Tillement, J.P. and Boissier, J.R. (1980) : The distribution of bound propranolol between the different serum proteins. Mol Pharmacol 17, 187-191.

Goldstein, A. (1949) : The interaction of drugs and plasma proteins. Pharmacol Rev 1, 102-165.

Goto, S., Yoshitomi, H. and Nakase, M. (1978) : Binding of sulfonylurea-related compounds with bovine serum albumin. Chem Pharm Bull (Tokyo) 26 (2), 472-480.

Goya, S., Takadate, A., Fujino, H., Otagiri, M. and Uekama, K. (1982) : New fluorescent probes for drug-albumin interaction studies. Chem Pharm Bull (Tokyo) 30 (4), 1363-1369.

Grafnetterová, J., Grafnetter, D., Schück, O., Tomková and Bláha, J. (1979) : The effect of endogenous compounds, isolated from sera of uremic patients, on chloramphenicol binding to proteins. Biochem Pharmacol 28, 2923-2928.

Graham, T. (1861) Trans R Soc London 151, 183.

Green, G.L. and O'Haver, T.C. (1974) : Derivative luminescence spectrometry. Anal Chem 46 (14), 2191-2196.

Greenblatt, D.J., Sellers, E.M. and Koch-Weser, J. (1982) : Importance of protein binding for the interpretation of serum or plasma drug concentrations. J Clin Pharmacol 22, 259-263.

Gridgeman, N.T. (1952) : Reliability of photoelectric photometry. Anal Chem 24 (3), 445-449.

Grigorova, A.-M., Cittanova, N. and Weber, G. (1980) : Existence of multiple sites for ANS in an alpha-fetoprotein fraction. Demonstration by fluorescence polarization. Biochem Biophys Res Commun 94 (2), 413-418.

Guilbault, G.G. (1973) : Practical Fluorescence - Theory, Methods and Techniques. Marcel Dekker, New York.

Gumpen, S., Hegg, P.O. and Martens, H. (1979) : Thermal stability of fatty acid - serum albumin complexes studied by differential scanning calorimetry. Biochim Biophys Acta 574, 189-196.

Hansch, C. (1968) : The use of substituent constants in drug modification. Farmaco (Sci) 23 (4), 293-320.

Hansen, E.H. and Ruzicka, J. (1982) : Flow-injection analysis. An idea complete - but yet far from fully exploited. J Automatic Chemistry 4 (4), 193.

Hawkins, D., Pinckard, R.N. and Farr, R.S. (1968) : Acetylation of human serum albumin by acetylalicylic acid. Science 160, 780-781.

Henry, J.A., Dunlop, A.W., Mitchell, S.N., Turner, P. and Adams, P. (1981) : A model for the pH dependence of drug-protein binding. J Pharm Pharmacol 33, 179-182.

Hertl, W. and Odstrchel, G. (1982) : Radiometric assay of dialysates. US Patent 4, 311, 687.

Hiji, Y., Sugiyama, M. and Yamada, M. (1978) : Dynamic dialysis utilizing a hollow fibre unit as a rapid method for studying protein binding. Arch Int Physiol Biochim 86, 531-541.

Holy, H.W. (1982) : Commentary : Flow-injection analysis - an idea incomplete? J Automatic Chemistry 4 (3), 111.

Horie, T., Sugiyama, Y., Awazu, S., and Hanano, M. (1982) : 1-anilino-8-naphthalene sulfonate binding site on human erythrocyte membrane using fluorescence lifetime and polarization. J Pharm Dyn 5, 73-80.

Howell, A., Sutherland, R. and Rolinson, G.N. (1972) : Effect of protein binding on levels of ampicillin and cloxacillin in synovial fluid. Clin Pharmacol Ther 13 (5), 724-732.

Hsia, J.C. (1981) : Evolutionary origin of the physiological ligand binding specificity of serum albumin - the allosteric domain model. Periodicum Biologorum 83 (1), 9-104.

Hsia, J.C., Er, S.S., Tan, C.T. and Tinker, D.O. (1982) : Human serum albumin : an allosteric domain model for bilirubin binding specificity. J Biol Chem 257 (4), 1724-1729.

Hsu, P.-L., Ma, J.K.H., Jun, H.W. and Luzzi, L.A. (1974) : Structure relationship for binding of sulfonamides and penicillins to bovine serum albumin by fluorescence probe technique. J Pharm Sci 63 (1), 27-31.

Itoh, M., Yamahata, K., Yagi, N., Sakamoto, M., Sekikawa, H., Kadowaki, J,-I., Ohnishi, M., Itoh, H. and Takada, M. (1981) : Biochemical and biophysical behaviours of plasma albumin. II. Comparison of plasma albumin from normal subjects and nephrotic patients. J Pharm Dyn 4, 901-906.

Iyer, K.S., Lau, S.-J., Laurie, S.H. and Sarkar, B. (1978) : Synthesis of the native copper (II) - transport site of human serum albumin and its copper (II) - binding properties. Biochem J 169, 61-69.

Jackson, G. and Porter, G. (1961) Proc R Soc Lond Ser A 260, 13-30.

Jacobsen, C. (1972) : Chemical modification of the high-affinity bilirubin-binding site of human serum albumin. Eur J Biochem 27, 513-519.

Jadetsky, O. and Wade-Jadetsky, N. (1965) : On the mechanism of the binding of sulphonamides to bovine serum albumin. Mol Pharmacol 1, 214-230.

Jähnchen, E., Blanck, K.J., Breuing, K.H., Gilfrich, H.J., Meinertz, T. and Trenk, D. (1981) : Plasma protein binding of azopropazone in patients with kidney and liver disease. Br J Clin Pharmacol 11, 361-367.

Janssen, L.H.M., Van Wilgenburg, M.T.and Wilting, J. (1981) : Human serum albumin as an allosteric two-state protein. Evidence from effects of calcium and warfarin on proton binding behaviour. Biochim Biophys Acta 669, 244-250.

Jonas, A. (1972) : Physiochemical properties of bovine serum high density lipoprotein. J Biol Chem 247 (23), 7767-7772.

José, M.V. and Larralde, C. (1982) : Alternative interpretation of unusual Scatchard plots : Contribution of interactions and heterogeneity. Math Biosci 58, 159-170.

Judis, J. (1982) : Binding of selected phenol derivatives to human serum proteins. J Pharm Sci 71 (10), 1145-1147.

Jusko, W.J. and Gretch, M. (1976) : Plasma and tissue protein binding of drugs in pharmacokinetics. Drug Metabolism Reviews 5 (1), 43-140.

Kakemi, K., Arita, T., Yamashina, H. and Konishi, R. (1962) : Absorption and excretion of drugs. X. The effect of the protein binding on the renal excretion rate of salicylic acid derivatives. J Pharm Soc Jap 82 (4), 536-539.

Karush, F. (1950) : Heterogeneity of the binding sites of bovine serum albumin. J Am Chem Soc 72, 2705-2713.

Karush, F. and Karush, S.S. (1971) : Equilibrium dialysis. In : Methods in Immunology and Immunochemistry 3 pp383-393, ed. by Williams, C.A. and Chase, M.W. : Academic Press, New York and London.

Keen, P. (1971) : Effect of binding to plasma proteins on the distribution, activity and elimination of drugs. Chapter 10 in Handbook of Experimental Pharmacology Vol. 28 (1) pp213-233, ed. by Brodie, B.B. and Gillette, J.R. : Springer-Verlag, Berlin.

Kendal, F.E. (1941) : Studies on human serum proteins. II. Crystallization of human serum albumin. J Biol Chem 138, 97-109.

Keresztes-Nagy, S., Mais, R.F., Oester, Y.T. and Zaroslinski, J.F. (1972) : Protein binding methodology : Comparison of equilibrium dialysis and frontal analysis chromatography in the study of salicylate binding. Anal Biochem 48, (1), 80-89.

Kernoff, L.M., Pimstone, B.L., Solomon, J. and Brock, J.F. (1971) : The effect of hypophysectomy and growth hormone replacement on albumin synthesis and catabolism in the rat. Biochem J 124, 529-535.

Klotz, I.M. (1946) : The application of the law of mass action to binding by proteins. Interactions with calcium. Arch Biochem 9, 109-117.

Klotz, I.M. (1953) : Protein interactions. Chapter 8 in The Proteins : Chemistry, Biological Activity and Methods, pp727-806, ed. by Neurath, H. and Bailey, K. : Academic Press, New York.

Klotz, I.M. (1982) : Numbers of receptor sites from Scatchard graphs : facts and fantasies. Science 217, 1247-1249.

Klotz, I.M. (1983) : Ligand-receptor interactions : what we can and cannot learn from binding experiments. Trends in Pharmacological Sciences 4 (6), 253-255.

Klotz, I.M. and Hunston, D.L. (1971) : Properties of graphical representation of multiple classes of binding sites. Biochemistry 10 (16), 3065-3069.

Klotz, I.M., Triwush, H. and Walker, F.M. (1948) : The binding of organic ions by proteins. Competition phenomena and denaturation effects. J Am Chem Soc 70, 2935-2941.

Kober, A., Jenner, Å., Sjöholm, I., Borga, O. and Odar-Cederlöf, I. (1978) : Differential effects of liver cirrhosis on the albumin binding sites for diazepam, salicylic acid and warfarin. Biochem Pharmacol 27, 2729-2735.

Kober, A., Sjöholm, I., Borga, O. and Odar-Cederlöf, I. (1979) : Protein binding of diazepam and digitoxin in uremic and normal serum. Biochem Pharmacol 28 1037-1042.

Koch-Weser, J. (1972) : Serum drug concentrations as therapeutic guides. N Engl J Med 287 (5), 227-231.

Koch-Weser, J. and Sellers, E.M. (1976a) : Binding of drugs to serum albumin (first of two parts). N Engl J Med 294 (6), 311-316.

Koch-Weser, J. and Sellers, E.M. (1976b) : Binding of drugs to serum albumin (second of two parts). N Engl J Med 294 (10), 526-531.

Koh, S.-W.M. and Means, G.E. (1979) : Characterization of a small apolar anion binding site of human serum albumin. Arch Biochem Biophys 192, 73-79.

Kolb, D.A. and Weber, G. (1975) : Cooperativity of binding of anilinonaphthalenesulfonate to serum albumin induced by a second ligand. Biochemistry 14 (20), 4476-4481.

Koshland, D.E.,Jr. (1958) : Proc Natl Acad Sci USA 44, 98.

Koshland, D.E.,Jr. Nēmethy, G. and Filmer, D. (1966) : Comparison of experimental binding data and theoretical models in proteins containing subunits. Biochemistry 5 (1), 365-385.

Kragh-Hansen, U. (1981) : Molecular aspects of ligand binding to serum albumin. Pharmacol Rev 33 (1), 17-53.

Kragh-Hansen, U. (1983) : Relations between high-affinity binding sites for L-tryptophan, diazepam, salicylate and Phenol Red on human serum albumin. Biochem J 209, 135-142.

Kremer, J.M.H., Bakker, G. and Wilting, J. (1982) : The role of the transition between neutral and basic forms of human serum albumin in the kinetics of the binding to warfarin. Biochim Biophys Acta 708, 239-242.

Kunin, C.M., Craig, W.A., Kornguth, M. and Monson, R. (1973) : Influence of binding on the pharmacologic activity of antibiotics. Ann NY Acad Sci 226, 214-224.

Kurono, Y. and Ikeda, K. (1982) : Classification and identification of drug binding sites on human serum albumin by using its esterase-like activities. J Pharm Dyn 5, s-50.

Kurono, Y., Ohta, N., Yotsuyanagi, T. and Ikeda, K. (1981) : Effects of drug binding on the esterase-like activity of human serum albumin. III. Evaluation of reactivities of the two active sites by using clofibric acid as an inhibitor. Chem Pharm Bull (Tokyo) 29 (8), 2345-2350.

Kurtz, H. and Fichtl, B. (1983) : Binding of drugs to tissues. Drug Metabolism Reviews 14 (3), 467-510.

Kurtz, H., Trunk, H. and Weitz, B. (1977) : Evaluation of methods to determine protein-binding of drugs. Equilibrium dialysis, ultrafiltration, ultracentrifugation, gel filtration. Arzneim Forsh/Drug Res 27 (2), 1373-1380.

Lagercrantz, C., Larsson, T. and Karlsson, H. (1979) : Binding of some fatty acids and drugs to immobilized bovine serum albumin studied by column affinity chromatography. Anal Biochem 99, 352-364.

Lakowicz, J.R. (1980) : Minireview : Fluorescence spectroscopic investigations of the dynamic properties of proteins, membranes and nucleic acids. J Biochem Biophys Methods 2, 91-119.

Lakusta, H. and Sarkar, B. (1979) : Equilibrium studies of zinc (II) and cobalt (II) binding to tripeptide analogues of the amino terminus of human serum albumin. J Inorgan Biochem 11, 303-315.

Lamola, A.A., Eisinger, J., Blumerg, W.E., Patel, S.C. and Flores, J. (1979) : Fluorimetric study of the partition of bilirubin among blood components : basis for rapid microassays of bilirubin and bilirubin binding capacity in whole blood. Anal Biochem 100, 25-42.

Langmuir, I. (1917). J Am Chem Soc 39, 1848.

Lassmann, A. (1981) : Stopped-flow investigations on the kinetics of drug binding to human serum albumin. In : Methods in Clinical Pharmacology 2 pp17-29, ed. by Reitbrock, N. and Woodcock, B.G. : Vieweg Braunschweig.

Lassmann, A. and Reitbrock, N. (1982) : Stopped flow studies on drug-protein binding. Analog-computer analysis of the pH-dependent binding kinetics of warfarin and human serum albumin. Nauyn Schmiedebergs Arch Pharmacol 320, 189-195.

Lau, S.-J. and Sarkar, B. (1979) : Inorganic mercury (II) - binding components in normal human blood serum. J Toxicol Environ Health 5 (5), 907-916.

Law, S.W. and Dugaiczyk, A. (1981) : Homology between the primary structure of α-fetoprotein, deduced from a complete cDNA sequence, and serum albumin. Nature (Lond) 291, 201-205.

Levine, R.L., Fredericks, W.R. and Rapoport, S.I. (1982) : Entry of bilirubin into the brain due to opening of the blood-brain barrier. Pediatrics 69 (3), 255-259.

Levy, G. (1973) : Relationship between plasma protein binding, distribution and anticoagulant action of dicoumarol. Ann NY Acad Sci 226, 195-199.

Lewis, R.J., Trager, W.F., Chen, K.K., Breckenbridge, A., Orme, A., Rowland, M. and Schary, W. (1974) : Warfarin : stereochemical aspects of its metabolism and the interaction with phenylbutazone. J Clin Invest 53, 1607-1617.

Lichtenwalner, D.M., Suh, B., Lorber, B., Rudnick, M.R. and Craig, W.A. (1981) : Partial purification and characterization of the drug-binding - defect inducer in uremia. J Lab Clin Med 97 (1), 72-81.

Lien, E.J. (1981) : Structure-activity relationships and drug disposition. Annu Rev Pharmacol Toxicol 21, 31-61.

Lim, C.S., Miller, J.N. and Bridges, J.W. (1978) : The use of polarizers to improve detection limits in fluorimetric analysis. Anal Chim Acta 100, 235-243.

Lim, C.S., Miller, J.N. and Bridges, J.W. (1980) : Automation of an energy-transfer immunoassay by using stopped-flow injection analysis with merging zones. Anal Chim Acta 114, 183-189.

Lloyd, J.B.F. (1971): Synchronized excitation of fluorescence emission spectra. Nature (Lond) 231, 64-65.

Lloyd, J.B.F. and Evett, I.W. (1977) : Prediction of peak wavelengths and intensities in synchronously excited fluorescence emission spectra. Anal Chem 49 (12), 1710-1715.

Longworth, J.W. (1981) : A new component in protein fluorescence. Ann NY Acad Sci 336, 237-245.

Ma, J.K.M., Hsu, P.-L. and Luzzi, L.A. (1974) : New fluorescent probes for drug-protein binding studies. J Pharm Sci 63 (1), 32-36.

Madsen, B.W. and Ellis, G.M. (1981) : Cooperative interaction of warfarin and phenylbutazone with human serum albumin. Biochem Pharmacol 30, (11), 1169-1173.

Maes, V., Engelborghs, Y., Hoebeke, J., Maras, Y. and Vercruysse, A. (1982) : Fluorimetric analysis of the binding of warfarin to human serum albumin. Equilibrium and kinetic study. Mol Pharmacol 21, 100-107.

Maliwal, B.P. and Guthrie, F.E. (1983) : Chemical modifications of the insecticide binding sites on human serum albumin : role of indole, bilirubin, and fatty acid binding sites. Pest Biochem Physiol 19, 104-113.

Mertens, M.L. and Kägi, J.H.R. (1979) : A graphical correction procedure for inner filter effect in fluorescence quenching titrations. Anal Biochem 96, 448-455.

Marks, V. (1979a) : New developments in immunoassays for therapeutic drug monitoring. Antibiotics Chemother 26, 16-26.

Marks, V. (1979b) : Clinical monitoring of therapeutic drugs. Ann Clin Biochem 16, 370-379.

Martin, B.K. (1965) : Potential effect of the plasma proteins on drug disposition. Nature (Lond) 207, 274-276.

McArthur, J.N., Dawkins, P.D., Smith M.J.H., and Hamilton, E.B.D. (1971) : Mode of action of antirheumatic drugs. Br Med J 2 (5763), 677-679.

McClure, W.O. and Edelman, G.M. (1966) : Fluorescent probes for conformational states of proteins. I. Mechanism of fluorescence of 2-p-toluidinylnaphthalene-6-sulfonate, a hydrophobic probe. Biochemistry 5 (6), 1908-1918.

McElnay, J.C. and D'Arcy, P.F. (1980) : Sites and mechanisms of drug interactions II. Protein binding, renal excretion and pharmacodynamic interactions. Int J Pharm 6, 205-223.

McElnay, J.C. and D'Arcy, P.F. (1983) : Protein binding displacement interactions and their clinical importance. Drugs 25, 495-513.

McLachlan, A.D. and Walker, J.E. (1977) : Evolution of serum albumin. J Mol Biol 112, 543-558.

McLachlan, A.D. and Walker, J.E. (1978) : Serum albumin domain secondary structure prediction. Biochim Biophys Acta 536, 106-111.

McMenamy, R.H. and Oncley, J.L. (1958) : The specific binding of L-tryptophan to serum albumin. J Mol Biol 233, 1436-1447.

McNamara, P.J. and Bogardus, J.B. (1982) : Effect of initial conditions and drug-protein binding on the time to equilibrium in dialysis systems. J Pharm Sci 71 (9), 1066-1068.

McNamara, P.J., Slaughter, R.L., Visco, J.P., Elwood, C.M., Siegel, J.H. and Lalka, D. (1980) : Effect of smoking on binding of lidocaine to human serum proteins. J Pharm Sci 69 (6), 749-751.

Means, G.E. and Wu, H.-L. (1979) : The reactive tyrosin residue of human serum albumin : characterization of its reaction with diisopropylfluorophosphate. Arch Biochem Biophys 194 (2), 526-530.

Meloun, B., Morávek, L. and Kostka, V. (1975) : Complete amino acid sequence of human serum albumin. FEBS Lett 58 (1), 134-137.

Meuldermanns, W.E.G., Hurkmans, R.M.A. and Heykants, J.J.P. (1982) : Plasma protein binding and distribution of fentanyl, sufentaril, alfentaril and lofentaril in blood. Arch Int Pharmacodyn 257, 4-19.

Meyer, M.C. and Guttman, D.E. (1968) : The binding of drugs by plasma proteins. J Pharm Sci 57 (6), 895-917.

Midgley, J.E. and Wilkins, T.A. (1982) : Assay for the free portion of substances in biological fluids. US Patent 4, 366, 143.

Miller, T.L., Willett, S.L., Moss, M.E., Miller, J. and Belinka, B.A., Jr. (1982) : Binding of crocetin to plasma albumin. J Pharmi Sci 71 (2), 173-177.

Mindegaard, J. (1979) : Flow multi-injection analysis - a system for the analysis of highly concentrated samples without prior dilution. Anal Chim Acta 104, 185-189.

Moll, G.W.,Jr. and Rosenfield, R.L. (1978) : Some limitations of using equilibrium dialysis to study human serum albumin - testosterone interaction. J Clin Endocrinol Metab 46 (3), 501-503.

Monod, C., Netter., Stalars, M.C., Martin, J., Royer, R.J. and Gaucher, A. (1983) : Difficulties in applying the Scatchard model of ligand binding to proteins - proposal of new mathematical tools - application to salicylates. J Pharm Sci 72 (1), 35-41.

Monod, J., Changeux, J.-P. and Jacob, F. (1963) : Allosteric proteins and cellular control systems. J Mol Biol 6, 306-329.

Monod, J., Wyman, J. and Changeux, J.-P. (1965) : On the nature of allosteric transitions : a plausible model. J Mol Biol 12, 88-118.

Moriguchi, I., Wada, S. and Nishizawa, T. (1968) : Protein bindings. III. Binding of sulfonamides to bovine serum albumin. Chem Pharm Bull (Tokyo) 16 (4), 601-605.

Morrison, B., Shenkin, A., McLelland, A., Robertson, D.A., Barrowman, M., Graham, S., Wuga, G. and Cunningham, K.J.M. (1979) : Intra-individual variation in commonly analyzed serum constituents. Clin Chem 25 (10), 1799-1805.

Mudge, G., Stibitz, G.R., Robinson, M.S. and Gemborys, M.W. (1978) : Competition for binding to multiple sites of human serum albumin for cholecystographic agents and sulfobromophthalein. Drug Metabolism and Disposition 6 (4), 440-451.

Müller, W.E. and Stillbauer, A.E. (1983) : Characterization of a common binding site for basic drugs on human α_1-acid glycoprotein (orosomucoid). Naunyn Schmeidebergs Arch Pharmacol 322, 170-173.

Müller, W.E. and Wöllert, U. (1975) : Influence of various drugs on the binding of L-tryptophan to human serum albumin. Res Commun Chem Pathol Pharmacol 10 (3), 565-568.

Müller, W.E. and Wöllert, U. (1979) : Human serum albumin as a 'silent receptor' for drugs and endogenous substances. Pharmacology 19, 59-67.

Munson, P.J. and Rodbard, D. (1980) : LIGAND : A versatile computerized approach for characterization of ligand-binding systems. Anal Biochem 107, 220-239.

Nakano, N.I., Shimamori, Y. and Yamaguchi, S. (1982) : Binding capacities of human serum albumin monomer and dimer by continuous frontal affinity chromatography. J Chromatogr 237, 225-232.

Neurath, H. (1965) : The Proteins : Composition, Structure and Function. Vol 3, 2nd edition. Academic Press, New York and London.

Newbould, B.B. and Kilpatrick, R. (1960) : Long acting sulphonamides and protein-binding. Lancet 1, 887-891.

Nikkel, H.J. and Foster, J.F. (1971) : A reversible sulfhydryl-catalyzed alteration of bovine mercaptalbumin. Biochemistry 10 (24), 4479-4486.

Norby, J.G., Ottolenghi, P. and Jensen, J. (1980) : Scatchard plot : common misinterpretation of binding experiments. Anal Biochem 102, 318-320.

Odell, G.B. (1959) : Studies in kernicterus. I. The protein binding of bilirubin. J Clin Invest 38, 823-833.

Odell, G.B. (1982) : Letter to the editor. Pediatrics 70 (4), 659-660.

Øie, S. and Guentert, T.W. (1982) : Stability of heparin and other fractions of glycosaminoglycan sulfates in human digestive juices. J Pharm Sci, 71(1), 127-128.

Øie, S. and Tozer, T.N. (1979) : Effect of altered plasma protein binding on apparent volume of distribution. J Pharm Sci 68 (9), 1203-1205.

Olsen, E. (1975) : Modern Optical Methods of Analysis. McGraw-Hill Book Company.

O'Reilly, R.A. (1967) : Studies on the coumarin anticoagulant drugs : interaction of human plasma albumin and warfarin sodium. J Clin Invest 46, 829-837.

O'Reilly, R.A. (1973) : The binding of sodium warfarin to plasma albumin and its displacement by phenylbutazone. Ann NY Acad Sci 226, 293-308.

O'Reilly, R.A. and Goulart, D.A. (1981) : Comparative interaciton of sulfinpyrazone and phenylbutazone with racemic warfarin : alteration in vivo of free fraction of plasma warfarin. J Pharmacol Exp Ther 291 (3), 691-694.

Otagiri, M., Hardee, G.E. and Perrin, J.H. (1978) : Microcalorimetric investigations of pharmaceutical complexes II. Drug-albumin interactions. Biochem Pharmacol 27, 1401-1404.

Parker, C.A. (1968) : Photoluminescence of Solutions. Elsevier, New York.

Parker, C.A. and Rees, W.T. (1960) : Correction of fluorescence spectra and measurement of fluorescence quantum effeciency. Analyst 85, 587-600.

Pedersen, S.M. (1981) : The binding of gold to human albumin in vitro. Intrinsic association constants at physiological conditions. Biochem Pharmacol 30 (23), 3249-3252.

Pennock, B.E. (1973) : A calculator for finding binding parameters from a Scatchard plot. Anal Biochem 56, 306-309.

Perrin, J.H. and Juni, K. (1982) : The effect of Ca^{++} on the binding of drugs to human serum albumin : pharmacokinetic implications. Biopharm Drug Dispos 3, 379-381.

Perucca, E. and Crema, A. (1982) : Plasma protein binding of drugs in pregnancy. Clin Pharmacokin 7 (4), 336-352.

Perucca, E., Ruprah, M. and Richens, A. (1981) : Altered drug binding to serum proteins in pregnant women : therapeutic relevance. J R Soc Med 74, 422-426.

Peters, T.,Jr. (1975) : Serum albumin. Chapter 3 in The Plasma Proteins Vol. 1, 2nd edition, pp133-181, ed. by Putnam, F.W. : Academic Press, New York and London.

Peters, T.,Jr. (1977) : Serum albumin : recent progress in the understanding of its structure and biosynthesis. Clin Chem 23 (1), 5-12.

Piafsky, K.M. (1980) : Disease-induced changes in the plasma binding of basic drugs. Clin Pharmacokin 5, 246-262.

Pinkard, N., Hawkins, D. and Farr, R.S. (1973) : The influence of acetylsalicylic acid on the binding of acetrizoate to human albumin. Ann NY Acad Sci 226, 341-344.

Porro, T.J. (1972) : Double-wavelength spectroscopy. Anal Chem 44 (4), 93A-103A.

Prendergast, F.G., Meyer, M., Carlson, G.L., Iida, S. and Potter, J.D. (1983) : Synthesis, spectral properties, and use of 6-acryloyl-2-dimethylaminonaphthalene (Acrylodan) J Biol Chem 258 (12), 7541-7544.

Putnam, F.W. (1975) : The Plasma Proteins. Vol 1, 2nd edition. Academic Press, New York and London.

Quinn, P.S., Gamble, M. and Judah, J.D. (1975) : Biosynthesis of serum albumin in rat liver. Isolation and probable structure of 'proalbumin' from rat liver. Biochem J 146, 389-393.

Ranger, C. (1981) : Flow injection analysis. Anal Chem 53, 20A-32A.

Reed, R.G., Feldhoff, R.C., Clute, O.L. and Peters, T.,Jr. (1975) : Fragments of bovine serum albumin produced by limited proteolysis. Conformation and ligand binding. Biochemistry 14 (21), 4578-4583.

Reidenberg, M.M. (1976) : The binding of drugs to plasma proteins from patients with poor renal function. Clin Pharmacokin 1, 121-125.

Reidenberg, M.M. (1981) : Is protein binding important? Chapter 2 in Therapeutic Drug Monitoring, ed. by Richens, A. and Marks, V. : Churchill Livingstone.

Ritter, D.A., Kenny, J.D., Norton, H.J. and Rudolph, A.J. (1982) : A prospective study of free bilirubin and other risk factors in the development of kernicterus in premature infants. Pediatrics 69 (3), 260-266.

Reijn, J.M., Van der Linden, W.E. and Poppe, H. (1980) : Some theoretical aspects of flow injection analysis. Anal Chim Acta 114, 105-118.

Rocks, B.F. and Riley, C. (1982) : Flow-injection analysis : a new approach to quantitative measurements in clinical chemistry. Clin Chem 28 (3), 409-421.

Roemelt, P.M., Lapen, A.J. and Seitz, W.R. (1980) : Selective analysis of binary fluorophor mixtures by fluorescence polarization. Anal Chem 52 (4), 769-771.

Roitt, I.V. (1979) : Essential Immunology. Blackwell Scientific Publications, Oxford.

Roosdorp, N., Wänn, B. and Sjöholm, I. (1977) : Correlation between arginyl residue modification and benzodiazepine binding to human serum albumin. J Biol Chem 252 (11), 3876-3880.

Romach, M.K., Piafsky, K.M., Abel, J.G., Khouw, V. and Sellers, E.M. (1981) : Methadone binding to orosomucoid (α_1-acid glycoprotein) : determinant of free fraction in plasma. Clin Pharm Ther 29 (2), 211-217.

Rondanelli, R., Autelli, F., Guarnone, E. and Ciardelli, L. (1983) : The clinical pharmacology of drug interactions. Int J Clin Pharm Ther Toxicol 21 (5), 224-228.

Rosenthal, H.E. (1967) : A graphic method for the determination and presentation of binding parameters in a complex system. Anal Biochem 20, 525-532.

Rothschild, M.A., Oratz, M. and Schreiber, S.S. (1973) : Albumin metabolism Gastroenterology 64 (2), 324-337.

Routledge, P.A., Stargel, W.W., Kitchell, B.B., Barchowsky, A. and Shand, D.G.) 1981) : Sex-related differences in the plasma protein binding of lignocaine and diazepam. Br J Clin Pharmacol 11, 245-250.

Rowland, M. (1980) : Plasma protein binding and therapeutic drug monitoring. Ther Drug Monitoring 2 (1), 29-37.

Ruprah, M., Perucca, E. and Richens, A. (1981) : Spuriously high values of unbound drug fraction in serum as determined by the new ultrafree anticonvulsant drug filters. Br J Clin Pharmacol 12, 753-755.

Růžička, J. and Hansen, E. (1975) : Flow injection analysis. Part 1. A new concept of fast continuous flow analysis. Anal Chim Acta 78, 145-157.

Růžička, J. and Hansen, E. (1978) : Flow injection analysis. Part X. Theory, techniques and trends. Anal Chim Acta 99, 37-76.

Růžička, J. and Hansen, E. (1979a) : Stopped flow and merging zones - a new approach to enzymatic assay by flow injection analysis. Anal Chim Acta 106, 207-224.

Růžička, J. and Hansen, E. (1979b) : Flow injection analysis. Chemtech 9, 756-764.

Růžička. J. and Hansen, E. (1980) : Flow injection analysis. Anal Chim Acta 114, 19-44.

Růžička, J. and Hansen, E. (1981) : Flow injection analysis. Chemical Analysis Volume 62 ed. by Elving, P.J. and Winefordner, J.D. : John Wiley and Sons.

Saeed, S.A., Denning-Kendall, P.A., Drew, M. and Collier, H.D.J. (1981) : Plasma albumin : recent progress in the understanding of its biological function. Biochem Soc Trans 9 (3), 222-223.

Sakamoto,,H., Nagata, I., Kikuchi, K., Aida, M. and Irie, M. (1983) : N-bromosuccinimide-oxidized human serum albumin as a tool for the determination of drug binding sites of human serum albumin. Chem Pharm Bull 31 (3), 971-978.

Sawyer, W.T. (1983) : Warfarin. In : Applied Clinical Pharmacokinetics, pp187-222, ed. by Mungall, D. : Raven Press, New York.

Scanu, A.M., Edelstein, C. and Keim, P. (1975) : Serum Lipoproteins. In : The Plasma Proteins Vol.1, 2nd edition, pp317- , ed. by Putnam, F.W. : Academic Press, New York and London.

Scatchard, G. (1949) : The attraction of proteins for small molecules and ions. Ann NY Acad Sci 51, 660-672.

Scheider, W. (1979) : The rate of access to the organic ligand-binding region of serum albumin is entropy controlled. Proc Natl Acad Sci USA 76 (5), 2283-2287.

Scheurlen, P.G. (1955) : Uber Serumeiweissveränderungen beim Diabetes mellitus. Klin Wochenschr 33, 198-205.

Schmid, K., Kaufmann, H., Isemura, S., Bauer, F., Emura, J., Motoyama, T., Ishiguro, M. and Nanno, S. (1973) : Structure of -acid glycoprotein. The complete amino acid sequence, multiple amino acid substitutions, and homology with the immunoglobulins. Biochemistry 12 (14), 2711-2724.

Scholtan, V.W. (1968) : Die Hydrophobe Binding der Pharmaka an Humanalbumin und Ribonucleinsaure. Arzeim Forsch 18, 505-517.

Schwertner, H.A. and Hawthorne, S.B. (1980) : Albumin-bound fluorescence in serum of patients with chronic renal failure. Clin Chem 26 (5), 649-652.

Sebille, B., Thuaud, N. and Tillement, J.-P. (1978) : Study of binding of low-molecular-weight ligand to biological macromolecules by high-performance liquid chromatorgraphy. Evaluation of binding parameters for two drugs bound to human serum albumin. J Chromatogr 167, 159-170.

Seliskar, C.J. and Brand, L. (1971a) : Solvent dependence of the luminescence of N-arylaminonaphthalenesulfonates. Science 171, 799-800.

Seliskar, C.J. and Brand, L. (1971b) : Electronic spectra of 2-aminonaphthaelene-6-sulfonate and related molecules. II. Effects of solvent medium on the absorption and fluorescence spectra. J Am Chem Soc 93 (21), 5414-5420.

Sellers, E.M. and Koch-Weser, J. (1970) : Potentiation of warfarin induced hypoprothrombinemia by chloral hydrate. N Engl J Med 283, 827-831.

Sellers, E.M., Lang-Sellers, M.L. and Koch-Weser, J. (1977) : Comparative warfarin binding to albumin from various species. Biochem Pharmacol 26, 2445-2447.

Silverman, W.A., Andersen, D.H., Blanc, W.A. and Crozier, D.N. (1956) : A difference in mortality rate and incidence of kernicterus among premature infants alloted to two prophylactic antibacterial regimens. Pediatrics 18, 614-625.

Simons, J.P (1971) : Photochemistry and Spectroscopy. Wiley Interscience.

Sjödin, T. (1977) : Circular dichroism studies of the inhibiting effect of oleic acid on the binding of diazepam to human serum albumin. Biochem Pharmacol 26, 2157-2161.

Sjödin, T., Hansson, R. and Sjöholm, I. (1977) : Isolation and identification of a trypsin-resistant fragment of human serum albumin with bilirubin- and drug binding properties. Biochim Biophys Acta 494, 61-75.

Sjöholm, I., Ekman, B., Kober, A., Ljundgstedt-Pahlman, I., Seiving, B. and Sjodin, T. (1979) : Binding of drugs to human serum albumin. XI. The specificity of three binding sites as studied with albumin immobilized in microparticles. Mol Pharmacol 16, 767-777.

Sjöholm, I., Kober, A., Odar-Cederlöf, I. and Borga, O. (1976) : Protein binding of drugs in uremic and normal serum : the role of endogenous binding inhibitors. Biochem Pharmacol 25, 1205-1213.

Sjöholm, I. and Ljungstedt, I. (1973) : Studies on the tryptophan- and drug-binding properties of human serum albumin fragments by affinity chromatography and circular dichroism measurements. J Biol Chem 248, 8434-8441.

Skeggs, L.T. (1957) : An automated method for colorimetric analysis. Am J Clin Pathol 28, 311-322.

Sogami, M. and Foster, J.F. (1968) : Isomerization reactions of charcoal-defatted bovine plasma albumin. The N-F transition and acid expansion. Biochemistry 7 (6), 2172-2182.

Sogami, M., Petersen, H.A. and Foster, J.F. (1969) : The microheterogeneity of plasma albumins. V. Permutations in disulphide pairings as a probable source of microheterogeneity in bovine albumin. Biochemistry 8 (11), 49-58.

Sollene, N.P. and Means, G.E. (1979) : Characterization of a specific drug binding site of human serum albumin. Mol Pharmacol 15, 754-757.

Sollene, N.P., Wu, H.-L. and Means, G.E. (1981) : Disruption of the tryptophan binding site in the human serum albumin dimer. Arch Biochem Biophys 207 (2), 264-269.

Solomon, H.M., Schrogie, J.J. and Williams, D. (1968) : The displacement of phenylbutazone - ^{14}C and warfarin - ^{14}C from human albumin by various drugs and fatty acids. Biochem Pharmacol 17, 143-151.

Soltys, B.J. and Hsia, J.C. (1977) : Fatty acid enhancement of human serum albumin binding properties. J Biol Chem 252 (12), 4043-4048.

Soltys, B.J. and Hsia, J.C. (1978) : Human serum albumin. On the relationship of fatty acid and bilirubin binding sites and the nature of fatty acid allosteric effects - a monoanionic spin label study. J Biol Chem 253 (9), 3023-3028.

Spector, A.A., Santos, E.C., Ashbrook, J.D. and Fletcher, J.E. (1973) : Influence of free fatty acid concentration on drug binding to plasma albumin. Ann NY Acad Sci 226, 247-258.

Steinhardt, J., Kryn, J. and Leidy, J.G. (1971) : Differences between bovine and human serum albumins : binding isotherms, optical rotatory dispersion, viscosity, hydrogen ion titration, and fluorescence effects. Biochemistry 10 (22), 4005-4015.

Stewart, K.K. (1982) : A reply to H.W. Holy. J Automatic Chemistry 4 (4), 193-194.

Stewart, K.K., Beecher, G.R. and Hare, P.E. (1974) : Fed Proc 33, 1439.

Stockley, I. (1974) : Interactions with oral anticoagulants. In : Drug Interactions and Their Mechanisms pp45-49, Collected reprints of series of articles first published in Pharmaceutical Journal.

Stratton, F., Chalmers, D.G., Flute, P.T., Lewis, S.M., MacIver, J., Nelson, M.G., Shinton, N.K., Stuart, J. and Swan, H.T. (1982) : Drug interaction with coumarin derivative anticoagulants. Standing advisory committee for haematology of the Royal College of Pathologists. Br Med J 285, 274-275.

Stroupe, S.D. and Foster, J.F. (1973) : Further studies of the sulfhydryl-catalyzed isomerization of bovine mercaptalbumin. Biochemistry 12 (20), 3824-3830.

Stryer, L. (1965) : The interaction of a naphthalene dye with apomyoglobin and apohemoglobin. A fluorescent probe of non-polar binding sites. J Mol Biol 13, 482-495.

Sturgeon, R.J. and Schulman, S.G. (1975) : Fluorimetric determination of arylamines by coupling with N-(1-naphthyl) ethylenediamine. Anal Chim Acta 75, 225-226.

Sudlow, G., Birkett, D.J. and Wade, D.N. (1973) : Spectroscopic techniques in the study of protein binding : the use of 1-anilino-8-naphthalenesulphonate as a fluorescent probe for the study of the binding of iophenoxic and iopanic acids to human serum albumin. Mol Pharmacol 9, 649-657.

Sudlow, G., Birkett, D.J. and Wade, D.N. (1975) : The characterization of two specific drug binding sites on human serum albumin. Mol Pharmacol 11, 824-832.

Sugiyama, Y., Iga, T., Awazu, S. and Hanano, M. (1980) : Binding protein for 1-anilino-8-naphthalenesulfonate in rat liver cytoplasm. Biochem Pharmacol 29, 2063-2069.

Sukow, W.W., Sandberg, H.E., Lewis, E.A., Eatough, D.J. and Hansen, L.D. (1980) : Binding of the Triton X series of nonionic surfactants to bovine serum albumin. Biochemistry 19 (5), 912-917.

Suzukida, M., Le, H.P., Shahid, F., McPherson, R.A., Birnbaum, E.R. and Darnall, D.W. (1983) : Resonance energy transfer between cysteine -34 and tryptophan -214 in human serum albumin. Distance measurements as a function of pH. Biochemistry 22 (10), 2415-2420.

Svenson, A., Holmer, E. and Andersson, L.-D. (1974) : A new method for the measurement of dissociation rates for complexes between small ligands and proteins as applied to the palmitate and bilirubin complexes with serum albumin. Biochim Biophys Acta 342, 54-59.

Swaney, J.B. and Klotz, I.M. (1970) : Amino acid sequence adjoining the lone tryptophan of human serum albumin. A binding site of the protein. Biochemistry 9 (13), 2570-2574.

Taylor, G. (1953) : Dispersion of soluble matter in solvent flowing through a tube. Proc R Soc Lond Ser A 219, 186-203.

Tillement, J.P., Lhoste, F. and Giudicelli, J.F. (1978) : Diseases and drug protein binding. Clin Pharmacokin 3, 144-154.

Tillement, J.P., Zini, R. and Glasson, S. (1981) : In vitro studies to assess plasma binding of a new drug in humans. In : Methods in Clinical Pharmacology 2, pp45-63 ed. by Rietbrock, N. and Woodcock, B.G.

Tsutsumi, E., Inaba, T., Mahon, W.A. and Kalow, W. (1975) : The displacing effect of a fatty acid on the binding of diazepam to human serum albumin. Biochem Pharmacol 24, 1361-1362.

Turner, D.C. and Brand, L. (1968) : Quantitative estimation of protein binding site polarity. Fluorescence of N-arylaminonaphthalenesulfonates. Biochemistry 7 (10), 3381-3390.

Udenfriend, S. (1962) : Fluorescence Assay in Biology and Medicine, Volume I, Academic Press, New York.

Udenfriend, S. (1969) : Fluorescence Assay in Biology and Medicine, Volume II, Academic Press, New York.

Urien, S., Albengres, E. and Tillement, J.-P. (1981) : Serum protein binding of valproic acid in healthy subjects and in patients with liver disease. Int J Clin Pharmacol Ther Toxicol 19 (7), 319-325.

Urien, S., Albengres, E., Zini, R. and Tillement, J.-P. (1982) : Evidence for binding of certain acidic drugs to α_1-acid glycoprotein. Biochem Pharmacol 31 (22), 3687-3689.

Valente, E.J., Trager, W.F. and Jensen, L.H. (1975) : The crystal and molecular structure and absolute configuration of (-) - (s) - warfarin. Acta Cryst B 31, 954-960.

Vallner, J.J. (1977) : Binding of drugs by albumin and plasma protein. J Pharm Sci 66 (4) 447-465.

Vallner, J.J. and Perrin, J.H. (1981) : Circular dichroic examination of the interaction of some planar acidic drugs with tryptophan-modified human serum albumin. J Pharm Pharmacol 33, 697-700.

Van der Geisen, W.F. and Wilting, J. (1983) : Consequences of the N-B transition of albumin for the binding of warfarin in human serum. Biochem Pharmacol 32 (2), 281-285.

Van Peer, A.P., Belpaire, F.M. and Bogaert, M.G. (1981) : Binding of drugs in serum, blood cells and tissues of rabbits with experimental acute renal failure. Pharmacology 22, 146-152.

Varma, D.R. (1981) : Protein deficiency and drug interactions : a review. Drug Dev Res 1, 183-198.

Vo-Dinh, T. (1978) : Multicomponent analysis by synchronous luminescence spectrometry. Anal Chem 50 (3), 396-401.

Waldmeyer, J., Korkidis, K. and Geacintov, N.E. (1982) : Relative contributions of tryptophan and tyrosine to the phosphorescence emission of human serum albumin at low temperatures. Photochem Photobiol 35, 299-304.

Walker, J.E. (1976) : Lysine residue 199 of human serum albumin is modified by acetylsalicylic acid. FEBS Lett 66, 173-175.

Wallevik, K. (1973) : Reversible denaturation of human serum albumin by pH, temperature and guanidine hydrochloride followed by optical rotation. J Biol Chem 248 (8), 2650-2655.

Wandell, M. and Wilcox-Thole, W.L. (1983) : Protein binding and free drug concentrations. In : Applied Clinical Pharmacokinetics, pp17-48, ed. by Mungall, D. : Rowen Press, New York.

Wanwimolruk, S. and Birkett, D.J. (1982) : The effects of N-B transition of human serum albumin on the specific drug-binding sites. Biochim Biophys Acta 709, 247-255.

Wanwimolruk, S., Birkett, D.J. and Brooks, P.M. (1982) : Protein binding of some non-steroidal anti-inflammatory drugs in rheumatoid arthritis. Clin Pharmacokin 7, 85-92.

Wartak, J. (1983) : Clinical Pharmacokinetics. A Modern Approach to Individualized Drug Therapy. Clinical Pharmacology and Therapeutics Series Volume 2. Praeger.

Watts, R.J. and Strickler, S.J. (1966) : Fluorescence and internal conversion in naphthalene vapor. J Chem Phys 44 (6), 2423-2426.

Weber, G. (1975) : Energetics of ligand binding to proteins. Adv Protein Chem 29, 1-83.

Weber, G. and Farris, F.J. (1979) : Synthesis and spectra properties of a hydrophobic fluorescent probe : 6-propionyl-2-(dimethylamino) naphthalene. Biochemistry 18 (14), 3075-3078.

Weder, H.G., Schildknecht, J. and Kesselring, P. (1971) : A new equilibrium dialysing system. American Laboratory 10, 15-21.

Weisiger, R., Gollan, J. and Ockner, R. (1981) : Receptor for albumin on the liver cell surface may mediate uptake of fatty acids and other albumin-bound substances. Science 211 (4486), 1048-1051.

Wennberg, R.P. and Ahlfors, C.E. (1982) : Free bilirubin is of importance. Pediatrics 70 (4), 658.

White, C.E. and Argauer, R.J. (1970) : Fluorescence Analysis : A Practical Approach. Marcel Dekkar.

Whittam, J.B., Crooks, M.J., Brown, K.F. and Pedersen, P V (1979) : Binding of nonsteroidal anti-inflammatory agents to proteins - I. Ibruprofen-serum albumin interaction. Biochem Pharmacol 28, 675-678.

Wilkinson, G.R. (1983) : Plasma and tissue considerations in drug disposition. Drug Metabolism Reviews 14 (3), 427-465.

Wilson, K. and Bromberg, T. (1981) : The influence of some disease states on drug disposition. Meth Find Exp Clin Pharmacol 3 (3), 189-200.

Wilting, J., Van der Giesen, W.F. and Janssen, L.H.M.(1981) : The effect of chloride on the binding of warfarin to albumin as a function of pH. Biochem Pbarmacol 30 (10), 1025-1031.

Wiseman, E.H. and Nelson, E. (1964) : Correlation of in vivo metabolism rate and physical properties of sulphonamides. J Pharm Sci 53, 992.

Winefordner, J.D., Schulman, S.G. and O'Haver, T.C. (1972) : Luminiscence Spectroscopy in Analytical Chemistry. Volume 38 in Chemical Analysis ed. by Elving, P.J. and Kolthoff, I.M.

Wojcikowski, C. and Sztabowicz, D. (1977) : Binding of sulfonylurea derivatives to bovine serum albumin. Pol J Pharmacol Pharm 29, 469-475.

Wood, M.B. and Wood, A.J.J. (1981) : Changes in plasma drug binding and α_1-acid glycoprotein in mother and newborn infant. Clin Pharmacol Ther 29 (4), 522-526.

Wosilait, W.D. and Ryan, M.P. (1979) : The effects of oleic acid, tolbutamide, and oxyphenbutazone on the binding of warfarin by human serum albumin. Res Commun Chem Pathol Pharmacol 25 (3), 577-584.

Yacobi, A. and Lai, C -M. and Levy, G. (1980) : Comparative pharmacokinetics of coumarin anticoagulants XLV; Pharmacokinetic and pharmacodynamic studies of acute interaction between warfarin and phenylbutazone in rats. J Pharm Sci 69 (1), 14-20.

Zierler, K. (1977) : An error in interpretation of double-reciprocal plots and Scatchard plots in studies of binding of fluorescent probes to proteins, and alternative proposals for determining binding parameters. Biophys Struct Mechanism 3, 275-289.

Zini, R., Barre, J., Bree, F., Tillement, J.-P. and Sebille, B. (1981) : Evidence for a concentration-dependent polymerization of a commercial human serum albumin. J Chromatogr 216, 191-198.